UNIVERSITÉ DU LUXEMBOURG

PhD-FSTM-2025-007
The Faculty of Science, Technology and Medicine

DISSERTATION

Defence held on 21/01/2025 in Esch-sur-Alzette

to obtain the degree of

DOCTEUR DE L'UNIVERSITÉ DU LUXEMBOURG

EN BIOLOGIE

by

Bianca BRANDUS
Born on 20 December 1995 in Oradea, (Romania)

EXPLOITING COMPLEMENT FOR TARGETED THERAPIES AGAINST PSEUDOMONAS AERUGINOSA INFECTION AND BREAST CANCER

Dissertation defence committee

Dr. Carole Devaux, dissertation supervisor
Group leader at Infection and Immunotherapy Research Group, Department of Infection and Immunity, Luxembourg Institute of Health

Dr Karita Haapasalo
Group leader at Haartman Institute, University of Helsinki

Dr Thomas Sécher
University of Tours, UFR·INSERM U 1100 Centre d'étude des pathologies respiratoires

Dr Paul Wilmes, Chairman
Professor, University of Luxembourg

Dr. Henry-Michel Cauchie, Vice-Chairman
Group leader at Environmental and Industrial Biotechnologies Group, Luxembourg Institute of Science and Technolog

A dissertation by

Bianca Brandus

submitted to the University of Luxembourg

in partial fulfilment of the requirements for the degree of

DOCTOR of PHILOSOPHY

1

Affidavit

I hereby confirm that the PhD thesis entitled “Exploiting complement for targeted therapies for *Pseudomonas aeruginosa* infection and breast cancer” has been written independently and without any other sources than cited. All necessary ethical approvals have been obtained in accordance with the relevant articles of the EU Directive 2010/63/EU on the protection of animals used for scientific purposes.

Luxembourg, 14/10/2024 Bianca Brandus

Acknowledgements

Earning a PhD is a journey, not a solitary destination. I am eternally grateful to the many people who shared their time, expertise, and passion for research, making this achievement possible.

Firstly, my deepest gratitude goes to Dr. Carole Devaux, my scientific supervisor. You didn't just offer me a unique opportunity, but truly mentored me every step of the way. The opportunity to work on such an innovative project alongside you was both an honour and a pleasure. You consistently supported my ideas, provided invaluable advice, and most importantly, encouraged me through the inevitable challenges.

My gratitude also extends to Dr. Xavier Dervillez, my co-supervisor and the visionary mind behind CoMiX molecules. Without his innovative work, this project wouldn't exist. His invaluable contributions included both guiding the design of the molecules and offering hands-on support in the lab. I am deeply indebted to his expertise and tireless collaboration.

My deepest thanks go to Aubin, Gilles, Jean-Yves and Camille for their invaluable contributions. Their expertise and dedication were crucial in designing and executing in vitro and in vivo experiments, propelling this project forward.

My sincere thanks extend to my thesis committee members; Prof. Dr. Paul Wilmes and Dr. Aurélie Poli, for their thoughtful feedback and insightful conversations not only enriched my research but also helped me grow as a scientist.

This thesis would not be complete without acknowledging the vital contributions of my collaborators. Dr. Mustapha Si-Tahar's unparalleled expertise in working with *Pseudomonas aeruginosa* was crucial, in guiding the design and execution of key experiments. Equally invaluable was the knowledge of Dr. Jacques Zimmer, whose insights into NK cells and the broader field of immunology provided invaluable depth and clarity to our research. Thank you for sharing your time and expertise.

Finally, to my family and friends, your unwavering love and support throughout this long and challenging journey have been my anchor. Thank you for reminding me that life exists outside of academia, for listening when I needed it most, and for the laughter and tears shared along the way. Especially to Anya, Apa and Vilmos my deepest gratitude goes to your unconditional love and support. This journey would

not have been the same without the arrival of my son, Mark. His presence has filled our lives with a new kind of wonder and love.

Furthermore, I acknowledge the critical financial support provided by the Luxembourg Research Fund (FNR).

This thesis is a testament to the collective effort, encouragement, and inspiration of many remarkable individuals. Thank you all from the bottom of my heart.

Table of contents

Table of figures

List of publications

Publications included in this thesis:

1. **Directed-complement killing of *Pseudomonas aeruginosa* protects against lethal pneumonia**

   Bianca Brandus*, Aubin Pitiot*, Gilles Iserentant, Camille Rolin, Jean-Yves Servais, Delphine Fouquenet, Benoit Briard, Mustapha Si-Tahar, Guillaume Desoubeaux, Yves Mely, Patrice Rassam, Ludovic Richert, Jacques Zimmer, Xavier Dervillez, Carole Seguin-Devaux

2. **Complement-Activating Multimeric Immunotherapeutic Complexes for HER2-breast cancer immunotherapy**

   Carole Seguin-Devaux*, **Bianca Brandus***, Jean-Marc Plesseria, Gilles Iserentant, Jean-Yves Servais, Georgia Kanli, Iris Behrmann, Jacques Zimmer, Jacques H M Cohen, Xavier Dervillez

   https://doi.org/10.1101/2024.02.02.578619

3. **Dimeric protein complexes and uses thereof**

   Xavier Dervillez, Rafaëla Maria Schober, **Bianca Brandus**, Carole Devaux, Jacques René Zimmer, Jacques Henri Max Cohen

   https://patents.google.com/patent/WO2023281120A1/en

Publications not included in this thesis:

1. **Multimeric immunotherapeutic complexes activating natural killer cells towards HIV-1 cure**

   Rafaëla Schober, **Bianca Brandus**, Thessa Laeremans, Gilles Iserentant, Camille Rolin, Géraldine Dessilly, Jacques Zimmer, Michel Moutschen, Joeri L. Aerts, Xavier Dervillez & Carole Seguin-Devaux

   Journal of Translational Medicine 21(1), 791 (2023)

   https://doi.org/10.1186/s12967-023-04669-4

Abbreviations

ACR	Arrestin-coupled receptor
ACT	Adoptive cell transfer
ADC	Antibody-drug conjugate
ADCC	Antibody-dependent cellular cytotoxicity
ADCP	Antibody-dependent cellular phagocytosis
Akt	Protein kinase B
AML	Acute myeloid leukemia
AP	Alternative complement pathway
APC	Antigen-presenting cell
AprA	Alkaline protease A
BiKE	Bispecific killer engager
BPPL	Bacterial priority pathogens list
BRCA1/2	Breast Cancer gene 1 and 2
C1-Inh	C1-inhibitor
C1q	Complement component 1q
C3	Complement component 3
C3aR	C3a receptor
C4BP	C4b-binding protein
C5	Complement component 5
C5aR	C5a receptor
CAR	chimeric antigen receptor
CCL	Chemokine (C-C motif) ligand
CCP	Complement control protein domain
ccRCC	Clear cell renal cell carcinoma
CD	Cluster of differentiation
CDC	Complement-dependent cytotoxicity
CDCP	Complement dependent phagocytosis
CF	Cystic fibrosis
CH	Heavy chain constant domain
CIT	Complement inhibitory threshold
CLP	Common lymphoid progenitor
CoMiX	Complement-activating multimeric immunotherapeutic complexes
CP	Classical complement pathway

CR	Complement receptor
CRC	Colorectal cancer
CRIT	Complement C2 Receptor Inhibitor Trispanning Protein
CRP	C-reactive protein
CRP	Complement regulatory protein
CRS	Cytokine release syndrome
cSCC	cutaneous squamous cell carcinoma
cSMAC	Central supramolecular activation cluster
DAF	Decay accelerating factor
DAMP	Danger associated molecular pattern
DC	Dendritic cell
DNA	Deoxyribonucleic acid
EBV	Epstein-Barr virus
ECIS	European Cancer Information System
ECM	Extracellular matrix
EF-Tu	Elongation factor Tu
EGFR	Epidermal growth factor receptor
EMT	Epithelial-mesenchymal transition
EPS	Extracellular polymeric substances
Erk-1/2	Extracellular signal-regulated kinase 1/2
EU	European Union
FAS	Fas cell surface death receptor
FasL	Fas ligand
FB	Factor B
FcγR	Fc-gamma receptor
FD	Factor D
FDA	Food and Drug Administration
FH	Factor H
FHL-1	Factor H-like protein 1
FHR	Factor H-related proteins
FI	Factor I
FISH	Fluorescence in-situ hybridization
GAG	glycosaminoglycan
GPCR	G protein-coupled receptor
GvHD	Graft-versus-host disease

GZM	Granzyme
HCC	Hepatocellular carcinoma
HER2	Human epidermal growth factor receptor 2
HER2+	HER2-positive
HIV	Human immunodeficiency virus
HSC	Hepatic stellate cell
HSV	Herpes simplex virus
iC3b	Inactive C3b
IFN-γ	Interferon-gamma
Ig	Immunoglobulin
IHC	Immunohistochemistry
int-FH	intracellular Factor H
JRC	Joint Research Centre
KIR	Killer immunoglobulin-like receptor
KLF5	factor Kruppel-like factor 5
LAG3	Lymphocyte activation gene-3
LDH	Lactate dehydrogenase
LP	Lectin complement pathway
LPS	Lipopolysaccharide
MAC	Membrane attack complex
MAPK	Mitogen-activated protein kinase
MASP	MBL-associated serine proteas
MBL	Mannose-binding lectin
MCP	Membrane cofactor protein
mCRP	Membrane-bound complement regulatory protein
MDSC	Myeloid-derived suppressor cells
MHC-I	Major Histocompatibility Complex class I
MHC-II	Major Histocompatibility Complex class II
MIC	Minimum inhibitory concentration
MIC-A/B	MHC class I chain-related A and B
MIRL	Membrane inhibitor of reactive lysis
miRNA	MicroRNA
mTOR	Mammalian target of rapamycin
NET	Neutrophil extracellular trap
NF-κB	Nuclear Factor –κB

NHS	Normal human serum
NK cell	Natural killer cell
NKCE	Natural killer cell engager
NKG2D	Natural-killer group 2, member D
NLR	Nucleotide-binding oligomerization domain (NOD)-like receptors
OD	Oligomerization domain
P	Pertuzumab
PAMP	Pathogen associated molecular pattern
PDAC	Pancreatic ductal adenocarcinoma
PD-L1	Programmed Cell Death Ligand 1
PI3K	Phosphatidylinositol 3-kinase
PMN	Polymorphonuclear neutrophil
PRF	Perforin
PRR	Pattern recognition receptor
pSMAC	Peripheral supramolecular activation cluster
PTX3	Pentraxin 3
QS	Quorum sensing
RLR	Retinoic acid-inducible gene I (RIG-I)-like receptors
RNA	Ribonucleic acid
ROS	Reactive oxygen species
SARS-CoV-2	Severe acute respiratory syndrome coronavirus 2
scFv	Single chain variable fragment
SMIPP-S	scabies mite proteolytically inactive serine protease paralogue
SYD985	Trastuzumab duocarmycin
T	Trastuzumab
T3SS	Type 3 secretion system
TAA	Tumor-associated antigen
TAM	Tumor-associated macrophage
TCF1	T cell factor 1
T-DC	Trastuzumab-drug conjugate
T-DM1	Trastuzumab emtansine
T-DXd	Trastuzumab deruxtecan
TetraKE	Tetraspecific killer engagers
TGF-β	Transforming growth factor beta

TIGIT	T-cell immunoreceptor with immunoglobulin and immunoreceptor tyrosine-based inhibitory motif domains
TIM-3	T-cell immunoglobulin and mucin domain-containing protein 3
TLR	Toll-like receptor
TME	Tumor microenvironment
TNF-α	Tumor necrosis factor α
TRAIL	TNF-related apoptosis-inducing ligand
Treg	Regulatory T cell
TriKE	Trispecific killer engager
TRP53	Transformation-related protein 53
TWIST1	Twist-related protein 1
ULBP	UL16 binding protein
VEGF	Vascular endothelial growth factor
VHH	Variable Heavy domain of Heavy chain
WHO	World Health Organization
WWOX	WW domain-containing oxidoreductase
XCL	Chemokine (C motif) ligand

165

166

I. Abstract

Complement is the primary defense mechanism against pathogens and in antitumor immunity. Complement activating Multimeric compleXes (CoMiX), a novel class of antibody-based therapeutics, activate the complement at the surface of pathogens or target cells. In this work, we have evaluated their potential in targeting and eliminating both *Pseudomonas aeruginosa* (*P. aeruginosa*) and HER2-positive breast cancer. These multimeric complexes are composed of three distinct functional components: a targeting moiety, an oligomerization domain, and an effector component.

In the context of *P. aeruginosa* infections, CoMiX were designed to target the Psl-exopolysaccharide of the bacterium. The effector component of CoMiX in this case was either an Fc region, which activated the classical complement pathway and immune cells, or Factor H-related protein 1 (FHR1), which competed with the complement inhibitor Factor H. In vitro studies demonstrated CoMiX's ability to bind to *P. aeruginosa* isolates, activate complement, and directly kill the bacteria. Importantly, CoMiX was shown to reduce dramatically bacterial load and mortality in a mouse model of acute *P. aeruginosa* lung infection.

For HER2-positive breast cancer, CoMiX were engineered to target HER2-expressing tumor cells. The effector component in this case was either FHR4, which activated the alternative complement pathway, or a triple Fc dimer, which activated the classical complement pathway and promoted NK cell activation and phagocytosis by macrophages. In vitro studies demonstrated CoMiX's ability to activate complement, induce complement-dependent cytotoxicity, and stimulate immune cell responses. In vivo studies in a xenograft model of human breast cancer showed that CoMiX could effectively inhibit tumor growth and overcome the resistance to trastuzumab.

Overall, these studies highlight the versatility and therapeutic potential of CoMiX in targeting and eliminating both bacterial pathogens and cancer cells. Subsequent research and clinical development are essential to comprehensively assess their potential benefits in patients.

II. Scope and objectives of the thesis

While *Pseudomonas aeruginosa* (*P. aeruginosa*) and HER2-positive breast cancer may seem like disparate diseases, they share a common and pressing challenge: the emergence of resistance to current treatments. Both *P. aeruginosa* and HER2-positive breast cancer cells have evolved sophisticated mechanisms to evade the immune system and resist conventional therapies, making them increasingly difficult to eradicate. *P. aeruginosa* has become resistant to multiple antibiotics, while HER2-positive breast cancer cells benefiting from potent therapeutic antibodies, often develop resistance to targeted therapies. This growing resistance has limited the effectiveness of standard treatments and increased the need for innovative approaches. Complement activating Multimeric compleXes (CoMiX), were engineered using the C4BP scaffold to offer a promising therapeutic approach for both diseases.

PART 1: Design and development of Complement activating Multimeric compleXes (CoMiX)

The multivalent proteins CoMiX combine specific targeting functions with effector mechanisms, selectively activating the complement system against target cells without causing excessive collateral damage. The C4BP scaffold provides a versatile platform for engineering CoMiX, allowing for the attachment of various functional components, including targeting domains that recognize specific antigens and effector functions that mediate therapeutic effects. The oligomerization strategy differed between the two types of diseases. For HER2-positive breast cancer, the C4BPα chain's oligomerization domain was used to form hexa- and heptamers whereas the C4BPβ chain was utilized to create dimers for *P. aeruginosa*.

CoMiX leverage the C4BP scaffold to link targeting domains such as single-chain variable fragments (scFv-s) for *P. aeruginosa* and variable heavy chains (VHHs) for breast cancer with effector functions (Fc region, FHR1 or FHR4). The specific targeting domains and effector functions differ between the two types of molecules to bind and kill the two different targets CoMiX molecules targeting *P. aeruginosa* utilize scFv-s derived from Panobacumab or MEDI3902 to recognize the Psl exopolysaccharide whereas CoMiX targeting breast cancer employ VHHs derived from trastuzumab or pertuzumab to recognize the HER2 tumor-associated antigen. Additionally, the effector functions binding to Factor H and linked to the C4BP scaffold vary: *P. aeruginosa*-targeting molecules utilize Factor H Related-protein 1 (FHR1), while HER2-

targeting molecules employ FHR4. In both cases, Fc-based CoMiX molecules were developed including one Fc dimer to kill *P. aeruginosa* and triple Fc dimers to kill of HER2-breast cancer.

PART 2: In vitro evaluation of CoMiX for *P. aeruginosa* and HER2-positive breast cancer

The in vitro studies conducted in these two investigations aimed to evaluate the efficacy, the mechanisms of actions and the safety of CoMiX against *P. aeruginosa* and HER2-positive breast cancer. The primary objectives of these studies were to:

1. Assess the complement-activating properties of CoMiX molecules: Both studies examined the ability of CoMiX to initiate the classical and alternative complement pathways, leading to the opsonization and lysis of target cells.
2. Investigate the synergistic effects of CoMiX with or as compared to existing therapies: The study on *P. aeruginosa* evaluated the combination of CoMiX with the antibiotic amikacin, while the breast cancer study explored the combination of the different CoMiX.
3. Assess the potential of CoMiX to kill multidrug-resistant strains of *P. aeruginosa* and a breast cancer cell line resistant to trastuzumab
4. Evaluate the safety of CoMiX in bronchial epithelium.

PART 3: In vivo efficacy and safety of CoMiX for *P. aeruginosa* and HER2-positive breast cancer

In vivo studies were conducted in mice to assess the therapeutic efficacy of CoMiX molecules against the two diseases. The primary objectives of these studies were to:

1. Evaluate the efficacy of CoMiX in vivo: The studies aimed to determine the therapeutic efficacy of CoMiX in animal models of acute pneumonia and tumor xenografts.
2. Assess the impact of CoMiX on disease progression: The studies sought to measure the effect of CoMiX on key disease parameters, such as survival rates, bacterial burden, and tumor growth.
3. Investigate the mechanisms of action of CoMiX in vivo: The studies aimed to elucidate the biological pathways through which CoMiX exert their therapeutic effects.
4. Evaluate the safety and tolerability of CoMiX in vivo: the studies assessed the potential side effects and toxicity of CoMiX in mice.

Overall, the aim of the study was to describe a novel targeted therapeutic approach harnessing the complement for combating both *P. aeruginosa* infections and HER2-positive breast cancer, two major challenges in modern medicine.

249

III. Synopsis

A. Introduction

1. Innate immunity in infection and cancer

The innate immune system offers a quick and wide-ranging response to pathogens, acting as the body's primary defense[1]. This system comprises various components of cellular and non-cellular components (skin, mucous membranes, complement proteins). These elements act as environmental sensors, swiftly responding to pathogens and initiating inflammation.

Unlike the adaptive immune system, acquired through exposure to pathogens, innate immunity is a pre-existing, genetically determined defense mechanism. It relies on genetically conserved specific receptors (PRRs)[2] to detect pathogen-associated molecular patterns (PAMPs). Toll-like[3], NOD-like[4], and RIG-like[5] receptors, as well as C-type lectins[6] and complement proteins, can detect a variety of pathogen components, including lipopolysaccharides, flagella, peptidoglycans, and viral nucleic acids. Upon PAMP recognition, innate immune cells are activated to release pro-inflammatory cytokines and chemokines[7]. This inflammatory response not only mobilizes additional immune cells to the infection site, increases vascular permeability, but also facilitates immune cell infiltration.

Despite limited specificity, the hallmark of innate immunity remains in a rapid and broad response to pathogens. Innate immunity is essential for controlling initial infection and creating an optimal environment for the subsequent adaptive immune response to achieve long-term immunological memory characteristics.

Beyond pathogen defense, innate immunity plays an important role in cancer immunosurveillance. Natural killer (NK) cells patrol the body for abnormal cells and destroy those with diminished or missing Major Histocompatibility Complex class I (MHC-I) expression[8]. Additionally, innate immune cells contribute to anti-tumor immunity by inducing inflammation and promoting tissue remodelling, which can suppress tumor growth. Upon encountering precancerous lesions or developing tumors, innate immune cells induce inflammation that can cause collateral damage to healthy tissues, but also serves the important function of recruiting other immune cells to the site, isolating the tumor, and promoting tissue remodelling[9]. This remodelling process can eliminate precancerous cells or create a microenvironment less hospitable for tumor growth.

However, pathogens and tumor cells exhibit remarkable immune-evasive capabilities[10, 11]. These evasive tactics often involve masking or altering surface molecules to evade recognition, producing proteins and immunosuppressive molecules that interfere with immune signalling pathways, or mimicking host molecules to blend in and avoid detection. Certain pathogens can evade extracellular immune surveillance by establishing an intracellular niche within host cells[12]. Cancer cells can suppress innate immune responses by reducing the expression of molecules that NK cells recognize or by releasing immunosuppressive substances.[13].

Ultimately, several regulatory mechanisms between innate immunity and pathogens or malignant cells can be used to generate novel immunotherapeutic approaches, especially by activating the complement.

2. The complement system

Complement is an essential element of the body's innate immune defenses, acting as a primary defense against pathogens and abnormal host cells. Consisting of over 40 proteins, complement proteins are primarily produced by the liver and can be found circulateing in the blood plasma, on cell surfaces and even intracellularly[14]. The complement system acts as a cascade, with proteins activating each other in a carefully ordered sequence. Beyond directly eliminating microbes, complement acts as a coordinator of the immune response, initiating a complex cascade of stimulations. This includes mediating inflammation, a crucial process for attracting immune cells to the infected area and facilitating efficient immune surveillance. The system also promotes the opsonization and clearance of cellular debris after apoptosis or necrosis as well as the removal of immune complexes, a crucial step in preventing the development of autoimmune reactions[15].

2.1. Complement activation

Complement activation is a sequential process initiated through the generation of active enzymes from their inactive precursor forms. This cascade-like mechanism ensures rapid and localized responses. Three pathways can trigger activation: the classical (CP), the lectin (LP), and the alternative pathway (AP) visualized on **Figure 1**.

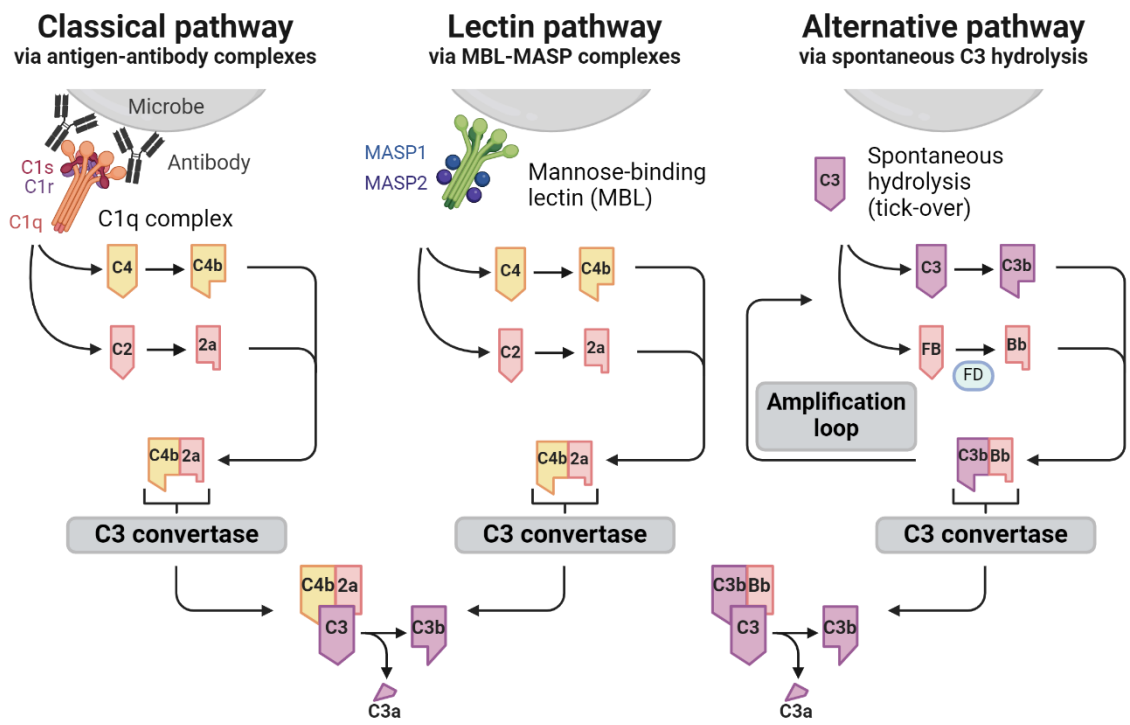

Figure 1: Schematic visualization of the complement cascade, depicting its three primary activation pathways. The CP is initiated by C1q binding to its ligands, while the lectin pathway begins with MBL or ficolins binding to activating surfaces. Conversely, the alternative pathway is always active through C3 hydrolysis to C3(H2O). All pathways meet at the C3 convertase that converts C3 into C3a and C3b. C3b functions as an opsonin, while C3a is a potent anaphylatoxin released into the circulation.

2.1.1. Classical pathway

The classical pathway (CP) was first described in the late 19th century. It was originally termed "classical" because it was believed to be activated solely by IgM or IgG antibodies bound to pathogens[16]. CP is activated through the recognition of specific ligands by the C1 complex[17]. This large, multi-component protein complex is composed of the ligand-binding protein C1q and a heterotetramer of Ca^{2+}-dependent serine proteases (C1r2s2). Primarily, C1q binds to the Fc region of immune complexes, particularly IgM or IgG monomers organized in specific hexameric structures. However, C1q's ligand repertoire extends beyond immunoglobulins, encompassing various PAMPs, including lipid A[18] and bacterial porins[19], as well as host-derived molecules such as C-reactive protein[20, 21] (CRP) or pentraxins[22]. This broad recognition capacity allows the CP to differentiate between pathogen surfaces, apoptotic cells, and healthy host cells.

Upon ligand binding, C1q triggers the activation of C1r followed by C1s. This active complex mediates the proteolysis of C2 and C4 into smaller (C2a, C4a) and bigger (C2b and C4b) fragments. These fragments assemble the CP C3 convertase (C4b2a), gaining the ability to cleave C3.

2.1.2. Lectin pathway

The lectin pathway (LP) operates similarly to the CP but is initiated by recognizing carbohydrate structures on the surfaces of microorganisms through mannose-binding lectin (MBL) or ficolins[23]. These detect carbohydrate moieties, including mannose, glucose, and N-acetyl glucosamine, are typically absent or rare on host cell surfaces.

Like C1q, these recognition-receptors are associated with enzymes (MASP: MBL-associated serine proteases[24]), which are homologous to C1r and C1s in structure as well as in function.

2.1.3. Alternative pathway

At the initial step of the alternative pathway (AP), C3 spontaneously undergoes hydrolysis to form C3(H2O), a process known as tick-over[25]. This initiates a cascade involving the Mg^{2+}-dependent factor B (FB) binding to C3(H_2O), followed by its Factor D (FD)-mediated cleavage. C3(H_2O)Bb, the initial AP C3 convertase, is unstable but can generate small amounts of C3b. Amplification occurs as C3b binds more FB, producing the more stable C3bBb convertase, stabilized by properdin. This convertase efficiently cleaves C3 into C3a, a potent anaphylatoxin, and C3b, an opsonin, further amplifying the pathway[26]. Importantly, unlike the other pathways, AP activation is not triggered by specific ligand recognition but rather by the intrinsic instability of C3. While serum inhibitors normally control this low-grade activation, surfaces lacking these inhibitors, such as pathogens, allow uncontrolled C3b deposition and subsequent AP amplification.

2.1.4. Opsonization and terminal pathway activation

The three pathways meet at the cleavage of C3 (**Figure 2**). Regardless of the initiating pathway, generated C3b molecules function as opsonins, enhancing phagocytosis and propagating the complement cascade. Additionally, C3b can associate with these convertases to form C3bC2aC3b or C3bBbC3b with altered substrate specificity for C5 (C5 convertases).

Proteolysis of C5 yields the potent anaphylatoxin C5a and C5b, the first component of the membrane attack complex (MAC)[27]. Subsequent binding of C6, C7, and C8 to C5b forms a pre-pore structure that inserts into the target cell membrane. Polymerization of C9 molecules into this structure creates a

transmembrane channel approximately 10 nm in diameter, resulting in osmotic lysis of susceptible cells[28]. The amplification inherent to the complement system ensures that over 80% of terminal complement activity is derived from this pathway. While the formation of C5b-9 complexes is robust, nucleated cells possess mechanisms to rapidly eliminate membrane-inserted MACs through endocytosis or membrane shedding, thereby evading complement-mediated lysis[29].

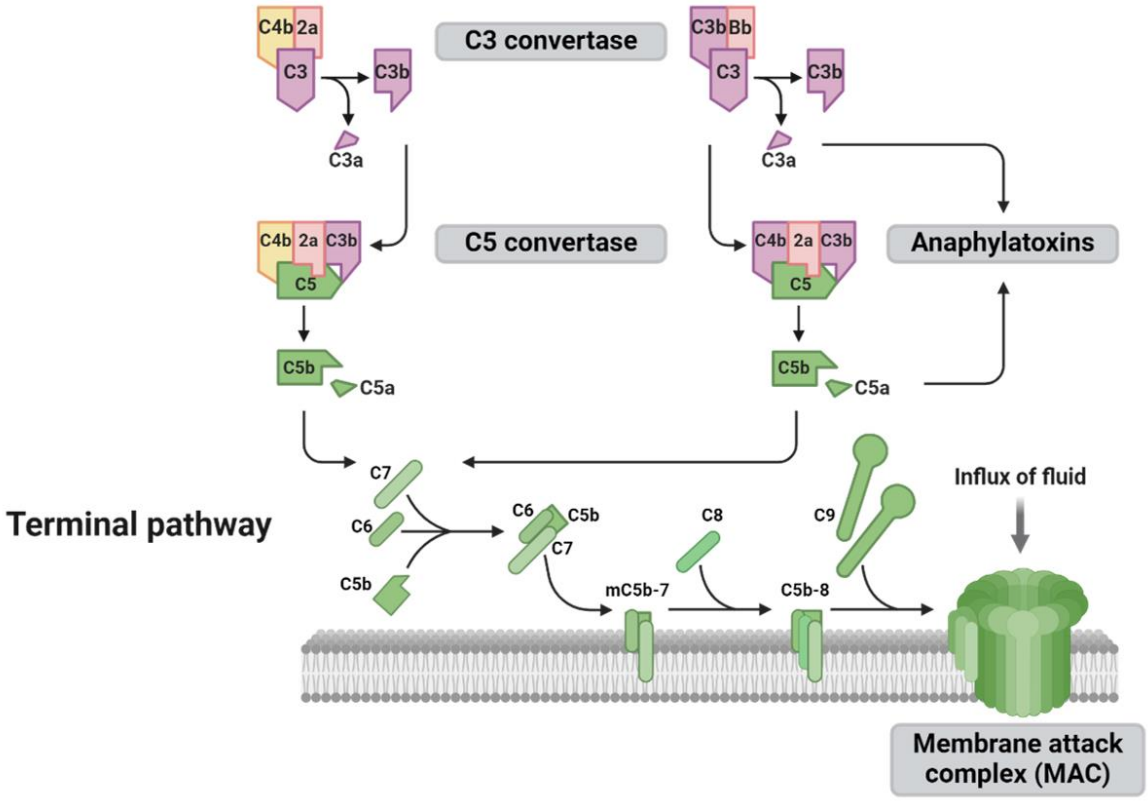

Figure 2: C5-convertase formation and terminal pathway. Cleavage of more C3 molecules by the C3 convertases facilitates the formation of new C3 convertases and C5 convertases with changed substrate specificity. Subsequent cleavage of C5 by C3bC2aC3b or C3bBbC3b produces C5a and C5b, resulting in the initiation of MAC assembly, leading to osmotic cell lysis.

2.2. Complement-mediated immune defenses

2.2.1. Clearance of cellular debris: a silent guardian

Complement proteins play a critical role in the efficient and regulated clearance of apoptotic cells, a process essential for maintaining tissue homeostasis[30]. During apoptosis, cells undergo structural and molecular changes, including the exposure of "eat-me" signals on their surface[31]. While C1q, along with

MBL and ficolins, can recognize and bind to these apoptotic cell surface changes, this binding alone is insufficient for silent removal. C1q's role is primarily to initiate the classical complement pathway. The key is that complement activation, regulated by complement control proteins, is required. This activation leads to opsonization of the apoptotic cell with C3 fragments, which are then recognized by phagocytic cells, promoting engulfment and silent removal. Critically, complement regulatory proteins tightly control this process, preventing inappropriate complement activation on healthy cells and ensuring that only apoptotic (or necrotic) cells are targeted, thus avoiding excessive inflammation and damage to self-tissues. This regulated cascade, not simply C1q binding, differentiates between apoptotic and necrotic cells and facilitates their efficient clearance.

2.2.2. Pathogen elimination through opsonization and anaphylatoxin-driven inflammation

The coating of microbial surfaces with complement proteins, particularly C3b and iC3b, makes them highly susceptible to phagocytosis. Phagocytes express a variety of complement receptors (CRs)[32] that recognize different C3 fragments, leading to pathogen internalization and destruction (**Figure 3**)[33].

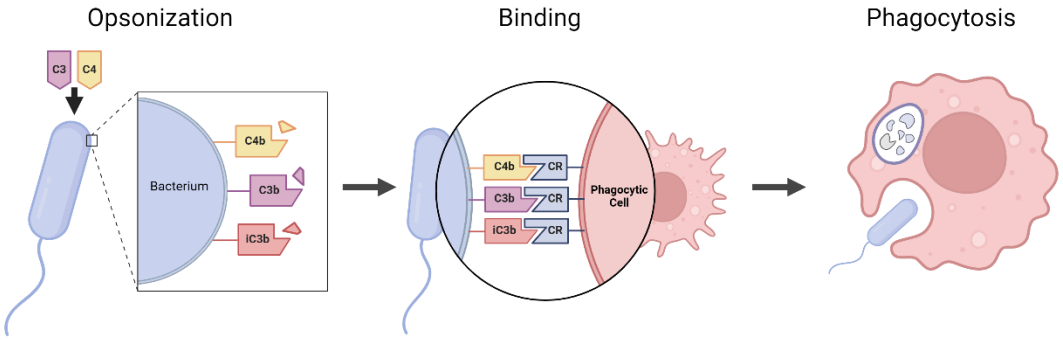

Figure 3: Opsonization and phagocytosis of microbes. This figure illustrates the process of opsonization by C3b, iC3b and C4b, binding to complement receptors and subsequent phagocytosis of microbes by immune cells.

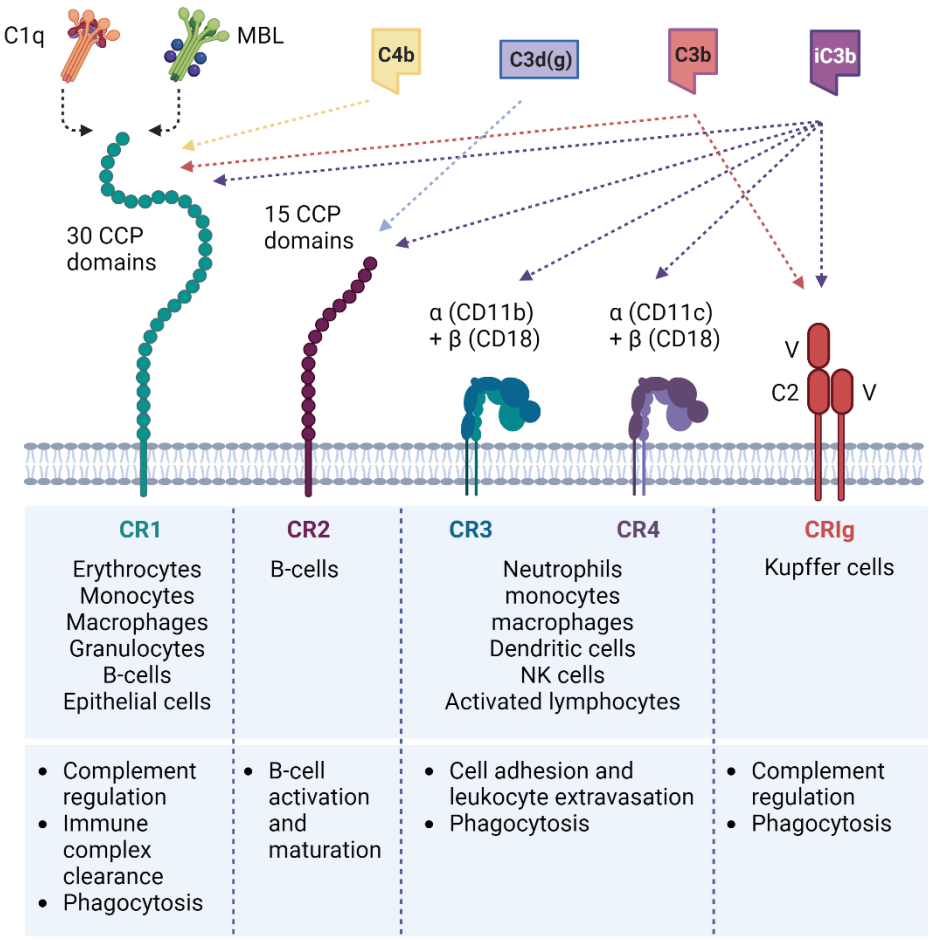

Figure 4: Complement receptors and their ligands. This figure provides an overview of complement receptors (CRs) and their ligands, as well as the cell types that express these receptors.

CR1, prevalent on both immune and other cells, binds to C3b and C4b. While it can inhibit complement activation, its primary role is to enhance phagocytosis by interacting with Fcγ receptors. Erythrocytes express CR1, allowing them to transport immune complexes to the spleen and liver for clearance[34]. CR2, primarily found on B cells, forms a complex with CD19 and CD81, acting as a co-receptor that recognizes iC3b and C3d. This interaction is crucial for B cell activation, as C3d acts as an adjuvant, significantly lowering the activation threshold[35].

CR3 and CR4, expressed on myeloid cells, are integrins that recognize iC3b and C3c, respectively[36]. These receptors have an important function in phagocytosis, immune complex clearance, and inflammation. Their expression and affinity are regulated by cellular activation, ensuring efficient pathogen uptake. CRIg, mainly expressed Kupffer cells, binds to C3b and iC3b, facilitating phagocytosis and complement

inhibition[37]. By directly interacting with C3b, CRIg prevents the formation of complement convertases, limiting excessive inflammation.

In addition to facilitating phagocytosis, complement activation generates potent inflammatory mediators known as anaphylatoxins[38]. These small peptides, primarily C3a and C5a, are cleaved from their respective complement proteins during the activation cascade. While C4a also shares some anaphylatoxin properties, its effects are less pronounced due to the absence of a dedicated receptor[39].

C3a and C5a mediate their functions through distinct transmembrane receptors (**Figure 5**). C3a selectively interacts with the C3a receptor (C3aR), while C5a binds to C5aR1 and C5L2 (C5aR2)[40]. The C3aR is a classic G protein-coupled receptor (GPCR) that signals through both Gi and Gq proteins, resulting in β-arrestin recruitment when activated. In contrast, C5aR1 signals through both Gi and β-arrestin pathways, whereas C5aR2 primarily utilizes β-arrestin-mediated signalling, hence its classification as an arrestin-coupled receptor (ACR)[41]. Upon receptor binding, anaphylatoxins induce intracellular signalling cascades that result in vasodilation, vascular permeability, and chemotaxis of inflammatory cells. Notably, C5a is a particularly strong chemoattractant for neutrophils and mast cells, amplifying the immune response[42]. To prevent excessive inflammation and tissue damage, anaphylatoxins are rapidly inactivated by carboxypeptidase N[43].

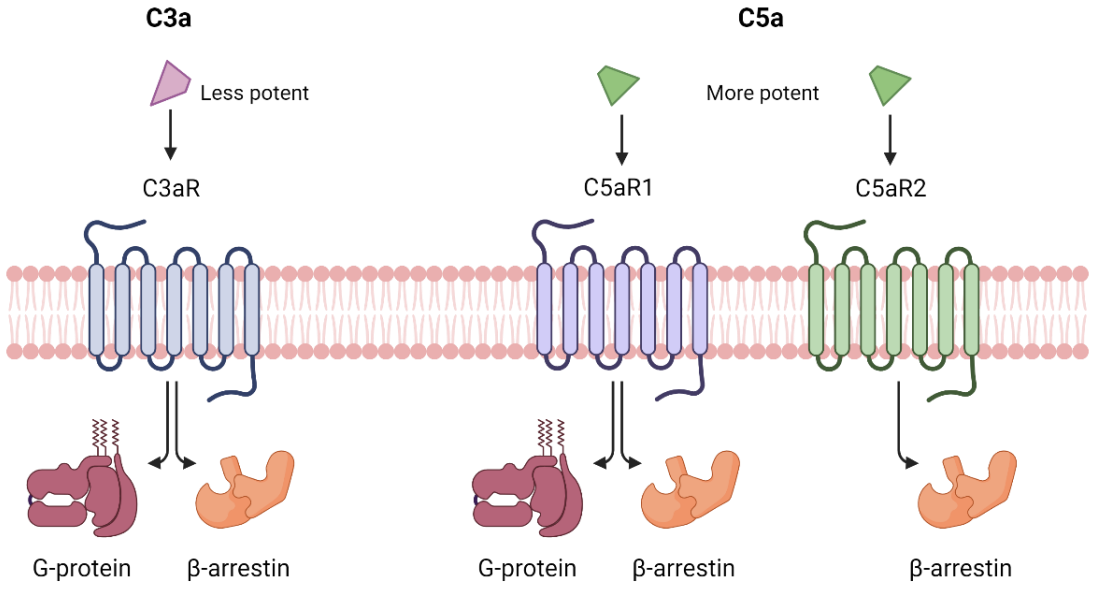

Figure 5 : Schematic representation of C3a and C5a receptors and signalling. C3aR and C5aR1 are GPCRs that signal via Gi and Gq. C5L2 is primarily an ACR signalling through β-arrestin. Receptor activation initiates intracellular cascades, leading to vasodilation, increased permeability, and inflammatory cell chemotaxis.

C3a and C5a also trigger mast cell activation, leading to histamine release and other inflammatory responses, and can induce smooth muscle contraction[44]. Beyond their role in inflammation, they contribute to immune regulation, and tissue repair, and are implicated in various pathologies, including autoimmune disorders[45], allergies[46], neurodegenerative conditions[47], and cancer[48].

Anaphylatoxins further contribute to the immune response by connecting innate and adaptive immune functions. C3a and C5a stimulate dendritic cell maturation into antigen-presenting cells (APCs) by upregulating MHC-II and CD86 molecules via their corresponding receptors[49]. Furthermore, recent findings indicate that intracellular cleavage of C3 and C5 into C3a and C5a can significantly influence cellular metabolism, homeostasis, and the dynamics of T-cell responses[50].

2.3. Modulating complement activation: regulatory proteins

The complement system requires precise regulation due to its rapid and diverse effector functions. Dysregulation of complement activation has been implicated in various diseases, including autoimmune diseases, inflammatory disorders, and reperfusion injury[51]. To prevent systemic damage while ensuring efficient local activity, a diverse array of soluble and membrane-associated regulatory proteins maintains complement homeostasis (**Figure 6**). These proteins fine-tune complement activation on appropriate targets, preventing collateral destruction to the host.

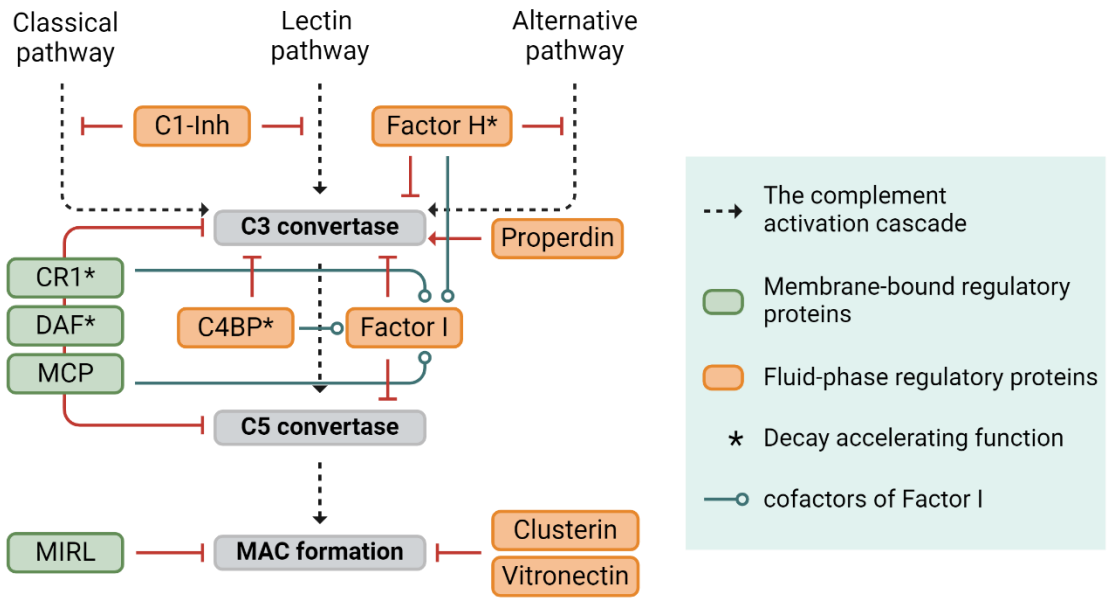

Figure 6: Mechanism of action of complement regulatory proteins. Membrane-bound and fluid-phase regulatory proteins modulate the complement cascade at multiple stages. C1-Inh suppresses initiation, while FH, C4BP, CR1,

DAF, MCP, and Factor I (FI) target the C3/C5 convertase. CR1, DAF, C4BP, and FI exhibit decay-accelerating functions, whereas CR1, MCP, FH, and C4BP possess cofactor activity. MIRL, clusterin, and vitronectin act at the terminal phase of the cascade.

2.3.1. Membrane-bound regulatory protein

Membrane-bound complement regulatory proteins (mCRPs) are essential for shielding host cells and tissues from excessive complement activation[52]. Four mCRPs have been identified: complement receptor 1 (CR1), membrane cofactor protein (MCP), decay accelerating factor (DAF), and membrane inhibitor of reactive lysis (MIRL), also known as protectin. Complement regulatory proteins are expressed on most cells but with varying levels across different tissues, likely reflecting tissue-specific immune interactions. These proteins can be divided into two groups. The first group of complement inhibitors targets C3b and C4b. These proteins, including CR1, MCP, and DAF have a role in preventing the formation or facilitating the decay convertases. The second group consists solely of MIRL, which prevents MAC formation.

CR1 is widely present on various cell types, including erythrocytes, leukocytes, and epithelial cells. It is a critical component of the complement regulatory system, possessing both cofactor and decay-accelerating activities. As a cofactor for FI, CR1 facilitates the cleavage and inactivation of C3b and C4b, preventing amplification. Additionally, CR1 exhibits decay-accelerating activity[53], disrupting the formation of the convertases. Beyond its regulatory functions, CR1 has a pivotal role in immune complex clearance, phagocytosis, and B cell activation[54], highlighting its complex involvement in immune responses.

MCP is found on all cells except erythrocytes. It comprises four complement control protein (CCP) domains and exists as four isoforms generated by alternative splicing[55]. MCP regulates all three complement pathways by being a cofactor for FI, facilitating the inactivation of C3b and C4b.

DAF, a GPI-anchored glycoprotein, shares a similar expression pattern with MCP. While it participates in regulating the CP and AP, DAF lacks cofactor activity for FI. Instead, as its name suggests, its primary function is to accelerate the decay of C3 and C5 convertases.

MIRL is also ubiquitously expressed. It functions as a terminal inhibitor of cell lysis by disrupting the formation of MAC. MIRL binds to the C8 component of the developing MAC, obstructing the recruitment of additional C9 molecules and consequently inhibiting pore formation[56].

2.3.2. Fluid-phase regulator proteins

Fluid-phase complement inhibitors differ from their membrane-bound counterparts in that they are not permanently anchored to the cell surface but are instead mobilized as needed. These proteins constitute a critical defense mechanism against uncontrolled complement activation. Circulating within the bloodstream, soluble complement regulatory proteins protect healthy tissues by blocking activation at various stages of the complement cascade.

One key inhibitor, C1 inhibitor (C1-INH), regulates both CP and LP[57]. Its C-terminal domain, homologous to other serpins, is responsible for the inhibitory function. In contrast, the heavily glycosylated N-terminal domain lacks homology to other serpins and does not contribute to protease inhibition. C1-INH exerts its inhibitory action by binding to and inactivating C1r, C1s, MASP1, and MASP-2[58].

Another crucial inhibitor, C4b binding protein (C4BP), also regulates the CP and LP[59]. Composed of multiple (tipically six-seven) α-chains and a single β-chain, C4BP exhibits a distinctive spider-like structure. The α-chains have eight CCP domains, with the initial three CCPs responsible for C4b binding[60]. While all α-chains possess C4b binding capacity, steric hindrance limits simultaneous binding to four C4b molecules. C4BP functions by accelerating the degradation of C4b through its cofactor activity for FI, thereby preventing the generation of convertases.

Factor H (FH) and its shorter counterpart, Factor H-like protein 1 (FHL-1), are the most important regulators of the AP and the amplification loop[61]. Primarily produced in the liver, FH is also locally synthesised in various tissues. As a large glycoprotein built of 20 CCP domains, FH interacts with multiple ligands, including C3b, glycosaminoglycans (GAGs), and inflammatory and cell signalling molecules through these domains[62]. In contrast, FHL-1 comprises seven CCP domains of FH with a distinct C-terminus. Both FH and FHL-1 function as fluid-phase regulators, preventing uncontrolled complement activation by inhibiting C3 convertase formation, accelerating its decay, and serving as cofactors for FI-mediated C3b inactivation. These regulatory activities primarily localize to the first four CCP domains. As a soluble inhibitor, FH competes with FB for C3b binding, hindering C3 convertase formation. While primarily a fluid-phase regulator, FH also binds to host cell membranes, protecting them from complement-mediated damage[14].

Factor I (FI) is a 66 kDa serine protease essential for regulating complement activation by cleaving C3b and C4b[63]. It specifically targets arginyl peptide bonds within these complement components, preventing convertase formation. Notably, FI requires cofactors such as FH, C4BP, MCP, and CR1 to exert its

proteolytic activity. Although circulating as an inactive form, FI becomes enzymatically active upon binding to both its substrate and a cofactor. Interestingly, thrombomodulin[64] and von Willebrand factor[65] can enhance FI activity in the presence of cofactors. Despite its importance, the precise mechanisms underlying FI regulation and its interactions with various cofactors remain areas of ongoing research.

Beyond the control mechanisms governing the formation of convertases, the assembly of the MAC is also strictly regulated. Two key soluble complement inhibitors, clusterin and vitronectin, play crucial roles in this process[66]. Clusterin inhibits MAC formation at multiple steps. It binds to C7, preventing its insertion into the membrane, and can also interact with C8β and C9, blocking the assembly of the terminal lytic complex[67]. Vitronectin, a multifunctional glycoprotein, also functions as a MAC inhibitor, by blocking its insertion into the target membrane. Additionally, vitronectin's heparin-binding domain binds to C5b-9, inhibiting C9 polymerization[68].

While the cascade is strictly controlled by inhibitory proteins, positive regulators are essential for effective immune responses. Properdin is a key example. The transient nature of the C3bBb complex necessitates stabilization for efficient complement activation[69]. Properdin fulfils this critical role by enhancing the C3bBb complex's stability five to tenfold. Produced by various immune cells, properdin exists as oligomers of varying sizes, with tetramers demonstrating superior stabilizing capabilities compared to dimers. Properdin binds to both the active C3bBb complex and its precursor, C3bB, as well as C3b independently. Upon binding to C3bBb, properdin induces conformational changes that interfere with FH binding, thereby protecting the complex from regulatory degradation[70]. This stabilization ensures a sustained amplification loop in the alternative complement pathway, promoting effective immune responses.

2.3.2.1. The Factor H protein family

The FH protein family is a group of serum glycoproteins encoded by a cluster of six genes on chromosome 1. Central to this family are FH and FHL-1, both products of the CFH gene. Additionally, five related proteins (CFHR1-5) are encoded by separate genes within this cluster (**Figure 7**)[71]. A common structural foundation of CCP domains form the basis of these proteins.

Figure 7: Gene organization of the FH protein family. FH and FHL-1 are both products of the CFH gene.

While FH is well-recognized for its role in complement inhibition, the functions of the Factor H-related proteins (FHRs) remain less clear and controversial[72]. Despite initial suggestions of an inhibitory role in complement activation, emerging evidence points to an involvement in complement activation[73, 74, 75, 76, 77].

Structurally, FHRs share significant homology with FH (**Figure 8**). Their N-terminal regions exhibit high sequence similarity, aligning with CCP domains 6-8 of FH, while the C-terminal regions show 37-100% similarity, corresponding to CCPs 19-20[78]. FHR-5 is distinct, displaying homology to a wider range of FH CCPs. These structural similarities enable FHRs to bind to ligands similar to FH, including heparin and complement activation fragments. However, lacking the essential complement regulatory domains present in FH, FHRs cannot inhibit complement activation. This suggests a potential competitive mechanism where FHRs might interfere with FH's complement inhibitory function by competing for ligand binding sites.

Certain FHR proteins can form dimeric structures. FHR-1, FHR-2, and FHR-5 can pair to create both identical (homodimeric) and mixed (heterodimeric) units[79]. While FHR-3 and FHR-4 typically exist as single molecules, FHR-1 can also combine with FHR-2. Although various dimeric configurations have been observed, recent research suggests a more limited range of these structures in circulation. Primarily, homodimers as well as FHR-1 and FHR-2 pairings predominate.

Their association with a variety of diseases emphasizes the clinical relevance of FHRs. Variations in FHR protein levels of CFHR genes have been linked to autoimmune conditions such as IgA nephropathy[80, 81, 82], age-related macular degeneration[83, 84, 85], and C3 glomerulopathy[86, 87, 88], as well as infectious diseases like invasive meningococcal disease[89] and atypical hemolytic uremic syndrome[90, 91, 92]. These findings suggest that FHR proteins offer potential for therapeutic and diagnostic applications.

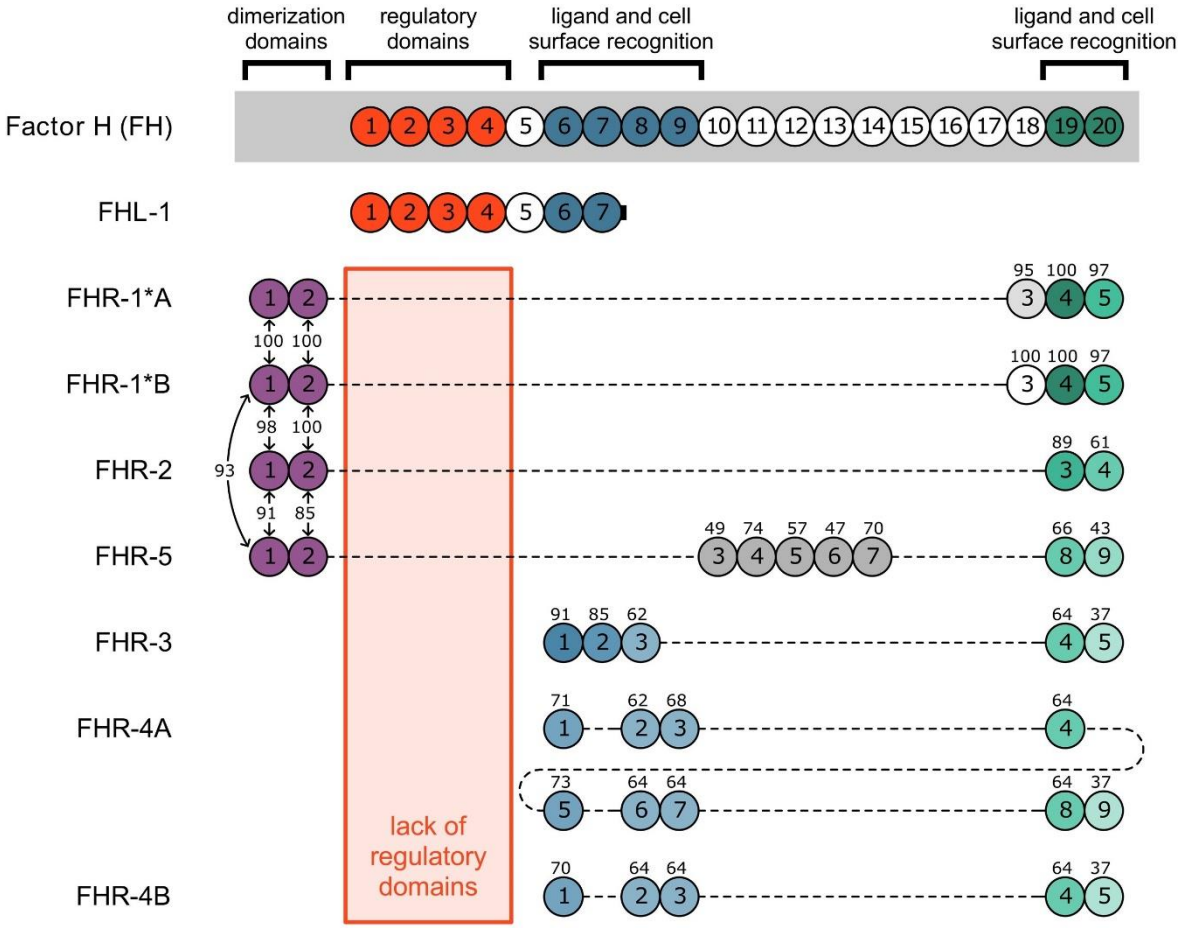

Figure 8: The human factor H protein family. Adapted from Cserhalmi et al. (2019).[78]

2.3.2.2. FHR1 and FHR4: Complex regulators of complement and inflammation

FHR-1 is a prominent glycoprotein within the factor H-related family, circulating in plasma at concentrations of 40-100 µg/mL. Its structure comprises five CCP domains, the latter three of which exhibit significant homology to CCP18-20 of FH[93]. Two glycoforms (FHR-1α, 37 kDa; FHR-1β, 41 kDa)[94] and two isoforms (FHR-1A, acidic; FHR-1B, basic) arise from differential glycosylation and amino acid sequence variations. The acidic isoform (H36.1 cDNA) and basic isoform (H36.2 cDNA) differ in CCP3 residues. Both isoforms share two amino acid substitutions in CCP5 compared to FH but vary in N-glycosylation sites (one in FHR-1A, two in FHR-1B). The functional impact of glycosylation on FHR-1 remains unclear[95].

FHR-1's C-terminal CCPs mimic FH's host-recognition and C3b-binding domains (**Figure 9**). Unlike FH, FHR-1 lacks cofactor and decay-accelerating activities. While initially proposed as a C5 convertase and membrane attack complex inhibitor[96], recent evidence suggests the opposite effect.

Like FH, FHR-1 binds heparin, endothelial cells, CRP and pentraxin 3 (PTX3)[97, 98]. It competes with FH for C3b[99], potentially reducing complement inhibition, especially the FHR-1B isoform due to greater FH homology. While the competitive interaction is established, the precise mechanisms of FHR-1-mediated complement deregulation in diseases like C3 glomerulopathy (linked to FHR-1 gene amplification) remain unclear[100]. Excess FHR-1 might displace FH from C3b, causing uncontrolled complement activation and tissue damage.

Beyond complement, FHR-1 emerges as a key player in inflammatory responses[101]. Unlike its role in complement regulation, FHR-1 acts as a potent inducer of inflammation when bound to oxidized lipid surfaces, characteristic of necrotic cells. Elevated FHR-1 levels are observed in various inflammatory diseases, including vasculitis, IgA nephropathy, and acute cellular rejection, correlating with disease severity. The ability of FHR-1 to distinguish between healthy and necrotic surfaces is crucial for understanding its dual function in both complement regulation and inflammation.

FHR-1's dual roles in complement regulation and inflammation highlight its complex involvement in immune responses.

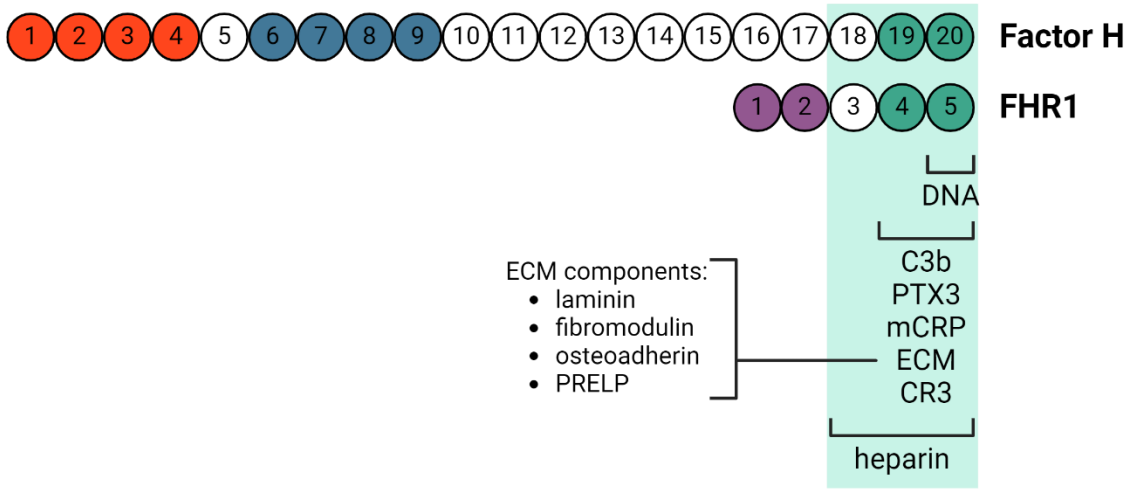

Figure 9: Common ligands of FH and FHR1. FH and FHR1 both interact with numerous different molecules, including C3b, PTX3, mCRP, extracellular matrix (ECM) components (laminin, fibromodulin, osteoadherin, PRELP), CR3, DNA and heparin.

FHR4, another factor H-related protein, also has an important role in modulating complement activation[102]. Uniquely among the FHRs, the FHR4 gene encodes two splice variants, FHR4A and FHR4B,

each with distinct structural features. FHR4A (86 kDa), composed of nine CCP domains, exhibits an internal duplication. In contrast, FHR4B (43 kDa) consists of only five CCP domains.

Unlike the inhibitory function of FH, FHR4 enhances complement activation. Hebecker et al. (2012) found that FHR4 facilitates the assembly of an AP C3 convertase by binding C3b[103]. The C3b bound to FHR4 has a prolonged capacity to bind FB and properdin, therefore to lyse more C3. Furthermore, mutations in the C-terminal domains of FHR4 significantly reduced C3b binding and AP activation. FHR4B demonstrated binding to both C3b and C3d when immobilized on microtiter plates. FHR4A, however, exhibited a broader binding capacity, binding to iC3b as well but not C3c. FHR4A exhibited a stronger affinity for C3b compared to FHR4B, approaching the binding strength of FH.

Mihlan et al. (2009) identified another role for FHR4 in the complement system[104]. They demonstrated that FHR4 binds to C-reactive protein (CRP) via its first domain, leading to CP activation. This interaction is enhanced by the pentameric form of CRP and suggests a role for FHR4 in the opsonization of necrotic cells. Hebecker et al. (2010) expanded on this finding, demonstrating that FHR4 can independently activate complement via the CP, without the involvement of FH[105]. Mutations in the CCP1 domain of FHR4 resulted in reduced CRP binding and subsequent complement activation. Unlike FH, which predominantly binds to the monomeric form of CRP, FHR4 exhibits a preference for the native pentameric form.

The potential therapeutic implications of FHR4 are significant. Our research group has previously developed heteromultimeric immunoconjugates incorporating FHR4 to selectively target and activate complement on tumor cells[106]. These multimeric proteins have shown promising results in preclinical studies, suggesting their potential as novel therapeutic agents.

2.4. Microbial escape: complement evasion tactics

Complement evasion is a critical survival strategy employed by many microorganisms, including viruses, bacteria, fungi, and parasites. To counteract the host's immune response, these pathogens have evolved sophisticated strategies to circumvent host complement attack. These strategies encompass a range of tactics; from hijacking host complement regulators to degrading complement components or establishing physical barriers that impede complement attack. By successfully evading complement, these microorganisms can establish and propagate infections within the host.

2.4.1. Viruses

Viruses have developed diverse strategies to evade complement-mediated elimination[107]. Many viruses bind host complement inhibitors to their surface, acting as decoys to inhibit complement activation. For example, dengue[108] and Zika[109] viruses, members of the *Flaviviridae* family, utilize this approach. Additionally, some viruses incorporate host regulatory proteins, like DAF and MIRL, into their envelopes, shielding themselves from complement attack. This is observed in enveloped viruses such as influenza[110] and the human immunodeficiency virus (HIV)[111]. SARS-CoV-2 exemplifies a distinct evasion strategy. The viral protein ORF8 mimics the human complement protein FI, enabling the virus to bypass complement activation[112]. This molecular mimicry effectively protects the virus from immune surveillance. Beyond these examples, some viruses directly inhibit complement activation. Herpes simplex virus (HSV) encodes a protein that cleaves complement components, preventing the formation of MAC[113]. Epstein-Barr virus (EBV) employs another tactic by using the gp350 glycoprotein to disrupt the immune response by interfering with the B cell-complement system interaction. It binds to CR2 on B cells, blocking C3d binding and preventing B cell activation[114].

2.4.2. Bacteria

Similar to viruses, bacteria have developed diverse tactics to avoid complement-mediated destruction. One common strategy is the recruitment of regulatory proteins to their cell surface. By binding and effectively utilizing host factors such as C4BP and FH (**Figure 10**), these pathogens can neutralize complement activation. For instance, *Streptococcus pneumoniae* cunningly employs PspA and PspC to interact with C4BP[115], while *Neisseria meningitidis* utilizes PorA for a similar purpose[116]. Similarly, a diverse range of pathogens, including *Borrelia burgdorferi*, *Neisseria meningitidis*, *Staphylococcus aureus*, and *Streptococcus pyogenes*, have evolved proteins capable of binding to FH, such as OspE[117], FHbp[118], SdrE[119], and M protein[120], respectively. These protein-protein interactions result in the disruption of the complement cascade, allowing these bacteria to successfully survive and proliferate within the host environment.

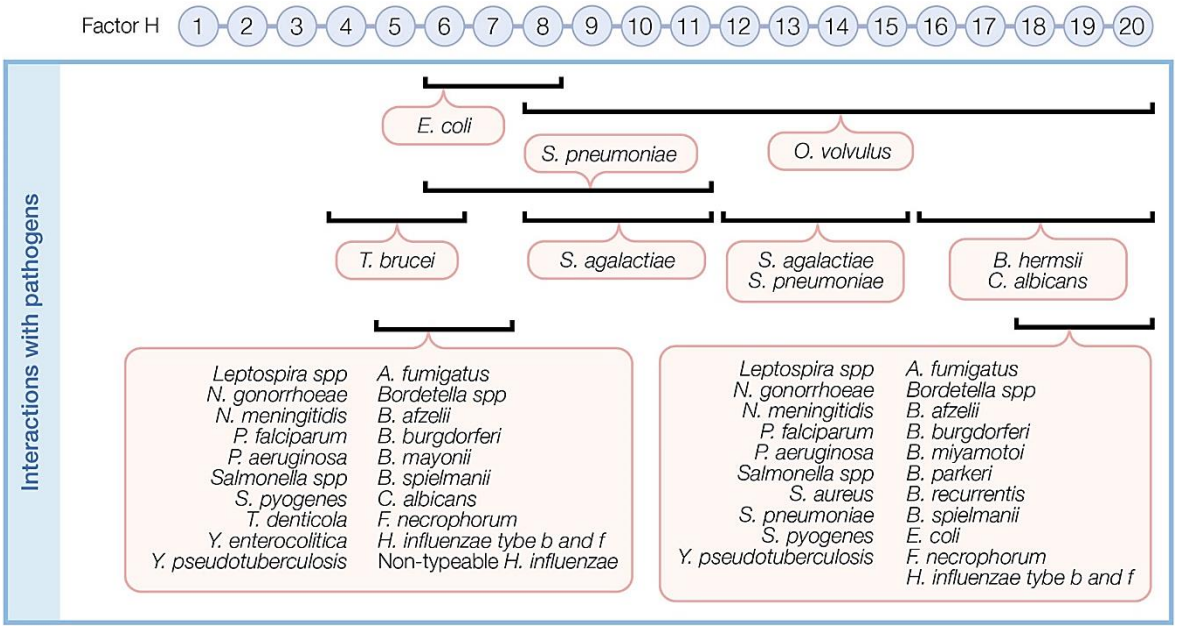

Figure 10: Pathogen-driven Factor H recruitment and complement evasion. Numerous human pathogens recruit FH, the most important complement regulatory protein of the AP. By binding to FH, these pathogens can successfully evade the complement system's destructive effects, promoting their survival and dissemination. The figure is adapted from Moore et al. (2021).[121]

Beyond the recruitment of complement regulatory proteins, bacteria have evolved other tactics to evade the host immune defenses. One such tactic entails the blocking of host antibodies. For example, *Staphylococcus aureus* produces enzymes like plasmin to degrade IgG, while its proteins A and G bind to the Fc region of IgG to prevent its essential effector functions[122]. Similarly, *Streptococcus pyogenes* utilizes PepO to hinder the binding of IgG to C1q, a pivotal step in classical pathway activation[123]. Some bacteria, such as *Salmonella typhi*, can conceal their surface antigens with a capsule (Vi antigen) to hinder antibody recognition[124]. Furthermore, certain pathogens, like *Streptococcus suis*, produce enzymes capable of inactivating IgA1 and IgM, effectively neutralizing these important antibody isotypes[125, 126, 127].

Another critical strategy employed by bacteria is the inhibition of C3 convertase, a key enzyme essential for complement activation. For instance, *Escherichia coli* lipopolysaccharide (LPS) prevents properdin binding, while *Streptococcus pyogenes* SpeB degrades both properdin and C3[128, 129]. Additionally, some bacteria, like *Staphylococcus aureus*, produce proteins such as SCIN[130] and Efb/Ecb[131, 132] that interfere with C3 convertase function. Other pathogens, including *Streptococcus agalactiae*[133] and *Borrelia burgdorferi*[134], have evolved proteins that effectively block C3 convertase assembly by preventing the interaction between C4b and C2.

Bacterial proteases represent another potent arsenal in the bacterial evasion of complement. These enzymes directly target and degrade essential complement components, disrupting the complement cascade at various critical stages. For instance, *Staphylococcus aureus* employs Aureolysin to cleave C3 into a non-functional form[135], while plasmin, produced by multiple bacteria including *Staphylococcus aureus*[136]*, Leptospira interrogans*[137], and *Streptococcus suis*[138], also degrades C3. Additionally, *Escherichia coli* EspP cleaves C3/C3b and C5[139], and *Tannerella forsythia* Mirolysin degrades multiple complement proteins, including ficolins, C4, and C5[140].

Bacteria have also developed strategies to inhibit the terminal steps of complement activation and subsequent host responses. One approach is to prevent the formation of MAC. For example, *Staphylococcus aureus* SSL-7 inhibits the interaction between C5 and the C5 convertase[141], while *Borrelia burgdorferi* SIC blocks the insertion of C5b-7 into the bacterial membrane[142]. In addition, several bacteria, including *Borrelia burgdorferi*[143] and *Helicobacter pylori*[144], express MIRL-like proteins that inhibit MAC formation. Beyond preventing direct killing by complement, bacteria have evolved mechanisms to counteract the host inflammatory response triggered by complement activation. *Staphylococcus aureus* CHIPS[145] and *Streptococcus pyogenes* GAPDH[146] inhibit neutrophil chemotaxis[147], while *Streptococcus pyogenes* ScpA cleaves C5a[148].

2.4.2.1. *Pseudomonas aeruginosa*

Pseudomonas aeruginosa (*P. aeruginosa*) is a versatile, Gram-negative bacterium renowned for its opportunistic nature. This microorganism thrives in diverse environments and poses a major threat to immunocompromised individuals. Demonstrating remarkable adaptability, *P. aeruginosa* can flourish in various conditions while evading the effects of antibiotics[149]. Moreover, its ability to form biofilms exacerbates treatment challenges[150], making it a primary cause of severe, often life-threatening infections such as pneumonia, skin infections, urinary tract infections, and bloodstream infections within healthcare settings.

2.4.2.1.1. Virulence factors

A variety of virulence factors contribute to the pathogenesis of *P. aeruginosa* by facilitating bacterial adherence, colonization, immune evasion, and immunosuppression (**Figure 11**)[151]. Type IV pili, filamentous structures on the bacterial surface, facilitate attachment to host cells, promote bacterial motility, and contribute to biofilm formation. Flagella, whip-like structures, facilitate swarming motility, biofilm formation, and bacterial adhesion, aiding in colonization and spreading within the host.

Additionally, the lipopolysaccharide (LPS) the outermost component of the outer membrane plays an important role in stimulating the host inflammatory response and providing resistance to serum killing and phagocytosis, allowing the bacterium to circumvent the host immune attack. *P. aeruginosa* also secretes a variety of factors that contribute to its virulence. Exopolysaccharides, including alginate, Pel, and Psl, have a role in biofilm formation, immune evasion, and bacterial adhesion[152, 153]. Siderophores, including pyoverdine and pyochelin, are secreted to chelate iron, a vital nutrient for bacterial growth[154]. Proteases, such as alkaline protease, elastase A and B, and protease IV, are secreted by *P. aeruginosa*[155, 156]. These enzymes degrade host proteins, resulting in tissue damage and interfering with the host immune response. Various toxins are also secreted by *P. aeruginosa*. Type 3 secretion system (T3SS) effectors, including ExoS, ExoT, ExoU, and ExoY, disrupt host cell functions, leading to cell death and tissue damage[157, 158]. Other toxins, such as exolysin[159] (a pore-forming toxin), exotoxin A[160] (which inhibits protein synthesis), and leukocidin[161](which impairs host immune functions), also enhance to the pathogenicity of *P. aeruginosa*. Additionally, lipase A[162], phospholipase C[163], and lipoxygenase[164] are secreted to damage host tissues, disrupt host signalling pathways, and control the bacterial invasion process.

In addition to these individual virulence factors, *P. aeruginosa* utilizes quorum sensing, a mechanism for cell-to-cell communication, to synchronise its behaviour and increase its virulence[165]. This allows *P. aeruginosa* to sense the population density of neighbouring bacteria and regulate the production of virulence factors accordingly. Quorum sensing (QS) plays a crucial role in coordinating the production of biofilm-related factors, swarming and twitching motilities. By responding to environmental cues and the presence of other bacteria, *P. aeruginosa* can optimize its survival and virulence strategies.

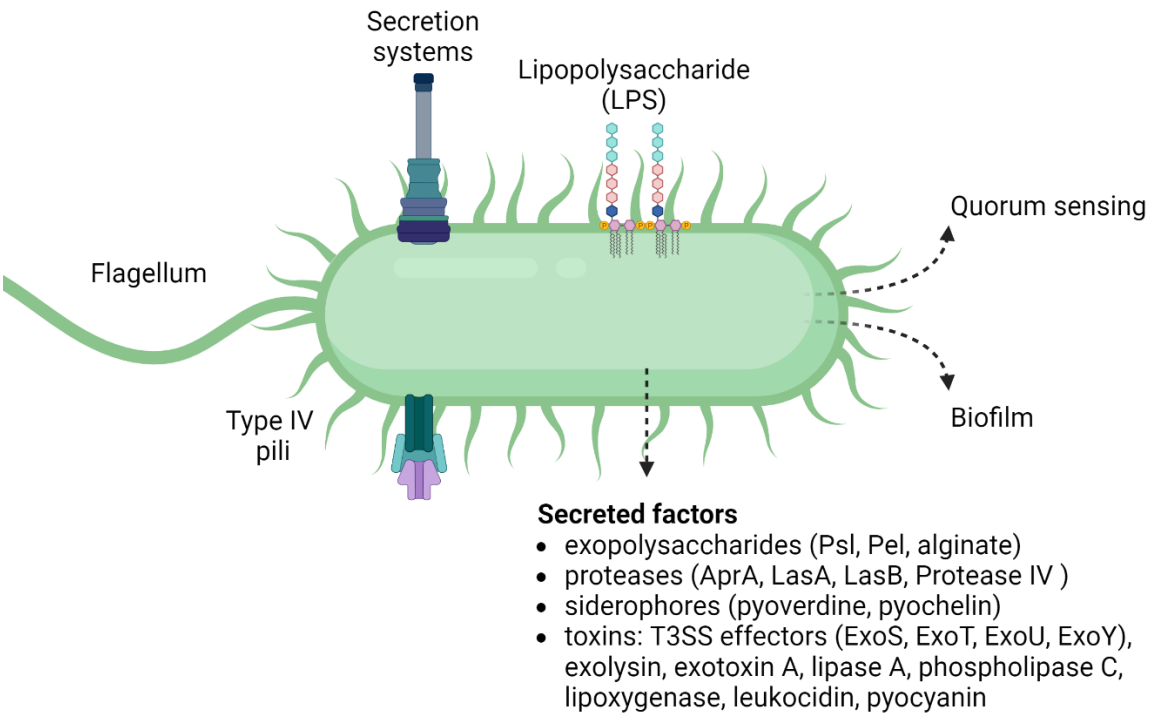

Figure 11: Virulence factors of *Pseudomonas aeruginosa*. This figure illustrates the diverse virulence factors employed by *P. aeruginosa*, that contribute to its adherence, colonization and immune evasion, including type IV pili, flagella, lipopolysaccharide, exopolysaccharides, siderophores, proteases, toxins, and quorum sensing molecules.

2.4.2.1.2. Complement evasion mechanisms employed by *Pseudomonas aeruginosa*

To evade the host's immune system, *P. aeruginosa* has evolved many strategies to combat the complement system. These tactics primarily involve interfering with complement activation, recruiting complement inhibitors, and modifying or degrading complement components.

Central to these strategies is the LPS, a complex molecule built up of lipid A, the core polysaccharide, and the O antigen (**Figure 12**)[166]. Anchored into the bacterial outer membrane by lipid A, LPS modulates the host immune response. For instance, alterations in lipid A structure can confer protection from antimicrobial peptides and trigger a more robust inflammatory response[167]. The inner core, covalently linked to lipid A, consists of conserved sugars indispensable for bacterial survival. The outer core, composed of varying sugar residues, often undergoes O-acetylation and connects to the O antigen, a repetitive sugar chain that determines LPS serotype and immunogenicity.

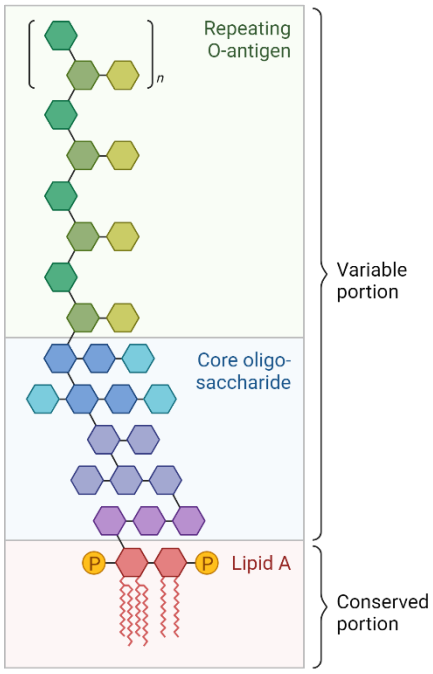

Figure 12: The building blocks of LPS. LPS, a complex molecule integral to the outer membrane of Gram-negative bacteria, consists of three primary components. The hydrophobic lipid A anchor (red), embedded within the membrane, is composed of fatty acids and phosphorylated sugars. Attached to lipid A is the core oligosaccharide (purple/blue), a polysaccharide chain that provides structural integrity and serves as an antigen. The O-antigen (green), a repeating polysaccharide chain connected to the core oligosaccharide, is highly variable among bacterial species and determines serotype specificity.

P. aeruginosa possesses two primary O antigen types: a conserved A-band and a variable B-band. The A-band consists of a repetitive D-rhamnose polysaccharide, while the B-band O antigen comprises diverse sugar structures across the 20 different O serotypes[168]. Interestingly, chronic infection-associated strains, such as those in cystic fibrosis (CF), frequently lack the O antigen (rough LPS), contrasting with the O antigen-presenting (smooth LPS) strains typically linked to acute infections. While smooth LPS strains exhibit resistance to serum killing, rough LPS strains are more susceptible. However, the precise O-side chain length required for optimal complement resistance remains an area of active research.

The genetic loci responsible for O antigen biosynthesis are clustered within the *P. aeruginosa* genome. The A-band gene cluster encodes enzymes involved in the production of the D-rhamnose backbone. In contrast, the B-band gene cluster is more complex, harbouring genes for the synthesis of diverse sugar monomers, their assembly into repeating units, and the attachment of these units to lipid A.

Of particular importance are the wzz genes, which encode a chain length-determining protein (**Figure 13**). Wzz regulates the length of the O antigen, influencing the overall structure and immunogenicity of the LPS molecule[169]. *Wzz1* is related to the regulation of long O antigen chains. It is often found in strains carrying the A-band LPS, which is characterized by a relatively short, homopolymeric O antigen. *Wzz1* functions as a chain length-determining factor by interacting with the O antigen polymerase, influencing the rate of polysaccharide chain elongation. In contrast, *Wzz2* is more commonly linked to the production of very long O antigen chains. It is frequently found in strains with the B-band LPS, which often exhibit longer, heteropolymeric O antigens. *Wzz2*, like *Wzz1*, interacts with the O antigen polymerase but exerts a different regulatory effect, allowing for the synthesis of longer polysaccharide chains.

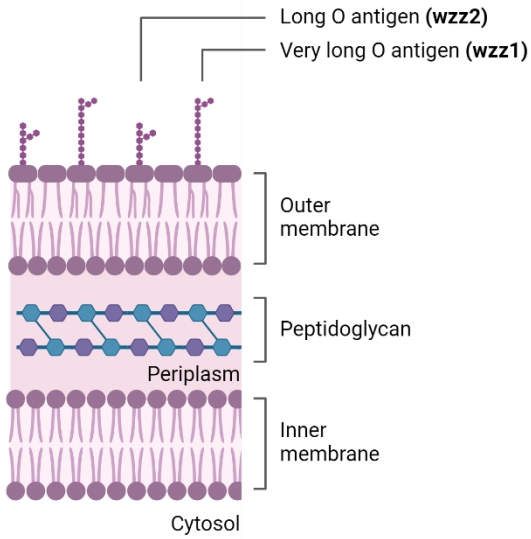

Figure 13: Wzz genes regulate the length of O antigen chains. Wzz1 is associated with the synthesis of long O antigen chains (A-band LPS), while Wzz2 is more commonly linked to very long O antigen chains (B-band LPS).

In addition to LPS, *P. aeruginosa* employs a repertoire of extracellular polysaccharides, including alginate, Psl, and Pel, to shield itself from the host immune system (**Figure 14**)[152, 153, 170]. Alginate modifications, such as acetylation, enhance its immune-evasive properties by masking hydroxyl groups and preventing complement opsonization. While alginate contributes to complement resistance, its primary mechanism involves preventing opsonization rather than directly inhibiting complement activation. Another extracellular polysaccharide, Psl, is essential for biofilm formation, cell adhesion, and complement evasion. Unlike alginate, Psl directly interferes with complement activation by reducing C3b deposition on the bacterial surface, thereby hindering opsonophagocytosis and promoting bacterial survival[171]. While the role of Pel in complement evasion is less clearly understood, it undoubtedly contributes to the overall

immune-avoiding properties of *P. aeruginosa*[172]. Collectively, these polysaccharides create a protective barrier that protects the bacterium from the host immune response.

To further enhance its survival, *P. aeruginosa* forms biofilms, complex communities encased in a matrix of extracellular polymeric substances (EPS)[173]. The EPS matrix serves as a barrier, protecting bacteria from immune defenses, antibiotics, and oxidative stress. The interaction between *P. aeruginosa* biofilms and the immune system is complex. While the complement system is effective against planktonic bacteria, its ability to eliminate biofilms is significantly reduced. This is particularly evident in cystic fibrosis, where *P. aeruginosa* biofilms can persist despite the presence of complement[174]. The cystic fibrosis lung environment, characterized by altered complement levels, further complicates the host response to *P. aeruginosa* biofilms.

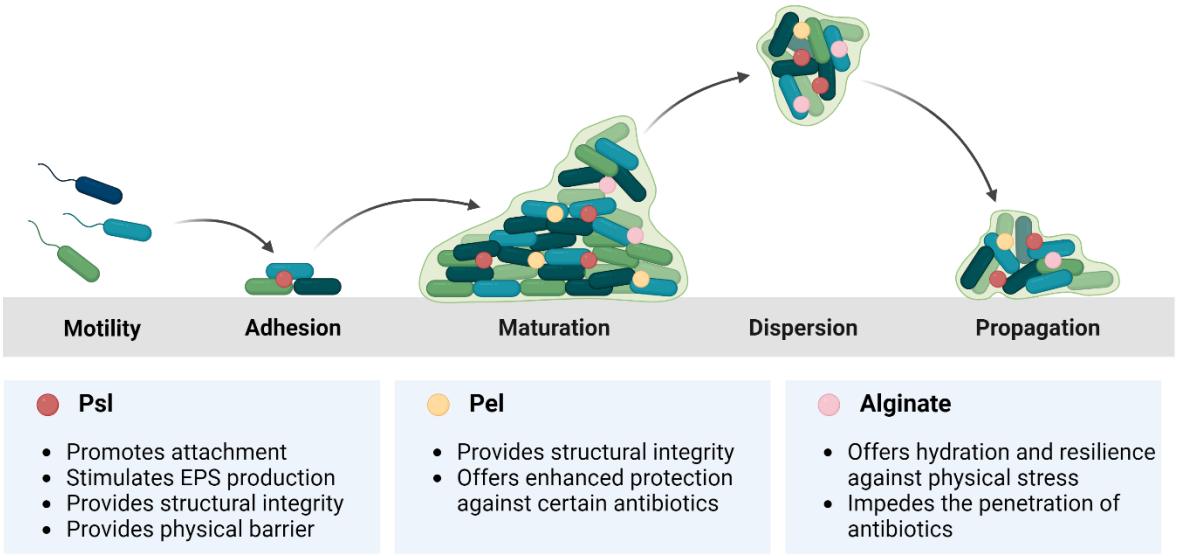

Figure 14: The role of Psl, Pel and alginate exopolysaccharides in biofilm formation and maturation. Psl and Pel, primarily produced by non-mucoid strains, facilitate initial attachment to surfaces and contribute to the biofilm's structural integrity. Alginate, more commonly associated with mucoid strains, provides a protective barrier against host defenses and antibiotics. The combination of these polysaccharides creates a robust matrix that enables the biofilm to persist and resist treatment.

P. aeruginosa also binds inhibitory complement regulatory proteins to its surface. Multiple bacterial proteins are involved in this process, including elongation factor Tu (EF-Tu)[175], Lpd[176], OprD[177], and OprG[76]. These proteins bind complement regulators, preventing MAC assembly and promoting bacterial survival.

Moreover, *P. aeruginosa* inactivates complement components by producing exoproteases. These proteolytic enzymes, namely elastase B, alkaline protease A, Protease IV, and Pseudomonas Small Protease, collectively disrupt critical complement functions. Elastase B, a zinc metalloprotease, demonstrates broad-spectrum activity against complement components, cleaving C1q, C3, C5, C8, and C9[178]. By targeting these proteins, elastase B effectively inhibits complement activation, thereby prevents the formation of the MAC. Alkaline protease A (AprA), another key exoprotease, contributes to immune evasion through its proteolytic activity on C2, C3, C1q, and C5a[155, 179]. In addition to inhibiting complement activation, AprA impairs neutrophil recruitment, a critical step in host defense against bacterial infections[180]. Protease IV and Pseudomonas Small Protease exhibit more focused proteolytic activities, primarily targeting C3 and C1q[181, 182]. By cleaving these complement components, these enzymes contribute to complement evasion and facilitate bacterial survival within the host.

Furthermore, *P. aeruginosa* employs other mechanisms to evade complement. Ecotin, a periplasmic and biofilm-associated protein, disrupts complement activation by inactivating MASP enzymes[183]. Another strategy involves the utilization of lytic polysaccharide monooxygenases. CbpD, a specific type of lytic polysaccharide monooxygenase, impairs C5 convertase assembly, a key enzyme complex for the terminal complement pathway[184]. This highlights the diverse approaches employed by *P. aeruginosa* to avoid complement attack and establish successful infections.

2.4.2.1.3. Therapeutic strategies and resistance mechanisms

Antibiotics are the first line of therapeutics used to combat *P. aeruginosa* infections, however due to the pathogens intrinsic and acquired resistance mechanisms, genetic plasticity and adaptability treatment is often challenging[185]. Conventional beta-lactams (e.g. penicillin, cephalosporin) are usually used in combination with an aminoglycoside, although novel antibiotics are also available. These include carbapenems (e.g. imipenem, meropenem)[186], cefiderocol[187] and finafloxacin[188]. Antibiotic combinations with β-lactamase inhibitors are also a potential treatment strategy[189, 190, 191]. These include ceftazidime-avibactam[192], ceftolozane-tazobactam[193], imipenem-cilastatin-relebactam[194], meropenem-vaborbactam[195]. To enhance their anti-pseudomonas effect antibiotics can also be used in combination with other substances, including metal chelators (EDTA + gentamycin)[196], fatty acids (linolenic acid + tobramycin)[197], amino acids (glutamine + ampicillin)[198] or metal nanoparticles[199]. A variety of therapeutics have been tested to prevent biofilm formation, including antimicrobial peptides[200], quorum-sensing inhibitors[201] or to demolish already formed biofilms like exopolysaccharide hydrolases[202], or bacteriophage therapy[203].

Antibody-based therapy has also been evaluated as an option for treating antibiotic resistant infections, especially infections caused by Gram-negative pathogens, such as those caused by *P. aeruginosa*. Contrary to broad-spectrum antibiotics antibodies offer a target-specific approach, limiting off-target effects on the normal bacterial flora. Despite promising preclinical data, several *P. aeruginosa* antibody-based therapeutics have failed to deliver in clinical trials. Challenges often arise from factors such as the pathogen's ability to rapidly evolve and develop resistance, the complexity of the host-pathogen interaction, and difficulties in achieving effective antibody delivery to the site of infection. Additionally, adverse effects, including immune-related reactions and off-target effects, can hinder the development of these therapies. Among the six anti-pseudomonas antibodies developed by 2022, only one progressed to Phase III clinical trials[204]. Unfortunately, this candidate also failed to meet its primary endpoint. Panobacumab recognising the O-antigen of lipopolysaccharide serotype O11 showed promising results in preclinical trials by binding to bacteria with high avidity, reducing lung bacterial load in a mouse model of pneumonia, as well as having synergistic effects with imipenem[205, 206, 207]. However further studies were not pursued due to panobacumab's limited serotype coverage. The bispecific antibody MEDI3902, designed to target both the Psl exopolysaccharide and Type III Secretion Protein PcrV, demonstrated encouraging outcomes in preclinical and initial human trials[208]. Nonetheless, it failed to decrease the occurrence of nosocomial pneumonia in patients with ventilator-associated pneumonia caused by *P. aeruginosa*[209]. Recently another anti-Pseudomonas antibody has been developed (WVDC-5244) showing promising results in preclinical trials, however, its epitope target remains unclear[210].

2.4.3. Fungi

Fungi utilize similar approaches to evade the complement system. For example, *Candida albicans* binds complement regulators such as FH and C4BP, inhibiting complement activation[211, 212]. Additionally, some fungi possess capsule-like structures that act as physical barriers, protecting them from complement attack. *Cryptococcus neoformans* is a prime example, with its capsule playing a crucial role in evading immune defenses[213]. Moreover, certain fungi can modify their cell surface components to avoid complement recognition or promote complement inactivation.

2.4.4. Parasites

Parasites have evolved diverse mechanisms to evade complement-mediated killing. One common strategy involves recruiting host regulatory proteins to inhibit complement activation. For instance, *Plasmodium falciparum* utilizes PfMSP3.1 to harness the host's C1-INH[214], and *Echinococcus granulosus*

employs InsP6 to recruit FH[215, 216], both preventing complement initiation. Additionally, parasites can acquire host complement inhibitors, such as *Plasmodium falciparum* obtaining MIRL through PfPIG-M, to hinder the formation of MAC[217].

Beyond these approaches, parasites have developed the ability to produce proteins that mimic host complement regulators. For example, *Schistosoma japonicum*[218] and *Trypanosoma cruzi*[219] express CRIT (Complement C2 Receptor Inhibitor Trispanning Protein), similar to the host's CRIT, to disrupt C2 activation. Similarly, *Schistosoma mansoni* produces a C3 receptor and SCIP-1, analogous to host complement regulators, to interfere with complement activation and the MAC[220]. By mimicking these host proteins, parasites effectively counteract the immune response.

Furthermore, parasites can synthesize proteins that directly target complement components. Calreticulin, expressed by various parasites, inhibits the CP and LP[219, 221, 222]. Other examples include paramyosin[223, 224, 225], which inhibits both the CP and MAC assembly, and SMIPP-Ss[226, 227], which interferes with the CP and AP.

These examples collectively demonstrate the diverse and sophisticated strategies employed by microorganisms to evade the complement system, highlighting the ongoing evolutionary arms race between pathogens and their hosts.

2.5. Complement in cancer: a double-edged sword

Within the dynamic ecosystem of the tumor microenvironment (TME), complement components exhibit different expression patterns. Both cancer, stromal and infiltrated immune cells contribute to the complement protein pool, influencing the local complement activation profile. While certain complement components can exert anti-tumor effects, such as promoting immune cell infiltration and mediating direct tumor cell lysis, others may facilitate tumor progression through mechanisms including angiogenesis and immune evasion (**Figure 15**)[228].

Complement factors, such as C1q, C3a, and C5a, can exert both pro-tumoral and anti-tumoral functions, influencing various immune cell types including macrophages, MDSCs, T cells, DCs, and B cells. Complement can promote tumor growth by increasing T-cell apoptosis, reducing T-cell proliferation and dendritic cell maturation, and recruiting M2 macrophages, MDSCs, and regulatory T-cells[229, 230]. These effects can suppress the overall anti-tumor immune response. Conversely, complement can also have anti-tumoral effects, such as improving therapeutic response, increasing immune cell infiltration and interferon-gamma (IFNγ) production.

Additionally, the complement system can impact angiogenesis, a crucial process for tumor growth. Depending on the specific cancer type and model, complement proteins can either stimulate or inhibit angiogenesis. Furthermore, complement-mediated modulation of signalling pathways within tumor cells can influence tumor growth and survival. Activation of pathways like Erk1/2-AKT-PI3K can promote tumor growth, while modulation of WWOX and FAS pathways can induce apoptosis of tumor cells[231].

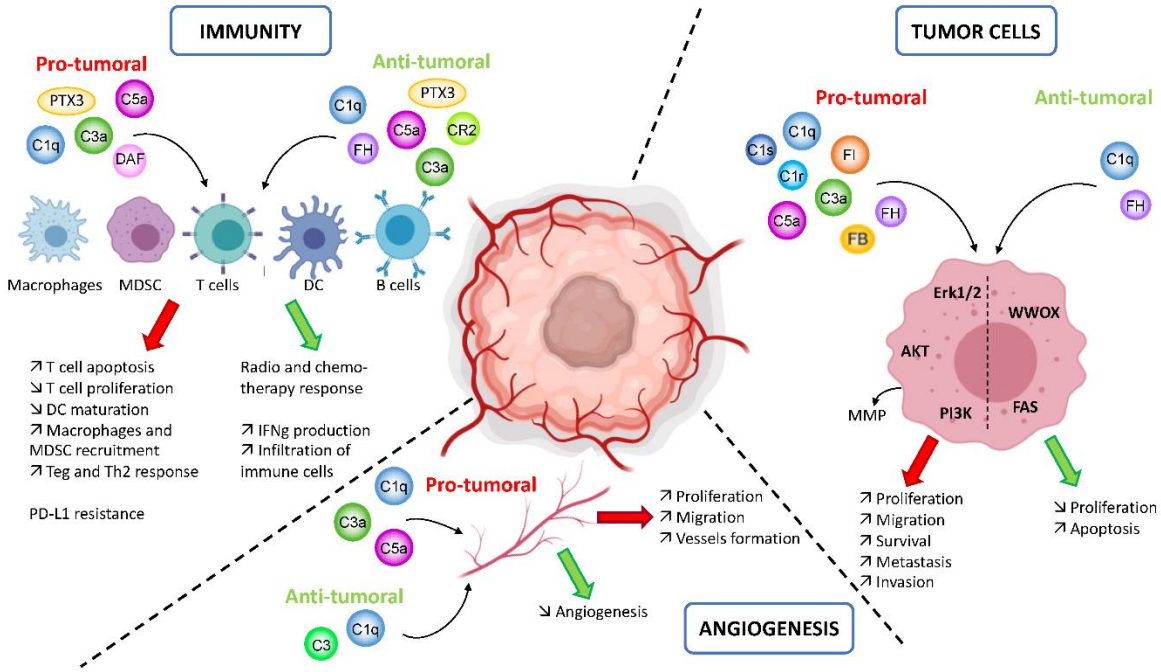

Figure 15: Complement's dual role in tumor progression. Complement proteins exert a diverse influence on tumor progression, modulating immune cell function, angiogenesis, and tumor cell phenotype. The figure is adapted from Revel et al. (2020)[231].

The dual nature of complement's involvement in cancer is further emphasized by the differential expression of complement genes across various cancer types. While some cancers exhibit a complement profile associated with a favourable prognosis, others display an aggressive phenotype linked to complement overexpression.

The subsequent sections provide a more comprehensive discussion of the detailed roles of complement proteins in anaphylatoxin-mediated inflammation, tumor angiogenesis, the function of complement regulators in cancer evasion, and the complosome's influence on tumorigenesis.

2.5.1. Impact of C3a/C3aR and C5a/C5aR on tumor growth and inflammation

Complement activation generates anaphylatoxins C3a and C5a, which significantly influence the TME. In addition to their well-established roles in immune regulation, anaphylatoxins have been involved in a variety of processes that contribute to cancer development. Emerging research indicates that these molecules can directly influence tumor cell behaviour by stimulating intracellular signalling pathways associated with cancer progression. Given the widespread expression of their receptors, C3aR and C5aR, on tumor cells, these anaphylatoxins can promote tumor growth and progression by stimulating cell proliferation, migration, and epithelial-mesenchymal transition (EMT).

Markiewski et al. pioneered research demonstrating the pro-tumorigenic role of complement[232, 233]. They showed that complement activation in a lung epithelial cancer model generated C5a, which attracted myeloid-derived suppressor cells (MDSCs) to the tumor via C5aR1. This led to suppressed CD8+ T-cell responses, suggesting a detrimental impact on anti-tumor immunity. Notably, mice deficient in C3, C4, or C5aR displayed slower tumor growth rates. Subsequent studies across various cancer models consistently supported the pro-tumorigenic role of C5aR1 signalling.

Both C3a/C3aR and C5a/C5aR1 signalling contribute to cancer progression. Nabizadeh et al. (2016) demonstrated the role of C3a-C3aR signalling in promoting melanoma growth[234]. Mice lacking C3aR exhibited slower tumor growth due to alterations in the tumor microenvironment, including increased neutrophils and CD4+ T lymphocytes but decreased macrophages. Depleting neutrophils reversed this tumor-inhibiting effect, suggesting that C3aR inhibition could be a potential therapeutic target. Xu et al. (2020) investigated the role of C3 in hepatic stellate cells (HSCs) and their impact on hepatocellular carcinoma (HCC)[235]. HSCs were found to promote HCC progression by suppressing T-cell function and facilitating myeloid-derived suppressor cell expansion. These effects were mediated through the C3 pathway, and knocking down C3 in HSCs suppressed HCC development in a mouse model. Davidson et al. (2020) employed single-cell RNA sequencing to analyse the tumor microenvironment in melanoma[236]. They discovered that complement component C3 was specifically expressed in the immune stromal population and supported the recruitment of C3aR-expressing macrophages. Disrupting the C3a-C3aR signalling pathway hindered immune infiltration and slowed tumor growth. Jackson et al. (2021) revealed the crucial role of C3 in the development of cutaneous squamous cell carcinoma (cSCC)[237]. C3 deficiency reduced tumor burden, while deficiencies in C5aR1, C5aR2, or the C3a receptor had the opposite effect. This suggests that C3 drives tumorigenesis independently of downstream C5a generation or the membrane attack complex. Ding et al. (2020) highlighted the importance of the C5a/C5aR1 signalling

pathway in colorectal cancer (CRC) tumorigenesis. C5a/C5aR1 signalling recruits myeloid-derived suppressor cells, impairs CD8+ T cells, and modulates cytokine production, initiating CRC. Targeting this pathway could be a promising preventive strategy for CRC[238]. Zha et al. (2019) found that tumor cells can produce C3, which is activated intracellularly to generate C3a[239]. C3a then modulates tumor-associated macrophages, suppressing antitumor immunity. Deleting C3 in tumor cells with high C3 expression enhanced the effectiveness of anti-PD-L1 treatment. Cho et al. (2016) found that the transcription factor TWIST1 binds to and upregulates the expression of C3 in malignant epithelial cells[240]. C3 promotes EMT by reducing E-cadherin expression in a C3a and KLF5-dependent manner. TWIST1 and C3 were co-localized at the invasive edges of tumors and developing tissues, suggesting their coordinated role in pathological and physiological EMT.

C5a, has also been extensively investigated for its role in tumorigenesis. Corrales et al. (2012) demonstrated that lung cancer cells can activate the complement system and produce the anaphylatoxin C5a[241]. C5 deposition and C5a release were higher in lung cancer cell lines compared to non-cancerous bronchial epithelial cells, both locally and systemically. In a 2014 study, Vadedvu et al. observed that the C5aR receptor plays an important role in the spread of breast cancer to the lungs in a mouse model[242]. Their research revealed that C5aR inhibits T-cell immune responses, facilitating cancer growth. This suppression is attributed to the influx of immature myeloid cells and the modulation of TGF-β and IL-10 levels, which promote the development of regulatory T cells and Th2 responses, leading to the impairment of CD8+ T cell function. Blocking C5aR pharmacologically or genetically reduced lung metastases, primarily due to the restoration of CD8+ T-cell function.

A key factor influencing the intratumoral concentration of C5a is PTX3. Bonavita et al. (2015) found that PTX3 deficiency in mice increased susceptibility to cancer development, including macrophage recruitment, elevated cytokine levels, blood vessel growth, and genetic alterations in the Trp53 gene[243]. By contrast, Netti et al. (2020) found that in humans PTX3 expression was elevated in clear cell renal cell carcinoma (ccRCC) and associated with lower survival rates[244]. PTX3 activated the complement system, promoting angiogenesis and inflammation. Higher serum PTX3 levels were correlated with advanced tumor stage and poorer patient outcomes. A 2015 study by Surace and colleagues demonstrated that radiation therapy activates the complement system in both mouse and human cancers[245]. The release of pro-inflammatory molecules C3a and C5a was essential for the anti-tumor benefits of radiation therapy and the development of a targeted immune response. However, the use of dexamethasone, a medication commonly administered alongside radiation therapy, was found to suppress complement activation and

diminish the effectiveness of the immune response. High levels of C5aR1 have been linked to poor patient outcomes in many of these cancers. Zhank et al. (2023) investigated the role of C5aR1 in high-grade serous ovarian cancer (HGSC)[246]. They found that C5aR1 expression was associated with poor prognosis and linked to an immunosuppressive subtype of HGSC characterized by increased infiltration of pro-tumor cells and impaired CD8+ T cell function. A C5aR1 inhibitor, PMX53, was shown to antagonize cancer growth, modulate immunosuppressive mechanisms, and synergize with PD-1 therapy. Xu et al. (2023) investigated the role of C5aR1 in colorectal cancer metastasis[247]. They found that C5aR1 expression was linked to a higher rate of CRC cell growth and spread. C5aR1 also accelerated the EMT process. Abdelbaset-Ismail et al. (2017) investigated the role of C3a and C5a in leukaemia cell migration[248]. They found that leukaemia cells respond to C3a and C5a by chemotaxis and adhesion. Activation through C3a and C5a receptors led to phosphorylation of p42/44 and p38 MAPK, and AKT.

Overall, the C3a/C3aR and C5a/C5aR1 pathways play crucial roles in cancer development and progression. Targeting these pathways offers potential therapeutic strategies for cancer treatment.

2.5.2. Complement activation and tumor angiogenesis

Angiogenesis, the creation of new blood vessels within a tumor, is crucial for its survival and expansion. Tumors, like normal tissues, require nutrients, oxygen, and a means to eliminate waste. To obtain these essentials, cancer cells, deeply embedded within the tumor, rely on the development of new blood vessels. While angiogenesis is a natural process involved in wound healing and reproduction, its persistent activation within tumors is abnormal. This hijacked process fuels tumor growth and metastasis. Research into the relationship between complement components and angiogenesis has revealed a complex interplay. While some studies suggest a supportive role of complement in blood vessel formation, others indicate an inhibitory effect.

Recent findings have unveiled a novel, complement-independent function for C1q[249]. In subcutaneous tumor models, C1q deficiency led to disruption of tumor vasculature and alterations in VEGF-C expression. However, the influence of C1q on angiogenesis appears context-dependent, as C1q deficiency has also been associated with increased angiogenesis and larger tumors in spontaneous breast cancer models[250].

While the role of C1q in angiogenesis remains complex, the impact of the anaphylatoxins C3a and C5a on this process has been better elucidated. Similar to C1q, C3 deficiency results in vascular abnormalities and altered VEGF levels[251]. Furthermore, C5a directly stimulates endothelial cell migration, proliferation, and

vessel formation[252]. Finally, the overall effect of complement on angiogenesis remains controversial, with some studies demonstrating anti-angiogenic properties in specific tumor contexts.

C3a and C5a contribute to tumor growth by activating mitogenic signalling pathways, promoting cell proliferation, and suppressing apoptosis[253, 254]. Additionally, the membrane attack complex has been implicated in activating cell cycle and oncogenic pathways[255]. In conclusion, the complement system is intricately involved in tumor progression, influencing angiogenesis, immunity, and tumor cell proliferation.

2.5.3. The role of complement regulators in cancer escape

Cancer cells have exploited the complement system by upregulating CRPs[256]. This overexpression serves as a protective mechanism, shielding tumor cells from opsonization and lysis. Studies demonstrated that various cancer types, including squamous cell carcinomas and uveal melanomas, express multiple CRPs, such as CD46, CD55, and CD59, at higher levels compared to normal tissues[257].

Beyond immune evasion, CRPs can actively contribute to tumor progression. One study by Daugan et al. unveiled a novel role for FH in driving tumor progression[258]. Traditionally recognized for its extracellular function in regulating the complement system, this work demonstrated that intracellular FH (int-FH) plays a crucial part in the development of ccRCC and lung adenocarcinoma. Int-FH was found to promote tumor growth by influencing essential cellular processes, including cell cycle progression, survival, and migration. Unexpectedly, this pro-tumorigenic effect was specific to these cancer types, highlighting a unique mechanism of action. Specifically, int-FH appears to influence tumor behaviour by affecting key cellular processes like p53 phosphorylation and NF-κB translocation. p53 is a tumor suppressor protein, and NF-κB is a protein involved in inflammation and cell survival. By inhibiting p53 and promoting NF-κB activity, int-FH creates a favourable environment for tumor growth. The clinical significance of CRP overexpression is evident in studies associating high CRP expression to poorer patient outcomes, including increased metastasis and reduced survival in cancers like breast cancer[259].

2.5.4. The complosome: a new player in cancer progression

The traditional view of the complement system as a solely extracellular player has undergone a significant shift with the discovery of its intracellular counterpart. This intracellular complement system, often termed 'complosome', is a cascade-like mechanism within cells that has been implicated in diverse cellular processes[260]. Initially characterized in immune cells, the complosome has been shown to regulate vital

functions such as T-cell metabolism, inflammation, and cell survival. Notably, its influence extends beyond immune cells, affecting the behaviour of cells in organs like the pancreas, lungs, and heart[261].

The cancer landscape has also been profoundly influenced by the complosome. Emerging research has unveiled specific mechanisms by which the complosome contributes to cancer progression. For instance, kidney cancer cells can autonomously express and utilize complement FH and C1s within the cellular environment, distinct from the classical complement cascade. FH has been linked to regulating tumor cell proliferation and survival, with high intracellular levels correlating with poor patient outcomes[258].

Expanding on this, Daugan et al. uncovered a complex dual role for C1s in ccRCC progression[262]. The study revealed a strong association between elevated C1s expression in tumor cells and poor patient prognosis. Intriguingly, this prognostic value was independent of complement activation, suggesting a novel, non-canonical role for C1s. Functional studies demonstrated that C1s promotes cancer cell proliferation and viability while inhibiting T cell activation. Moreover, C1s influenced the tumor microenvironment by attracting macrophages and T cells. These findings underscore C1s as a pivotal player in ccRCC progression, operating through both complement-dependent and independent mechanisms that modulate the tumor cell phenotype and immune response.

Riihilä et al. further emphasized the complosome's role in cancer by demonstrating a critical function for C1r and C1s in cSCC progression[263]. The study revealed significantly increased C1r and C1s expression in cSCC cells compared to normal skin. Importantly, these complement components promoted cSCC growth by facilitating tumor angiogenesis and cellular proliferation. Mechanistically, C1r and C1s activated signalling pathways involved in cell survival and proliferation, while their inhibition suppressed tumor growth and angiogenesis.

The critical role of the complosome in cancer progression is further illustrated by the work of Shimazaki et al., who elucidated the importance of FB in pancreatic ductal adenocarcinoma (PDAC)[264]. FB was significantly overexpressed in PDAC cells, where it played a critical role in promoting cell growth by inhibiting cellular senescence. Clinically, high stromal FB expression correlated with poor patient outcomes and an immunosuppressive tumor microenvironment.

Ding et al. added to this knowledge by unveiling a novel intracellular pathway involving C5 in colorectal cancer progression[238]. Intracellular C5 is cleaved to generate C5a, which subsequently activates intracellular C5aR1, leading to β-catenin stabilization and tumorigenesis. Importantly, C5aR1 inhibition suppressed tumor growth.

Extensive research has highlighted the critical role of tumor-derived complosome components, especially C3 and its cleavage product C3a, in cancer progression. The intracellular activation of tumor-produced C3 suppresses the infiltration and function of CD8+ T cells by fostering an immunosuppressive TME[239]. Notably, eliminating C3 within cancer cells exhibiting high C3 levels enhances the effectiveness of anti-PD-L1 therapy.

While these studies collectively highlight the different aspects of the complosome's role in cancer, it is essential to acknowledge potential cancer-specific variations in complement protein function. Identifying these differences is crucial for developing targeted therapeutic interventions.

2.5.5. Breast cancer

Breast cancer continues to be a serious issue across Europe. According to data from the European Cancer Information System (ECIS), an estimated 374,800 women and 4,400 men were diagnosed with the disease in 2022 (**Figure 16**). Despite therapeutic progress, breast cancer is the primary contributor to cancer mortality among women in the European Union (EU), representing 16.7% of cancer fatalities. The lifetime risk of developing breast cancer is notably higher for women (1 in 11) compared to men (1 in 909). These statistics highlight the importance of early detection, prevention efforts, and continued research to combat this prevalent form of cancer.

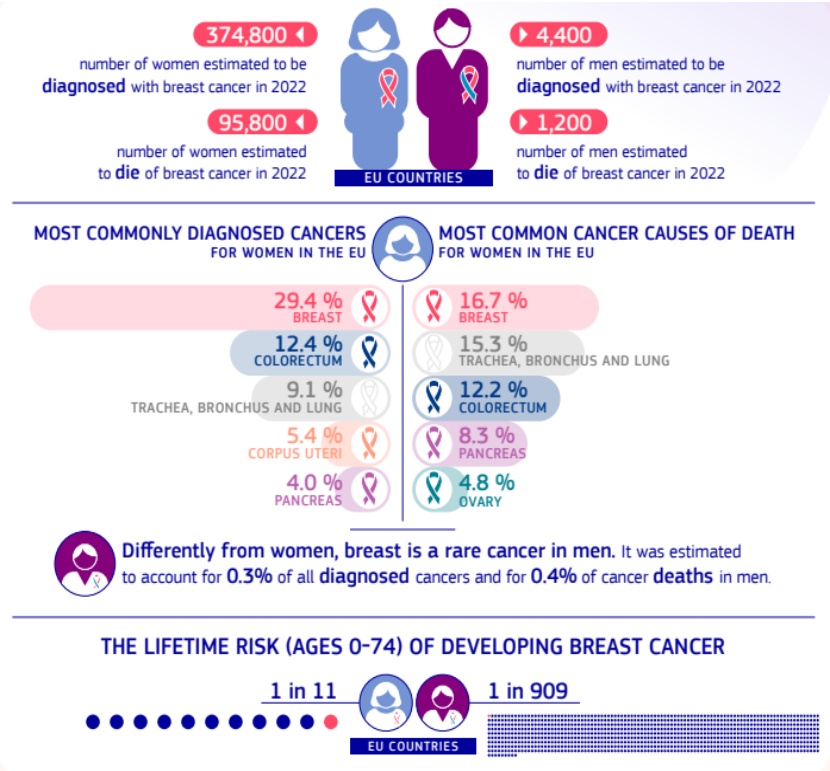

Figure 16: Breast cancer incidence and mortality in Europe. Source: European Commission, Joint Research Centre (JRC). (2022). Cancer estimates factsheet in EU-27 countries for 2022.

2.5.5.1. Breast Cancer Subtypes: A Complex Landscape

Breast cancer is a diverse disease with a wide range of biological and clinical characteristics. Its classification into distinct subtypes has evolved significantly with advancements in molecular and immunohistochemical techniques.

In conventional breast cancer classification, estrogen, progesterone, and human epidermal growth factor receptor 2 (HER2) expression are key determinants[265].

Luminal A breast cancers exhibit high hormone levels and low HER2 expression, often associated with a more favourable prognosis. While sharing similarities, luminal B breast cancers tend to have higher HER2 expression and a more aggressive biological profile. HER2-positive (HER2+) breast cancers are characterized by excessive HER2 gene activity, driving rapid tumor growth and an increased risk of metastasis. Triple-negative breast cancers, lacking receptors for estrogen, progesterone, and HER2, present a more complex treatment challenge due to limited targeted therapy options.

While these subtypes provide a foundational understanding, the complexity of breast cancer necessitates a comprehensive evaluation of each patient's tumor profile. Emerging research has emphasized the importance of additional molecular markers, such as microRNAs (miRNAs)[266, 267] and genetic mutations (BRCA1/2, p53)[268, 269], in refining breast cancer classification.

2.5.5.2. HER2+ breast cancer

HER2+ breast cancer is defined by an overabundance of the HER2 protein, resulting from either an increased number of copies of the HER2 gene or overactive gene function[270]. This overexpression leads to abnormal cell growth and proliferation. Approximately 15-20% of breast cancers exhibit HER2 positivity. HER2 status is typically determined through immunohistochemistry (IHC) staining or fluorescence in-situ hybridization (FISH)[271]. IHC assesses HER2 protein levels, while FISH quantifies HER2 gene copies. A diagnosis of HER2+ breast cancer is established when IHC shows a 3+ score or FISH reveals an amplification of the HER2 gene.

HER2/neu is a receptor tyrosine kinase belonging to the ErbB family, which comprises four related proteins: EGFR, HER2/neu, HER3, and HER4[272]. Like its family members, HER2/neu is composed of three

main regions: an extracellular domain of approximately 105 kDa, a short transmembrane part, and an intracellular domain with tyrosine kinase activity[273].

The HER2 signalling pathway plays a crucial role in tumorigenesis (**Figure 17**)[274, 275, 276, 277]. Upon ligand binding, HER2 undergoes dimerization and autophosphorylation, activating downstream signalling cascades, primarily the PI3K/AKT and MAPK pathways. These pathways stimulate cell proliferation, survival, angiogenesis, and metastasis.

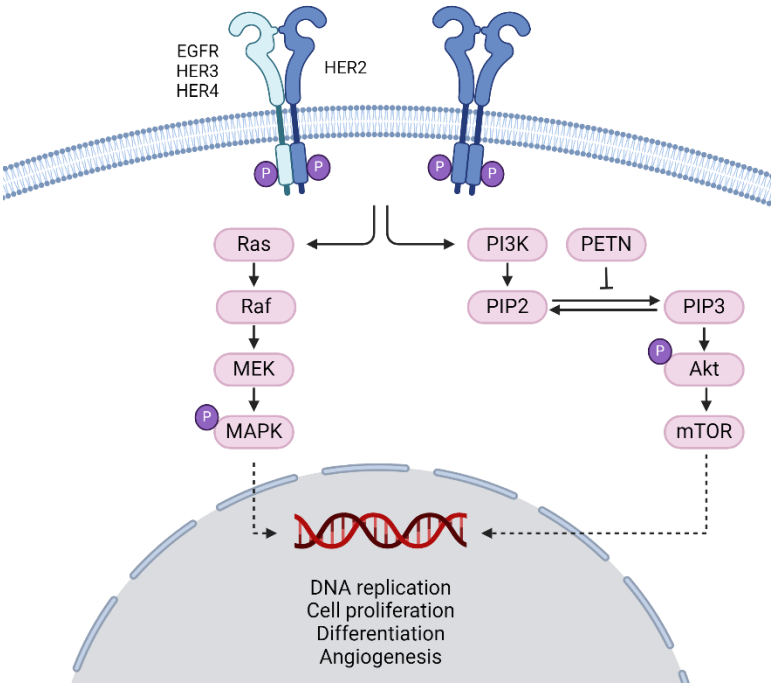

Figure 17: HER2 signalling pathways. The HER2 signalling cascade is initiated by the activation of HER2 receptors on the cell membrane. HER2 can form both homomeric and heteromeric complexes with other ErbB family members. Upon ligand binding, such as epidermal growth factor or neuregulin, receptor dimerization occurs, leading to autophosphorylation. This event triggers the recruitment of intracellular signalling molecules. Key downstream signalling pathways involved include the Ras-Raf-MEK-MAPK cascade, which regulates cell division and specialization.

2.5.5.3. Anti-HER2 therapeutic strategies

The introduction of monoclonal antibodies has fundamentally changed the treatment paradigm for HER2+ breast cancer. While these therapies have significantly advanced patient outcomes, a substantial proportion of patients exhibit resistance or derive limited benefit from current treatment regimens. To

optimize therapeutic strategies and enhance patient care, a comprehensive understanding of the underlying mechanisms of action is imperative. HER2 has emerged as a critical therapeutic target.

2.5.5.3.1. Trastuzumab

Trastuzumab, a monoclonal antibody binding to HER2's extracellular domain, was the first HER2-targeted therapy approved by the Food and Drug Administration (FDA)[278, 279, 280]. Its mechanism of action is complex, involving both extracellular and intracellular pathways[281].

A primary mode of action for trastuzumab involves antibody-dependent cellular cytotoxicity (ADCC). This immune-mediated process is initiated when the antibody binds to HER2 overexpressed on the tumor cell surface. The Fc portion of trastuzumab then interacts with Fc receptors, primarily on NK cells, leading to the recognition and destruction of the cancer cell. While ADCC is a well-established mechanism contributing to trastuzumab's efficacy, ongoing research is dedicated to enhance its immune effects through strategies such as augmenting NK cell activity, modifying the antibody structure, and employing inhibitors of immune checkpoint proteins.

While the extracellular actions of trastuzumab are more defined, its intracellular effects are less understood[282]. Initially hypothesized to inhibit HER2-mediated intracellular signalling, subsequent studies have shown a more nuanced picture. Although trastuzumab can influence intracellular signalling pathways, the precise mechanisms and their clinical relevance remain under investigation. Proposed intracellular effects include modulation of HER2 signalling, where trastuzumab can downregulate HER2 signalling under certain conditions, though its impact on key signalling pathways like Akt and ERK is often inconsistent and context-dependent. In addition, trastuzumab can interfere with the proteolytic cleavage of HER2, preventing the formation of truncated, oncogenic HER2 fragments (p95HER2). Early studies suggested a role for trastuzumab in inhibiting DNA repair, but these findings require further validation[283]. Furthermore, in addition to its direct antitumor activity, trastuzumab has demonstrated anti-angiogenic properties in preclinical models.

15% of patients treated with adjuvant trastuzumab may experience disease recurrence[284, 285]. Furthermore, a majority of those with metastatic disease develop resistance to trastuzumab within the first year of therapy, highlighting the urgent need for innovative treatment approaches. Approximately 35% of patients may exhibit de novo resistance, while 70% may develop resistance after initial treatment.

Alterations in HER2 expression or structure, activation of compensatory signalling pathways involving other HER receptors or downstream effectors, and the emergence of bypass mechanisms can all

contribute to treatment failure. Constitutive activation of the PI3K-Akt-mTOR pathway, frequently resulting from genetic alterations, is a key mechanism driving resistance to therapy. Therefore, there is still the need to improve immunotherapies based on trastuzumab.

Antibody-drug conjugates (ADCs) have significantly augmented the therapeutic potential of trastuzumab. T-DCs, which utilize trastuzumab as a selective antibody to deliver cytotoxic drugs into cancer cells, have demonstrated remarkable clinical outcomes. Trastuzumab emtansine (T-DM1), an early success in the field, links the anti-tubulin agent emtansine to trastuzumab, targeting HER2-expressing cancer cells with a potent cytotoxic payload[286, 287, 288]. T-DM1 has shown efficacy in various HER2-positive cancers, including breast-, gastric-, and non-small cell lung cancer. More recently, trastuzumab deruxtecan (T-DXd) has emerged as a promising ADC[289, 290, 291, 292, 293]. Leveraging deruxtecan, a novel, highly potent toxin, T-DXd has exhibited superior efficacy not only in HER2-positive breast cancers but also in HER2-low and HER2-mutant lung cancers. Given the prevalence of HER2-low breast cancer, T-DXd holds significant potential to benefit a substantial patient population. SYD985 (trastuzumab duocarmycin) is another promising ADC for HER2-positive cancers[294]. Combining trastuzumab with the potent cytotoxic payload duocarmycin, SYD985 has shown promising results in clinical trials across various tumor types, including breast cancer, gastric cancer, urothelial cancer, and endometrial cancer. While further research is warranted, SYD985 offers potential benefits for patients with HER2-positive malignancies.

2.5.5.3.2. Pertuzumab

Unlike trastuzumab, which targets the extracellular portion of the HER2 protein (domain IV), pertuzumab binds to a different region (subdomain II), preventing HER2 from dimerization with other HER family members[295, 296]. This distinct mode of action sets it apart from other treatments that target HER2.

By binding to subdomain II, pertuzumab physically blocks the receptor's ability to form dimers with other HER family members, primarily HER3. Dimerization is a crucial step in activating downstream signalling pathways (PI3K/Akt and MAPK), which are essential for cell growth, proliferation, and survival.

Preventing dimerization effectively inhibits HER2 activation and subsequent downstream signalling. While pertuzumab alone might have limited effects on Akt phosphorylation compared to trastuzumab, the combination of both antibodies has shown synergistic anti-tumor activity[282].

2.5.5.3.3. Complement activation drives synergy of Trastuzumab and Pertuzumab

The combination of trastuzumab and pertuzumab has demonstrated enhanced efficacy in treating HER2+ cancers. Although preliminary studies suggested that the synergistic effect arises from distinct mechanisms—pertuzumab blocking HER2 heterodimerization and trastuzumab stimulating the immune response against the tumor—concrete in vivo evidence supporting this theory has been scarce.

Recent research by Tsao et al. has elucidated a novel mechanism underlying the therapeutic efficacy of this combination (**Figure 18**)[297]. Their findings indicate that the joint activation of the CP is essential for the observed synergy. While both antibodies independently trigger ADCC and antibody-dependent cellular phagocytosis (ADCP), their combined administration potently activates the complement pathway, resulting in complement-dependent cytotoxicity (CDC) and phagocytosis (CDCP). This concerted action significantly augments tumor cell elimination.

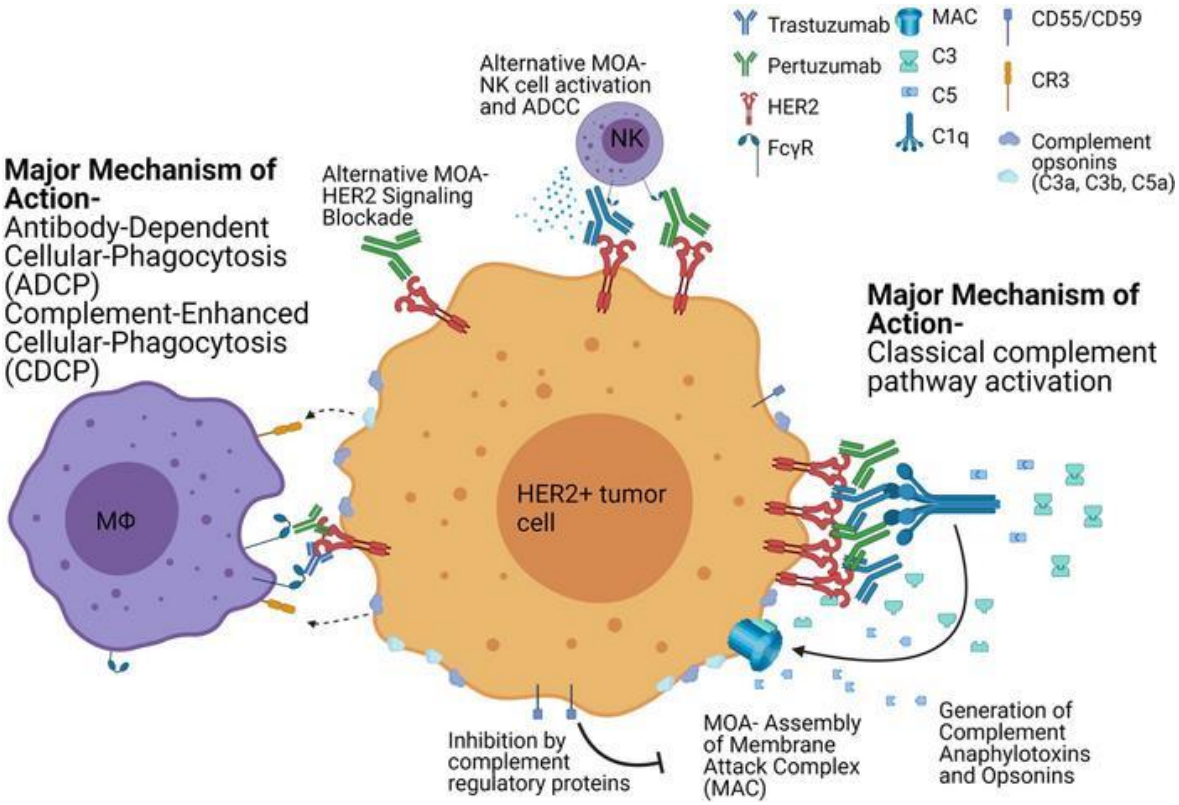

Figure 18: Complement activation mediates synergistic antitumor effects of trastuzumab and pertuzumab. Adapted from Tsao et el. (2022)[297]

Furthermore, the study emphasizes the important role of complement activation in vivo, as demonstrated by the attenuated anti-tumor activity observed upon complement inhibition. Notably, correlations

between complement regulator expression and patient outcomes suggest potential prognostic and therapeutic implications. These findings challenge the previously established understanding of the synergistic relationship between trastuzumab and pertuzumab. While differential HER2 receptor targeting and composition-independent inhibition may contribute to the observed efficacy, the compelling evidence for complement activation as a primary driver of therapeutic benefit warrants further investigation.

This activation leads to both CDC and CDCP of HER2+ tumor cells. Importantly, the study identified a correlation between elevated tumor C1q expression and improved survival in HER2+ breast cancer patients, while complement regulators CD55 and CD59 demonstrated an inverse correlation with patient outcome. These observations confirm the clinical importance of complement activation in the context of trastuzumab and pertuzumab therapy.

3. Cellular components of innate immunity

Innate immunity relies on a diverse array of cellular effectors to provide rapid and non-specific defense against pathogens and cancer cells[298]. Phagocytes, including neutrophils, monocytes, and macrophages, are instrumental in pathogen clearance through phagocytosis and the generation of reactive oxygen species (ROS). Dendritic cells, while primarily bridging innate and adaptive immunity, also contribute to pathogen elimination. NK cells exert cytotoxic activity against virus-infected and tumor cells through the release of lytic granules[299]. Collectively, these cells mediate inflammatory responses, antigen presentation, and direct pathogen killing.

3.1. Phagocytes

Phagocytosis is characterized by the cellular engulfment and subsequent degradation of foreign particulates, including pathogens and apoptotic debris[300, 301]. Distinct from the non-specific fluid uptake of pinocytosis, phagocytosis is a receptor-mediated process that selectively targets solid particles for internalization. Primarily executed by neutrophils, monocytes, and macrophages, this complex cellular mechanism involves the extension of pseudopodia to surround and enclose the target within a phagosome. Subsequent fusion with lysosomes creates a phagolysosome, where oxidative burst and hydrolytic enzymes dismantle the ingested material. Beyond pathogen elimination, phagocytosis contributes to tissue homeostasis, inflammation resolution, and antigen presentation, demonstrating its essential role in maintaining overall health and immune function.

3.1.1. Neutrophils

Polymorphonuclear neutrophils (PMNs) comprise a substantial portion of circulating leukocytes, constituting 50-70% of the total[302]. Continuously generated within the bone marrow, these cells are the primary effectors of acute inflammation. PMNs possess three granule types: azurophilic, specific, and gelatinase, containing key enzymes such as myeloperoxidase, lactoferrin, and metalloproteinase 9, respectively[303].

To eliminate pathogens, PMNs employ multiple strategies. Intracellularly, microorganisms are engulfed within phagosomes and neutralized through the generation of (ROS)[304] or the action of antimicrobial proteins, including cathepsins, defensins, lactoferrin, and lysozyme[305]. Extracellular pathogens may also be targeted through the release of antimicrobial substances via degranulation. Additionally, PMNs can undergo a process termed neutrophil extracellular trap (NET) formation, wherein chromatin, histones, and granular proteins are expelled to capture and kill microbes (**Figure 19**)[306, 307]. A variety of stimuli, including pathogens, damage-associated molecular patterns (DAMPs), platelets, immune complexes, and other factors, can trigger both lytic and non-lytic NETosis[308].

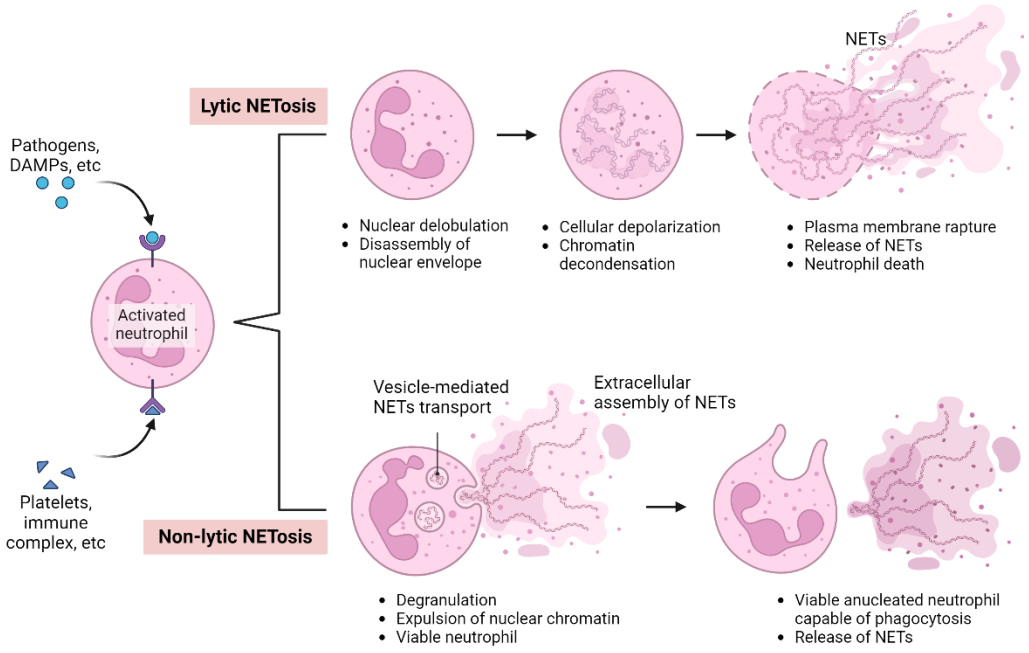

Figure 19: Neutrophil extracellular trap (NET) formation. NETosis is a unique immune response where neutrophils release chromatin and antimicrobial proteins in the form of extracellular traps (NETs) to combat pathogens. Lytic NETosis involves the death of the neutrophil. Activated neutrophils undergo nuclear delobulation, disassembly of the nuclear envelope, and chromatin decondensation, followed by plasma membrane rupture and NET release. Non-

lytic NETosis allows neutrophils to survive and maintain their phagocytic function. In this pathway, neutrophils expel nuclear chromatin and degranulate, releasing NETs without cell death.

Neutrophils, once considered primarily as first responders in innate immunity, have emerged as complex players in cancer progression[309, 310]. Their role extends beyond a binary classification of pro- or anti-tumorigenic, with increasing evidence suggesting a more nuanced and context-dependent involvement. The neutrophil/lymphocyte ratio has emerged as a potential prognostic biomarker, highlighting the clinical significance of these cells in cancer patients[311].

The tumor microenvironment is a dynamic milieu that influences neutrophil phenotype and function[309]. There is growing recognition of neutrophil plasticity, enabling them to adapt to diverse cancer contexts and exhibit a spectrum of behaviours. While neutrophils can contribute to tumor growth, angiogenesis, and metastasis through the release of pro-inflammatory factors and extracellular matrix degradation, they also possess anti-tumor capabilities, including phagocytosis of cancer cells and the formation of NETs[312].

A compelling hypothesis suggests that the cancer microenvironment can induce a pro-tumorigenic reprogramming of neutrophils[313, 314]. This shift in phenotype may be a critical factor in cancer progression and therapeutic resistance. Consequently, strategies aimed at preventing or reversing this reprogramming hold promise as novel cancer treatments.

3.1.2. Monocytes

Monocytes are circulating innate immune cells originating from common myeloid progenitors within the bone marrow[315]. While traditionally considered precursors to tissue-resident macrophages, recent research underscores their distinct functional capacities beyond this role. Additionally, monocytes can be rapidly mobilized from reserve pools located in the spleen and lungs.

Monocytes can be categorized into three primary subsets based on their surface expression of CD14 and CD16: classical, intermediate, and non-classical[316] (**Figure 20**).

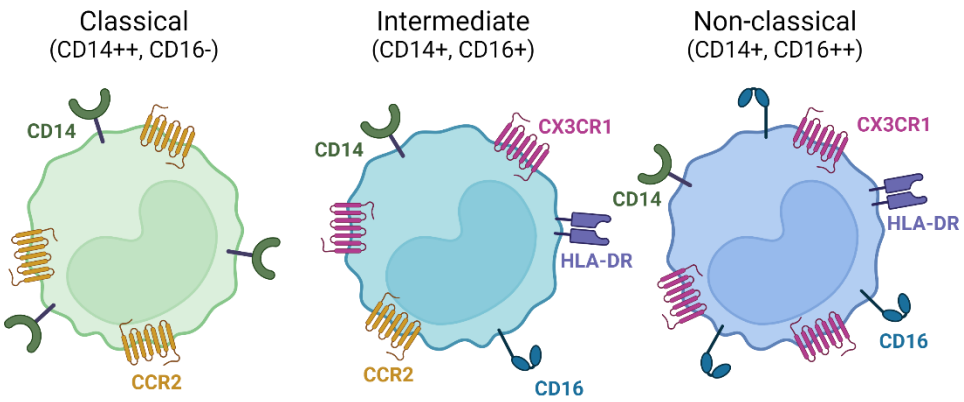

Percentage	80-95%	<10%	<10%
Primary function	Phagocytosis	Antigen presentation, T cell activation	Surveillance
Key markers	high CD14, CCR2, CD26L, low CX3CR1	CXCR1, CCR2, CCR5, CD16, HLA-DR	low CCR2, high CX3CR1, high CD16, HLA-DR
Cytokine production	IL-10, IL-6	TNFα, IL-1β, IL-6	TNFα, IL-1β, IL-6

Figure 20: Key characteristics of human monocyte subsets. Monocytes can be divided into subsets based on their expression of surface markers and their functional properties. These subsets include classical monocytes, which are involved in inflammation and phagocytosis, intermediate monocytes, which have properties of both classical and nonclassical monocytes, and nonclassical monocytes, which are primarily involved in patrolling the blood vessels and detecting pathogens.

While classical monocytes constitute the majority and rapidly differentiate into tissue-resident macrophages, non-classical monocytes exhibit a longer lifespan and patrol the vasculature, contributing to endothelial integrity. The function of intermediate monocytes is unclear, but they appear specialized in antigen presentation. Beyond their differentiation potential, monocytes possess diverse effector functions. They can internalize, process, and present antigens, influencing T-cell responses. Moreover, monocytes exhibit both pro- and anti-inflammatory activities, contributing to tissue remodelling.

3.1.3. Macrophages

Macrophages are versatile immune cells with diverse origins and functions. Their origins can be traced to hematopoietic stem cells within the yolk sac, a transient organ during embryogenesis. From these progenitors, macrophage precursors migrate to various tissues, differentiating into specialized subsets. While certain macrophage populations, such as those in the brain and liver, are established early in development and persist throughout life, others, like skin and connective tissue macrophages, can be replenished by circulating monocytes from the bone marrow[317].

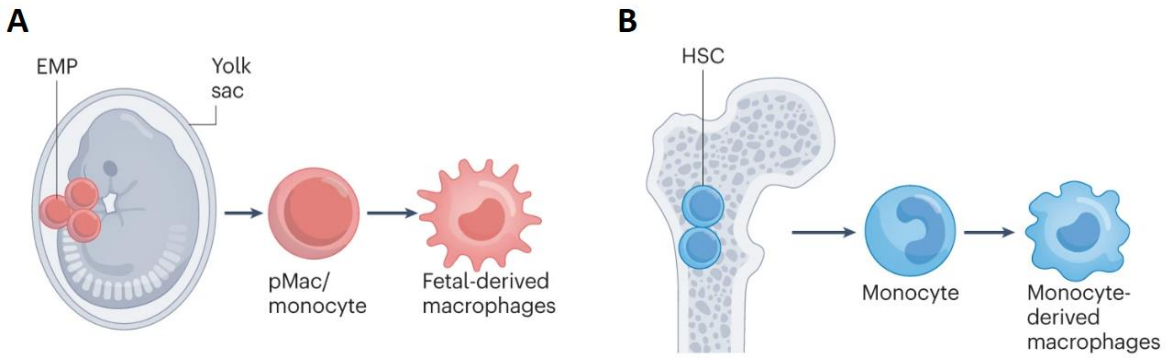

Figure 21: Dual origins of tissue macrophages. Tissue macrophages arise from two main sources. Erythro-myeloid progenitors (EMPs) differentiate into pre-macrophages (pMac)/monocytes, which can mature into fetal-derived macrophages. These resident macrophages exhibit a high capacity for self-renewal and typically do not require continuous input from hematopoietic stem cells (HSCs). Conversely, HSCs can also develop into monocytes that differentiate into macrophages in response to various stimuli. These macrophage populations often rely on a steady supply of monocytes throughout adulthood. The figure was adapted from Mass et al., 2023[318].

Demonstrating remarkable plasticity, macrophages adapt to various microenvironments, fulfilling critical roles in immunity, tissue repair, and homeostasis[319]. Distinct macrophage subsets occupying specific tissues carry out specialized roles. For example, Kupffer cells in the liver tissue eliminate toxins and pathogens[320], while microglia contribute to brain equilibrium[321]. Additionally, macrophages within lymphoid organs, including marginal zone and medullary macrophages, regulate immune responses, clearing cellular debris and initiating antiviral defenses[322]. Intestinal macrophages maintain tolerance to the gut microbiota while combating enteric pathogens[323]. Alveolar macrophages are specialized phagocytic cells residing within the alveoli of the lungs[324]. These cells serve as an important component of the pulmonary immune system, functioning to engulf and eliminate inhaled pathogens, particulate matter, and cellular debris. In alignment with other tissue-resident macrophages, their role extends beyond phagocytosis, including the regulation of inflammatory responses, tissue repair, and the maintenance of lung homeostasis.

M1/M2 classification has been proposed to offer a simplified framework for understanding macrophage functional diversity[325, 326]. However, it is essential to recognize the significant heterogeneity in macrophage phenotypes across different microenvironments (**Figure 22**).

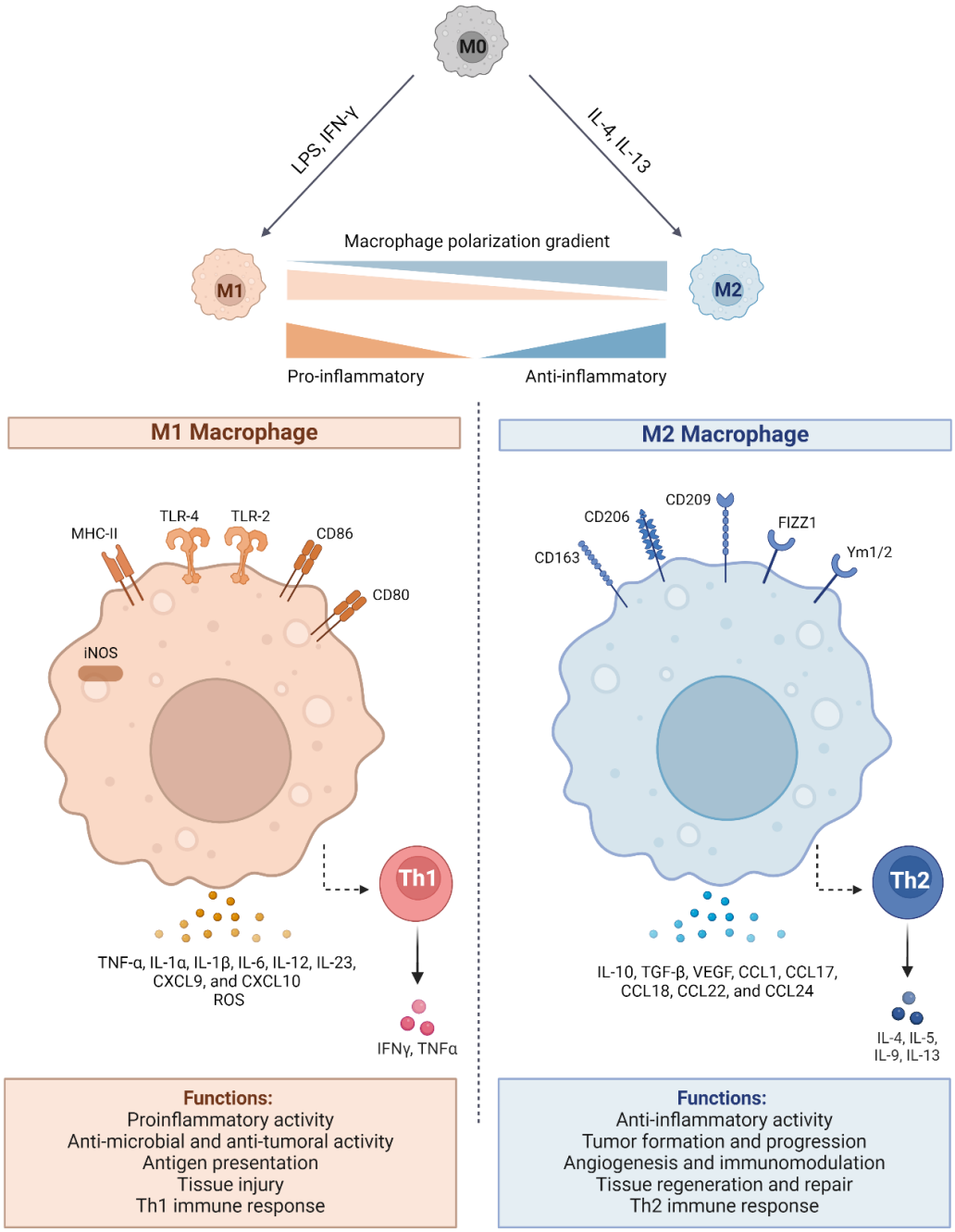

Figure 22: Comparison of M1 and M2 macrophages. The figure illustrates the key distinguishing features, activation cytokines, cellular markers, secreted molecules, and functional roles of M1 and M2 macrophages.

Primarily targeting intracellular pathogens, M1 macrophages are activated by IFN-γ and LPS. Excelling in phagocytosis and microbial killing, they produce pro-inflammatory cytokines (TNF-α, IL-1β, IL-6, IL-12) to recruit additional immune cells[327]. Moreover, they generate reactive oxygen species to eliminate

pathogens. M1 macrophages also present antigens to activate T cells, contributing to acute inflammation and potential tissue damage[328].

Predominantly involved in tissue repair, wound healing, and immune regulation, M2 macrophages are activated by IL-4 and IL-13[329]. They promote tissue remodelling and angiogenesis while suppressing inflammation through cytokines like IL-10 and TGF-β. Furthermore, they help with tissue repair, fibrosis, and responses to allergic reactions and parasitic infections.

Macrophages exhibit significant plasticity and heterogeneity, complicating their characterization within the complex TME[330, 331]. While initially contributing to anti-tumor responses, M1 macrophages often transition to an M2-like phenotype, promoting tumor growth along with tumor maturation. Indeed, most tumor-associated macrophages (TAMs) display M2-like characteristics.

The number and phenotype of macrophages dynamically evolve throughout tumor progression. Although their accumulation often correlates with early tumor growth, their prognostic value remains uncertain. As tumors advance, they actively recruit and reprogram macrophages towards the M2 phenotype[332]. Factors like CSF-1, secreted by cancer cells, contribute to TAM accumulation and M2 polarization by suppressing CD8+ T cell infiltration. Mature tumors harbour a dense population of M2-like macrophages, which secrete growth factors, inflammatory cytokines, and proteases to support cancer growth, angiogenesis, and invasion. These interactions create a positive feedback loop, exacerbating tumor malignancy and establishing macrophages as prognostic indicators of advanced cancer[333].

3.1.3.1. Tailoring therapeutics for macrophage engagement in cancer

Upon binding to target cells, antibodies activate Fcγ receptors (FcγRs) on macrophages, leading to the formation of a phagosome that engulfs and degrades the tumor cell. This is an important mechanism of action for several monoclonal antibodies, including daratumumab (anti-CD38) in multiple myeloma[334] and the anti-CD20 antibodies rituximab, ofatumumab in chronic lymphocytic leukemia[335]. Furthermore, Shi et al. (2015) demonstrated that macrophages play an important role role in trastuzumab-mediated cancer cell elimination, by engulfing antibody-opsonized tumor cells[336].

However, the presence of inhibitory FcγRs can hinder the clearance of cancer cells. To overcome this limitation, bispecific antibodies (BsAbs) have been developed that target both macrophage receptors and specific TAAs. BsAbs targeting Fc receptors have emerged as a promising therapeutic strategy to enhance ADCP. By engaging FcγRs and FcαRI, these BsAbs can effectively induce phagocytosis of tumor cells.

Additionally, BsAbs that interfere with checkpoint inhibitors, such as the SIRPα-CD47 pathway, have shown potential in overcoming immune evasion mechanisms employed by cancer cells.

Various FcγR-targeting BsAbs have been developed for different types of cancers. For example, MDX-210[337] and MDX-H210[338], targeting HER-2, were evaluated in clinical trials for HER2-positive cancers but were ultimately discontinued. H22xKi4 targeting CD30, demonstrated promising preclinical efficacy against lymphoma, however the compound failed to meet its primary endpoints in Phase I clinical trial and was subsequently discontinued.[339, 340].

Several FcαRI-targeting BsAbs have also been developed. For example, A77xKi-4 CD30 and A77x520C9 HER-2 are being investigated in preclinical models for lymphoma and carcinoma, respectively. CD20xFcαRI is being evaluated for B cell malignancies and lung cancer, while TrisomAb and gp75xFcαRI are being studied for colorectal cancer and melanoma, respectively.

Macrophages express SIRPα, an inhibitory receptor that can bind to CD47, a protein frequently overexpressed by cancer cells. This binding interaction transmits a "don't eat me" signal to the macrophage, enabling cancer cells to evade immune surveillance. Consequently, CD47/SIRPα-targeting bispecific antibodies (BsAbs) have emerged as a promising therapeutic approach. A notable example of such a BsAb was developed by Ring et al. in 2017. KWAR23 specifically targets SIRPα on myeloid cells and CD70 on cancer cells. CD70 is an antigen that exhibits limited expression in normal tissues but is highly expressed in various malignancies. This selective expression pattern makes CD70 an attractive therapeutic target for cancer immunotherapy.

FcαRI (CD89) is a receptor on neutrophils and macrophages that also can be targeted by bispecific myeloid cell engagers. These engagers, such as anti-CD20 × anti-FcαRI, can effectively mediate ADCC of cancer cells and stimulate tumor regression in animal models. These studies, along with other immune cell engagers, have been recently reviewed by Rolin et al. (2024)[341].

3.2. NK-cells

NK cells originate from CD34+ hematopoietic precursors in the bone marrow and develop through the common lymphoid progenitor (CLP) lineage[342]. Historically, human NK cells were primarily categorized into CD56bright and CD56dim subsets based on the density of CD56 on their surface and their capacity to kill target cells[343, 344, 345]. These subsets exhibit distinct characteristics in terms of function, appearance, and location within the body. Characterized by high levels of cytotoxic proteins (perforin, granzyme B), the CD56dim NK cell subset, which is predominant in the bloodstream, also expresses the activating CD16

receptor and multiple killer immunoglobulin-like receptors (KIRs). These cells effectively eliminate target cells and can also release cytokines in response to activating signals. Conversely, the CD56bright NK cell subset is less common in the bloodstream and primarily resides in lymph nodes. These cells display lower levels of perforin, granzyme B, and KIRs, and their primary role involves producing cytokines and chemokines in response to soluble factors.

Recent advances in single-cell RNA sequencing have unveiled a more nuanced understanding of NK cell diversity (**Figure 23**)[346, 347]. Unsupervised classification algorithms have identified three primary NK cell subsets with distinct tissue distributions: NK1, NK2, and NK3. Predominant in the blood and endowed with potent cytotoxic functions, NK1 cells correspond to the CD56dimCD16+ NK cell population. These cells are also abundant in the bone marrow and spleen. In contrast, NK2 cells, equivalent to CD56brightCD16- NK cells, exhibit a unique transcriptional profile marked by granzyme K, specific chemokines, and the TCF1 transcription factor. Enriched in the lungs, tonsils, lymph nodes, and intestines, NK2 cells demonstrate a distinct tissue tropism. Lastly, NK3 cells, primarily composed of CD16dim NKG2Chigh NK cells, exhibit memory-like characteristics and mount enhanced responses to diverse stimuli.

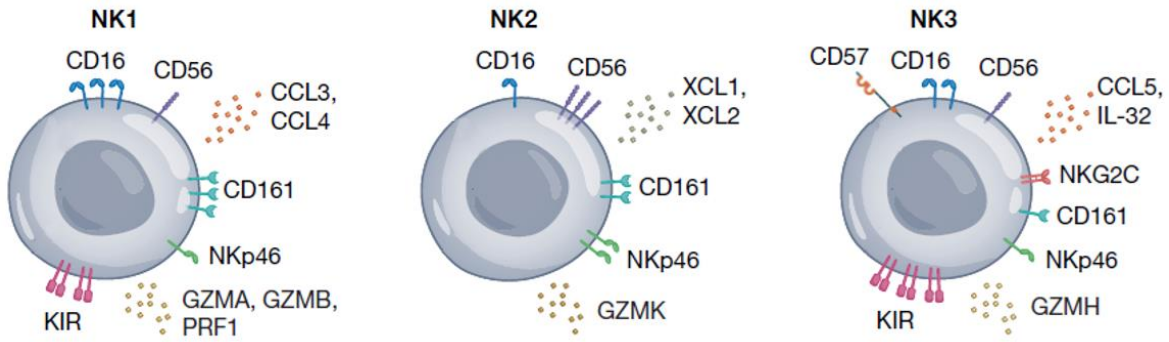

Figure 23: Characterization of human NK cell subsets in peripheral blood. Three distinct NK cell subsets exist: NK1, NK2, and NK3. This figure depicts the secreted molecules, and cell surface receptors that define each subset. Adapted from Vivier et al. (2023)[347]

3.2.1. The immunological synapse

The immunological synapse (IS) is a specialized intercellular junction formed when NK cells engage with target cancer cells[348, 349]. This dynamic structure undergoes distinct phases: recognition, initiation, effector phase, and termination[350].

Upon recognition of stress-induced or tumor-associated antigens, NK cells initiate adhesion through integrins and other adhesion molecules. This initial contact leads to the formation of the immunological synapse (IS), characterized by a central supramolecular activation cluster (cSMAC) containing signalling molecules including NKG2D, NKp46, KIRs, DAP10, DAP12, Src family kinases (Lck, Fyn), and Syk[351]. A peripheral supramolecular activation cluster (pSMAC) primarily composed of adhesion molecules[352].

Activated NK cells primarily exert their effector functions through two distinct mechanisms. These include the secretion of cytotoxic granules (NK-mediated cytotoxicity), composed of perforin, granzymes, and human-specific granulysin, as well as the engagement of death receptors through ligands like Fas ligand (FasL) and TNF-related apoptosis-inducing ligand (TRAIL)[353].

When NK cell receptors bind to cancer cell ligands, a signalling cascade is initiated. Receptor clustering and phosphorylation lead to adaptor protein recruitment and activation. Syk kinase is activated, initiating downstream signalling pathways, including calcium mobilization, MAPK activation, and PI3K activation[354].

Downstream signalling events converge to promote the directed movement of lytic granules containing perforin and granzymes to the IS. Lytic granules undergo exocytosis, releasing their contents towards the target cell[355]. Perforin, a pore-forming cytolytic protein, polymerizes to create transmembrane channels within the target cell membrane[356]. These perforin pores disrupt the integrity of the target cell, rendering it susceptible to the influx of cytotoxic molecules.

This disruption of membrane integrity facilitates granzyme internalization into the target cell. Granzymes initiate a cascade of apoptotic events, directly activating caspases such as caspase-3 and -7. Additionally, granzyme B indirectly induces apoptosis by cleaving Bid and Mcl-1, ultimately leading to the disruption of the mitochondrial outer membrane and the initiation of the intrinsic apoptotic pathway[357].

NK cells possess the ability to induce target cell death not only through the perforin-granzyme pathway but also via the death receptor pathway. NK cells express FasL and TRAIL, which can bind to death receptors on target cells[299, 353]. Activation of these receptors initiates a caspase cascade resulting in apoptosis.

NK cells have inhibitory receptors that bind to MHC-I molecules, protecting healthy cells from unintentional destruction. Binding of these inhibitory receptors counteracts activating signals and prevents NK cell-mediated cytotoxicity[358]. However, absent or decreased MHC-I presentation by cancer cells can lead to reduced inhibitory signalling, allowing NK cells to effectively target and eliminate tumor cells.

The final stage involves the termination of the interaction between the NK cell and its target. Following detachment, the NK cell either proceeds to serially kill additional targets or enters a state of exhaustion. Disruption at any point in this cascade of events can impair the killing of infected target cells.

3.2.2. NK cell receptors: a balance of activation and inhibition

The interplay between activating and inhibitory signals determines the result of the interaction between NK cells and cancer cells[359, 360]. A strong activating signal, coupled with reduced inhibitory signalling, can lead to efficient target cell killing. Conversely, a dominant inhibitory signal can prevent NK cell-mediated cytotoxicity, allowing cancer cells to escape immune surveillance.

Activating receptors are often stimulated by stress-induced molecules expressed by transformed or infected cells. Upon ligand engagement, NK cells initiate a cascade of intracellular signalling events culminating in cytotoxic granule release, cytokine production, and ADCC. For instance, NKG2D recognizes a variety of stress-induced ligands, such as MIC-A, MIC-B, and ULBPs, commonly expressed by tumor and virus-infected cells[361]. NKp46, another critical activating receptor, interacts with a diverse array of cellular ligands, including viral proteins and tumor-associated antigens[362].

Counterbalancing the stimulatory influence of activating receptors are inhibitory receptors. Primarily recognizing self-molecules, particularly MHC class I molecules expressed by healthy cells, these receptors attenuate NK cell activation, thereby safeguarding healthy tissue from inadvertent destruction. KIRs exemplify this category, binding to various MHC class I allotypes and exerting a highly polymorphic regulatory effect on NK cell function[363].

The equilibrium between activating and inhibitory signals serves as the ultimate determinant of target cell fate. A predominance of activating signals empowers NK cells to eliminate the target, whereas a dominant inhibitory signal prevents NK cell-mediated lysis. Furthermore, both receptor types are dynamically regulated by various stimuli, including cytokines, growth factors, and viral infections.

By manipulating the equilibrium between activating and inhibitory signals, it may be feasible to enhance anti-tumor activity while at the same time minimizing adverse effects.

3.2.3. NK cell therapies: a promising frontier

NK cell-based therapies have rapidly gained attraction as a promising modality in cancer treatment[364, 365, 366]. Two primary approaches are being investigated to enhance the antitumor response of NK cells.

Antibody-based therapies focus on enhancing NK cell activity through the use of immune checkpoint inhibitors, as well as by employing monoclonal antibody-derived NK engagers that stimulate activating NK cell receptors, such as NK cell engagers. The second therapeutic strategy involves the direct administration of modified NK cells to patients. These cells, which may be cultured, genetically engineered, or equipped with chimeric antigen receptors (CARs), exhibit enhanced antitumor properties.

3.2.3.1. Improving NK cell efficacy through antibody-based strategies

Several receptors like NKG2A, LAG3, TIM-3, and TIGIT, which function on both NK and T cells, can mediate this inhibition. The CD94-NKG2A receptor can be blocked by antibodies like monalizumab[367, 368]. This unleashes T cell and NK cell anti-tumor responses. Monalizumab is being studied in various lung cancer combinations. LAG3 interacts with MHC-II molecules and other proteins[369]. Its exact function is not fully understood, but it has become a promising target with over 20 therapies in clinical trials[370]. Relatlimab, combined with nivolumab, is approved for melanoma[371, 372]. Preclinical data suggests LAG3 blockade boosts NK cell anti-tumor immunity[373]. TIM-3 is higher in NK cells from cancer patients. Blocking TIM-3 reverses NK cell dysfunction in melanoma and lung adenocarcinoma patients but also restores NK cell killing in multiple myeloma[374]. TIGIT, expressed on T and NK cells, inhibits NK cytotoxicity and cytokine release and is expressed on NK cells in various cancers. Blocking TIGIT restores NK cell function and promotes anti-tumor immunity in different cancer models[375].

To enhance the therapeutic efficacy of NK cells, researchers have developed innovative biomolecules known as NK cell engagers (NKCEs)[376]. These engineered constructs redirect and amplify NK cell cytotoxicity towards specific target cells, such as cancer cells or those infected with viruses. Leveraging the inherent properties of NK cells, including rapid response, potent killing ability, and a favourable safety profile, NKCEs offer a promising therapeutic approach for cancer and infectious diseases[341].

One class of NKCEs, bispecific killer engagers (BiKEs), bridges NK cells and tumor cells. By simultaneously binding to CD16a on the NK cell and a tumor-associated antigen (TAA), BiKEs activate NK cells, leading to target cell destruction. Demonstrating their potential, BiKEs targeting CD16a and CD30 have shown promise in treating Hodgkin's lymphoma[377], while those targeting CD16a and BCMA are being investigated for multiple myeloma[378]. Early clinical studies have confirmed the efficacy of BiKEs against various TAAs in both haematological malignancies and solid tumors. Moreover, their potential to combat viral infections, particularly HIV, is under exploration[379].

Building on the BiKE platform, trispecific killer engagers (TriKEs) incorporate an additional functional element to augment NK cell activity and anti-tumor efficacy. The inclusion of cytokines like IL-15 or targeting additional NK cell activating receptors, such as NKp46, has shown improved preclinical outcomes[380]. TriKEs targeting specific TAAs are currently undergoing clinical evaluation for haematological malignancies, with GTB-3550, targeting CD16a, IL-15, and CD33, being tested for acute myeloid leukaemia (AML)[381]. Another TriKE targeting CD16a, NKp46, and CD123 has shown promise in preclinical models for AML treatment[382].

As the field of NK cell engager therapy progresses, tetraspecific killer engagers (TetraKEs) have emerged as a novel approach. By combining four distinct functional elements, TetraKEs aim to further optimize NK cell activation, target cell recognition, and anti-tumor response. While in early-stage development, TetraKEs targeting CD16a, two tumor antigens, and IL-15 or CD16a, NKp46, CD20, and the IL-2 receptor beta chain have shown potential for enhanced anti-tumor activity, particularly against CD20-low tumor cells[383]. The future of TetraKEs in revolutionizing cancer immunotherapy is promising.

3.2.3.2. Cell-based therapies

Adoptive cell transfer (ACT) is a therapeutic approach where a patient's immune effector cells are isolated, grown ex vivo, and readministered back into the patient to enhance their anti-tumor immunity. NK ACT therapy involves the manipulation of NK cells to improve their potency and persistence in the tumor microenvironment[384, 385]. There are two main approaches to ACT with NK cells: autologous and allogeneic[386].

Allogeneic NK cell therapy entails the administration of NK cells derived from a donor to a patient[387]. This approach offers several advantages. First, donor-derived NK cells can be prepared and stored, ensuring immediate availability for treatment. Second, these cells often demonstrate robust anti-tumor activity against a broad spectrum of cancer types. Finally, allogeneic NK cells carry a lower risk of graft-versus-host disease (GvHD) compared to T cells, a significant benefit. However, to mitigate the risk of rejection, patients undergoing allogeneic NK cell therapy typically require preconditioning with immunosuppressive drugs, which can lead to adverse side effects.

In contrast, autologous NK cell therapy utilizes the patient's own NK cells[388, 389]. This approach eliminates the risk of rejection, as the cells are genetically identical to the patient. Consequently, there is no need for preconditioning, reducing the potential for treatment-related side effects. Additionally, autologous NK cells may be specifically tailored to the patient's tumor, potentially enhancing treatment efficacy.

CAR-NK therapy is another promising approach in tumor immunotherapy, leveraging the natural cytotoxic capabilities of NK cells[390, 391]. By engineering these cells with CARs, researchers aim to improve their ability to target and eliminate cancer cells. CARs are engineered proteins composed of an extracellular antigen-binding domain and intracellular signalling domains, designed to activate immune cells upon target recognition.

CAR-NK cells differ from their T-cell counterparts in several key aspects[392, 393, 394]. While CAR-T cells have demonstrated exceptional effectiveness in haematological malignancies, challenges such as GvHD, complex manufacturing, and severe cytokine release syndrome (CRS) limit their broader application. In contrast, allogeneic CAR-NK cells possess intrinsic cytotoxicity, requiring no prior sensitization, and offer potential advantages including reduced GvHD risk, more consistent product quality, and a lower incidence of CRS. Their shorter lifespan compared to CAR-T cells is a factor to consider. Additionally, the inherent characteristics of NK cells, such as their resistance to the immunosuppressive TME, may confer benefits in solid tumor settings. Furthermore, the manufacturing process for CAR-NK cells is often more conducive to large-scale production compared to CAR-T cells.

CAR-NK cell therapies are being evaluated for various solid tumors. NKG2D is a target antigen for both ovarian and colorectal cancers. For ovarian, testicular, and endometrial cancers, CLDN6, AXL, GPC3, and mesothelin are being explored as potential targets[395]. TROP2 is being investigated as a target for lung, breast, ovarian, and pancreatic cancers[396]. Additionally, DLL3 is specifically targeted for small-cell lung cancer[397, 398]. PD-L1 is being explored as a target for gastric and head/neck cancers[399]. Finally, CD70 is under investigation for kidney, lung, and bone cancers[400].

4. CoMiX: A Novel Approach to Complement-Mediated Therapy

Targeted activation of complement is a promising approach for the development of new therapeutics against a range of diseases, including cancer and infectious diseases. By selectively triggering the complement system to attack specific target cells, this strategy offers the potential to achieve greater efficacy and specificity compared to traditional therapies.

The development of multivalent proteins represents a promising approach for enhancing therapeutic efficacy and selectively targeting cells for elimination through effector functions. The therapeutic potential of multimeric proteins, particularly those based on the Fc region of IgG, has gained significant attention due to their ability to mimic the immunomodulatory effects of intravenous immunoglobulin[401]. By inducing Fc multimerization, these molecules can enhance avidity and target specific FcγR-s, leading to

various effector functions such as ADCC and complement activation. Recent advancements in engineering techniques, like the use of the self-assembling tetramerization domain from p53, have enabled the creation of multivalent antibody formats, known as Quads[402]. These Quads offer a promising approach to increase binding potency and neutralize target molecules, such as TNF, with greater efficacy. By understanding the mechanisms underlying Fc multimerization and exploring novel engineering strategies, researchers aim to develop a new class of therapeutics with enhanced potency and specificity for autoimmune and inflammatory diseases.

C4BP, a plasma glycoprotein involved in complement regulation, presents a unique structural platform for developing such multivalent proteins[403, 404, 405]. Its modular architecture comprises multiple complement control protein (CCP) domains and C-terminal oligomerization domains (ODs) within its α and β chains. C4BP exists in four isoforms: the predominant 7α1β, and the less abundant α1β, 7α, and 6α isoforms. While the α chains, containing eight CCPs and one OD, are primarily responsible for complement inhibition through their N-terminal CCP1-CCP3 domains and binding ligands such as C3b, C4b, heparin, pentraxins, CD91, DNA, and microbial surface proteins, the β chains, composed of three CCPs and one OD, bind to protein S through its CCP1 domain and are involved in coagulation.

The OD domains within both α and β chains lack immunological function, making them ideal sites for grafting therapeutic peptides. The inherent ability of C4BP to form multimers, specifically heptamers for the α chain and dimers for the β chain, offers the potential to enhance the valency, binding affinity, stability, and pharmacokinetic properties of the attached peptides. By combining multiple peptides onto a single C4BP scaffold, it is possible to create complex molecules with tailored functionalities. By strategically positioning protein-binding domains on this platform, it is possible to optimize interactions with multimeric target receptors. The first study to utilize C4bp as a scaffold for multimerizing recombinant molecules was conducted by Libyh et al. in 1997[406]. They demonstrated the feasibility of creating a multivalent anti-Rh(D) recombinant protein by combining a single chain variable fragment (scFv) antibody binding site with a multimerizing domain from C4bp. Another study utilizing the C4bp scaffold was conducted in 2000 by Christiansen et al[407]. They created a chimeric fusion protein, sCD46-C4bpα, by linking the CD46 ectodomain to the C4bpα chain. The octameric form of this protein exhibited enhanced binding affinity to measles virus hemagglutinin, inhibited virus-induced cell-cell fusion, and protected mice from lethal measles virus infection.

Our group has previously demonstrated that this scaffold enables the creation of heteromultimeric immunoconjugates that selectively activate the complement system on tumor cells. We aimed to develop

a therapeutic strategy that would stimulate complement-dependent cytotoxicity on HER2-positive tumors. We designed conjugates consisting of FHR4 as a positive regulator of the complement alternative pathway, a targeting function against HER2, and a fluorescent protein serving as a tracking function[106]. By selecting the clones with high number of FHR4 molecules within the CoMiX molecules, we were able to overcome the complement inhibitory threshold (CIT) and enhance C3b deposition, membrane attack complex formation, and cancer cell lysis. Moreover, opsonized tumor cells were efficiently phagocytosed by macrophages. This technology has been patented in 2017 as "Multifunctional heteromultimeric constructs" (WO2017202776A1) and granted in 2022 in USA[408]. This patent describes the techniques for creating heteromultimeric protein complexes with specific ratios of different functional elements with either targeting-, tracking-, or effector functions. These complexes were designed to trigger complement-dependent cytolysis of cancer cells for our current study on HER2+ breast cancer cells. Using the C4bpα-scaffold anti-HER2 scFv-s derived from either Trastuzumab or Pertuzumab were coupled with the effector function of the Fc region or FHR4 through the OD domain of the C4BPα- or C4BPβ chain.

In 2023, we further developed dimeric protein complexes comprising two polypeptides, each with a functional component and the C-terminal OD of the C4bp beta-chain and patented the technology as "Dimeric protein complexes and uses thereof" (WO2023281120A1). The OD of the C4BP β chain was employed to fuse the targeting capabilities of anti-O11 or anti-Psl single-chain variable fragments (scFv-s) with the effector functions of either the Fc region (for classical pathway activation and immune cell recruitment) or the CCP3-5 domains of FHR1 (for alternative pathway activation and overcoming FH competition).

Both types of protein complexes were generated for the scope of this project and have potential applications in various targeted therapies for infectious diseases and cancer.

4.1. Directed-complement killing of *Pseudomonas aeruginosa* protects against lethal pneumonia

Pseudomonas aeruginosa (*P. aeruginosa*), a ubiquitous gram-negative bacterium, is a dangerous pathogen with a remarkable ability to adapt to diverse environments, including the human body. Its versatility and resilience have made it a significant cause of healthcare-associated infections, particularly in immunocompromised patients and those with chronic illnesses.

The clinical relevance of *P. aeruginosa* is highlighted by its association with a wide range of infections, including pneumonia, urinary tract infections, bloodstream infections, and skin infections. *P. aeruginosa*'s ability to form biofilms, microbial communities embedded in a self-produced matrix, is a major contributing factor to its recalcitrance to treatment. Moreover, *P. aeruginosa* can produce various virulence factors, such as exotoxins, proteases, and alginate, which contribute to its pathogenicity and exacerbate the severity of infections.

Current treatment strategies for *P. aeruginosa* infections typically involve a combination of antibiotics and supportive care. However, the emergence of antibiotic resistance, particularly to carbapenems and aminoglycosides, has limited the effectiveness of traditional therapies. This has led to a growing concern about the potential for untreatable *P. aeruginosa* infections. *P. aeruginosa* is part of the 2024 World Health Organization (WHO) Bacterial Priority Pathogens List for prioritization in research and development in the fight against antimicrobial resistance.

To address these challenges, our research group has pioneered a novel antibody-based therapeutic strategy: complement-activating multimeric immunotherapeutic complexes (CoMiX). These innovative molecules harness the power of the complement system to facilitate the elimination of *P. aeruginosa*, overcoming the limitations of existing treatments.

We designed two types of CoMiX molecules recognizing *P. aeruginosa*. Both constructs utilize the C-terminal oligomerization domain of C4bpβ to promote multimerization, thereby enhancing their potency.

ScFv-s are genetically engineered nanobodies designed to recognize and bind to specific molecular targets. An scFv consists of the variable heavy and light chain regions of an antibody, joined together into a single polypeptide chain. This unique structure allows the scFv to impart bacterial specificity, enabling it to target and interact with particular bacterial antigens. The two scFvs initially used in CoMiX were derived from either Panobacumab or MEDI3902. Panobacumab is a humanized monoclonal antibody that

binds to the O-polysaccharide moiety of *P. aeruginosa* serotype IATS O11. By neutralizing LPS, Panobacumab inhibits bacterial virulence and inflammation. Preclinical studies have demonstrated its efficacy in reducing lung inflammation and bacterial clearance in both neutropenic and immunocompetent mice infected with *P. aeruginosa*. The second scFv tested was derived from MEDI3902 (gremubamab), a novel bispecific antibody designed to target two distinct virulence factors of *P. aeruginosa*: PcrV protein and Psl exopolysaccharide. This dual-targeting approach effectively disrupts the bacterium's ability to cause cellular damage and colonize tissues. Preclinical studies have demonstrated MEDI3902's efficacy in preventing lethal infections and mitigating the production of inflammatory cytokines. For our molecular design, we focused exclusively on the anti-Psl component of MEDI3902 as a targeting system.

After evaluating two distinct scFvs on their binding capacities on primary clinical strains we also investigated two alternative effector functions. CoMiX-Fc and CoMiX-FHR1 engage different activating pathways. CoMiX-Fc, incorporating the Fc region of an IgG1 antibody, initiates the classical pathway, leading to opsonization and potential target cell lysis. In addition, it triggers Fcγ receptor-mediated cellular responses, such as phagocytosis by neutrophils and macrophages, and ADCC by NK cells. In contrast, CoMiX-FHR1 leverages the last three domains of FHR1 to initiate alternative pathway activation. These novel CoMiX platforms, with their distinct mechanisms of action, offer two therapeutic options to compare in this study to combat *P. aeruginosa* infections, particularly in high-risk populations.

4.1.1. Results

To explore the potential therapeutic applications of our CoMiX molecules, we conducted a comprehensive assessment of their interactions with *P. aeruginosa*. Our investigations focused on the molecules' ability to target bacterial strains, activate complement, enhance phagocytosis, and protect human bronchial epithelial cells from infection.

We initially compared the binding affinities of anti-Psl (derived from MEDI3902) and anti-O11 (derived from panobacumab) scFv-s to a panel of clinically relevant *P. aeruginosa* isolates. These strains, obtained from patients on mechanical ventilation in intensive care units or suffering from cystic fibrosis, included multiple multidrug-resistant isolates. The anti-O11 scFv's binding specificity was restricted to 20% of the clinical isolates, indicating a low occurrence of the O11 serotype.In contrast, the anti-Psl scFv exhibited significantly broader targeting, recognizing 82% of all strains, and was selected for therapeutic development.

Next, to validate the specificity of the anti-Psl targeting system, we examined its dose-dependent binding to two reference strains (PAO1, IP5944) and one selected clinical isolate (IPP6247290) resistant to multiple antibiotics. The molecule demonstrated highly specific recognition of *P. aeruginosa*. Conversely, the irrelevant control molecule with an scFv targeting *Aspergillus fumigatus* demonstrated no binding to *P. aeruginosa*.

Besides their specificity, both CoMiX-Fc and CoMiX-FHR1 significantly augmented C3b deposition and MAC (C5b9) formation on *P. aeruginosa* strains PAO1 and IPP6247290 compared to controls, in a dose dependant manner. CoMiX-Fc consistently demonstrated a more pronounced effect on C3b and C5b9 deposition than CoMiX-FHR1, suggesting a potentially enhanced ability to activate the complement cascade. Confocal microscopy corroborated these findings, visually demonstrating increased complement activation on bacterial cell surface.

Furthermore, CoMiX-Fc and CoMiX-FHR1 demonstrated direct killing efficacy against *P. aeruginosa* strains PAO1 and IPP6247290 in the presence of 10% normal human serum (NHS). Both CoMiX molecules significantly reduced bacterial viability by 40% (CoMiX-Fc) and 35% (CoMiX-FHR1), compared to controls, and exhibited synergistic effects with amikacin, an aminoglycoside antibiotic, enhancing bacterial killing compared to their individual use. The strongest synergy was observed at sub-MIC (minimum inhibitory concentration) concentrations of amikacin, specifically 2 μg/ml for the reference strain and 10 μg/ml for the clinical isolate. Remarkably, CoMiX-Fc consistently demonstrated a stronger synergistic effect with amikacin compared to CoMiX-FHR1, likely due to its enhanced ability to activate the classical complement pathway.

As another mode of action, CoMiX-Fc demonstrated a substantial increase in the phagocytosis of *P. aeruginosa* by PBMC M1-derived macrophages, but not FHR1. These findings suggest that only CoMiX-Fc can enhance phagocytosis through FcγRIIIa-mediated ADCP but not through C3b receptor-mediated CDCP with CoMiX-FHR1, two essential pathways for pathogen clearance.

To evaluate the safety and efficacy of CoMiX molecules, their effects were assessed on the BEAS-2B cell line, a human bronchial epithelial cell model. BEAS-2B cells are derived from the bronchial epithelium, the lining of the bronchi, and are used to study airway functions such as inflammation, mucus production, and ciliary beating. When used alone, CoMiX molecules were well-tolerated by these cells and did not induce any adverse effects. However, when tested on *P. aeruginosa*-infected cells, CoMiX-Fc, but not CoMiX-FHR1, significantly reduced *P. aeruginosa*-induced cytotoxicity as measured by lactate dehydrogenase

(LDH) release. Furthermore, both CoMiX molecules enhanced IL-6 production by BEAS-2B cells, suggesting a potential role in modulating the host immune response. These findings indicate that CoMiX-Fc may have protective effects against *P. aeruginosa*-mediated damage to bronchial epithelial cells and could contribute to a more effective immune response.

To evaluate CoMiX's efficacy in vivo, we administered two treatment regimens: prophylactic and therapeutic. In both cases, 8-week-old female mice were intranasally infected with a lethal dose of luciferase-positive *P. aeruginosa*. In the prophylactic regimen, the mice were intranasally treated with 100 µg of anti-Psl CoMiX-Fc, anti-Psl CoMiX-FHR1, or an irrelevant control 3 hours before and 3 hours after infection. All control mice had to be euthanized within 48 hours, whereas all treated mice survived until Day 2. After 6 days, survival rates were 87% for the anti-Psl CoMiX-FHR1 group and 62% for the anti-Psl CoMiX-Fc group. Treated mice began to regain weight after Day 3. Bioluminescence imaging revealed lung colonization by *P. aeruginosa*. Luciferase activity was assessed at 24 and 48 hours post-infection. The control group exhibited a high bacterial burden in the lungs, while both treatment groups demonstrated a clear lung phenotype with the infection localized to the nasal cavity. The percentage of luciferase-positive mice in each group was measured on days 1 and 2. All control mice were luciferase-positive on both days. In contrast, the CoMiX-Fc and CoMiX-FHR1 groups exhibited significantly lower percentages of luciferase-positive mice. Specifically, 43% of CoMiX-Fc-treated mice and 37% of CoMiX-FHR1-treated mice were positive on day 1. These percentages decreased to 18% and 25%, respectively, on day 2.

The therapeutic regimen was similar to the prophylactic regimen, except that the molecules were administered only once, 1 hour after infection. Mice treated with CoMiX-Fc or CoMiX-FHR1 exhibited significantly higher survival rates than the control group. Body weight changes were comparable across all groups. The percentage of luciferase-positive mice was also assessed on days 1, 2, and 3.

To elucidate the mechanisms underlying CoMiX's protective effect against acute *P. aeruginosa* infection in the therapeutic protocol, we conducted a comprehensive analysis. Macroscopic observations revealed that mice treated with the irrelevant CoMiX control exhibited severe lung injury characterized by hemorrhagic lungs. In contrast, mice treated with CoMiX-Fc or CoMiX-FHR1 displayed less severe lung damage with reduced hemorrhage and visible areas of healthy tissue. Bacterial load measurement demonstrated that mice treated with the irrelevant CoMiX control had significantly higher bacterial loads in the bronchoalveolar lavage (BAL) and lungs compared to CoMiX-Fc or CoMiX-FHR1-treated mice. Notably, CoMiX-Fc and CoMiX-FHR1 treatments rapidly reduced bacterial load, suggesting a direct antimicrobial effect. Complement activation was assessed, and results indicated that CoMiX-Fc and

CoMiX-FHR1 induced higher levels of cleaved C3 fragments in the blood compared to the irrelevant control. Complement activation was observed early at 4 hours post-infection (*p.i.*) and subsequently decreased by 16 hours *p.i*. Immune cell response analysis revealed that CoMiX-Fc and CoMiX-FHR1 treatments resulted in fewer total immune cells in the BAL. Furthermore, specific immune cell populations, including neutrophils, macrophages, and eosinophils, were also reduced in these groups. Inflammatory cytokines were measured, and IL-6 levels were found to be significantly decreased in CoMiX-Fc and CoMiX-FHR1-treated mice compared to the irrelevant control.

In conclusion, our findings demonstrate the significant therapeutic potential of CoMiX molecules against *P. aeruginosa* in acute lung infections. Both CoMiX-Fc and CoMiX-FHR1 displayed promising properties, including broad targeting of *P. aeruginosa* strains, enhanced complement activation, and protection of bronchial epithelial cells from bacterial damage. In addition, in vivo studies revealed superior survival rates and reduced bacterial burden in mice treated with both CoMiX molecules compared to controls.

4.1.2. Discussion

Multidrug-resistant *P. aeruginosa* is a significant public health concern due to its ability to resist a broad spectrum of antibiotics. Its inclusion as a high-priority pathogen in the World Health Organization's (WHO) updated Bacterial Priority Pathogens List (BPPL) 2024 underscores the urgent need for innovative therapeutic strategies. The bacterium's prevalence in healthcare settings, where it can easily spread among patients, exacerbates its public health impact. This often leads to outbreaks, increasing morbidity and mortality rates. Given its global distribution and ability to affect people of all ages, the burden of *P. aeruginosa* infections is substantial.

In response to the urgent global health threat posed by *P. aeruginosa*, our research team has developed novel complement-activating immunotherapeutic complexes (CoMiX) as a potential therapeutic solution. Our findings suggest that by leveraging the complement system's potent effector functions, CoMiX could potentially overcome the limitations of traditional antibiotic therapies and provide a valuable therapeutic option for infected patients with targeted bacteria resistant to multiple drugs.

In the present study, we developed two unique CoMiX constructs, CoMiX-Fc and CoMiX-FHR1, specifically designed to initiate the classical and alternative complement pathways for the elimination of *P. aeruginosa,* respectively. CoMiX-Fc, through its Fc region, activates the classical pathway and mediates phagocytosis through Fcγ receptor engagement, while CoMiX-FHR1 enhances the alternative pathway by competitively inhibiting FH, the main negative regulator of complement activation. Our findings support

the notion that FHR-1 plays a crucial role in promoting opsonization by disrupting FH-mediated complement inhibition, aligning with previous studies on Group A Streptococcus, Plasmodium falciparum, and other biological contexts.

CoMiX's innovative structure is specifically tailored to target *P. aeruginosa* by utilizing an scFv directed against the exopolysaccharide Psl. Psl, a key virulence factor, plays a crucial role in promoting adhesion (initial step of biofilm formation), cell-cell interactions, and immune evasion. Previous research has demonstrated the efficacy of anti-Psl antibodies in hindering *P. aeruginosa* infections by preventing attachment of bacteria to epithelial cells and facilitating phagocytosis by immune cells. Notably, Psl is highly prevalent in clinical isolates, particularly those associated with non-cystic fibrosis infections. Our findings align with this, showing broad recognition of our Psl-targeting scFv across a variety of clinical isolates, including multi-drug-resistant strains.

Both CoMiX molecules facilitated the deposition of complement components C3b and C5b9 onto the target cell surface, leading to their opsonization and elimination by immune cells. Since CoMiX exhibited a synergistic effect with amikacin, a broad-spectrum aminoglycoside antibiotic widely used in clinical practice, their combination could allow for lower therapeutic doses of amikacin, reducing the risk of adverse side effects, improving efficacy against antibiotic-resistant strains and preventing the development of further resistance. Amikacin while effective, can indeed cause common significant side effects such as nausea, vomiting, diarrhea, and headache, but also lead to more serious adverse reactions, including hearing loss, kidney damage, and hypersensitivity reactions.

The timely clearance of *P. aeruginosa* from the lungs is crucial to prevent severe respiratory complications, such as pneumonia, sepsis, and respiratory failure. Our data demonstrate that CoMiX treatment significantly modulates the host immune response, facilitating this clearance, and revealed no evidence of toxicity to the BEAS-2B human bronchial epithelial cell line, suggesting a favourable safety profile. Notably, we observed a marked increase in IL-6 production by human bronchial epithelial cells. Elevated IL-6 levels are well-established to promote enhanced neutrophil recruitment, phagocytosis, and macrophage efferocytosis, which are key downstream effector mechanisms critical for bacterial clearance.

Finally, in vivo studies in a murine model of acute *P. aeruginosa* lung infection further demonstrated both the therapeutic and prophylactic potential of CoMiX. Both prophylactic and therapeutic CoMiX treatments significantly improved survival and reduced bacterial load compared to a control group receiving

irrelevant CoMiX-Fc. While CoMiX-FHR1 showed slightly better prophylactic efficacy, CoMiX-Fc was more effective therapeutically, possibly due to the two model variabilities. Infection severity differed between control groups in prophylactic and therapeutic treatments, likely influenced by factors like initial bacterial load, host susceptibility, and experimental conditions. In the prophylactic treatment, the control group experienced a more severe infection, leading to complete mortality within 48 hours.

While previous studies using antibodies targeting *P. aeruginosa* have shown potential in preclinical and early clinical stages, large-scale trials have not consistently demonstrated significant efficacy. For instance, MEDI3902, a bispecific antibody designed to bind both the exopolysaccharide Psl and the Type III Secretion Protein PcrV, initially displayed promising results but ultimately failed to significantly reduce nosocomial pneumonia in late-phase trials. These findings emphasize the limitations of solely antibody-based approaches. CoMiX offer several advantages over traditional antibody-based therapies. For example, the Psl targeting system in CoMiX enables broader recognition of *P. aeruginosa* isolates compared to Panobacumab, which only targets a limited subset. Additionally, CoMiX facilitates rapid and localized activation of the complement system, leading to efficient bacterial clearance at the early stages of infection. Furthermore, CoMiX-FHR1 molecules engage the alternative pathway of the complement system, resulting in a more robust immune response compared to relying solely on the classical pathway.

CoMiX has therefore potential versatility for clinical applications, as it could be used to prevent infections in high-risk individuals or to treat established infections. CoMiX could enhance traditional antibiotics like antipseudomonal penicillins, cephalosporins, carbapenems, aminoglycosides, and fluoroquinolones, especially for chronic infections or antibiotic-resistant strains. Additionally, CoMiX could be used with non-antibiotic therapies like surgical drainage, wound care, and supportive measures. For chronic infections, inhaled antibiotics and mucolytic agents might complement CoMiX. Beyond treatment, CoMiX could be used preventively before surgery in immunocompromised patients or in intensive care units (ICUs) to reduce the risk of healthcare-associated infections.

The versatility of CoMiX's modular design lies in its ability to tailor both targeting and effector functions. This allows for the creation of highly specific therapeutics for diverse diseases. For instance, in chronic infections, CoMiX could be equipped with effector components to target quorum sensing and biofilm formation. Potential additions include quorum sensing inhibitors, such as natural brominated furanones or synthetic halogenated furanones, to disrupt bacterial communication and virulence. Additionally, biofilm formation inhibitors like enzymes like dispersin B from bacteria or synthetic peptides could be

integrated to disassemble existing biofilms and prevent new ones from forming. This adaptability makes CoMiX a promising platform for developing innovative solutions to address complex medical challenges.

By preventing infections or treating them early, CoMiX could potentially lead to significant improvements in patient outcomes and a reduction in healthcare costs across various clinical settings. This includes its application in homecare centers for the elderly, ICUs, pre-surgery care for immunocompromised patients, and as a local treatment for infections, potentially reducing the need for systemic antibiotics. Such reductions can contribute to faster healing and mitigate the risk of antibiotic resistance. Before CoMiX can be widely adopted, rigorous clinical trials must thoroughly evaluate its safety and efficacy in these specific applications.

4.2. Complement-Activating Multimeric Immunotherapeutic Complexes for HER2-breast cancer immunotherapy

Breast cancer remains a significant global health burden, with the HER2-positive subtype posing unique challenges. While monoclonal antibodies have revolutionized treatment, resistance and limited efficacy remain pressing concerns.

In the present article, we have developed a novel therapeutic approach for HER2+ breast cancer: complement-activating multimeric immunotherapeutic complexes (CoMiX). These innovative molecules leverage the complement system to enhance tumor cell elimination, addressing the challenges of resistance and limited efficacy associated with current therapies. CoMiX incorporates FHR4 (CoMiX-FHR4), a complement regulatory protein, to de-regulate complement inhibition and activate the complement amplification loop. We have further engineered CoMiX-Fc, a variant featuring a multimeric Fc domain, to enhance the complement classical pathway and immune cell activation targeting HER2-expressing tumor cells.

CoMiX incorporate the tumor-targeting capabilities of Variable Heavy domains (VHH) derived from the therapeutic antibodies trastuzumab or pertuzumab. They possess two different effector functions, either the Fc region of IgG1 antibodies or FHR4. The targeting (VHH) and effector functions (Fc or FHR4) are linked through an oligomerization domain derived from C4BP. This scaffold enables multimerization without activating the immune system. This unique combination allows CoMiX molecules to potentially interact with and modulate the immune response against targeted cells. The Fc-based CoMiX (CoMiX-Fc) contains a hinge segment inserted before the IgG1 constant CH2-CH3 domains, while the FHR4-based

CoMiX (CoMiX-FHR4) lacks this hinge region and instead incorporates the FHR4 effector function. The hinge region plays a critical role in the structural integrity and functional capabilities of CoMiX. Characterized by its high proline content, this region allows for independent movement of the scFv fragments enhancing their ability to recognize and bind their bacterial antigens.

4.2.1. Results

Both CoMiX demonstrated potent complement activation and tumor cell death. C3b and C5b9 deposition, along with complement-dependent cytotoxicity (CDC), were increased on HER2+ BT474 tumor cells. Notably, combining the different CoMiX led to significantly enhanced complement activation and cytotoxicity compared to individual treatments.

We first determined the complement pathway activation mechanism by which both CoMiX induce C3b deposition and CDC in the presence or absence of Ca^{2+} ions. Ca^{2+} is a prerequisite for the activation of the classical and lectin complement pathways. Conversely, the alternative pathway can be initiated independently of Ca^{2+}. CoMiX-FHR4 molecules retained their complement-activating properties in the absence of Ca^{2+}, indicating their utilization of the alternative pathway. In contrast, CoMiX-Fc-s and therapeutic antibodies lost their activity, suggesting their dependence on the classical pathway.

Fc-based CoMiX molecules possess multiple Fc regions within their structure, prompting the investigation of their potential to activate NK cells. NK cells bind to FcγRIIIa receptors (CD16) on IgG antibodies and mediate target cell destruction through ADCC. CoMiX-Fc molecules, particularly VHH(P)/Fc, significantly upregulated the degranulation marker CD107a and IFN-γ expression on NK cells, indicating NK cell activation. The hinge region was indispensable for the effective activation of NK cells by CoMiX-Fc molecules. In the absence of the hinge, these molecules failed to induce NK cell activation.

Previous studies have demonstrated that FHR4 can effectively induce complement-dependent phagocytosis of tumor cells mediated by macrophages. In this study, we sought to compare the relative abilities of CoMiX-Fcs, CoMiX-FHR4s, therapeutic antibodies, and their various combinations to stimulate phagocytosis of BT474 cells. This comparative analysis aimed to provide a deeper understanding of the cellular mechanisms underlying tumor cell clearance. CoMiX-VHH(P)/Fc significantly enhanced phagocytosis, while CoMiX-VHH(T)/Fc did not. Enhanced phagocytosis was observed with all CoMiX molecule/therapeutic antibody combinations, excluding the trastuzumab/pertuzumab and trastuzumab/FHR4(VHH(P)). These findings confirmed the functionality of Fc/FcγR interactions in CoMiX-Fc mediated phagocytosis and the essential role of the hinge region for functional CoMiX-Fc assembly.

To evaluate the potency of CoMiX in inhibiting tumor growth, a xenograft mouse model utilizing BT474 cells sensitive and resistant to trastuzumab was employed. Treatment with CoMiX-FHR4 molecules lead to a substantial reduction in tumor volume compared to control groups. Notably, CoMiX-FHR4 demonstrated effectiveness in suppressing tumor growth even in mice bearing trastuzumab-resistant BT474 cells. CoMiX-FHR4 exhibited superior infiltration into tumor tissue compared to CoMiX-Fc molecules, leading to widespread complement activation within the tumor mass. This suggests that CoMiX-FHR4 may be a more potent therapeutic agent for targeting and eradicating tumors, having a distinct mode of action that the standards of care trastuzumab or pertuzumab. Trastuzumab showed a superior anti-tumor activity in xenografts sensitive to trastuzumab as compared to both CoMiX, while CoMiX-Fc with the scFv derived from pertuzumab was superior to pertuzumab in reducing tumor growth.

Immunohistochemistry analysis was also conducted on xenografts at day 25 or when they reached a volume of 1000 mm^3. Xenografts from mice treated with trastuzumab or various combinations exhibited significant leukocyte infiltration, which was less prominent in those treated with FHR4-VHH(T), FHR4-VHH(P), or VHH(P)/Fc. Within these infiltrates, NK cells were detected in multiple areas, while T cells were more concentrated at the tumor periphery or near blood vessels in mice treated with trastuzumab, VHH(P)/Fc, FHR4-VHH(P), and FHR4-VHH(T). All combination treatments resulted in substantial leukocyte infiltration, including NK and T cells. Serum analysis revealed varying levels of anti-HER2 antibodies in mice treated with different drugs compared to PBS. While statistical significance was not reached, a tendency towards higher anti-HER2 antibody levels was observed in trastuzumab-treated mice and those receiving trastuzumab plus pertuzumab.

Our in vitro studies and animal experiments collectively demonstrate the proof of concept that targeted complement activation on HER2+ breast cancer cells can be a therapeutic option, particularly in trastuzumab-resistant tumors.

4.2.2. Discussion

HER2-targeted therapies have revolutionized the treatment of HER2+ breast cancer, significantly improving patient outcomes. Trastuzumab and pertuzumab are commonly used first-line treatments for advanced disease. However, the emergence of resistance to these therapies remains a clinical challenge. Novel therapeutic approaches are urgently needed to address this issue.

Directed complement activation through immunotherapy presents a promising opportunity for overcoming anti-HER2 therapy resistance. The classical complement pathway's fundamental role in the

therapeutic efficacy of Rituximab, a chimeric IgG1 monoclonal antibody, highlights the complement system's cancer-fighting potential. As demonstrated by Lara et al. (2022), CDC is a key mechanism of action for Rituximab to eradicate CD20+ B-cell lymphoma.

Factor H (FH), a pivotal plasma complement regulator, can be exploited by pathogens and tumor cells to avoid opsonization and lysis. Factor H-related protein 4 (FHR4) has been identified as a positive regulator of the alternative complement pathway. FHR4 shares structural similarities with FH, especially in domains 6 to 9 and the C-terminal domains 19, and 20, which are involved in C3b binding. FHR4 binds to C3b on cell surfaces, competing with FH and thereby promoting immune activation. On the other hand, FHR4 lacks the regulatory domains of FH, preventing it from inactivating C3b. Upon binding to C3b, FHR4 facilitates the attachment of FB and properdin, leading to the formation of FHR4-C3bBb convertases that are resistant to FH-mediated decay. This amplification of the complement cascade enhances opsonization and aids in the recognition of dying cells or pathogens by the host's immune system, ultimately resulting in their elimination through direct cell killing or phagocytosis. Our earlier research indicated that BT474 tumor cells exhibit a threshold of complement inhibition. This threshold can be surpassed by directing CoMiX molecules with high FHR4 valences to the tumor cell surface.

In this study, we investigated the complement-activating potentials of CoMiX-FHR4 and compared it to a novel type of CoMiX-Fc against HER2+ BT474 cancer cells. The triple Fc dimers in CoMiX-Fc-s mediates multiple effector functions, including ADCC, ADCP and CDC through classical complement pathway activation.

Both types of molecules effectively activated complement in vitro and in a mouse xenograft model, leading to direct tumor cell lysis. FHR4/VHH(T) and FHR4/VHH(P) exhibited substantially greater in vitro complement activation and complement-dependent cytotoxicity than CoMiX-Fcs and therapeutic antibodies used in clinical practice. CoMiX-FHR4 molecules preferentially activate the alternative complement pathway, which is calcium-independent, while CoMiX-Fc-s primarily activate the calcium-dependent classical pathway. This dual activation mechanism offers a potential advantage, as the alternative pathway remains active even in environments with reduced calcium levels, which can be beneficial in various conditions, such as hypocalcemic states or certain tumor microenvironments. Moreover, CoMiX-Fc molecules were observed to stimulate NK cells and induce phagocytosis of tumor cells by M2 macrophages.

In vivo experiments revealed, at first, the tumor growth-inhibitory effects of CoMiX in a murine xenograft model using BT474 cells sensitive to trastuzumab. Following systemic administration, CoMiX rapidly penetrate the tumor tissue, demonstrating efficient distribution within the tumor environment. Within six hours of injection, a robust activation of the complement system was detected within the tumor, indicating that the CoMiX molecules could effectively engage and trigger the immune response. FHR4/VHH(T), FHR4/VHH(P), and VHH(P)/Fc demonstrated significant tumor growth inhibition, whereas the VHH(T)/Fc molecule exhibited reduced efficacy. This diminished effectiveness can be attributed to its impaired ability to induce macrophage phagocytosis and NK cell degranulation. In contrast, the VHH(P)/Fc molecule demonstrated superior capabilities in these immune effector functions, likely contributing to its enhanced tumor-suppressing activity. These data suggest than the scFv binding to the pertuzumab epitope could induce a better presentation of the Fc dimers to the cellular FcγR than the ScFvs binding to the trastuzumab epitope. Trastuzumab emerged as the most effective treatment in this study, suggesting that its combined effects of complement activation, cell signalling inhibition, and ADCC / ADCP are more beneficial in combating tumor growth than complement activation alone. Specifically, trastuzumab's ability to target a specific epitope on the HER2 receptor, distinct from the epitope targeted by pertuzumab, appears to be crucial for these enhanced therapeutic effects. Notably, VHH(P)/Fc outperformed pertuzumab in reducing tumor progression in the in vivo xenograft model. This superior efficacy can potentially be attributed to VHH(P)/Fc's enhanced ability to activate NK cells and initiate phagocytosis through complement and Fc gamma receptors.

The simultaneous use of two CoMiX-FHR4 molecules targeting distinct HER2 epitopes resulted in a significant amplification of opsonization by C3b deposition, MAC assembly, CDC, and overall therapeutic efficacy in vivo. While this combination demonstrated promising results, its efficacy still fell short of that achieved by trastuzumab. However, when evaluated against a BT474 cell line resistant to trastuzumab, the most effective combination of FHR4/VHH(T) and FHR4/VHH(P) exhibited a pronounced tumor growth suppression up to 25 days when the tumor relapsed.

Immunohistochemistry revealed significant leukocyte infiltration in xenografts treated with trastuzumab or its combinations, with NK and T cells being prominent. Among the VHH-based treatments, FHR4-VHH(T), FHR4-VHH(P), and VHH(P)/Fc showed less pronounced leukocyte infiltration. Serum analysis showed a trend towards higher anti-HER2 antibody levels in trastuzumab-treated mice and those receiving trastuzumab plus pertuzumab, although statistical significance was not reached.

These findings suggest that CoMiX-FHR4 molecules may offer a potential therapeutic option for patients with trastuzumab-resistant HER2-positive breast cancer. An optimization of dose and timing for drug delivery is necessary to achieve tumor remission.

Advances in HER2 breast cancer treatment currently focus on antibody-drug conjugates (ADCs), including trastuzumab-emtansine and trastuzumab deruxtecan or bispecific antibodies that target two different HER2 epitopes for increased effectiveness. Dual HER2 inhibition with trastuzumab and pertuzumab has shown improved outcomes in patients with HER2+ metastatic breast cancer compared to single-agent HER2 inhibition. The CoMiX approach, which uses dual HER2 targeting, may overcome limitations in HER2 binding. It is therefore possible that a future CoMiX including both HER2 targeting, could enhance its effectiveness in its current form or when used as an ADC or in combination with a checkpoint inhibitor. Various strategies to stimulate the immune response against HER2+ tumor cells are being investigated, and CoMiX may offer such possibilities.

The complement system is a tightly regulated inflammatory process. Membrane-anchored complement regulatory proteins and soluble complement inhibitors prevent excessive complement activation on host cells. This regulation prevents excessive complement activation on healthy cells, making it a potentially safe anti-cancer therapy when focused on targeted tumor cells. By targeting complement activation specifically to tumor cells, CoMiX-based therapies could represent a safe and effective anticancer approach. Unlike existing antibody treatments like trastuzumab, external recruitment of the complement system is highly unlikely to induce treatment resistance.

It is important to note that complement components can influence the tumor microenvironment, affecting both tumor growth and suppression. A comprehensive understanding of these mechanisms will be crucial for the clinical development of CoMiX.

CoMiX-based therapies could potentially offer advantages over other immunotherapeutic approaches, such as checkpoint inhibitors, by targeting a different mechanism of tumor cell elimination. CoMiX molecules could be combined with other therapies, such as chemotherapy or radiation therapy, to enhance their efficacy. Further studies are needed to evaluate the safety and tolerability of CoMiX-based therapies in patients.

In conclusion, our findings demonstrate that targeted complement activation can effectively reduce tumor growth in vivo and that CoMiX are as effective as pertuzumab, potentially overcoming trastuzumab resistance. Combining the two CoMiX designed against trastuzumab and pertuzumab further enhances

tumor growth inhibition, suggesting synergistic therapeutic effects. Given the high rate of resistance to conventional monoclonal antibodies, CoMiX could be valuable second-line treatments, particularly when trastuzumab resistance arises.

CoMiX's unique mechanism of action, which involves rapid and efficient complement activation within tumors, distinguishes it from trastuzumab and pertuzumab. This approach holds promise for stimulating the immune response and potentially circumventing resistance mechanisms associated with HER2-targeted therapies.

5. Conclusions and Perspectives

The two studies presented here provide the proof of concept of directed-complement activation on target cells for further killing and inducing the immune response. Our work highlights the promising potential of complement-activating multimeric immunotherapeutic complexes (CoMiX) as a novel therapeutic approach for both *P. aeruginosa* infections and HER2-positive breast cancer. These diseases were selected due to their increasing prevalence and the emergence of resistance mechanisms, which pose significant challenges to current treatment options.

P. aeruginosa has developed resistance to a wide range of antibiotics through various mechanisms, including efflux pumps, β-lactamase production, altered porin proteins, and target site modifications. Additionally, its ability to form biofilms creates a protective barrier, often leading to chronic and difficult-to-treat infections.

Similarly, HER2-positive breast cancer, defined by the overexpression of the HER2 protein, presents significant challenges due to its aggressive nature and the emergence of resistance to targeted therapies like trastuzumab and pertuzumab. Factors such as HER2 gene amplification, HER2 mutations, altered downstream signalling pathways, and immune escape contribute to resistance. Furthermore, the high metastatic potential of HER2-positive breast cancer poses significant challenges for treatment once the disease has spread.

By leveraging the complement system's potent effector functions, CoMiX offers a potential solution to these challenging diseases. By effectively targeting and eliminating both pathogens and cancer cells, CoMiX may provide a new approach for therapeutic intervention.

All CoMiX are comprised of three distinct functional components: a targeting scFv, an oligomerization domain, and an effector component. The oligomerization scaffold utilized differed between the two studies. In the HER2+ breast cancer study, the molecules employed the alpha chain of C4BP to facilitate multimerization, typically forming hexa- and heptamers whereas the *P. aeruginosa* study utilized the oligomerization domain of the beta chain, resulting in the formation of dimers.

Both studies demonstrated that CoMiX effectively activated the complement system, initiating both the classical and alternative pathways. In the study focusing on *P. aeruginosa*, CoMiX utilize FHR1 as an effector function to activate the alternative complement pathway. In the study on HER2-positive breast

cancer, CoMiX incorporated FHR4 to enhance complement activation on tumor cells. Both FHR1 and FHR4 share a high sequence similarity with FH, the main soluble inhibitor of the alternative pathway and amplification loop but lack the regulatory functions of FH. Both FHR1 and FHR4 compete with FH for antigen binding and for binding to C3b, a central activation product and opsonin.

This activation leads to opsonization, phagocytosis, and direct cell killing. Notably, CoMiX shows particular promise in addressing resistance mechanisms. In the HER2-positive cancer model, CoMiX delayed the onset of resistance, potentially "buying time" for surgical intervention or chemotherapy. While antibiotics remain a cornerstone of P. aeruginosa infection treatment, CoMiX offers a promising strategy to overcome antibiotic resistance, as demonstrated by synergistic effects observed in combination with amikacin. These findings establish a strong proof-of-concept for developing novel CoMiX-based therapies with significant therapeutic potential.

Moreover, in vitro and in vivo studies suggest that CoMiX have minimal toxicity to host cells, indicating favourable safety profiles. While these studies provide compelling evidence for the therapeutic potential of CoMiX, further research is necessary to fully pursue their clinical application. Building on these results, the next research phase should focus on addressing challenges and maximizing CoMiX benefits. To mitigate resistance in the HER2-positive breast cancer model, a novel CoMiX construct with two scFvs targeting both trastuzumab and pertuzumab epitopes can be developed. Immunogenicity studies in immunocompetent mice should be conducted to assess safety and tolerability. In vivo studies will determine the optimal CoMiX dose and administration timing for maximizing immune cell activation. Pharmacokinetic investigations will define CoMiX half-life, which is anticipated to be shorter than that of traditional therapeutic antibodies (>28 days). In the *P. aeruginosa* infection model, CoMiX efficacy against biofilms, a significant challenge in chronic infections like COPD and cystic fibrosis, should be evaluated. To enhance clinical relevance, a more sophisticated in vitro human lung model should be established. This model will likely involve an air-liquid interface (ALI) culture, which mimics the physiological environment of the lung. ALI cultures allow lung cells to be grown on a permeable membrane, with one side exposed to air and the other to a liquid medium, promoting the formation of a more physiologically relevant tissue structure and allowing for the study of interactions with airborne substances, such as bacteria or therapeutic agents like CoMiX.

A crucial aspect of preclinical research, particularly for novel immunotherapeutics like CoMiX, involves the use of animal models, most commonly mice, to assess both efficacy and safety. While mouse models offer valuable insights, translating findings from these preclinical studies to humans presents significant

challenges, particularly in the context of complement research. The mouse and human complement systems, while sharing core components, exhibit notable differences in several key aspects. These include variations in the specific sequences and structures of complement proteins, which can affect their interactions with CoMiX and target cells. For example, the binding affinity of CoMiX for mouse C3 or C4 might differ from its affinity for human C3 or C4, influencing the strength and duration of complement activation. Furthermore, the regulatory mechanisms governing complement activation can vary between species. Mice may express different levels or isoforms of complement regulators like Factor H or CD59, potentially leading to exaggerated or diminished complement activation compared to humans. This is particularly relevant for CoMiX, which are designed to manipulate complement activation. The mouse immune system as a whole, beyond just the complement cascade, may respond differently to complement activation induced by CoMiX. For instance, the recruitment and activation of immune cells like neutrophils and macrophages, which are crucial for CoMiX-mediated target cell clearance, might differ between mice and humans. This could impact the overall therapeutic efficacy observed in preclinical models. Therefore, careful consideration of these species-specific differences, including potential variations in complement protein interactions, regulatory mechanisms, and overall immune response, is essential when interpreting data from mouse models and designing subsequent clinical trials to ensure the safety and efficacy of CoMiX in human patients.

In addition to their standalone efficacy, CoMiX also hold promise in combination with other established treatments. In the context of *P. aeruginosa* infections, CoMiX could be combined with traditional antibiotic treatments, including antipseudomonal penicillins, cephalosporins, carbapenems, aminoglycosides, and fluoroquinolones to improve efficacy. For instance, the synergistic effects observed between CoMiX and amikacin in vitro studies suggest that CoMiX could enhance the activity of antibiotics against *P. aeruginosa*. This could be particularly beneficial in cases of chronic infections or antibiotic-resistant strains.

CoMiX may also be employed in conjunction with non-antibiotic therapies. Non-antibiotic treatments may include surgical drainage of abscesses, wound care, and supportive measures like intravenous fluids. For chronic infections, particularly in patients with cystic fibrosis, inhaled antibiotics and mucolytic agents, including hypertonic saline, mannitol, N-acetylcysteine (NAC), or dornase alfa, may be beneficial in clearing mucus and reducing the bacterial burden. It is essential to recognize that treatment regimens can vary based on the severity of the infection, the patient's health status, and the specific *P. aeruginosa* strain involved.

Beyond their therapeutic potential, CoMiX could also serve as a preventive approach for sensitive populations. For example, CoMiX might be used pre-surgery to reduce the risk of infections in immunocompromised patients or in intensive care units (ICUs) to prevent healthcare-associated infections among critically ill patients.

Beyond their applications in infectious diseases, CoMiX could also be explored in conjunction with other emerging cancer therapies. Translating these findings to clinical practice requires considering current standard of care. In early-stage HER2-positive breast cancer (surgery, chemotherapy, trastuzumab +/- pertuzumab), CoMiX may be considered if resistance develops. In advanced-stage disease (chemotherapy, trastuzumab, pertuzumab, tyrosine kinase inhibitors), CoMiX could offer a more tolerable alternative to antibody-drug conjugates (e.g., Trastuzumab-emtansine, Trastuzumab-deruxtecan), particularly given ADC side effects, but this requires clinical investigation. CoMiX could potentially be used preoperatively to reduce tumor volume and improve surgical outcomes, or postoperatively to eliminate residual tumor cells. Combining CoMiX with radiation therapy could enhance tumor response and reduce recurrence risk. CoMiX could increase chemotherapy efficacy and reduce side effects, as with trastuzumab. In hormone-sensitive cancers, CoMiX could be combined with hormone therapy. Finally, CoMiX could be combined with immunotherapy (checkpoint inhibitors, CAR therapy) to enhance immune-mediated tumor killing. For example, combining CoMiX with checkpoint inhibitors (anti-PD-1, anti-PD-L1) could increase tumor cell visibility to the immune system. CoMiX could activate complement, directly killing tumor cells and promoting immune cell activation and infiltration. CoMiX could potentially reduce immunosuppressive mechanisms within the tumor microenvironment. Further research is needed to explore optimal combinations and dosing schedules. These potential combinations highlight CoMiX versatility and capacity to enhance existing cancer treatment efficacy. However, additional preclinical and clinical studies are needed. Future investigations should focus on early-stage clinical trials to confirm CoMiX safety and efficacy in humans. A deeper understanding of CoMiX mechanisms of complement activation and interaction with target cells is needed to optimize design and therapeutic potential and anticipate resistance. Strategies to address potential CoMiX resistance should be developed. Exploring CoMiX effectiveness in combination with other modalities (chemotherapy, immunotherapy) could enhance efficacy and diminish side effects. These potential combinations highlight the versatility of CoMiX and their capacity to enhance the efficacy of existing cancer treatments. However, additional preclinical and clinical studies are necessary to fully elucidate the optimal combinations and dosing schedules for different cancer types and patient populations.

Future investigations should focus on conducting early-stage clinical trials to confirm the safety and efficacy of CoMiX in human patients since the mode of action of CoMiX is quite distinct from therapeutic antibodies by activating complement on target human cells. Additionally, a deeper understanding of the precise mechanisms by which CoMiX activate the complement system and interact with target cells is needed to optimize their design and therapeutic potential and anticipate resistance issues. Strategies to address potential resistance to CoMiX-based therapies should also be developed.

The oligomerization scaffold offers a versatile platform for combining various targeting and effector functions within the CoMiX molecule. This flexibility allows for the customization of both the targeting and effector functions, enabling the development of highly specific and effective therapeutic agents. The targeting function, typically a scFv antibody, can be easily swapped out to target different pathogens or cancer types. This modular design expands the potential applications of CoMiX to a wide range of diseases. Additionally, the effector function can be modified to achieve diverse biological outcomes. For example, quorum sensing inhibitors like furanones and acyl-homoserine lactones can disrupt bacterial communication, while biofilm formation inhibitors such as dispersin B and polymyxins can prevent bacteria from forming protective biofilms. We can propose a novel version of CoMiX-Fc and CoMiX-FHR1 including anti-biofilm drugs[409] into the C4bp-β scaffold to counteract the main challenges of bacterial biofilm during chronic infection.

The modular design of CoMiX enables the exploration of a diverse range of cytotoxic payloads, including those currently used in ADCs and novel agents with enhanced therapeutic potential. By coupling potent anti-tumor agents to the CoMiX scaffold, the platform can leverage the specificity of the targeting function to deliver these payloads directly to cancer cells, minimizing off-target toxicity. This flexibility allows for the optimization of potency, selectivity, and pharmacokinetics, potentially addressing limitations encountered with existing ADC therapies. Additionally, CoMiX can be engineered to incorporate multiple payloads, enabling targeted delivery of different therapeutic agents to simultaneously address complex disease states including the challenging tumor microenvironment.

For instance, CoMiX could be coupled with traditional ADC payloads such as MMAE, MMAF, DM1, DM4, calicheamicins, and PBDs, as well as novel protein degraders like PROTACs and DEGRADES, which target specific proteins for degradation. In addition, CoMiX could include immunomodulators such as toll-like receptor agonists, cytokines, and immune checkpoint inhibitors, or radioisotopes such as 225Ac, 177Lu, and 67Cu, for targeted radiation therapy.

By incorporating these payloads into CoMiX molecules, the platform can develop highly effective and targeted cancer therapies with the potential to overcome limitations associated with traditional treatments. Combining multiple effector functions within a single CoMiX molecule can create even more potent and targeted therapies.

In conclusion, CoMiX represent a promising therapeutic approach with the potential to address significant unmet medical needs. Further research and development are warranted to fully explore their potential benefits for patients.

6. Appendix of original publications

6.1. Directed-complement killing of *Pseudomonas aeruginosa* protects against lethal pneumonia

Bianca Brandus[1]*, Aubin Pitiot[1]*, Gilles Iserentant[1], Camille Rolin[1], Jean-Yves Servais[1], Delphine Fouquenet[2], Benoit Briard[2], Mustapha Si-Tahar[2], Guillaume Desoubeaux[2], Yves Mely[3], Patrice Rassam[3], Ludovic Richert[3], Jacques Zimmer[1] , Xavier Dervillez[1,] Carole Seguin-Devaux[1†]

1. Department of Infection and Immunity, Luxembourg Institute of Health, Luxembourg
2. Research Center for Respiratory Diseases, INSERM U1100, University of Tours, France
3. Laboratory of Bioimaging and Pathology, UMR 7021 CNRS/Unistra, University of Strasbourg, France

* Contributed equally.

† Corresponding author: Carole Devaux; Department of Infection and Immunity, Luxembourg Institute of Health, 29 Rue Henri Koch, Esch-Sur-Alzette, Luxembourg; Carole.Devaux@lih.lu

ABSTRACT

By causing a wide-array of infections in individuals with compromised immune defenses, multi-drug resistant *Pseudomonas aeruginosa* raise major clinical concerns. We developed two different Complement-activating Multimeric immunotherapeutic compleXes (CoMiX) targeting the bacterium through a scFv directed against the exopolysaccharide Psl, and carrying one of two different effector functions, Factor H Related protein 1 (FHR1) or Fc dimer, to kill *P. aeruginosa*. CoMiX-FHR1 and CoMiX-Fc effectively deposited C3b and C5b9 at the surface of multi-drug resistant clinical isolates, leading to their opsonization and/or direct killing. Both CoMiX synergize with amikacin and protect human epithelial cells against *P. aeruginosa*-induced cytotoxicity by stimulating their IL-6 production. Prophylactic and therapeutic treatment with both CoMiX significantly improved the survival of mice in a model of acute pneumonia by reducing the local bacterial burden through higher induction of C3b and decreased inflammation in the lung. Our findings highlight the therapeutic potential of directed-complement activation to combat multi-drug resistant bacteria.

Keywords

Pseudomonas aeruginosa, Immunotherapy, Complement system, FHR-1, Multidrug resistance

INTRODUCTION

Pseudomonas aeruginosa is a Gram-negative opportunistic bacterium responsible for life-threatening infections in immunocompromised individuals. It exhibits a broad tropism colonizing various tissues and causes a wide array of infections, including respiratory infections[410]. *P. aeruginosa*-associated lung infections are now considered a leading cause of morbidity and mortality worldwide. As part of the updated Bacterial Priority Pathogens List (BPPL) 2024 [411], *P. aeruginosa* is known for its extensive multidrug resistance (MDR), prompting the World Health Organization (WHO) to classify carbapenem-resistant *P. aeruginosa* as a high priority for novel therapeutic development[412].

Antibody-based therapies are emerging as a promising alternative to combat infections caused by MDR bacteria, particularly Gram-negative pathogens like *P. aeruginosa*[413]. These targeted therapies offer the distinct advantage of minimizing disruption of the normal bacterial flora and mitigating off-target effects. Beyond their neutralizing efficacy, antibodies can trigger potent effector functions, promoting pathogen clearance, usually through the engagement of their Fc-region to the Fc-receptors (FcRs). Among them, antibody-dependent cellular cytotoxicity (ADCC) triggers the release of cytotoxic granules by Natural Killer cells, antibody-dependent cellular phagocytosis (ADCP) activates phagocytosis by macrophages and neutrophils, and complement-dependent cytotoxicity (CDC) leads to opsonization of bacteria and their direct lysis[414, 415]. However, so far, antibodies directed against *P. aeruginosa* have failed in early clinical trials. One example is the MEDI3902, a bispecific antibody recognizing both the exopolysaccharide Psl and a Type III Secretion Protein PcrV[208] that showed promising results in preclinical and Phase I trials. In late Phase trials, the latter was nevertheless unsuccessful in reducing nosocomial pneumonia incidence in infected ventilator-associated pneumonia patients[209], indicating a limiting effect of therapeutic antibodies against *P. aeruginosa* infections.

Targeted therapies that activate the complement against bacterial infections remain poorly investigated. The preponderant role of the complement system is nevertheless well established in host anti-bacterial defenses and might offer a novel alternative against *P. aeruginosa* infections. Actually, both complement-depleted mice and complement-deficient knock-out mice show higher susceptibility to *P. aeruginosa* pneumonia[416], inability to clear the bacterial burden from the lungs, and increased mortality [417, 418]. In humans, recent studies revealed the complement system as the primary defense mechanism against *P. aeruginosa* infection[76, 419]. The complement system can be initiated through three distinct pathways: the classical pathway is usually initiated *via* C1q binding to the Fc region of antigen-bound immunoglobulins; the mannose-binding lectin (MBL) pathway is triggered by the binding of MBL or ficolins to specific

carbohydrates on pathogens whereas the alternative pathway begins with the spontaneous hydrolysis of C3[420]. Engagement of any of the complement pathways culminates to the generation of the enzyme C3 convertase. The cleavage of C3 by this enzyme yields C3b, which opsonizes target surfaces, and C3a, a potent anaphylatoxin and chemotactic molecule. C3b can subsequently bind to the C3 convertase, resulting in the enzyme C5 convertase. This novel enzyme complex cleaves C5, generating C5a, a potent chemoattractant peptide, and C5b, necessary for the assembly of the membrane attack complex (MAC) at the bacterial surface[421]. The complement system can thus eradicate pathogens, including *P. aeruginosa*, through a multifaceted approach: direct lysis *via* the MAC formation, opsonization of microbes by C3b/iC3b facilitating their phagocytosis, or release of C3a and C5a anaphylatoxins mediating chemotaxis and immune cell activation[15].

P. aeruginosa has however developed various mechanisms to evade complement-mediated killing[422]. Among them, the creation of physical barriers hinders complement component access to the bacterial surface (e.g. modulation of LPS O antigen, increase expression of exopolysaccharides)[423, 424, 425], the secretion of proteases cleaves and inactivates complement molecules at various stages of the cascade[178, 426, 427], or the binding of host complement regulatory proteins like Factor H (FH)[428, 429] that promotes C3b degradation and inhibits the alternative pathway. Interestingly, Factor H-related proteins (FHRs), with conserved ligand and cell surface recognition domains[78], lack the complement regulatory domains of Factor H (FH). This suggests that FHRs may function as positive regulators of complement activation and opsonization, counteracting the inhibitory effect of FH[77]. FHR1, the most abundant FHR in the blood is known to bind to various ligands of FH (e.g. C3b, pentraxins, heparin), and the FH-binding proteins of *P. aeruginosa*, (elongation factor Tuf[428], LPD[430] and OprG[76]) and has been shown recently to promote complement deposition at the surface of *P. aeruginosa* bacteria[76].

We have previously developed complement-activating immunotherapeutic complexes (CoMiX)[106, 431] targeting HER2-positive cancer cells. Our strategy uses the C-terminal oligomerization domain of the α- or the β-chain of C4b-binding protein (C4BP) as a multimerizing scaffold[403, 432], bridging a targeting function (e.g. single-chain fragment variables targeting HER2-positive cancer cells) and an effector function exploiting complement-activating properties (e.g. Fc-region or Factor H-related protein 4 (FHR4)). CoMiX treatment has been shown to increase C3b- and C5b9-deposition on tumor cells, their phagocytosis by macrophages, and a significant decrease of the growth of the tumor in a xenograft model.

In the current study, we evaluated this novel therapeutic approach against *P. aeruginosa* acute infection using single-chain variable fragments (scFv) targeting the exopolysaccharide Psl. The targeted activation

of complement on *P. aeruginosa* is mediated either by the Fc region (CoMiX-Fc) or the C-terminal domain of Factor H-related protein 1 (CoMiX-FHR1). We show that both CoMiX-Fc and CoMiX-FHR1 significantly enhanced complement deposition and activation at the surface of the bacterium, resulting in either direct bacterial lysis or, for CoMiX-Fc, a better opsonization of the bacteria potentially leading to enhanced phagocytosis by macrophages. Remarkably, we showed that intranasal administration of targeted CoMiX provided an optimal defense against *P. aeruginosa* in a murine model of acute lung infection, facilitating local bacterial burden clearance, reducing lung inflammation and injury and significantly improving mouse survival.

MATERIAL AND METHODS

Bacterial strains

Pseudomonas aeruginosa strain serotype IATS O11 was obtained from the American Type Culture Collection (ATCC) (strain number 33358). The luciferase-expressing strain PAO1 (PAO1-Lux) was kindly provided by Dr. Eric Morello (University of Tours, France). Reference strain PAO1 and twenty-nine clinical isolates of *Pseudomonas aeruginosa* were kindly obtained from Dr. Guillaume Desoubeaux (University of Tours, France, protocol number 2016-003 approved by the ethics committee of the CHRU of Tours). These clinical strains were isolated from patients with cystic fibrosis or from patients in intensive care units who underwent a tracheostomy. Antimicrobial susceptibility testing was performed on all strains. All bacterial cells were grown in tryptic soy broth (TSB) at 37°C with shaking or on TSB solidified with 1.5% agar (TSA) plates. In synergy experiments, TSB was supplemented with 2 µg/ml or 10 µg/ml of amikacin (39831-55-5, Santa Cruz Biotechnology).

Production and purification of CoMiX

The recombinant plasmid DNA for the expression of CoMiX using the C4bp β chain was previously described[432]. The following sequences were synthesized by ProteoGenix SAS (Schiltigheim, France): scFv anti-O11 scFv derived from Panobacumab, (patent WO2006/084758A1), human C4bp C-terminal β chain (UniProt nr. P20851.1, aa 137-252), human IgG1 H chain constant gamma (UniProt nr. P01857.1), scFv anti-Psl derived from the bispecific antibody MEDI3902 (patent WO2017/095744A1), human FHR1 CCP3-5 (UniProt nr. Q03591, aa 145-329), scFv anti-Aspergillus directed against the Chitin ring formation 2 (Crf2) protein of *A. fumigatus* (MS112-IIB1, Schütte et al., 2009). The production of CoMiX molecules was performed as previously reported[106] by transfecting HEK293T cells (ATCC CRL-3216) with the CoMiX expressing plasmid using Lipofectamine 3000 (ThermoFisher Scientific, USA) according to the manufacturer's instructions. Forty-eight hours' post-transfection, cells were trypsinized and seeded into 10 cm culture dishes containing complete DMEM medium and selected using 10 to 20 µg/ml puromycin (InvivoGen, USA).

Supernatants from these clonal cultures were subsequently analyzed by whole-cell ELISA. *P. aeruginosa* strain PAO1 or O11 ATCC 33358 were immobilized onto Maxisorp 96 well Nunc immunoplates (Thermofisher). After blocking with 4% BSA (Roth, Keerbergen, Belgium) in PBS, wells were incubated with CoMiX-FHR1 or CoMiX-Fc. Bound CoMiX was detected using either an HRP-conjugated anti-His antibody (Sigma-Aldrich Cat# A7058, RRID:AB_258326, Overijse, Belgium) for CoMiX-FHR1 or an HRP-conjugated

anti-Fc antibody (Abcam Cat# ab97225, RRID:AB_10680850, Abcam, Cambridge, UK) for CoMiX-Fc. Tetramethylbenzidine (Biolegend, USA) was used as a substrate, the reaction was stopped with H_2SO_4, and the absorbance was at 450 nm using a Polarstar spectrophotometer (BMG Labtech, Germany). Clones exhibiting the highest CoMiX expression were expanded in flasks and further seeded at confluence into a 5-chamber CellSTACK® culture system (Corning Incorporated, USA) containing complete DMEM medium for larger production. CoMiX-Fc was purified with Protein G Sepharose® 4 Fast Flow resin (GE Healthcare, GE17-0618-01; 1 ml bed volume) and CoMiX-FHR1 with HisTrap HP column (Cytiva Life Sciences, Marlborough, MA, USA) using a Bio-Rad NGC™ chromatography system (Bio-Rad Laboratories, Hercules, CA, USA). After elution, CoMiX were washed of all potential buffer and antibiotics contaminant, and concentrated using Amicon® Ultra centrifugal filter devices (MilliporeSigma). The final concentration was determined using a NanoDrop™ micro-volume spectrophotometer. All proteins were stored at -20°C.

Molecular and binding analysis of the CoMiX

The molecular pattern of the recombinant proteins was analyzed by SDS/PAGE, SYPRO Ruby protein gel staining and western blotting. Purified CoMiX molecules (3 µg) were mixed with 4 µl of 4X Laemmli sample buffer (Bio-Rad) only (non-reducing conditions), or supplemented with 10% β-mercaptoethanol (reducing conditions). Samples were loaded onto 4-15% Mini-PROTEAN® Tris-Glycine Extended (TGX™) precast gels (Bio-Rad) and electrophoresed using XT MES running buffer (Bio-Rad) according to the manufacturer's instructions. Following electrophoresis, the gel was fixed in a solution of 50% methanol and 7% acetic acid (v/v) for 30 minutes, then stained with SYPRO Ruby protein gel stain (Thermo Fisher Scientific) overnight at 4°C, following the manufacturer's protocol. The gel was washed with 10% methanol and 7% acetic acid (v/v) for 30 minutes and was visualized using an Amersham™ Typhoon™ biomolecular imager (Cytiva, MA, USA) with the Cy5 filter. For western-blot**,** proteins from the SDS-PAGE gel were transferred to a low-fluorescence PVDF membrane (activated in methanol prior to use) using TTB (25 mM Tris, 192 mM glycine, 0.01% (v/v) SDS, 20% (v/v) methanol, pH 8.8) blotting buffer. The membrane was blocked with 4% BSA in PBS to prevent non-specific antibody binding. The membrane was then probed with specific antibodies: anti-Fc AF647 (SouthernBiotech Cat# 2048-31, RRID:AB_2795692, Birmingham, USA) for CoMiX-Fc and rabbit anti-His antibody (Bethyl Cat# A190-114A, RRID:AB_67321, Merelbeke, Belgium) followed by polyclonal goat anti-rabbit AF647 (Jackson ImmunoResearch Labs Cat# 111-607-008, RRID:AB_2632470, Sanbio B.V., The Netherlands) for CoMiX-FHR1. Protein bands were detected using an Amersham™ Typhoon™ biomolecular image (Cytiva, MA, USA).

The binding of the purified CoMiX was confirmed on bacterial strains using whole cell ELISA. Briefly, a bacterial suspension containing 1 x 10^6 colony-forming units (CFU) per well was immobilized overnight onto Nunc MaxiSorp™ 96-well flat-bottom polystyrene ELISA plates. After washing the plates five times with PBS containing 1% BSA, the wells were blocked with 100 µL of 5% BSA in PBS solution for 1 hour at 4°C. Purified CoMiX and irrelevant controls were added to the plates for incubated for 1 hour at 4°C. Then, depending on the CoMiX variant used (Fc-tagged or FHR1-tagged), either HRP-conjugated goat anti-human IgG Fc antibody or HRP-conjugated anti-His antibody was added at a concentration of 1 µg/mL (100 ng/well) and incubated for 1 hour at 4°C. Finally, the binding was revealed by the chromogenic substrate, TMB/H_2SO_4 as described above. To test the competition between FH and CoMiX-FHR1, coated-wells of PAO1 bacteria were blocked with PBS - 1% BSA, and incubated with either PBS as control or FH (20 µg/ml) and a range of concentrations of CoMiX-FHR-1 (40-0 µg/ml). FH was then detected with the specific mouse monoclonal antibody OX-24 (Abcam), followed by an HRP-conjugated goat anti-mouse IgG (Biolegend), and developed by the chromogenic substrate, TMB/H_2SO_4. Washing steps with PBS-Tween 0.05% were included between each incubation.

C3b- and C5b9-deposition measurement by ELISA and microscopy

Reference strain PAO1 or clinical isolate IPP6247290 were immobilized onto Nunc MaxiSorp™ 96-well flat-bottom polystyrene ELISA plates following the previously described protocol. After blocking with 100 µL of PBS 5% BSA, plates were incubated with serially diluted purified CoMiX proteins (1:3 dilutions starting from 1000 ng/well) for 1 hour at 4°C. Following washes, plates were incubated with 2% normal human serum (NHS) or decomplemented NHS (ΔNHS) diluted in GVB++ buffer (final volume of 100 µL/well) for 30 minutes at 37°C. After additional washing steps, the plates were incubated with a mouse monoclonal antibody (mAb) anti-human C3/C3b/iC3b CL7636AP (clone 7C12; Cedarlane, Sanbio B.V.) for 1 hour at 4°C. Finally, HRP-conjugated goat anti-mouse IgG 405306 (Biolegend, Amsterdam, The Netherlands) was added at 100 ng/well and incubated for 1 hour at 4°C. The plate was developed with TMB/H_2O_2 and read at 450 nm. To investigate the formation of membrane attack complexes (MAC) following C3b deposition, the same protocol was employed using this time 4% NHS/ΔNHS. Here, the ELISA was revealed with a mouse mAb anti-human C5b9 ab66768 (clone aE11, Cedarlane).

Confocal microscopy was employed to visualize complement activation on PAO1 bacteria treated with CoMiX. Briefly, an overnight culture of *P. aeruginosa*-GFP (ATCC 15692GFP) was grown to log-phase. After treatment with CoMiX and normal or 10% C5-deficient human in GVB++ medium, as previously described, cells were pelleted by centrifugation (8000g for 5 minutes) and washed with PBS. Complement deposition

was detected with a goat anti-C3b (Invitrogen) and a goat anti-C5b9 (ebioscience), for MAC fornation, for 2 hours at room temperature followed by an anti-goat-AF647 (Jackson ImmunoResearch) secondary antibody for 2 more hours. Bacterial cells were fixed with 2% formaldehyde for 30 minutes at room temperature and mounted onto a pre-prepared agarose pad. Briefly, a 1.5 x 1.6 cm Gene Frame matrix (Thermo Scientific) was adhered to a microscope slide (Thermo Fisher). The Gene Frame was then filled with 200 µl of 1% TSB-agarose gel and a glass coverslip (Menzel Gläser #1) was placed on top. Samples were analyzed with a Leica SP8 confocal microscope and Leica LasX Life Sciences Software at the EuroBioimaging platform (University of Pharmacy, Strasbourg). The chosen pictures were processed with ImageJ before integrated inside the figures.

Complement-dependent killing assay

Bacterial strains PAO1 and IPP6247290 were cultured in Tryptic Soy Broth (TSB) at 37°C to an exponential growth phase and resuspended in PBS. 10^6 colony-forming units (CFU) was incubated with 10% (v/v) NHS in the presence or absence of CoMiX (30 µg/mL) or an irrelevant control for 2 hours at 37°C. Bacterial suspensions were diluted in PBS, plated onto Tryptic Soy Agar (TSA) plates, incubated overnight at 37°C, and the number of CFU was enumerated. For the PAO1-Lux strain, an identical culture protocol was followed. In this instance, the luminescence-based reporter system of PAO1-Lux was used for real-time monitoring of bacterial growth. Briefly, luminescence output (RLU) was measured every hour using the POLARStar Omega microplate reader, providing a quantitative assessment of bacterial viability and proliferation. We investigated the combined effect (synergy) of amikacin, a widely used aminoglycoside antibiotic (39831-55-5, Santa Cruz Biotechnology), and CoMiX against two *P. aeruginosa* strains: the reference strain PAO1 and a multidrug-resistant clinical isolate (IPP6247290). The minimum inhibitory concentration (MIC) of amikacin was determined using the broth micro dilution method as previously described (Kowalska-Krochmal, 2021). Overnight cultures of PAO1 and the clinical isolate IPP6247290 were grown in Tryptic Soy Broth (TSB) medium. To achieve exponential growth, 1 ml of each cell suspension was transferred to 3 ml of fresh TSB medium one hour before treatment. 10^6 CFU was incubated with 10% NHS in the presence or absence of 30 µg/mL of CoMiX or irrelevant control.

Additionally, various sub-MIC concentrations of amikacin were tested for each strain. The samples were incubated for 2 hours at 37°C under agitation before dilution and plating on TSA agar plates. CFU-s were counted the following day. The synergy coefficient was calculated using the equation adapted from Chaudhry et al., 2017: log(C) – log(SA) – log(SB) + log(SAB), where C represents the CFU in the untreated control well, SA represents the surviving CFU after treatment with amikacin alone, SB represents the

surviving CFU after treatment with the CoMiX molecules alone, and SAB represents the surviving CFU after combined treatment with amikacin and CoMiX. This equation defines whether synergy exists between amikacin and CoMiX. A synergy coefficient less than zero (< 0) indicates synergy between the two treatments.

Phagocytic killing assay

Peripheral blood mononuclear cells (PBMCs) from healthy donors (Luxembourg Red Cross, MAN_SCE_24_008) were isolated from buffy coats and differentiated into M1 macrophages using and following the manufacturer's instructions of PromoCell macrophage generation medium (PromoCell, Germany). Briefly, fresh PBMC were plated and incubated in monocyte attachment medium (MAM) for two hours, before removal by aspiration of the floating contaminating cells. Adherent cells were washed three times with MAM, and M1-Macrophage Generation Medium DXF (containing GM-CSF and a mix of cytokines) was directly added onto the cells. Cells were incubated for 9 days at 37°C with 5% CO2 with medium changes in between. One week before the assay, cells were harvested from the flasks, counted, and dispatched into 96 wells plates in RPMI, Glutamax, 10% FBS, 1% Penicillin/Streptavidin. M1-polarized macrophages were activated by treatment with 100 nM phorbol 12-myristate 13-acetate (PMA) (Sigma) for 5 days. Prior to the phagocytosis assay, cells were washed twice with PBS to remove any residual antibiotics, and resuspended in serum/antibiotics free RPMI medium.

PAO1 bacteria from an overnight culture were counted, fixed in PFA 2% and stained with pHrodo dye (P35372, Thermo Fisher Scientific) following the manufacturer's instructions. PBMC M1-derived macrophages were co-incubated with the pHrodo-stained bacteria at a 1:12 macrophage-to-bacteria ratio with normal human serum (10%), and in the presence or absence of CoMiX (15µg/mL). Cells were incubated in the Incucyte, and pictures under x4 were taken every 15 minutes for at least 2 hours.

PBMC M1-derived macrophages were also cultured on Lab-tek (Nunc, Loughborough, UK) 8 chamber slides. PAO1 bacteria were fixed from an overnight culture with ethanol PFA 2%, stained with CellTrace™ CFSE (C34554, Thermo Fisher Scientific, USA), and then added in the Lab-Tek at a 1:12 macrophage-to-bacteria ratio for 1 hour in the presence of human serum (10%) and CoMiX (15µg/mL). Following co-incubation, the cytoplasmic membrane of macrophages was stained for 10 minutes with AF647-Wheat Germ Agglutinin (WGA). Cells and bacteria were finally fixed with 2% paraformaldehyde. Slides were viewed on an Axio Observer fluorescence microscopy (Zeiss, Germany). Images of the two stains (green and red) were overlaid.

Effect of CoMiX on BEAS-2B cells

Immortalized human bronchial epithelial BEAS-2B cells (ATCC® CRL-9609™) were cultured in Ham's F-12 medium (Gibco™) supplemented with 10% fetal bovine serum (FBS), 1% penicillin-streptomycin, and 1% L-glutamine, and maintained at 37°C in a humidified incubator with 5% CO_2. For infection assays, cells were detached using 0.05% trypsin-EDTA and seeded into 96-well plates at a density of 2 x 10^4 cells/well in complete F-12 medium overnight to reach 80% confluence. Prior to infection with PAO1 reaching exponential growth phase, the cells were washed with PBS to remove antibiotics and resuspended in antibiotic- and serum-free F-12 medium. Cells were infected with PAO1 at a multiplicity of infection (MOI) of 10:1 in presence or not of CoMiX (15 µg/mL) and 10% NHS. The plates were incubated for 6 hours at 37°C, and cell culture supernatants were collected, centrifuged at 10,000 rpm for 5 minutes and frozen at -20°C. Lactate dehydrogenase (LDH) activity in the supernatants was measured using the CyQUANT™ LDH Cytotoxicity Assay kit (C20300, Thermo Fisher Scientific) according to the manufacturer's instructions. LDH release was expressed as a percentage of the total LDH activity measured in the positive control wells (representing 100% cell lysis). IL-6 and IL-8 levels in the culture supernatants were quantified using the human IL-6 ELISA Max Standard Set kit (30501, BioLegend) and the human IL-8 ELISA Max Deluxe Set kit (431505, BioLegend) following the manufacturer's protocol.

Acute pneumonia model in C57BL/6jrj (B6) mice

Adult female C57BL/6jrj (B6) mice (7 weeks old) were obtained from Janvier Laboratories (Le Genet Saint Isle, France). All mice were housed under specific-pathogen-free conditions at the Plateforme Scientifique et Technique Animaleries (PST-A) animal facility (Tours, France) and had access to food and water *ad libitum*. All animal experiments complied with the European and French legislative, regulatory and ethical requirements and the protocol was approved by the ethics committee in animal experimentation of the Centre - Val de Loire region under the referral number 7590 issued by the Ministry of Higher Education, Research and Innovation.

Mice were infected with a freshly prepared inoculum. Briefly, bacteria from a frozen stock were grown overnight in 4 mL of Luria broth (LB) under agitation at 220 rpm. The following day, bacteria were transferred into fresh LB medium and grown until their mid-log phase, as measured by an optical density (OD) of about 0.4, corresponding to a titer of 2 × 10^8 bacteria/mL. The bacterial culture was centrifuged at 3000 × g for 10 min, washed twice with PBS, and finally diluted to give a desired inoculum of 3 × 10^6 bacteria/40 µL. Each inoculum was verified for accuracy by serial dilutions and direct plating on LB agar plates. Mice were anesthetized by intra-peritoneal injection of a mixture of ketamine-xylazine 1:1. 40 µl

of the bacterial suspension ($3x10^6$ cfu/mice) was administrated by intranasal instillation and mice were then immediately held upright to facilitate bacterial inhalation until normal breathing resumed. In all experiments, the animals' mortality and body-weight were monitored daily. For ethical reasons, animals found moribund or with a body-weight loss >25% were sacrificed. Survival of the infection was assessed for 7 days.To administrate CoMiX, mice were anaesthetized with 3% isoflurane. Three hours before the infection (Prophylactic treatment) or one hour after the infection (Therapeutic treatment), anti-Psl CoMiX-Fc (100 µg/animal), anti-Psl CoMiX-FHR1 (100 µg/animal) or an irrelevant CoMiX control, anti-CFS1 CoMiX-Fc (100 µg/animal) were administered by intranasal instillation as previously described. A boost of molecules was administered 3 hours after the infection for animals following the prophylactic treatment. Photon emission of luminescent *P. aeruginosa* (PAO1-Lux) in the mouse was measured using the IVIS Lumina XR system (Revvity, USA), including an IVIS charge-coupled device camera coupled to the LivingImage software package (Revvity, USA). Analysis of photons was done under isoflurane inhalation anesthesia, generating a digital false-color photon emission image of the mouse where photons were counted using a 3-min acquisition time using the following settings: binning factor 4, Field of View: 10 cm, f1.

Bronchoalveolar lavages, lung and blood sampling and bacterial load assay

At 4 and 16 hours after *P. aeruginosa* infection, mice were euthanized using a lethal dose of pentobarbital (Exagon). Blood was collected in EDTA and non-EDTA tubes and stored at -80°C. BAL was recovered by cannulating the trachea and washing sequentially the lung twice with 1 mL of PBS at room temperature. The lavage fluid was centrifuged at 400 g for 10 min at 4 °C, leaving the supernatant of the first lavage to be stored at −80 °C until analysis, and the cell pellet to be resuspended in PBS, counted in a hemocytometer chamber and used for subsequent analysis.

Lungs were perfused with 10 mL of PBS and harvested in GentleMACS C tubes (Miltenyi Biotec, Germany) containing 2 mL of RPMI medium (Invitrogen, France) for flow cytometry or GentleMACS M tubes (Miltenyi Biotec, Germany) containing 1 mL of PBS for assessment of the bacterial load. Lung homogenates from PBS-filled tubes, containing broad-spectrum protease inhibitors (Sigma, France), were processed using a GentleMACS tissue homogenizer (Miltenyi Biotec, Germany). The homogenates were centrifuged at 800 g for 10 min at 4 °C, and stored at −20 °C until analysis. Lung homogenates were were then digested with 25 µg/mL of Liberase (Roche, France) and 100 µg/mL of DNAse I (Sigma, France) for 30 minutes at 37°C under agitation. After washes, red blood cells were eliminated using ACK Lysing Buffer (Thermofisher

Scientific, France) according to manufacturer's instructions. Samples were then filtered over 100 µm and 40 µm nylon mesh.

Bacterial load in BAL (before centrifugation) and lung homogenates was determined by plating tenfold serial dilutions on LB agar plates. Plates were incubated at 37°C, and the CFU were counted after 24 hours.

Flow cytometry

Cell pellets from BAL and lung homogenates were resuspended in FACS buffer (PBS, 2% FBS, 2mM EDTA, and 1X murine Fc-block), counted in a hemocytometer chamber, and stored at 4°C until staining. Cells were stained in FACS buffer for 20 minutes at 4°C with appropriate dilutions of the following Abs: CD45-APC-Cy7 (30-F11), Ly6G FITC (1A8), CD11c PE, Ly6C PeCy7, CD64 APC, CD11b AF700 from Biolegend and Siglec-F BV421 (E50-2440) from Becton Dickinson as well as the LIVE/DEAD Fixable Aqua Dead Cell Staining kit (Thermofisher Scientific, France) and acquired on a CytoFLEX (Beckman-Coulter, USA) flow cytometer. Analyses were performed using Kaluza software (Beckman Coulter, USA).

Cytokines, complement and CoMiX measurements

CoMix-Fc and CoMix FHR1 were quantified in serum and in BALF using a sandwich ELISA. Briefly, Maxisorp 96-well plates (ThermofisherScientific, France) were coated with 10^6 PAO1 bacteria, prepared from overnight cultures. The plates were then blocked with 1% BSA-PBS, and serum or BALF samples, as well as a concentration range of CoMiX were incubated for 2 hours. CoMiX-FHR1 molecules were revealed using a mouse anti-His IgG Ab added for 1 hour, followed by a HRP-goat anti-mouse IgG Ab for 1 hour. CoMiX-Fc were revealed using a mouse anti-human Fc IgG Ab added for 1 hour followed by a HRP-goat anti-mouse IgG for 1 hour. Between each step, plates were thoroughly washed in 0.05% Tween20-PBS. Tetramethylbenzidine was used as a substrate, and the absorbance was measured at 450 nm using a microplate reader (Molecular Devices, CA, USA).

Secreted mediator's concentrations in BALF was assessed by a multi-array U-plex assay, simultaneously measuring IL-1β, IL-6, mKC, GM-CSF, MIP1 and TNFα, following the manufacturer's instructions. All incubations were performed at room temperature with shaking. Briefly, a 96 well plate was coated with a mix of capture antibodies linked to their specific linker. Samples and calibrators, diluted in assay diluent, were then added and incubated for 2 hours. After washing the plate with PBS-0.05% Tween-20, a mix of detection antibodies was added and the plates incubated for an additional hour. A final washing step was performed, followed by the addition of read buffer. The plates were read using the MESO QuickPlex SQ

120MM (MSD, UT, USA). Cytokines and chemokines concentrations were determined using a curve fit model with by Meso Scale Discovery software provided with the instrument.

To assess quantitatively the amount of cleaved and activated C3 fragments (C3b, iC3b, C3c, C3a), and thus the activation of the complement cascade, the serum and BAL, sampled in EDTA and kept on ice to avoid *ex-vivo* activation, of mice was used in a C3b mouse ELISA Kit (Hycult, Uden, The Netherlands), following the manufacturer's instructions.

Statistical analysis

All *in vitro* tests were analyzed based on at least three independent experiments. Statistical differences between experimental groups were determined by using one-way analysis of variance (ANOVA) followed by Tukey's multiple comparisons test (allowing comparison of all groups). Student's t-test was used for comparison between two groups and paired analysis was used when comparing the same donor. Groups size for *in vivo* mouse studies were determined beforehand using power analysis to ensure sufficient statistical power. Log-rank test was used for survival analysis, and a Kruskal-wallis test followed by Dunn's post-test (allowing comparison of all pair of groups) helped to compare the effect of each molecules to the irrelevant molecule. Association between two experimental results was analyzed by Pearson's correlation coefficient. All tests were performed with GraphPad Prism version 10 for Windows (GraphPad Software, San Diego, CA, USA). All data are presented as individual data with the bars representing mean +/- standard error of the mean. A p-value inferior to 0.05 was considered statistically significant (*$p < 0.05$, **$p < 0.01$, ***$p < 0.001$, ****$p < 0.0001$).

Supplemental material

Fig. S1 shows the characterization of purified CoMiX-Fc and CoMiX-FHR1 by western blot and SYPRO Ruby Staining. Fig. S2 shows the binding of anti-O11 and anti-Psl scFv-based CoMiX to 29 *P. aeruginosa* clinical isolates. Fig. S3 shows the dose-dependent binding of CoMiX to two *P. aeruginosa* reference strains and one multidrug resistant clinical isolate. Fig. S4 shows the dose-dependent complement deposition on *P. aeruginosa* by CoMiX. Fig. S5 shows the BAL inflammatory profile of mice infected by P. aeruginosa infection and treated by CoMiX.

Table S1 shows the antibiotic resistance profile of clinical *P. aeruginosa* strains isolated from cystic fibrosis patients and patients who have undergone tracheostomy.

RESULTS

Anti-Psl CoMiX exhibits a broad recognition of *P. aeruginosa* clinical isolates

We engineered two distinct complement-activating multimeric immunotherapeutic complexes (CoMiX) targeting *P. aeruginosa* (**Figure 1**) using two different scFvs recognizing either the 011 serotype lipopolysaccharide (LPS) or the exopolysaccharide Psl. Both CoMiX designs incorporate the C-terminal oligomerization domain of the β-chain of the C4b-binding protein (C4bpβ, in gray) to facilitate dimerization. The single-chain variable fragment (scFv) confers bacterial specificity (in red). CoMiX-Fc (**Figure 1A**) employs the Fc domain of an IgG1 antibody (blue) to activate the classical complement pathway and Fc receptor-mediated cellular responses. Conversely, CoMiX-FHR1 (**Figure 1B**) utilizes the C-terminal domains (CCP3-5, green) of Factor H-related protein 1 (FHR1) to engage the alternative pathway. The profile of both molecules were verified by western blot, where we observed that the CoMiX-Fc was expressed as a dimeric form whereas the CoMiX-FHR1 was preferentially expressed as a monomeric form, an expression profile dependent on the clone chosen to express the protein **(Supplementary figure 1)**.

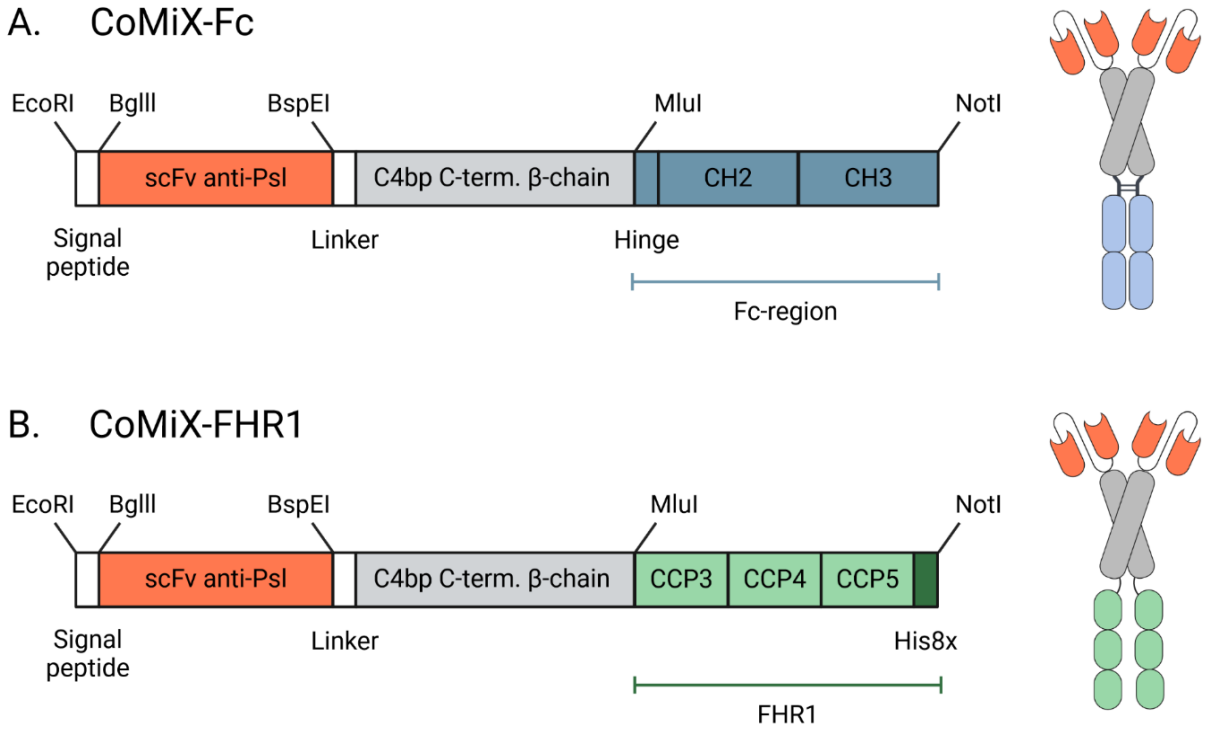

Figure 1. Schematic representation of CoMiX-Fc (A) and CoMiX-FHR1 (B) molecules. The oligomerization scaffold derived from the β-chain of C4b-binding protein (C4bpβ) is used to combine the targeting function of the scFv recognizing *Pseudomonas aeruginosa*, to either an Fc-region (CoMiX-Fc, A) or the CCP4-5 domains of Factor H-related protein 1 (CoMiX-FHR1, B). Both proteins can then be purified through the use of a protein G column for CoMiX-Fc and a Nickel column binding the His-tag found at the C-terminal end of CoMiX-FHR1.

We assessed the targeting potential of the scFv fragments by comparing the binding affinities of the anti-Psl CoMiX-Fc and the anti-O11 CoMix-Fc to a clinically relevant panel of 29 bacterial strains (**Supplementary Figure 2**). These strains, isolated from patients with either tracheostomy in intensive care units (n=17) or cystic fibrosis (n=11), included multidrug-resistant isolates (**Supplementary table 1**) reflecting a critical challenge in the clinic. The anti-O11 scFv bound to only about 20% of the strains, suggesting a low prevalence of the O11 serotype in this patient population. In contrast, the anti-Psl scFv displayed significantly broader targeting. It recognized 45% of cystic fibrosis strains and remarkably, 100% of isolates from tracheostomy patients. Overall, 82% of all strains were bound by the anti-Psl scFv, and we further selected the anti-Psl scFv for therapeutic development.

To further validate the specificity of our anti-Psl CoMix-Fc and CoMiX-FHR1, we tested their binding to the reference strain PAO1 **(Figure 2A)** and a multidrug-resistant clinical isolate IPP6247290 isolated from a patient's sputum in an intensive care unit **(Figure 2B)**. We used two irrelevant controls for both CoMiX containing an anti-Aspergillus scFv[433]. The anti-Psl CoMiX displayed significantly higher binding to both strains compared to controls ($p<0.0001$), confirming its specific recognition of *P. aeruginosa*. Additionally, dose-dependent binding of molecules (starting concentration: 10 µg/mL to 40 ng/mL, 1:3 dilutions) for each strain was also confirmed **(Supplementary Figure 3)**.

It was recently demonstrated that FHR-1 was able to compete with FH for its binding on *P. aeruginosa*. Those findings suggested a major role of FHR1 in the promotion of complement activation and the host-defense against the bacterium[76]. To validate that CoMiX-FHR1 was able to disrupt FH binding to *P. aeruginosa*, unimpaired by the scaffold and targeting system of the molecule, we conducted a competition ELISA between recombinant FH and CoMiX-FHR1. After a co-incubation of bacterial cells with a fixed concentration of FH and decreasing concentrations of CoMiX FHR-1, we observed a reduction of bound FH to the bacteria (around 40% for an initial CoMiX-FHR1 concentration of 40 µg/mL), in a dose-dependent manner **(Figure 2C)**, indicating that CoMiX-FHR1 competes with FH, and could be used to improve host-immunity against *P. aeruginosa*.

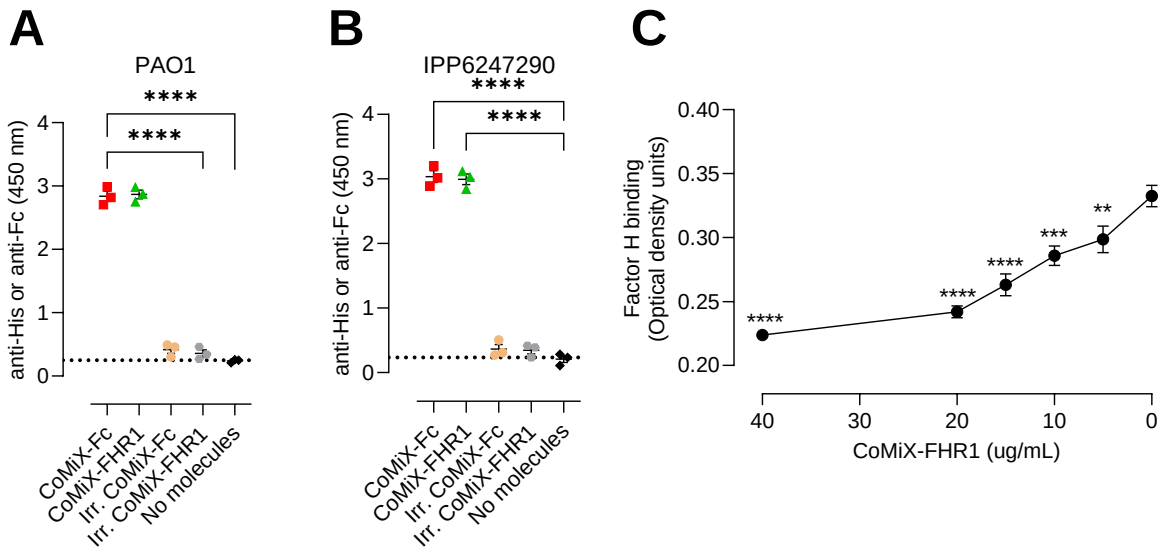

Figure 2. Anti-Psl CoMiX bind to *P. aeruginosa* strain PAO1 and clinical isolate IPP6247290, with CoMiX-FHR1 competing with FH. The binding of CoMiX to reference strain PAO1 **(A)** and clinical isolate IPP6247290 **(B)** was analyzed by whole-cell ELISA. Immobilized bacteria were incubated with 15 µg/ml of CoMiX and irrelevant controls. Bound CoMiX was detected using specific antibodies: anti-His for CoMiX-FHR1 and anti-Fc for CoMiX-Fc. Data are presented as the mean values ± SEM. Results correspond to three pooled independent experiments (1 replicate per experiment). Statistical analysis was performed using one-way ANOVA followed by Tukey's post-hoc test. ****p < 0.0001. To investigate the competition between FH and CoMiX-FHR1, recombinant FH (20 µg/ml) and increasing concentrations of CoMiX-FHR1 were added to PAO1 bacteria. The binding of FH to bacterial cells was detected with the FH-specific monoclonal antibody OX-24 **(C)**. Data are presented as the mean values ± SEM. Results correspond to three pooled independent experiments (3-4 replicates per experiment). Statistical analysis was performed using one-way ANOVA followed by Tukey's post-hoc test and indicate significant differences for the binding of FH in absence versus presence of CoMiX-FHR1. **p < 0.01; ***p < 0.001; ****p < 0.0001.

CoMiX significantly increase C3b- and C5b9-deposition

We first confirmed that CoMiX-Fc and CoMiX-FHR1 significantly enhanced C3b deposition ($p < 0.0001$) on both the reference strain PAO1 and the clinical isolate IPP6247290 as compared to all controls using whole cell ELISA and fluorescence microscopy imaging (**Figure 3)**. CoMiX-Fc induced a stronger C3b deposition increase (**Figure 3A**) on PAO1 (64%, 2.4-fold) compared to CoMiX-FHR1 (40%, 1.6-fold) as well as for the clinical isolate, with CoMiX-Fc (90%, 3.9-fold) displaying a slightly greater effect than CoMiX-FHR1 (51%, 2.1-fold). Similar patterns were observed for C5b9 deposition, indicating that both molecules trigger the membrane attack complex (MAC) assembly (**Figure 3C**). CoMiX-Fc increased deposition by 120% (2.2-fold) and 92% (1.9-fold) on PAO1 and the clinical isolate, respectively. CoMiX-FHR1 induced a 163% (2.6-fold)

increase on PAO1 and a 128% (2.3-fold) increase on the clinical isolate. Similarly as the binding assay, we further confirmed a dose-dependent complement activation at lower CoMiX concentrations (**Supplementary Figure 4**). Our observation, by confocal microscopy imaging, of the interactions between GFP-expressing PAO1 bacteria and the complement (C3b and C5b9 in red fluorescence) confirmed the results from the ELISA, indicating a higher deposition of complement in presence of CoMiX (**Figure 3 B and D**).

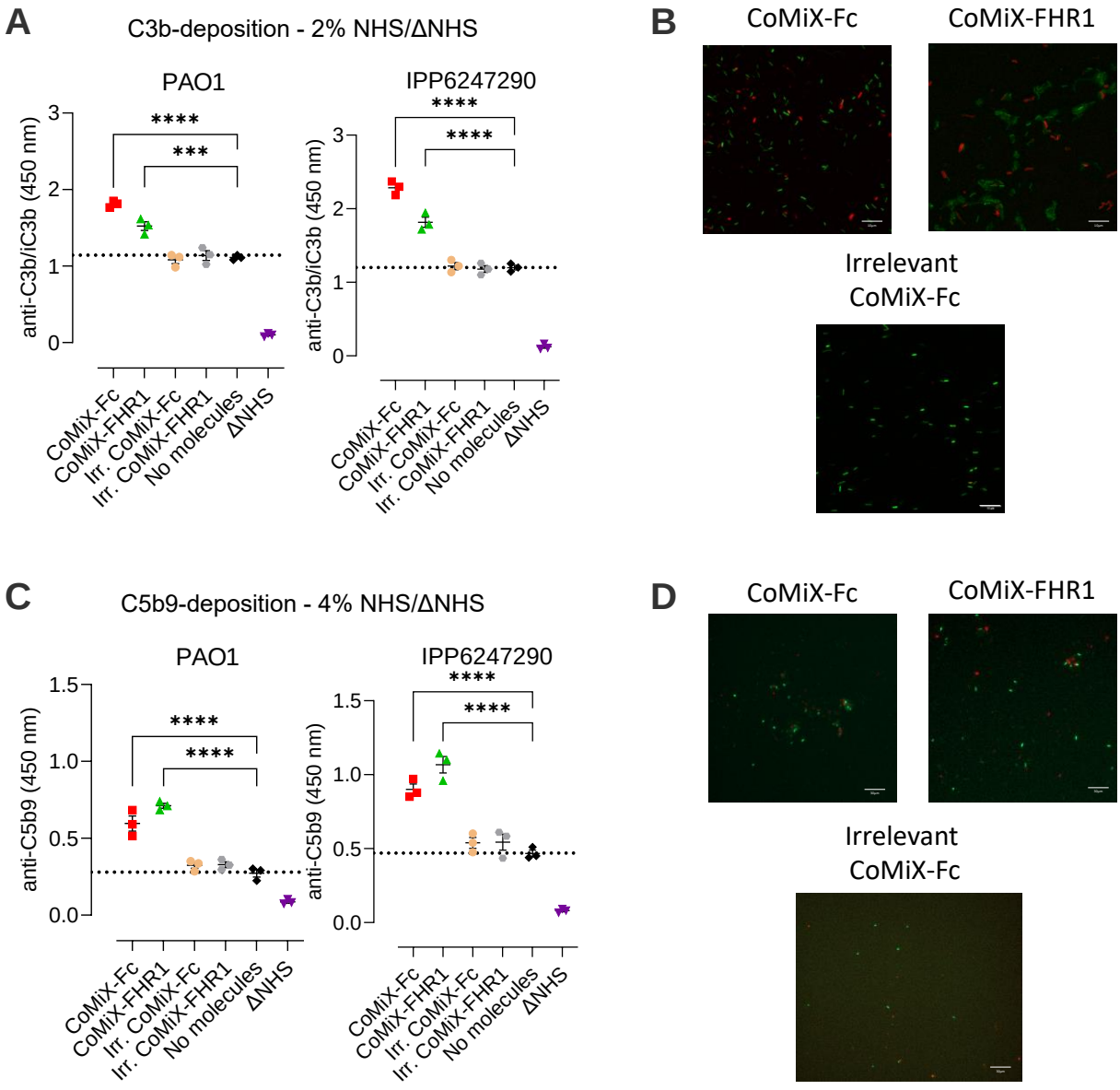

Figure 3. Anti-Psl CoMiX enhance C3b opsonization and membrane attack complex (C5b9/MAC) formation on *P. aeruginosa*. Immobilized bacterial cells of the *P. aeruginosa* reference strain PAO1, and the clinical isolate

IPP6247290 were incubated with 15 µg/ml of CoMiX, before the addition of either 2% (C3b) or 4% (C5b9/MAC) of normal human serum (NHS) or heat-inactivated human serum (ΔNHS) at 37°C for 30 minutes. Complement deposition at the bacterial surface was measured by ELISA, with C3b **(A)** being detected using a monoclonal mouse anti-human C3/C3b/iC3b antibody, while C5b9/MAC **(C)** being detected by a specific mouse anti-human C5b9 mAb. Data are presented as the mean values ± SEM. Results correspond to three pooled independent experiments (1 replicate per experiment). Statistical analysis was performed using one-way ANOVA followed by Tukey's post-hoc test. ****$p < 0.0001$. GFP-expressing PAO1 bacteria were incubated with 10% C5-deficient serum (C3b) or normal human serum (C5b9/MAC) at 37°C for 1 hour, in the presence or absence of 10 µg/ml of CoMiX molecules. Bacteria were then incubated with either a goat anti-C3b or goat anti-C5b9 antibody, followed by a secondary anti-goat AF647. Once stained, bacteria were mounted onto an agarose gel pad and visualized by microscopy in order to detect C3b deposition **(B)** or C5b9 deposition **(D)**. Green=GFP-expressing PAO1, red=C3b or C5b9 deposition by anti-goat Alexa Fluor 647. Scale bar = 10 µm.

CoMiX enhance the complement-mediated killing of *P. aeruginosa* and have a synergistic effect with amikacin.

We further investigated the direct killing efficacy of CoMiX-Fc and CoMiX-FHR1 (30 µg/mL) against *P. aeruginosa* strains PAO1 and the multidrug-resistant clinical isolate IPP6247290 in the presence of human serum (**Figure 4**). We observed a significant reduction in bacterial viability for both strains when treated with CoMiX molecules for 2 hours compared to the control groups resulting in an approximate 40% and 35% reduction in CFU for CoMiX-Fc and CoMiX-FHR1, respectively (**Figure 4A**). Consistently with the CFU data, CoMiX treatment resulted in around 40% reduction in relative luminescence units (RLU) after 2 hours of treatment on a PAO1 Luc strain, indicating decreased activity and bacterial growth (**Figure 4B**). To evaluate the potential for synergistic interaction, we combined CoMiX-Fc and CoMiX-FHR1 with the aminoglycoside antibiotic amikacin against the *P. aeruginosa* strain PAO1 and the clinical isolate IPP6247290 (**Figure 4C**). This clinical isolate exhibited inherent resistance to amikacin, requiring a higher MIC (40 µg/ml) compared to the reference strain PAO1 (8 µg/ml). Multiple sub-MIC concentrations of amikacin were tested for both strains. We calculated a synergy coefficient, as described by Chaudhry et al.[434], and observed the strongest synergy between the two treatments at 2 µg/ml of amikacin for PAO1 and 10 µg/ml of amikacin for IPP6247290. Notably, the irrelevant CoMiX control combined with amikacin displayed synergy coefficient values of 0.002 for PAO1 and 0.025 for IPP6247290, indicating the absence of synergy and highlighting the specificity of the antibacterial effect of CoMiX-Fc and CoMiX-FHR1. Interestingly, CoMiX-Fc consistently exhibited a more negative synergy coefficient compared to CoMiX-

FHR1 for both strains (PAO1: -0.061 vs. -0.052; IPP6247290: -0.027 vs. -0.002), suggesting a potentially stronger synergistic effect with amikacin in reducing *P. aeruginosa* viability.

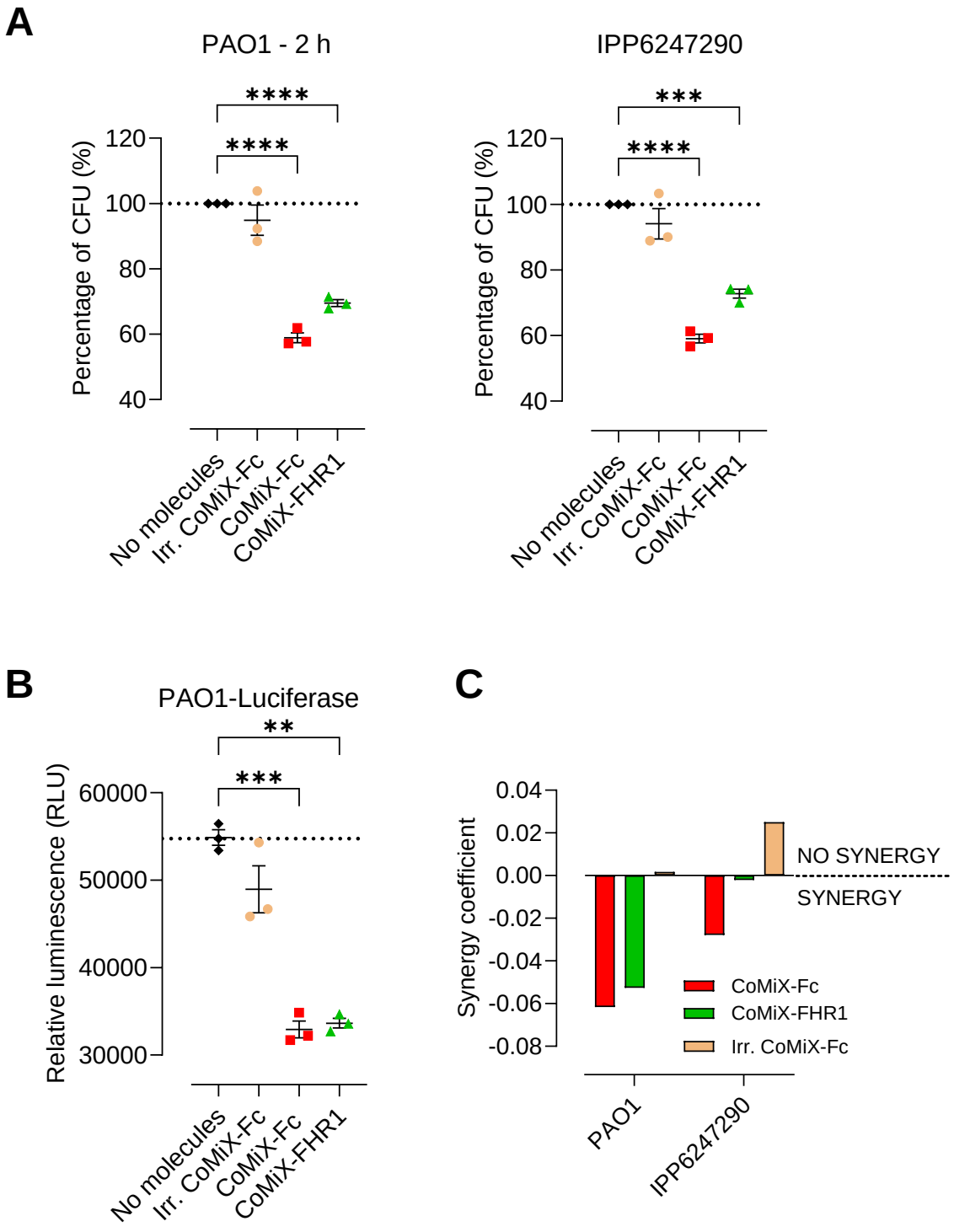

Figure 4. CoMiX enhance complement-mediated killing of *P. aeruginosa* and display synergy with amikacin. (A) Bacterial reference strain PAO1, and clinical isolate IPP6247290 strain were incubated with 10% normal human serum (NHS) in the presence or absence of 30 µg/ml CoMiX or irrelevant control for 2 hours at 37°C. Bacteria were plated, and colony forming units (CFU) were enumerated to assess bacterial viability. Data are presented as the mean values ± SEM. Results correspond to three pooled independent experiments (3 replicates per experiment). Statistical analysis was performed using one-way ANOVA followed by Tukey's post-hoc test. ***$p < 0.001$; ****$p < 0.0001$. **(B)** A mutated PAO1 bacterial strain with a luminescence-based reporter system (PAO1-Lux) was used in the same protocol as in A to monitor in real-time bacterial growth. The luminescence of bacteria (RLU) was measured after two hours of incubation on the POLARStar Omega microplate reader, as it is known that luminescence of bacteria correlates well with its concentration. Data are presented as the mean values ± SEM. Results correspond to three pooled independent experiments (3 replicates per experiment). Statistical analysis was performed using one-way ANOVA followed by Tukey's post-hoc test. ***$p < 0.001$; ****$p < 0.0001$. **(C)** To assess the potential of CoMiX in combinaison with the antibiotic amikacin, both the reference strain PAO1, and clinical isolate IPP6247290 strain were incubated with 10% NHS in the presence or absence of 30 µg/mL of CoMiX or irrelevant control, as well as various sub-MIC concentrations of amikacin (2 µg/ml for PAO1, 10 µg/ml for IPP6247290) for two hours at 37°C. Bacteria were plated, and colony forming units (CFU) were enumerated to assess bacterial viability. A synergy was admitted when the synergy coefficient (log(C) – log(SA) – log(SB) + log(SAB) < 0 (where C is CFU without treatment, SA is CFU with amikacin only, SB is CFU with CoMiX only, and SAB is CFU with both)), was negative. Data are presented as synergy coefficient calculated from the mean of three independent experiments (3 replicates per experiment).

CoMiX-Fc enhances phagocytosis of *P. aeruginosa* by PBMC-derived macrophages.

Beyond their complement-dependent lysis of bacteria, we decided to investigate the effects of CoMiX on the phagocytosis of *P. aeruginosa* by human peripheral blood mononuclear cell-derived macrophages. As described in the literature, pHrodo-stained bacteria only release fluorescence in an acidic environment, corresponding in our set up to the endosomes and lysosomes compartment. Using the incucyte, we were able to watch over time the engulfment of bacteria, and the emission of fluorescence when reaching the designated compartment **(Figure 5)**. To assess this phagocytosis, we measured the intensity of pHrodo in the cells **(Figure 5C)**. After 30 minutes, we already observed that the treatment by CoMiX-Fc produced a higher intensity of pHrodo compared to serum alone, synonym of a higher phagocytosis **(Figure 5A)**. This trend was confirmed after one hour in the co-culture when CoMiX-Fc treatment significantly increased the intensity of pHrodo in positive macrophages compared to the untreated group, but also to the irrelevant control **(Figure 5B)**. However, CoMiX-FHR1 did not displayed a higher effect than the control, suggesting that the ability of the serum to opsonize by itself the bacteria was not increased in the presence of CoMiX. The effect observed for the CoMiX-Fc seemed to be rather dependent on the liaison between

Fc and FcR. After two hours, no more differences were observable between the groups, due to the phagocytosis of nearly all bacteria. Fluorescent microscopy was used to confirm and visualize the phagocytosis of bacteria by PBMC-derived macrophages. Surprisingly, only a small amount of bacteria was detected in the cells (1-2 bacteria/cells) suggesting that MAC formation and direct lysis of bacteria was

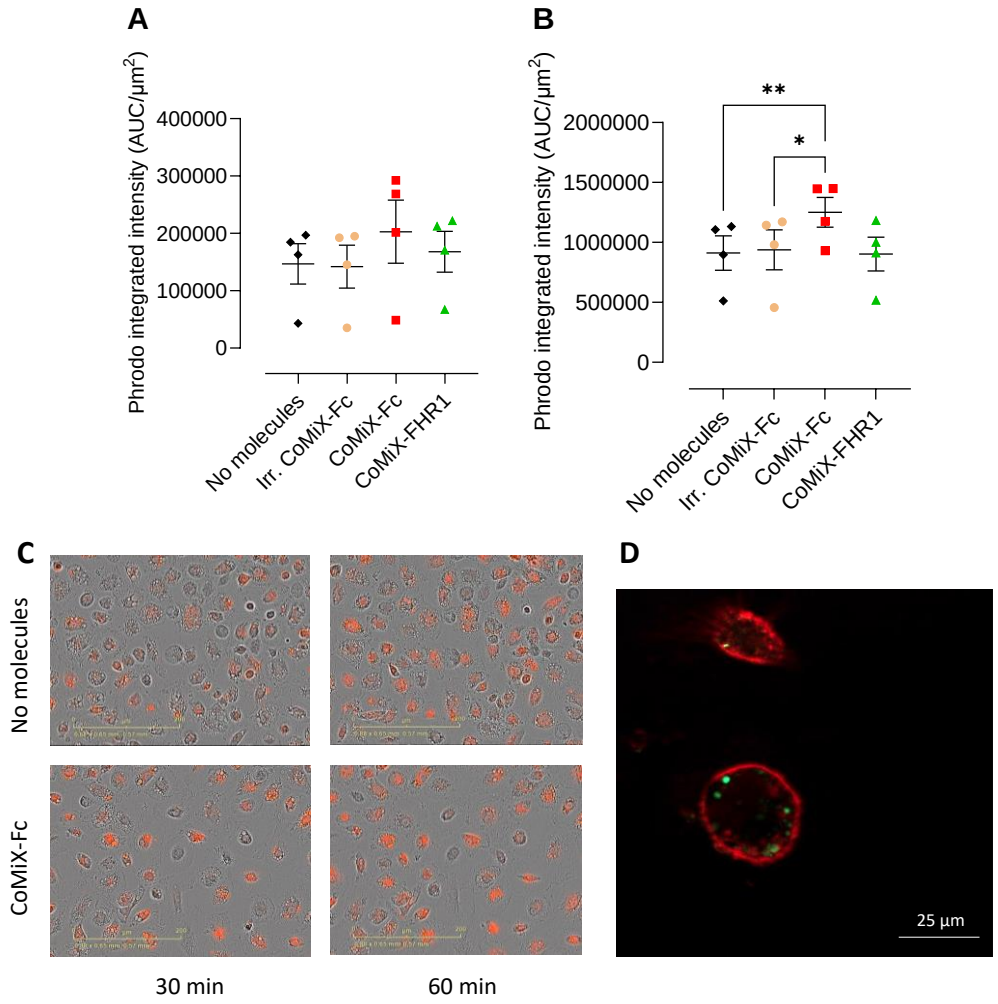

the preferential mechanism of action of CoMiX-Fc (**Figure 5D**).

Figure 5. CoMiX-Fc enhances phagocytosis of *P. aeruginosa* by PBMC-derived M1 macrophages. PMA-activated M1 macrophages were co-incubated with pHrodo-stained *P. aeruginosa* (PAO1) at a 1:12 ratio with 10% NHS and in the presence or absence of 15 µg/ml CoMiX-Fc or CoMiX-FHR1 or CoMiX-irrelevant. Phagocytosis was assessed after 30 minutes **(A)** and 1h **(B)** by taking pictures by the Incucyte microscope. The intensity of pHrodo as a marker of phagocytosis was measured, rationalized over the surface of cells and calculated as integrated intensity. Data are presented as the mean values ± SEM. Results correspond to two independent experiments (two healthy donors per experiment). Statistical analysis was performed using paired one-way ANOVA (to smooth inter-donor variability), followed by Tukey's post-hoc test: *$p < 0.05$; **$p < 0.01$. **(C)** Representative incucyte images for the phagocytosis

induced by serum and CoMiX-Fc after overtime. **(D)** Fluorescence microscopy image of phagocytosed *P. aeruginosa* bacteria by PBMC-derived M1 macrophages in presence of 10% serum and 15 µg/ml CoMiX-Fc. Red=wheat germ agglutinin Alexa-647, staining carbohydates residues of macrophages membranes; green= CellTrace™ CFSE stained *P. aeruginosa* bacteria.

CoMiX reduce the cytotoxicity of infected BEAS-2B human epithelial cells.

We used the human bronchial epithelial BEAS-2B cell line to closely mimic the physiological characteristics and function of the bronchial epithelium of the lung affected by *P. aeruginosa* infection. To assess CoMiX's intrinsic cytotoxicity, we initially evaluated its effect on BEAS-2B cell viability in the presence of serum without bacterial infection. Our findings revealed no significant increase in LDH release upon CoMiX treatment compared to the untreated control group (**Figure 6A**) suggesting a favorable safety profile. In contrast, PAO1 infection caused a substantial increase in LDH release (**Figure 6B and C**), signifying a pronounced elevation of cytotoxicity mediated by PAO1. Co-administration of CoMiX-Fc with PAO1 during infection significantly reduced LDH release (-47%) compared to PAO1 alone but not the co-administration of CoMiX-FHR1 or the irrelevant control. These data imply that CoMiX-Fc is able to mitigate PAO1's detrimental effects on BEAS-2B cells. This was confirmed by the measurement of IL-6 production by BEAS-2B cells in the supernatant (**Figure 6C**). Interestingly, treatment with both CoMiX resulted in a significant increase in IL-6 production by approximately 50% ($p < 0.05$) which could contribute to clear *P. aeruginosa* infection in the lung.

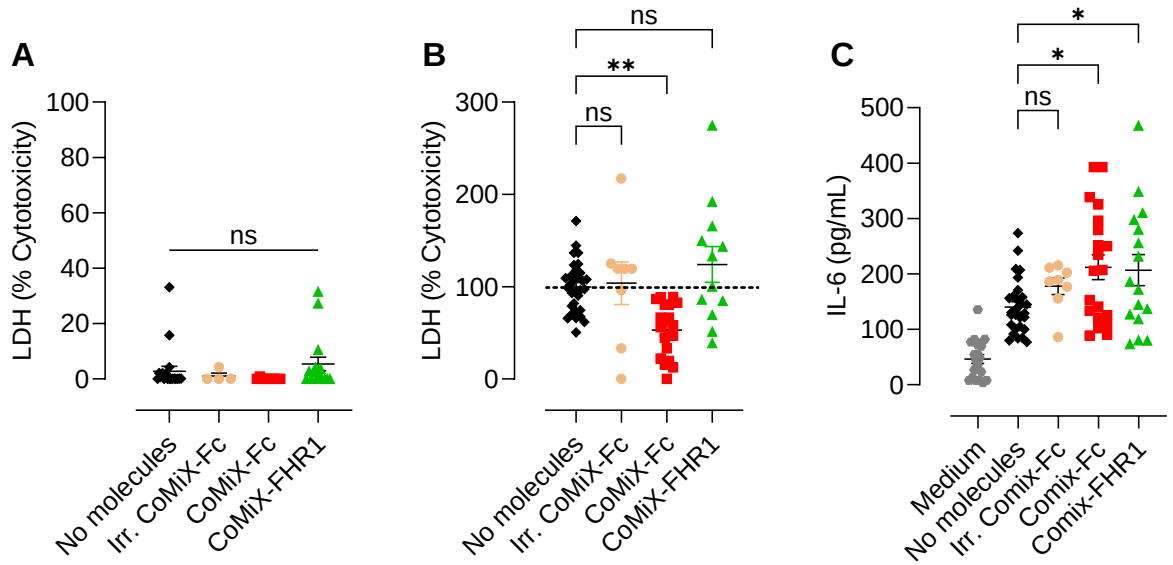

Figure 6. CoMiX are non-immunogenic for BEAS-2B bronchial epithelial cells, can protect against *P. aeruginosa* infection and modulate immune response. BEAS-2B epithelial cells were treated only with CoMiX (15 µg/mL) in

presence of 10% normal human serum. **(A)** Cell viability was assessed by measuring lactate dehydrogenase (LDH) release in the culture supernatant after 6 hours. Cells were infected with PAO1 at an MOI:10 in the presence of 10% NHS and CoMiX-Fc (15µg/mL), CoMiX-FHR1 (15µg/mL), CoMiX irrelevant (15µg/mL) or no molecules for 6 hours. **(B)** Cell viability was assessed by measuring lactate dehydrogenase (LDH) release in the culture supernatant after 6 hours. LDH was expressed as % of response over infected-untreated conditions (positive control for cell death). **(C)** IL-6 produced in the cell culture supernatant was measured as a marker of the epithelial response. Data are presented as the mean values ± SEM. Results correspond to at least three pooled independent experiments (3-6 replicates per experiment). Statistical analysis was performed using one-way ANOVA followed by Tukey's post hoc test: *$p < 0.05$; **$p < 0.01$.

CoMiX administered intranasally protects mice against an acute lung infection by facilitating the clearance of *P. aeruginosa*

To initially assess the efficacy of our molecules, we employed a prophylactic mouse model involving two doses administered 3 hours before and 3 hours after infection with Pseudomonas aeruginosa (**Figure 7**). Seven-week-old female C57BL/6J mice were intranasally challenged with a lethal dose of bioluminescent PAO1 (PAO1-lux) to establish infection in the lung. The mice were divided into three treatment groups: CoMiX-Fc, CoMiX-FHR1, or an irrelevant CoMiX control (anti-aspergillus CoMiX-Fc). Treatments, consisting of 100 µg/mL of molecules, were administered at a time point three hours prior to infection (T_{-3}) and again at a time point three hours' post-infection (T_3) (**Figure 7A**). Survival was monitored daily throughout the experimental period (**Figure 7B**). Body weight was also measured daily to evaluate the impact of the treatments on host health (**Figure 7C**). Bioluminescence imaging of the luciferase-expressing *P. aeruginosa* PAO1 strain within the lungs was conducted using an IVIS Lumina system on days 1, 2, and 3 following infection (**Figure 7D**, **E**). Bioluminescence intensity served as a quantitative measure of bacterial burden within the lungs and nasal cavity.

Administration of CoMiX significantly enhanced the survival of mice compared to the control group ($p < 0.0001$, **Figure 7B**). While all control mice required euthanasia by day 2 post-infection due to the administration of the irrelevant CoMiX, all mice in the treatment group survived until this point. By day 6, 62.5% of mice treated with CoMiX-Fc and 87.5% of mice treated with CoMiX-FHR1 were alive and exhibited weight gain from day 2 (**Figure 7C**). Bioluminescence imaging using the IVIS Lumina system was performed 24 hours' post-infection to assess bacterial burden (**Figure 7D**). After 24 hours' post-infection only 43.75% of mice in the CoMiX-Fc treatment group and 37.5% of mice in the CoMiX-FHR1 treatment group exhibited lung or nasal cavity luciferase activity, indicating reduced bacterial colonization compared to the control group, where all mice were luciferase-positive.

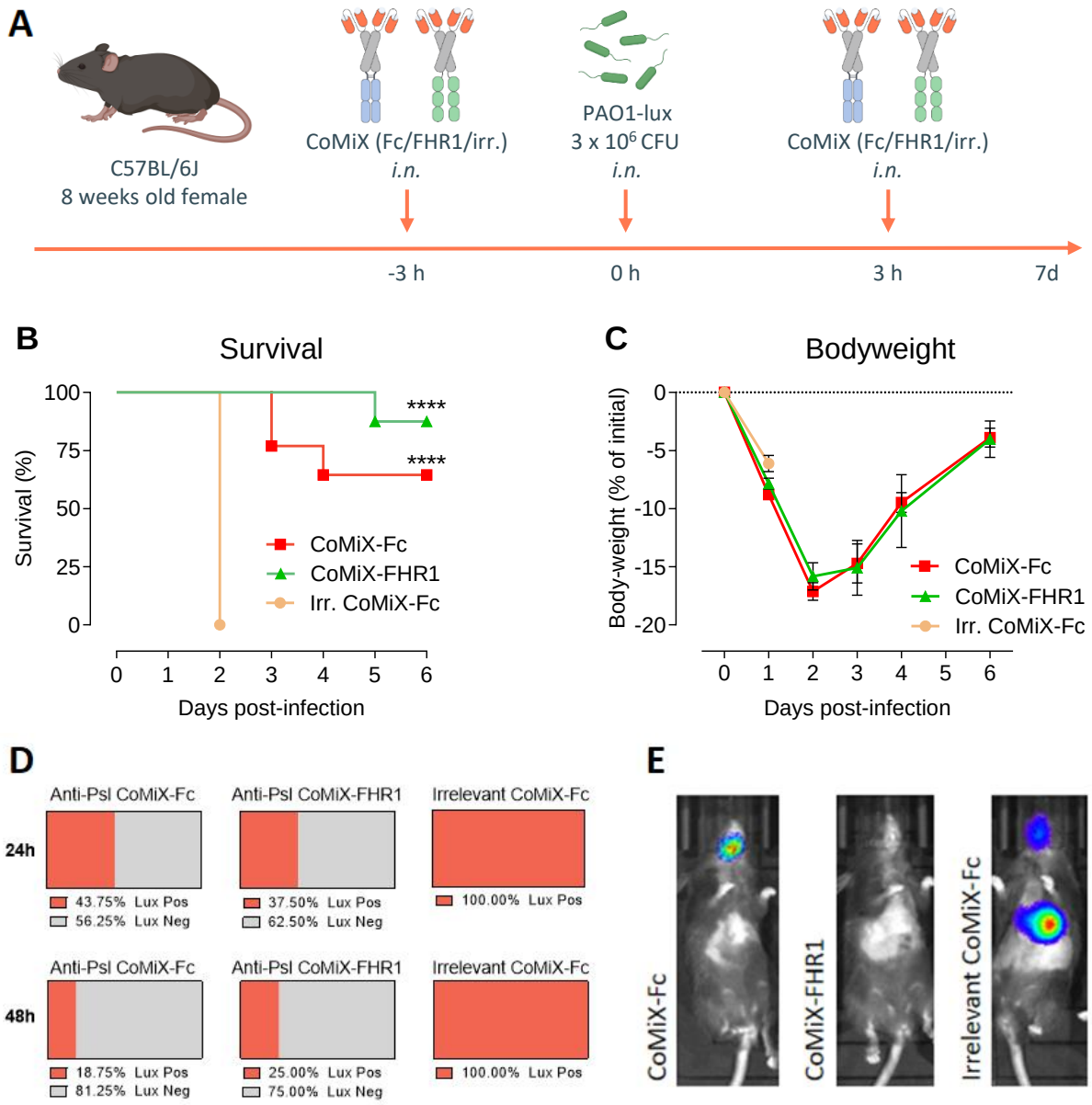

Figure 7: Prophylactic treatment with anti-Psl CoMiX protect mice from lethal *Pseudomonas aeruginosa* lung infection. (**A**) Seven-week-old female C57BL/6J mice were infected intranasally (*i.n.*) with a lethal dose (3 x 10^6 CFU) of luciferase-expressing PAO1 strain. Mice were treated with anti-Psl CoMiX-Fc, anti-Psl CoMiX-FHR1, or an irrelevant CoMiX control three hours before and after intranasal infection with luciferase-positive *Pseudomonas aeruginosa* PAO1. Survival (**B**) and body weight (**C**) were assessed daily for six days following infection. The data were analyzed using a log-rank test (Mantel-Cox), revealing statistically significant differences between groups (***p < 0.001, ****p < 0.0001). Results are presented as mean values ± standard error of the mean (SEM). (**D**) Bioluminescence imaging comparison of colonization by *P. aeruginosa* in mice treated with anti-Psl CoMiX-Fc, anti-Psl CoMiX-FHR1, or control. Luciferase activity was assessed 24 hours and 48 hours' post-infection. The figure illustrates the distribution of

luciferase-positive and luciferase-negative mice in each group. (**E**) A representative image of a mouse from each group is provided.

We next assessed CoMiX potency in a therapeutic model (**Figure 8**) where molecules were administered one-hour post-infection. All groups received a single intranasal dose of 100 µg of their respective CoMiX molecule diluted in PBS (**Figure 8A**). Treatment with the anti-Psl CoMiX significantly improved survival rates compared to the control group (**Figure 8B**). By day 2 post-infection, 50% of control mice succumbed to infection. In contrast, all mice treated with CoMiX-Fc or CoMiX-FHR1 survived up to this point, demonstrating the protective efficacy of CoMiX. By the study endpoint (day 7) only 31% of mice were still alive in the irrelevant control group, while all mice survived in the CoMiX-Fc treatment group and 93% survived in the CoMiX-FHR1 group. While body weight changes were similar between groups up to day 2, mice in the CoMiX-treated groups exhibited a faster recovery of body weight from day 2 onwards, suggesting potential improvement in their overall health status (**Figure 8C**). Compared to the control group, CoMiX treatment resulted in a significant reduction in bacterial burden (**Figure 8D and E).** At day 1, only 50% and 61.5% of mice treated with CoMiX-Fc and CoMiX-FHR1, respectively, displayed detectable bioluminescence, indicating a substantial decrease in bacterial colonization compared to the control group, where all mice were luciferase-positive. By day 2, the percentage of luciferase-positive mice remained lower in the CoMiX-treated groups (50% for CoMiX-Fc, 62.5% for CoMiX-FHR1) compared to the control group (71.4%). Finally, at 72 hour's post-infection, only 12.5% of mice in both CoMiX treatment groups were luciferase-positive, while 33.3% of mice in the control group remained positive, representing a 2.66-fold increase in the proportion of persistently infected mice as compared to the CoMiX-treated groups.

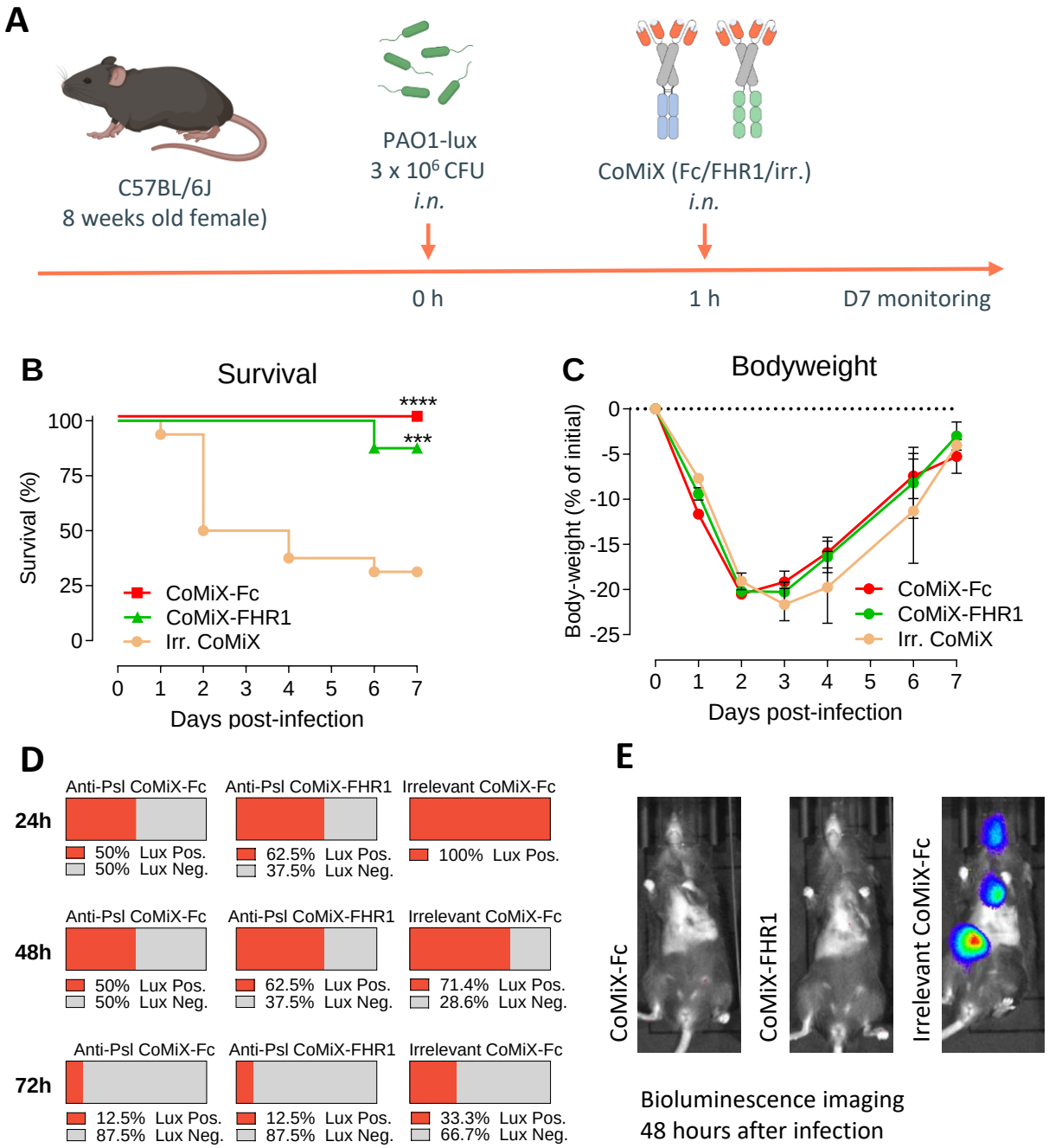

Figure 8. CoMiX protect mice from acute lung infection of *P. aeruginosa*. **(A)** Seven-week-old female C57BL/6J mice were infected intranasally (*i.n.*) with a lethal dose (3 x 10^6 CFU) of luciferase-expressing PAO1 strain. Mice were treated one hour later with 100 µg of CoMiX-Fc, CoMiX-FHR1 or an irrelevant CoMiX via *i.n* administration. Survival **(B)** and body weight **(C)** were monitored for 7 days after infection. Data are presented as the mean values ± SEM. Results correspond to two pooled independent experiments (*n* =16 mice per group). Statistical analysis was

performed using the log-rank test (Mantel-Cox). ***$p < 0.001$; ****$p < 0.0001$. **(D, E)** Lung infection was assessed by visualizing *P. aeruginosa*-associated luminescence emission in live animals during the first 3 days after the infection. One representative mouse image for each group is displayed. Data are presented as a percentage of mice with negative versus positive signal for bacteria. Results correspond to two pooled independent experiments (n =16 mice per group). Image of representative animal for each group.

CoMiX neutralize bacteria *in vivo* through complement activation, allowing for an enhanced control of local lung inflammation

We investigated the mechanisms underlying the protective effect promoted by CoMiX against *P. aeruginosa* acute infection in the therapeutic animal protocol. First, when looking at representative lungs from each group at 16 hours *p.i*, macroscopic differences could already be observed between the groups. Mice treated with the irrelevant CoMiX had lungs fully hemorrhagic, a typical presentation of severe lung injury due to *P. aeruginosa* infection whereas mice treated with either CoMiX-Fc or CoMiX-FHR1 had lungs with a lesser injury, a reduced stage of hemorrhage, and clear visible healthy areas **(Figure 9A)**. In agreement with the bacteria luminescence inside the lungs, we confirmed that mice treated with the irrelevant control presented the higher bacterial load in both the BAL (6 log CFU/mL) and the lungs (7 log CFU/mL) from 4h, only accentuated to 16h **(Figure 9B and C)**. In contrast, the therapeutic administration of both CoMiX-Fc and CoMiX-FHR1 reduced significantly the bacterial load in comparison to the irrelevant control, with a reduction of one log of the CFU in the BAL and the lungs ($p < 0.01$). The rapid and strong decrease in the number of CFU (already at 4h *p.i.*) suggests a direct killing effect of CoMiX rather than a longer process with activation of immune cells.

In concordance with their mode of action, both CoMiX-Fc and CoMiX-FHR1 induced a higher concentration of cleaved C3 fragments in the blood and in the BAL as compared to the mice that received the irrelevant control ($p < 0.01$) **(Figure 9D and E)**. This increased concentration, observed as a fast complement activation, was only detected at 4h *p.i.* and was downregulated after 16h. Concentrations of cleaved C3 molecules were correlated with an increased bacterial load in the BAL ($p< 0.0001$) **(Figure 9F)**. Overall, our results suggest that the protection of mice against an acute *P. aeruginosa* infection depends on their complement-dependent killing activity, and disappears fast enough causing less damage to the lung.

To further investigate the stimulation of the immune system involved in the enhanced clearance of *P. aeruginosa*, we measured the total number of cells and specific immune populations of leukocytes (CD45+) in the airways by flow cytometry **(Figure 9G)**. We observed that the mice receiving CoMiX-Fc and CoMiX-FHR1 had significantly fewer cells in their BAL than the mice treated with the irrelevant control,

demonstrated consistently at 4h (tendency) and 16 hours *p.i.* ($p < 0.01$). In a similar way, the mice that control acute infection in the CoMiX-Fc and CoMiX-FHR1 groups had also fewer immune cells, such as neutrophils **(Figure 9I)**, macrophages **(Figure 9H)** or eosinophils **(Figure 9K)** as compared to the irrelevant group ($p < 0.05$, $p < 0.01$). This suggests that the activation of the complement system limits the activation of the cellular immune system, especially the influx of neutrophils in the lungs. Interestingly, when the protected mice had fewer neutrophils in the BAL than the control, they tended to be more activated ($p < 0.05$ for CoMiX-Fc vs irrelevant and $p = 0.0647$ for CoMiX-FHR1 vs irrelevant) **(Figure 9J)**. The higher deposition of the complement on the bacteria induced a better control of the infection with a limited cell recruitment and a potential enhanced phagocytosis. CoMiX, by rapidly clearing part of the infection, could modulate the cellular immune response and limit the local inflammatory response, often associated with poor outcomes during *P. aeruginosa* acute lung infection.

To confirm those findings, we investigated the production of the pro-inflammatory cytokines and chemokines associated with innate immunity in cell-free BAL using the MSD U-plex assay. At 4h *p.i.*, animals that received CoMiX-Fc and especially CoMiX-FHR1, had significantly lower levels, compared to mice that received the irrelevant control ($p < 0.05$ and $p< 0.01$), of cytokines IL-6, TNF-α **(Figure 9L and M)**, and to a lesser extent IL-1β and GM-CSF **(Supplementary Figure 5A and B),** as well as chemokines KC/CXCL1 **(Figure 9N)** and MIP1α **(Supplementary Figure 5C)**. At a later time-point, 16h *p.i.*, the levels of pro-inflammatory mediators were similar for all groups of mice. As such, the rapid complement-dependent killing of *P. aeruginosa* infection was enough to lessen the expression of pro-inflammatory mediators, and participate, in the same manner as the immune cells, to an early resolution of the acute local inflammation.

Overall, our data suggest that the protection of the mice is mainly attributable to the fast CoMiX-dependent activation of the complement pathway, which by resolving rapidly the acute infection, limits global inflammation of the lungs and its deleterious effects.

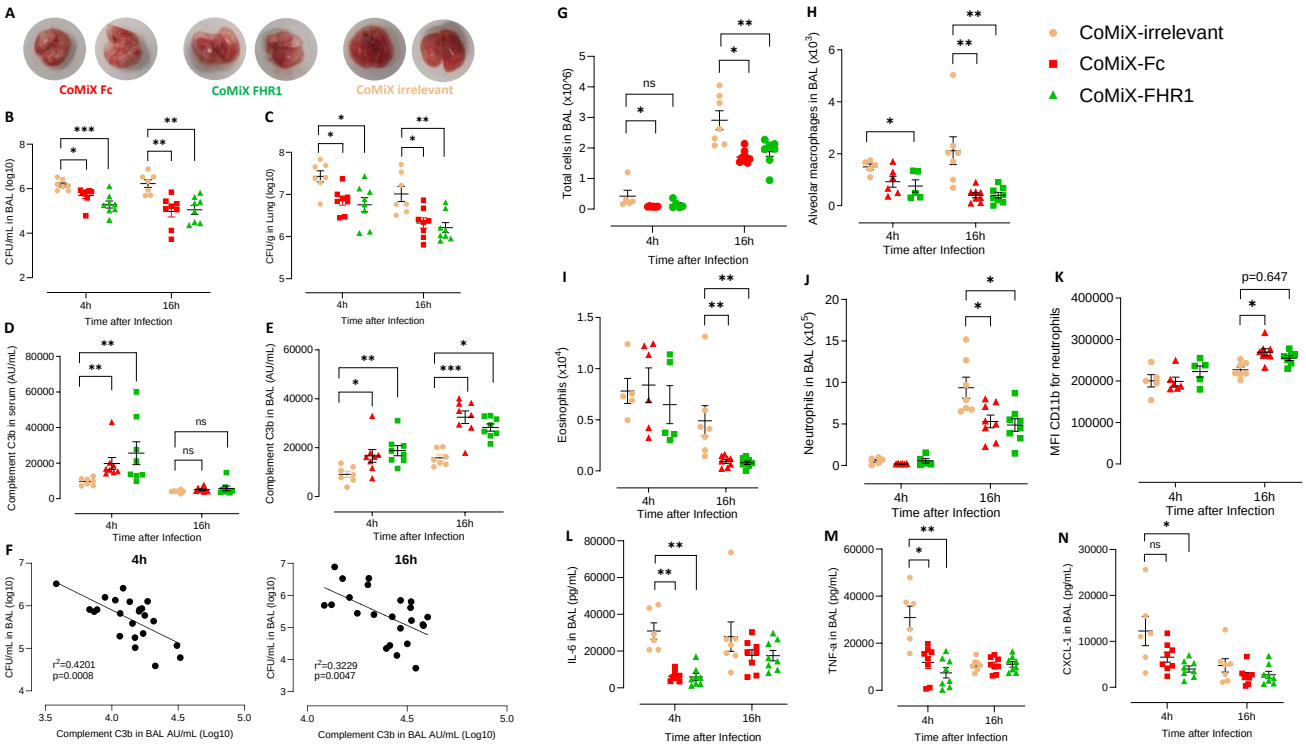

Figure 9. CoMiX in vivo protection depends on local complement activation and is associated with improved lung inflammation. Mice were infected/treated as described in Fig 7A, sacrificed at 4h and 16h post-infection, and lungs, BAL and blood were collected. **(A)** Lungs were first perfused for a visual assessment of inflammation. Bacterial load in BAL **(B)** and lungs **(C)** were determined after serial dilution and plating on petri dishes. To assess the activation of the complement cascade, the concentration of activated fragments of the mouse complement protein C3 was determined by ELISA, systemically in the serum **(D)** and locally in the BAL **(E)**. **(F)** Concentration of local C3 activated fragments was correlated with the BAL bacterial load. Data are shown as individual values (n=23 mice). As a reflection of lung inflammation, the BAL was assessed by flow cytometry for its number of total immune cells **(G)**, alveolar macrophages **(H)**, neutrophils **(I, J)** and eosinophils **(K)**, as well as its production of IL-6 **(L)**, TNF-α **(M)** and CXCL-1 **(N)**, measured by a MSD assay. All data are quoted as the mean values ± SEM and the results correspond to one experiment per time-point (n = 7-8 mice per group). Unless otherwise stated, all statistical analyses were performed using the Kruskal-Wallis test followed by a Dunn's post-test for comparisons between the groups, *: $p < 0.05$; **: $p < 0.01$; ***: $p < 0.001$. BAL = broncho-alveolar lavage; CFU = colony-forming unit; h = hours; SEM = standard error of the mean; IL= interleukin; TNF = tumor necrosis factor.

DISCUSSION

In the last decade, the emergence of multidrug-resistance in *Pseudomonas aeruginosa* bacteria combined to increased prevalence of infections in hospitalized patients has made the treatment of *P. aeruginosa* infections highly challenging. Those infections can be associated with severe and acute pneumonia but also with persistent infections, such as ones found in cystic fibrosis (CF) patients. The decline of antibiotic efficacy, and sometimes their complete failure against multi-resistant strains, necessitate the development of novel therapeutic strategies strategies[412, 435]. With success in the treatment of HIV or COVID-19 infections, antibody-based therapies show now great promise against infectious diseases[436].

In this work, we engineered and evaluated two anti-bacterial CoMiX, a novel class of complement-activating immunotherapeutic complexes, intended for the fast and directed-killing of multi-drug resistant *P. aeruginosa*. If current therapies targeting the complement system aim to inhibit its effect, deleterious in diseases such as the anti-neutrophilic cytoplasmic antibodies–associated vasculitis (AAV)[437], we, and others[438] aim in contrast to enhance its selective activity, as shown on cancer cells model, by blocking complement inhibitors on target cells to prevent undesired inflammation. Both recombinant proteins utilize the C-terminal oligomerization domain of the C4b-binding protein (C4BP). C4bp has long been recognized as a valuable tool for therapeutic applications in protein engineering and synthetic biology[403, 439, 440], and our group pioneered its application in developing therapeutic agents against HER2-positive breast cancer[106] and HIV infection[432]. CoMiX-Fc was designed to activate the classical pathway through Fc receptor engagement on immune cells and binding to C1q molecule. CoMiX-FHR1 was generated to enhance the alternative pathway by exploiting a novel mechanism, recently described[76], where FHR-1 disrupts FH-mediated cofactor activity for C3b degradation and C3 convertase decay, ultimately leading to increased C3 deposition on *P. aeruginosa*. These findings align with other previous reports demonstrating FHR-1's role as a competitive inhibitor of FH in various contexts, including Group A *Streptococcus*[441], *Plasmodium falciparum*[77], and interactions with DNA and dead cells[73]. Our data bring the evidence that FHR-1 promotes opsonization by limiting FH-dependent complement inhibition.

The main bottleneck of targeted therapies against infectious diseases is the selection of the right target. Indeed, the expression of a target at the surface of a pathogen can differ between strains, between disease contexts, even between infection sites as observed by *Enterobacteraciae* which can preferentially present fimbriae in the urinary tract, or capsular polysaccharides in the blood[442]. Therefore, while past attempts using antibodies targeting *P. aeruginosa* have shown initial promise in preclinical and early clinical studies, large-scale trials have not yet demonstrated consistent efficacy. A prime example concerns

the candidate KB001-A targeting the Type III Secretion System (T3SS) protein PcrV, able to reduce pneumonia incidence in mechanically ventilated patients colonized with *P. aeruginosa*, but failing to offer protection against the bacterium in CF patients, probably due to the reduction expression of T3SS in isolates colonizing CF patients[443, 444]. Here, we initially compared the binding of two scFvs (anti-O11 and anti-psl) in CoMiX to a diverse panel of clinical isolates. We found a broad recognition (82%) of the Psl scFv, including those exhibiting multi-drug resistance (MDR) to conventional antibiotics, especially to non-CF bacteria (96%). This broad targeting contrasted with the limited efficacy of anti-O11 scFv, reflecting the lower prevalence (20%) of the O11 serotype, nevertheless tested in clinical trial under the name of Panobacumab[445]. In addition, Psl is an attractive target with the ability to hinder *P. aeruginosa* infections and to prevent bacterial attachment and biofilm[446,447].

Both CoMiX-Fc and CoMiX-FHR1 effectively deposited the complement components C3b and C5b9 on the surface of *P. aeruginosa*, participating in the direct lysis of the bacteria by MAC formation, but also in its opsonization and subsequent phagocytosis by immune cells. From the *in vitro* data, it seems that this effect takes place rapidly after the treatment but lose rapidly its effect with regain of growth of the bacteria after 6 hours. This indicates a bacteriostatic activity of CoMiX, which might be due the limited delivery of complement in serum, provided here only at the beginning of the infection. The concentration of convertase enzymes or of complement component tends to decrease over its use. As reported by others, the resolution of infection uses high amount of complement. Once the system is depleted, the infection can regain strength[448]. This limited effect could fortunately be overcome *in vivo*, in the presence of an ever-replenishing pool of complement. Interestingly, CoMiX displayed a synergistic effect with the aminoglycoside antibiotic amikacin against both reference and clinical *P. aeruginosa* isolates. As CoMiX and antibiotics have different mode of actions, acting on different pathways, the synergistic interaction could lead to potential enhancement of their respective effects, and allowing for lower therapeutic doses. Furthermore, as their pharmacokinetic properties are different, their ratio and concentrations in blood and at the infection sites should vary overtime, lessening the selective pressure on the bacteria and preventing the emergence of further resistance[449]. Testing combinations of CoMiX with antipseudomonal antibiotics (e.g. penicillins, cephalosporins, etc…) could offer new perspectives on enhanced efficacy of the drugs, or even participate in the slowing of resistance evolution[450].

Furthermore, in a cytotoxic assay we showed no significant detrimental effects of CoMiX on human bronchial epithelial cells suggesting a favorable safety profile, which was corroborated by reduced cytotoxicity of BEAS2B cells induced by *P. aeruginosa* infection by CoMix-Fc but not CoMix-FHR1. The

difference could be explained by FcR and FcRn, the latter being expressed in epithelial cells, and known to contribute to the immune responses against several bacterial and viral infections, mediating local protection via its transport functions[451]. The activation of FcRn by the Fc fragment of CoMiX-Fc may limit pathological damages due to bacterial infection, and the activation of FcR could induce a higher secretion of anti-microbial peptides by the epithelial cells as shown with *Citrobacter rodentium*, *Clostridioides difficile* or *Helicobacter heilmannii* and *H. pyloriin* in mice models of infection[452]. Interestingly, both CoMiX targeting the bacteria could increase IL-6 secretion by epithelial cells, revealing that CoMiX treatment could modulate the host immune response in response to a pathogen, contributing to bacterial clearance. IL-6 is a pleiotropic cytokine with both pro-inflammatory and immunoregulatory functions[453], and has been shown to enhance neutrophil recruitment and phagocytosis[454], as well as being a key mediator for the increased efferocytosis observed in macrophages[455]. While we showed this increase *in vitro*, we observed an overall decrease of IL-6 in the BAL of mice treated with CoMiX 4 hours *p.i*. Previous studies have proposed that IL-6 is induced by a number of immune cells *in vivo*[456, 457], potentially obscuring its direct protective effects. In this case, the *in vitro* data could provide a more detailed understanding of the mechanisms of action that may be masked *in vivo* due the rapid clearance of bacteria, and a reduced overall pro-inflammatory environment.

The *in vivo* studies conducted in a murine model of acute *Pseudomonas aeruginosa* lung infection demonstrated the therapeutic potential of CoMiX. Both prophylactic and therapeutic treatments with CoMiX significantly enhanced survival rates and reduced bacterial burden compared to control groups receiving the irrelevant CoMiX treatment. While CoMiX-FHR1 exhibited slightly superior efficacy in the prophylactic model, the opposite was observed in the therapeutic model probably reflecting the variability of the animal model. The observed variation in infection severity between the control groups in the prophylactic and therapeutic treatments could be attributed to factors such as initial bacterial load, host susceptibility, and experimental conditions. In the prophylactic treatment, while all mice receiving the irrelevant CoMiX control died 48 hours after infection, 93 % of the mice receiving CoMiX-FHR1 survived. The reduced local bacterial burden was correlated with higher concentrations of C3b in the therapeutic protocol, confirming the critical part of the complement system in the host defense against pathogens. Activation of complement was detected rapidly at the site of infection in the BAL but also in the blood. No severe side effects were however observed with CoMiX treatment during 7 days, confirming the safety of targeted activation of complement. The reduction of complement to nearly normal levels after 16 hours, implied a transient activation of complement, thus avoiding its chronic activation and confirming the promise of CoMiX for therapeutic development.

Interestingly, a shared mechanism of anti-*P. aeruginosa* immunity, and general lung infection, involved improved cell activation and rapid neutrophil recruitment to the site of the infection which will phagocyte and kill the bacteria[458]. However, with the administration of CoMiX in our model of infection, we did not observe this rapid and massive recruitment of neutrophils, even at the early time *p.i*. in comparison to the control, neither did we observed the recruitment of other type of cells. The rapid resolution of the infection by the targeted action of complement could have early on limited this recruitment, preventing local inflammation, which may have favored the survival of the mice. Indeed, during acute lung infection, an excessive inflammation can lead to tissue injury and chronic activation of immune cells, resulting in the death of the host[459]. The decrease of pro-inflammatory mediators in the BAL of the mice treated with CoMiX was in accordance with the reduced presence of immune cells. The early control of *P. aeruginosa* in lungs was associated with C3b concentrations resulting in improved survival. If the overall *in vivo* efficacy of CoMiX-FHR1 and CoMiX-Fc was comparable, suggesting similar promising therapeutic potential, CoMiX-FHR1 had the advantage of engaging the alternative pathway. Studies have shown that this alternative pathway functions preferentially as a protective mechanism during critical illness resulting in a more robust activation compared to relying solely on the classical pathway[460].

Apart from the development of resistance in bacteria, the main problem of antibiotics is their broad range of action, which far from being specific to a bacterium can destroy the positive environmental bacteria, as found in the microbiota[461]. The use of targeted therapies, such as therapeutic antibodies has already shown its use to protect the microbiota. The activation of complement in those cases would be highly beneficial as its physiology and activation pattern is modulated in different compartments: in the gut, as the complement is nearly deprived of its terminal components, pathways are stopped before the level of MAC formation, sparing the commensals bacteria, but engaging the pathogens[462]. Beyond the practical aspect of CoMiX to treat successfully acute infections, *P. aeruginosa* is also known to be persistent bacteria, developing into biofilm and inducing chronic infections. The bacterium can evolve and colonize the host by forming 3D structures engulfed in a specific micro-environment, or grow in mucus, difficult to access for therapeutics. The use of the exopolysaccharide Psl, one typically conserved element of the extracellular polymeric substances (EPS), as a target, stands as a smart choice as it should disrupt the formation of the biofilm[152]. However, CoMiX can only bind to 45% of the CF isolates. Moreover, once the biofilm is formed, the accessibility to Psl would be impaired making it more difficult for the complement to find its target[463]. The use of CoMiX in combinations with mucolytic agents, antibiotics, or quorum-sensing inhibitors could reduce the effect of the protective barrier and restore part of the complement action[464]. Examining in details the expression of the biofilm could also help find new targets, more

expressed on bacterial strains. Ultimately, the biggest advantage of CoMiX is their molecular design allowing for customization of both targeting and effector functions. This versatile platform enables the development of highly specific therapeutic agents for a wide range of diseases. In the case of chronic infections, quorum sensing inhibitors, or biofilm formation inhibitors might be incorporated into CoMiX to address bacterial communication and biofilm formation challenges, respectively[465]. Besides airways infections, our antibacterial therapeutics may be useful to provide protection in immuno-suppressed or immuno-deficient individuals, to reduce the toxicity associated with high antibiotic doses, and to save time and costs in hospital with healthcare-associated infections.

If therapies are needed to treat everyday patients, the use over the years of vaccination helped Humans to live through pandemics such as for the last COVID-19. Other antibody-based constructs have already been used in prophylaxis, notably by serving as a preventive approach during pre-surgery for reducing the risk of infections in immunocompromised patients or in ICUs to prevent healthcare-associated infections[466]. As many licensed vaccines elicit production of neutralizing antibodies, and the complement can enhance their neutralization, it seems logical to consider that induction of complement could be a new tool to improve vaccination[467]. Furthermore, in recent years, the actions of the complement have been deeply analysed, and it is now admitted that it can lead to more than just the direct resolution of an infection, or cancer, but could in fact activate and regulate the adaptive immune system, important in the generation of a long-term immunity[468]. One impressive example is the binding of complement activation products C3a and C5a on T cells, able to signal T-cell proliferation, decrease their apoptosis and induce an increase T-cell response[469]. As we showed in our model, the prophylactic administration of CoMiX was able to rescue the animals against an acute lung infection, which could be an indication of its efficiency as a vaccine. In our model, we have yet to look at the activation of T-cells, but from other studies, we know that the target for complement-activating antibodies are usually excellent vaccine antigens, such as the case for fHbp of *N. meningitidis*, considered unique and now in phase III clinical trials[470]. Indeed, the complement plays a crucial role in host defense against *N. meningitidis.* Before the trial to test this antigen as a vaccine, targeted antibodies against fHbp used the complement to induce direct bacteriolysis through the classical pathway, promote phagocytosis, and block binding of factor H, increasing the activation of the alternative pathway, just as CoMiX-FHR1 is capable.

Recombinant antibody therapeutics have the potential to address a wide range of infectious diseases and to be cost-effective when used in high-risk individuals[471]. Although the cost of antibody-based drugs is still

a limitation, this cost should continue to decrease with the advent of new technologies, production methods and manufacturing[472]

In summary, this proof of concept of efficient directed-killing of *P. aeruginosa* by the complement offers solid perspectives for the further clinical development of CoMiX as a therapeutic strategy against bacterial infections. Future studies should focus on raising compelling evidence on the long-term potential of CoMiX, including the aspect of pharmacokinetics, potential off-target effects, or vaccine like effects, in order to improve the safety and optimize the efficacy of CoMiX in human affected by P. aeruginosa infections.

Acknowledgments

We would like to thank the Red Cross of Luxembourg for access to buffy coats from healthy donors. We also would like to thank the PST-animaleries from Tours for the caring of the animals used in this study. This study was supported by the “Fonds National de la Recherche” (PRIDE17/11823097/MICROH-DTU) and PSEUDO/2022) and the Ministry of Higher Education and Research of Luxembourg (LIH GBB 98000005).

Authors contributions

Conceptualization, A.P., C.S.D., G.D.; methodology, A.P., B.B, G.I, C.R, J.Y.S, D.F, B.B, M.S.T, G.D, Y.M, P.R, L.R, J.Z, X.D, C.S.D; validation, A.P., B.B., G.I., J.Y.S, C.S.D., G.D.; analysis, A.P., B.B, G.I, C.R, J.Y.S, D.F, B.B, M.S.T, G.D, Y.M, P.R, L.R, J.Z, X.D, C.S.D; data curation, A.P., B.B, C.S.D.; writing—original draft preparation, A.P., B.B, C.S.D. ; writing—review and editing, A.P., B.B, G.I, C.R, J.Y.S, D.F, B.B, M.S.T, G.D, Y.M, P.R, L.R, J.Z, X.D, C.S.D; resources, C.S.D, G.I., J.Y.S, A.P., J.Z., X.D.; funding acquisition, C.S.D., G.D. All authors have read and agreed to the published version of the manuscript.

Competing interests

A patent application has been filed for CoMiX (LIH-023-PCT WO2023281120) by the inventors (B.B., J.Z., X.D., C.S.D.). The authors have declared that no other conflict of interest exists.

Supplementary Figures

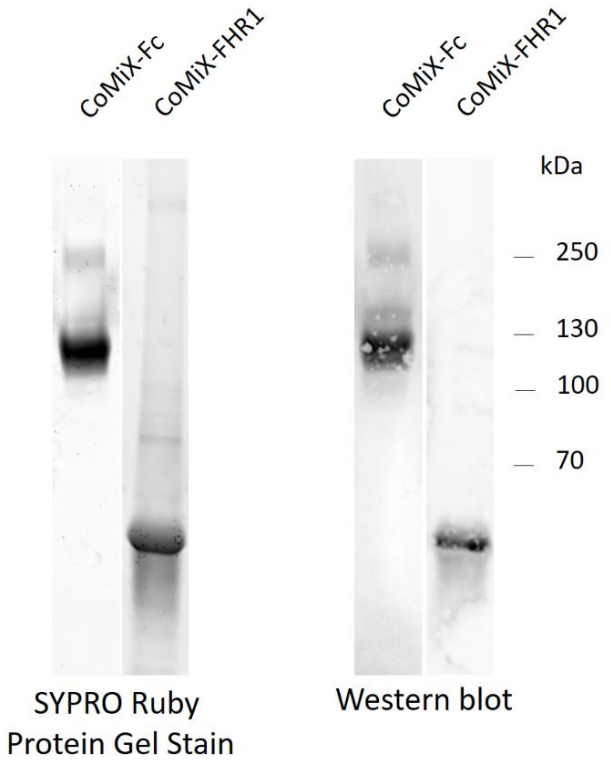

Supplementary Figure 1. Characterization of Purified CoMiX-Fc and CoMiX-FHR1 Proteins. (A) SYPRO Ruby Staining: 3 µg-s of CoMiX-Fc and CoMiX-FHR1 proteins were loaded onto 4-15% SDS-PAGE gels and stained with SYPRO Ruby according to the manufacturer's instructions. Briefly, gels were fixed in a solution of 50% methanol and 7% acetic acid (2x 50 mL) for 30 minutes, followed by overnight incubation with SYPRO Ruby stain (60 mL) and subsequent washing with 10% methanol/7% acetic acid solution. Protein bands were visualized using an Amersham Typhoon scanner. **(B)** Western Blotting: Proteins from the SDS-PAGE gel were transferred to a low-fluorescence PVDF membrane. The membrane was blocked with 4% BSA in PBS, then probed with specific fluorochrome-conjugated antibodies: anti-Fc AF647 for CoMiX-Fc and anti-His AF647 for CoMiX-FHR1. Protein bands were detected using an Amersham Typhoon scanner. The predicted molecular weight of CoMiX-Fc is approximately 120 kDa, while CoMiX-FHR1 has a smaller size of around 53 kDa.

Pseudomonas aeruginosa strains	Beta-lactams							Beta-lactamases inhibitors Beta-lactams Combination		Polymyxin	Aminoglycoside				Fluoroquinolone	
	TIC (75 µg)	CEF (30 µg)	PIP (30 µg)	AZT (30 µg)	CAZ (10 µg)	IPM (10 µg)	MEM (10 µg)	TZP (30/6 µg)	TCC (75/10 µg)	CL (50 µg)	GEN (10 µg)	AMK (30 µg)	NET (10 µg)	TOB (10 µg)	CIP (5µg)	LVX (5 µg)
Tracheostomy (n = 8):	5	3	2	1	2	3	2	2	6	1	1	0	0	1	2	1
Of which IPP6247290	R	R	R	I	R	R	R	R	R	S	S	S	S	S	R	R
Cystic fibrosis (n = 11):	7	5	7	3	5	3	4	6	6	0	5	4	3	4	2	5
Of which IPP119459	R	R	R	I	R	R	R	R	R	S	R	R	S	R	S	S
Total n = 19 (%)	12 (63.2)	8 (42.1)	9 (47.3)	4 (21.1)	7 (36.8)	6 (31.6)	6 (31.6)	8 (42.1)	12 (63.2)	1 (5.2)	6 (31.6)	4 (21.5)	3 (15.8)	5 (26.3)	4 (21.5)	6 (31.6)

Supplementary Table 1: Antibiotic resistance profile of clinical *P. aeruginosa* strains isolated from cystic fibrosis patients and patients who have undergone tracheostomy. The number of resistant strains is mentionned for the samples collected from tracheostomy of patients in intensive care units and from cystic fibrosis patients. The profile of IPP6247290 and IPP119459 is detailed as follow: R, resistant, S, sensitive, I intermediate. TIC, Ticarcillin; CEF, Cefepime; PIP, Piperacillin; AZT, Aztreonam; CAZ, Ceftazidime; IPM, Imipenem; MEM, Meropenem; TZP, Piperacillin + Tazobactam; TCC, Ticarcilline+Clavulanic acid, CL, Colistin; GEN, Gentamicin; AMK, Amikacin; NET, Netilmicin; TOB, Tobramycin; CIP, Ciprofloxacin; LVX, Levofloxacin.

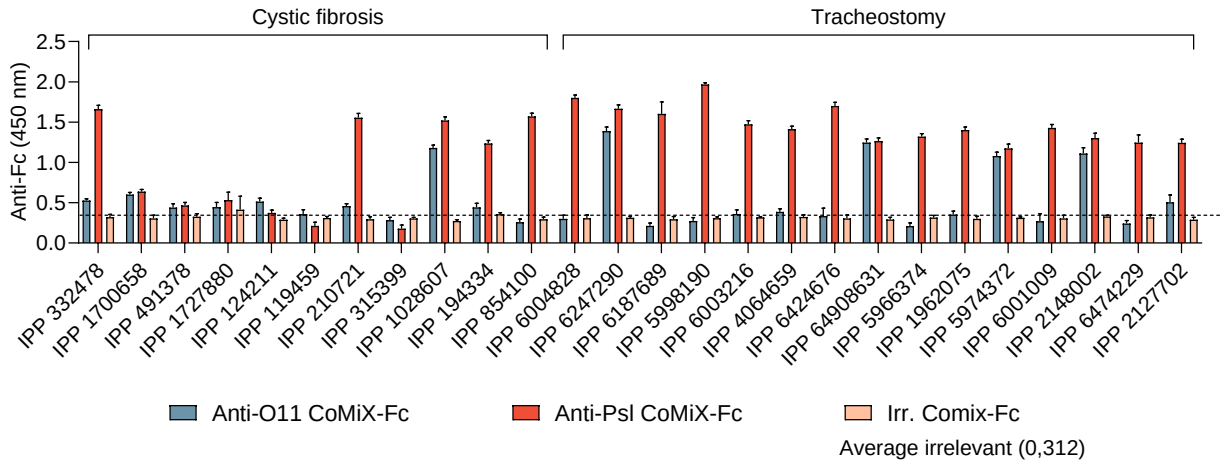

Supplementary Figure 2. Comparison of anti-O11 and anti-Psl scFv-s on 29 *P. aeruginosa* clinical isolates. We evaluated the binding of anti-O11 and anti-Psl scFv targeting moieties to a panel of 29 clinical *P. aeruginosa* strains isolated from patients with either tracheostomy (n=18) or cystic fibrosis (n=11). The strains were immobilized on ELISA plates, blocked with 4% BSA in PBS, and incubated with 100 ng of anti-O11 CoMiX-Fc, anti-Psl CoMiX-Fc, or an irrelevant control anti-Aspergillus CoMiX-Fc. The anti-O11 scFv bound to ~17% of the strains, indicating limited prevalence of the O11 serotype. In contrast, the anti-Psl scFv-Fc displayed broader recognition, binding to 45% of cystic fibrosis isolates and 100% of tracheostomy isolates. No binding was observed for the anti-Asp CoMiX-Fc control (Average signal: 0,312 O.D.), demonstrating the specificity of the anti-Psl scFv for *P. aeruginosa*.

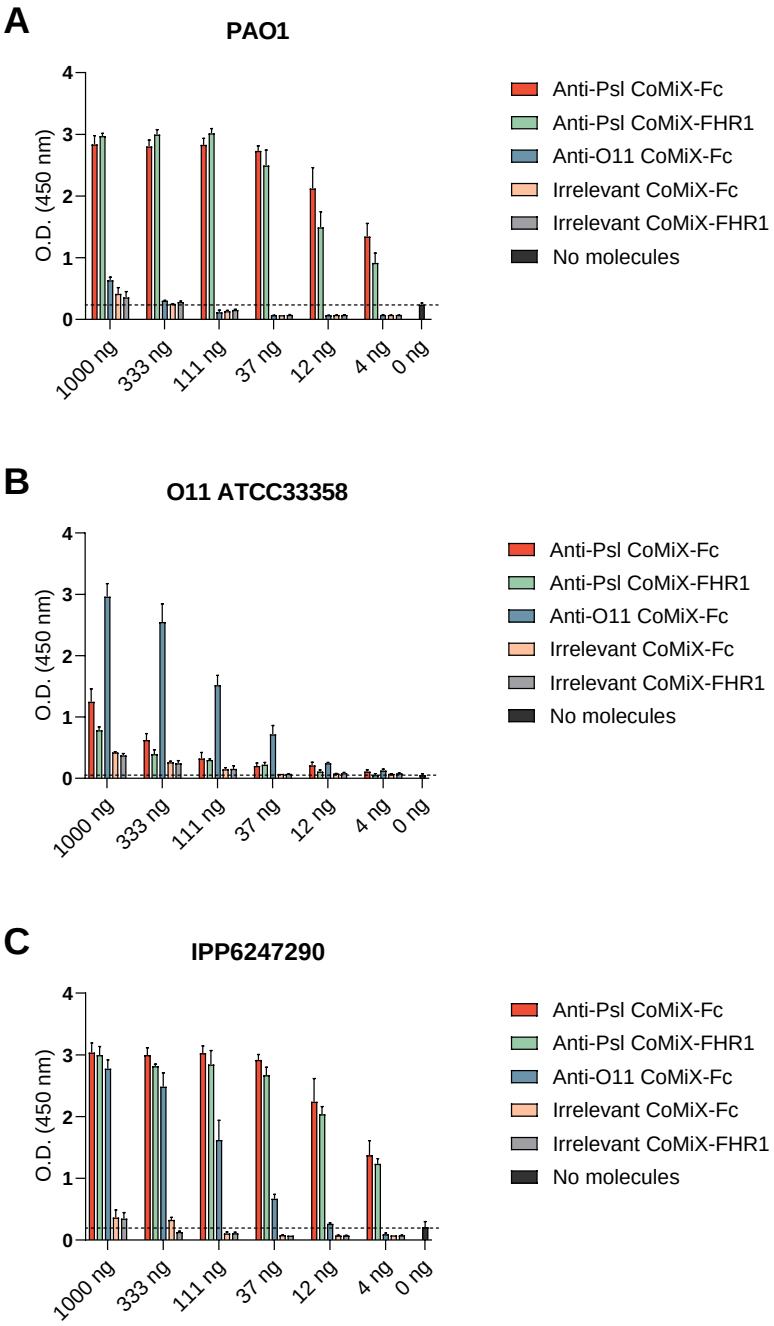

Supplementary Figure 3. Dose-dependent binding of Anti-Psl CoMiX-Fc, anti-Psl CoMiX-FHR1, anti-O11 CoMiX-Fc and irrelevant controls to *P. aeruginosa* reference strains PAO1 (A) and O11 ATCC33358 (B) and multidrug resistant clinical isolate IPP6247290 (C). The binding of molecules to reference strains and clinical isolate IPP6247290 was analyzed by whole-cell ELISA. Bacteria were immobilized and incubated with serially diluted CoMiX (starting concentration: 10 µg/mL, 1:3 dilutions). Bound CoMiX was detected using the follwoing antibodies: anti-His for CoMiX-FHR1 and anti-Fc for CoMiX-Fc. Bars represent the mean of three independent experiments with error bars indicating standard deviation (SD).

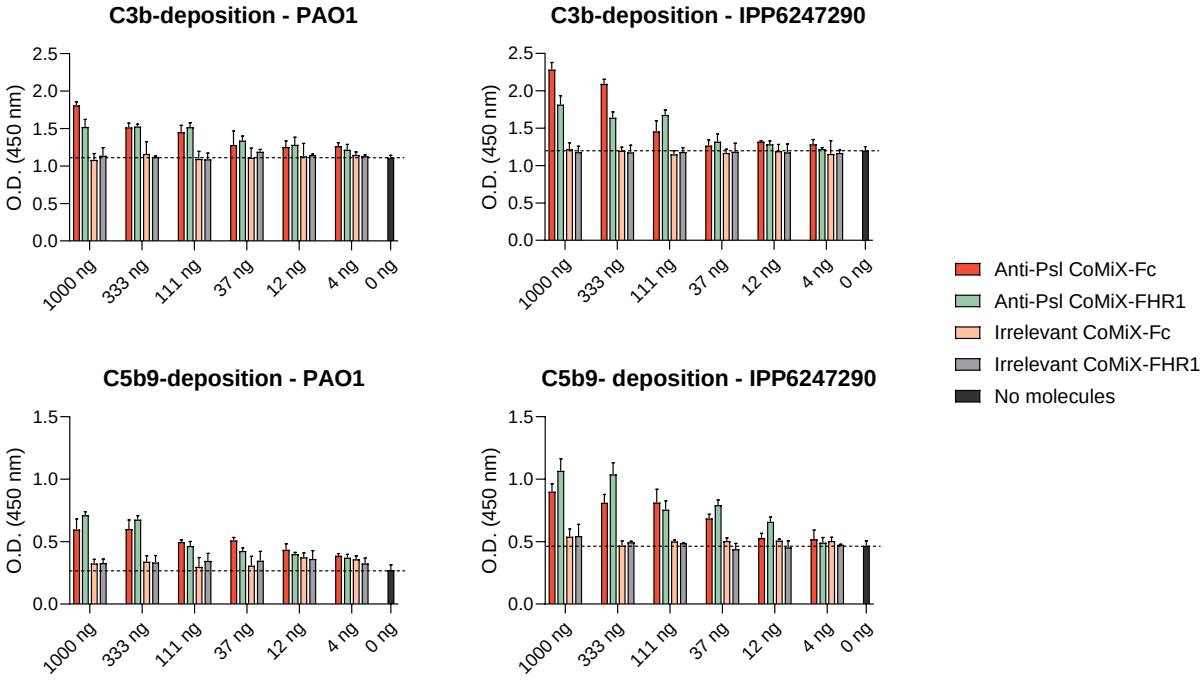

Supplementary Figure 4: CoMiX-Fc and CoMiX-FHR1 promote C3b and C5b9 deposition on *Pseudomonas aeruginosa* in a dose-dependent manner. Immobilized *P. aeruginosa* strains (PAO1, IPP6247290) were incubated with serially diluted CoMiX (starting concentration: 10 µg/ml, 1:3 dilution). Following washes, the bacteria were incubated with either 2% normal human serum (NHS) for C3b detection or 4% NHS for C5b9/membrane attack complex (MAC) detection. Heat-inactivated human serum (ΔNHS) served as a negative control. All serum incubations were performed at 37°C for 30 minutes. C3b deposition was measured using a monoclonal mouse anti-human C3/C3b/iC3b antibody, while C5b9 deposition was detected by a specific mouse anti-human C5b9 mAb. Data are presented as means ± SD from three independent experiments. Notably, CoMiX-mediated complement activation, as indicated by C3b and C5b9 deposition, was only observed at concentrations exceeding 333 ng/well for PAO1 and 111 ng/well for the clinical isolate. Interestingly, the clinical isolate demonstrated a higher propensity for complement activation compared to the reference strain, evident by increased C3b and C5b9 deposition at all CoMiX concentrations tested.

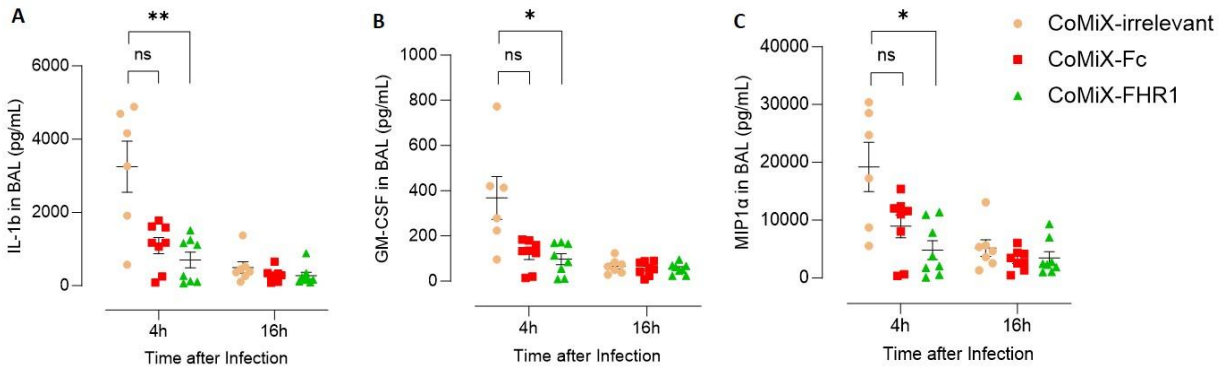

Supplementary Figure 5. CoMiX treatment during *P. aeruginosa* infection is associated with decrease in pro-inflammatory mediator's secretion in BAL. Mice were infected/treated as described in Fig 7A, sacrificed at 4h and 16h post-infection, and BAL were collected. As a reflection for lung inflammation, BAL was assessed by MSD assay for secreted production of IL-1β **(A)**, GM-CSF **(B)** and MIP1α **(C)**. All data are quoted as the mean values ± SEM and the results correspond to one experiment per time-point (n = 7-8 mice per group). All statistical analyses were performed using the Kruskal-Wallis test followed by a Dunn's post-test for comparisons between the groups, *: $p < 0.05$; **: $p < 0.01$; ***: $p < 0.001$.

6.2. Complement-Activating Multimeric Immunotherapeutic Complexes for HER2-breast cancer immunotherapy

Carole Seguin-Devaux[1*], Bianca Brandus[1*], Jean-Marc Plesseria[1], Gilles Iserentant[1], Jean-Yves Servais[1], Aubin Pitiot[1], Georgia Kanli[2], Iris Behrmann[3], Jacques Zimmer[1], Jacques H M Cohen[4], Xavier Dervillez[1,3]

[1] Department of Infection and Immunity, Luxembourg Institute of Health, Esch sur Alzette, Luxembourg

[2] Department of Oncology, Luxembourg Institute of Health, Luxembourg, Luxembourg

[3] Department of Life Sciences and Medicine, University of Luxembourg, Belval, Luxembourg

[4] University of Reims Champagne Ardennes, Reims, France

[*] Shared first co-authorship

Running title: CoMiX induce CDC and inhibit BT474 xenografts in NUDE mice

Keywords. Immunotherapy, HER2-breast cancer, complement dependent cytotoxicity, NK cell activation, phagocytosis, xenograft model.

Corresponding author: Carole Devaux, Luxembourg Institute of Health, Department of Infection and Immunity, 29, rue Henri Koch, L-4354 Esch-sur-Alzette. Luxembourg

Tel: +352 26970-224 , e-mail: carole.devaux@lih.lu

Conflict of interests: A patent application has been granted in USA for CoMiX (WO2017202776) by the inventors (C.S.D, J.H.M.C, X.D). The authors have declared that no other conflict of interest exists.

Funding information: This study was supported by the "Fonds National de la Recherche" (POC17/12252709/COMIX and PRIDE17/11823097/MICROH-DTU) and the Ministry of Higher Education and Research of Luxembourg (LIH GBB 98000005).

ABSTRACT

Directing selective complement activation towards tumor cells is an attractive strategy to promote their elimination. We have generated Complement-activating Multimeric immunotherapeutic compleXes (CoMiX) stimulating either the alternative pathway, using Factor H Related protein 4 (FHR4) or the classical pathways using triple Fc dimers, on HER2- expressing tumor cells. We used the C4bp C-terminal-α-/β-chain multimerising scaffolds to generate CoMiX-FHR4 and CoMiX-Fc with 2 different V_HH anti-HER2, V_HH(T) and V_HH(P), recognising trastuzumab- or pertuzumab-competing HER2 epitopes, respectively. Both CoMiX FHR4/V_HH(T) and FHR4/V_HH(P) led to the highest C3b and C5b9 depositions and CDC on BT474 tumor cells ($p<0.0001$), both individually and in combinations with their CoMiX-Fc counterparts, surpassing the very low complement activating capacity of trastuzumab and pertuzumab. All CoMiX induce BT474 cell death and phagocytosis of tumor cells by macrophages while CoMiX-Fc stimulate NK cell activation. In human BT474 breast cancer xenografts sensitive to trastuzumab in NUDE mice, CoMiX-FHR4 reduced the tumor volume compared to the PBS control ($p< 0.05$) to a lesser extent than trastuzumab ($p< 0.001$) while V_HH(P)/Fc led to a tumor volume reduction similar to pertuzumab. Combination of the two CoMiX-FHR4 or the two CoMiX-Fc were more potent, similarly to the combination of trastuzumab and pertuzumab, leading to NK and T cells infiltration in the xenografts. Importantly, CoMiX-FHR4 delayed the growth of trastuzumab-resistant cancer cells by inducing a large NK cell infiltration. We demonstrated here that directed-complement activation on tumor cells is an alternative to therapeutic antibodies, promising for combination therapy, in particular when resistance to standard-of-care treatment occurs.

Synopsis

Complement-activating multimeric immunotherapeutic complexes (CoMiX), as a novel complement-directed tumor cell destruction approach, inhibit BT474 xenografts growth by stimulating complement activation on tumor, cell death, NK cell activation, and phagocytosis by macrophages.

INTRODUCTION

Recombinant monoclonal immunoglobulin gamma antibodies (IgG) have become a major weapon in cancer immunotherapy [473]. The classical complement pathway is activated when antibody–antigen complexes are formed on cell surfaces, followed by binding of C1q to the constant region of the antigen-bound antibody [474]. Few therapeutic antibodies (Abs), such as rituximab targeting CD20, efficiently recruit the complement protein C1q of the complement system which binds to the C-terminal half of the CH2 domain of Fc and leads to complement-dependent cytotoxicity (CDC)[475]. All three complement pathways, activated by antibodies or by structural elements on target cells or pathogens, converge at the level of C3 amplification loop, which is cleaved by C3 convertase to produce the anaphylatoxin C3a and the component C3b, followed by the sequential recruitment and activation of C5 [475]. The assembly of the terminal complement proteins C5b–C9, the membrane attack complex (MAC), results in pore formation and subsequent lysis of the target cell. C3b degradation products [476] on tumor targets (iC3b, C3dg and C3d) are recognized by effector cells through CD11b and CD11c, leading to complement-dependent cell cytotoxicity (CDCC) or phagocytosis (CDCP), which allows the clearance of target cells. In addition, complement activation stimulates pro-inflammatory mediators such as C3a and C5a, the latter upregulating the FcγRs on phagocytes to enhance phagocytosis but also tumor cytolysis [477].

Both Fc and Fab regions contribute to the stimulation of the immune response and the inhibition of tumor growth of Abs [478, 479]. Association of two Abs recognizing different epitopes of the same Tumor Associated Antigens (TAAs) can also lead to efficient complement activation, despite not activating complement when used individually. Trastuzumab, the first humanized mAb approved for cancer treatment, inhibits the human epidermal growth factor receptor 2 (HER2) and EGFR signaling pathways [480]; Pertuzumab binds to a distinct epitope on HER2 blocking HER2 heterodimerization but includes the same IgG1 Fc domain as trastuzumab. Both antibodies can trigger antibody-dependent cell-mediated cytotoxicity (ADCC)[297, 481]. Several critical factors determine the ability of an antibody to activate the classical complement pathway, including epitope recognition, size, target protein density, membrane fluidity, and the internalization kinetics of the targeted receptor following antibody-epitope interactions [482]. The ability to recruit C1q is also influenced by the orientation and geometry of Abs following their binding to their epitope including hexamerization of IgG antibodies for efficient C1q binding, facilitating significant complement activation [483].

Nevertheless, despite the attractiveness of Abs, many patients do not respond to current therapies due to inherited or acquired resistance [285]. Improvement of Ab's efficacy are thus needed. Modification of the effector functions using Fc bioengineering [484] or antibody drug-conjugation

combining anticancer drug such as trastuzumab-emtansine (T-DM1)[485] or trastuzumab–deruxtecan (T-DXd) are the main approaches. Complement activation represents a substantial part to improve the overall biological activity of few Abs used in cancer immunotherapy [477]. The alternative pathway represents another critical component of the complement pathway that can be harnessed against tumor progression [231, 486]. Factor H-related protein 4 can activate complement by serving as a platform for the assembly of alternative pathway C3 convertase by competing with factor H (FH) for C3b binding.

We have developed a novel anti-tumor complement-mediated strategy by exploiting the complement activating effects of FH-related protein 4 (FHR4) towards HER2-overexpressing cancer cells [487]. We used the C4bp C-terminal α-chain multimerising scaffold (C4bpα) [488] to generate complement-activating multimeric immunotherapeutic complexes (CoMiX) that display multivalent FHR4 complement effector moieties and elicit C3b deposition, MAC formation and CDC by overcoming the complement inhibitory threshold on cancer cells [487]. In the present work, we have extended the use of the C4bpα multimerizing scaffold to express CoMiX-Fc harboring multimeric Fc that assemble as functional triple Fc-dimers. We used 2 different V_HH anti-HER2, V_HH(T) and V_HH(P), recognizing trastuzumab- or pertuzumab-competing HER2 epitopes, respectively, to generate 2 types of CoMiX-FHR4 [FHR4/V_HH(T) and FHR4/V_HH(P)] and 2 types of CoMiX-Fc [V_HH(T)/Fc and V_HH(P)/Fc]. CoMiX-FHR4 and CoMiX-Fc were first evaluated *in vitro*, individually or in combination, and their therapeutic efficacy was assessed *in vivo* on xenografts established in NUDE mice from human HER2-expressing BT474 breast cancer cell lines that are sensitive or not to trastuzumab. Our study demonstrates for the first time that the recruitment of directed complement on cancer cells is an effective approach to inhibit tumor growth *in vivo*. CoMiX might be effective in combination therapy in clinical conditions of immunotherapeutic failure.

MATERIAL AND METHODS

Transfection and clone selection

All CoMiX were generated from HEK293T cells transfected with 4 µg of recombinant plasmid DNA using Lipofectamine-3000 (Invitrogen, Thermo Fisher Scientific BVBA, Merelbeke, Belgium) following the manufacturer's instructions. CoMiX-FHR4 were produced as previously described [487] using double co-transfection whereas CoMiX-Fc, hinge deficient CoMiX-Fc (Δhinge) and multimeric V_HH(T) control, lacking any effector functions, were produced using single transfection. Well transfected clones selected by puromycin (Westburg, Leusden, The Netherlands) were further cultured. Protein expression in the supernatants were analyzed by sandwich ELISA. Briefly, 100 ng/well goat anti-human Fc (Abcam, Cambridge, UK, #ab97221) or rabbit anti-His (Bethyl, Antwerpen, Belgium, #A190214A) pAbs were immobilized onto a NUNC MaxiSorp™ 96-well flat-bottom polystyrene plate overnight at 4°C. After blocking with 5% (w/v) bovine serum albumin in PBS, each clone supernatant was incubated for 1 hour at 4°C. CoMiX-Fc were detected with a HRP-conjugated goat anti-human Fc pAb (Abcam, #ab97225), whereas CoMiX-FHR4 and V_HH controls were detected with a HRP-conjugated mouse anti-His mAb (Sigma-Aldrich). The plate was revealed with OPD/H_2O_2 substrate and absorbance was measured at 492 nm on a spectrophotometer. Clones with the highest production were selected and expanded in cellSTACKs® (Corning) in complete DMEM medium (10% FBS, Penicillin/Streptomycin and L-Glutamine).

Flow cytometry

HER2-positive BT474 cancer cells were incubated for 1 hour at 4°C with 3-fold serial dilutions of 15 µg/well CoMiX, V_HH controls and Abs, or 7.5 µg/well of two molecules for the combinations. Tumor cells were then incubated with 25% normal human serum (NHS) diluted in two different gelatin veronal buffer (GVB^{++}: 141 mM NaCl, 0.3 mM $CaCl_2$, 1 mM $MgCl_2$, 0.1% gelatin, 1.8 mM Na-barbital & 3.1 mM barbituric acid, pH 7.3-7.4) (GVB+: 3 mM $MgCl_2$ and 5 mM EGTA without Ca^{2+} ions) for 30 minutes at 37°C. Complement activation was detected with mouse anti-human C3/C3b/iC3b mAb (Cedarlane, Sanbio B.V., Uden, The Netherlands) followed by goat anti-mouse IgG AF647 (Invitrogen), mouse anti-human C5b9 (Novus, USA, Centennial), and Live/Dead (L/D) staining (Invitrogen). Washing steps were performed between each steps. The samples were fixed with 1% PFA and analyzed with a BD LSR Fortessa™ cell analyzer. The percentage of dead cells was calculated by dividing the number of L/D-positive cells by the total number of cells analyzed.

To analyze the NK-activating properties of CoMiX, we incubated BT474 cells with 5-fold diluted CoMiX starting at 20 µg/condition for 1 hour at 4°C. Cells were then co-incubated with human CD16-expressing NK cells ($NK92^{humCD16}$) for 4 hours at 37°C, and then stained with BV421™ anti-human CD107a (Biolegend) antibody as a degranulation marker. GolgiStop™ (BD Biosciences) and GolgiPlug™ (BD Biosciences) were added after 1 hour of incubation.

CoMiX-mediated cellular phagocytosis of BT474 cells

M2 macrophages were derived from monocytes of Peripheral blood mononuclear cells (PBMCs) from healthy donors (Luxembourg Red Cross) as previously described [13, 14]. Macrophages were plated into Lab-Tek 8-chamber slides (Nunc, Thermo Fisher Scientific) and stained with PKH26 (Sigma-Aldrich). BT474 cells were stained with CFSE (Invitrogen, Thermo Fisher) and then incubated for 30 min with 20 µg/ml of controls, CoMiX, trastuzumab, pertuzumab or their combination in GVB++ supplemented with 25% C5-deficient NHS to prevent lysis. CFSE-stained complement-coated tumor cells were washed, added to the KHP26-stained M2 macrophages (2:1) and incubated for 18 h at 37°C/5% CO2 in complete RPMI medium. Cells were fixed with 1% PFA, stained with DAPI and analyzed by confocal microscopy on the CSU-W1 Spinning Disk/High Speed Widefield confocal microscope lens X4. Three series of 10 pictures were taken for each experimental condition. Phagocytosis was evaluated on 400 macrophages for each condition.

In vivo models of human BT474 breast cancer xenografts in NUDE mice

Mice were housed in specific-pathogen-free facilities with a 12h light-dark cycle with food and water supplied *ad libitum*. Experiments were approved by the animal welfare committee of the Luxembourg Institute of Health (DII-2018-15) and the Ministry of Agriculture of Luxembourg (LUPA2019/82). Five weeks old female BALB/c NUDE mice (± 25 g) were anesthetized with isoflurane and injected subcutaneously with $5x10^6$ Matrigel-mixed (1:1) trastuzumab-sensitive BT474 cells into the mammary fat pads. Tumor growth was measured with calipers and their volumes calculated (Volume = (Length x Width x Width)/2). After tumors reached 60 mm^3 (in 30-40 days), mice were randomly divided into 11 groups (5 mice/group). Each group was treated 9 times with 100 µg of each molecules, or their combinations (50 µg of molecules). Tumors were measured every second or third day for 25 days or until the tumor size reached 1000mm^3. Magnetic Resonance Imaging (MRI) was performed on one representative mice of each group. Briefly, mice were sacrificed at day 11 post-treatment and placed in tubes containing cold solution of 4% PFA. MRI was performed on a 3T preclinical horizontal bore scanner (MR Solutions, Guilford, UK),

equipped with a quadrature volume coil designed for rodent head imaging, with a 17 cm horizontal bore. The heads were placed in a tube with fluorinert (3M, MN, USA). Anatomical FSE T2w (Spatial Resolution: 0.15 × 0.15 × 1mm; Number of Slices: 30; TE\TR: 68\7000 ms; Number of Averages: 1) were used to calculate the tumor volumes per animal which was calculated by the ImageJ software [489]. The effects of the most efficient CoMiX, FHR4/V_HH(P) or combination, [FHR4/V_HH(T), FHR4/V_HH(P)] were further explored in xenografts of trastuzumab-resistant BT474 cells (ATCC-CRL-3247) using the same animal protocol (4 groups , 5 mice/group).

Analysis of immune responses in xenografts

To analyze complement activation on xenografts, a single dose of 100 µg of the combination of CoMiX-FHR4 [50 µg FHR4/V_HH(T) + 50 µg FHR4/V_HH(P)], of the combination of CoMiX-Fc [50 µg V_HH(T)/Fc + 50 µg V_HH(P)/Fc], of the V_HH(T) control or the combination of each commercial antibody was injected intravenously into the lateral tail vein of 8 weeks old female BALB/c NUDE mice (4 mice/molecule). One or 6 hours after injection, mice were sacrificed by cervical dislocation. The tumors were surgically removed, placed in OCT cryomold, and instantly frozen in liquid nitrogen for immunohistochemistry analysis (supplemental materials). At sacrifice, BT474 xenografts sensitive to trastuzumab were surgically removed, placed in 4% PFA overnight, stored in ethanol 60% before shipping for immunohistochemistry staining at HistoWiz, Inc. (supplemental materials). The sera of mice was sampled and anti-HER2-specific IgG were measured by sandwich ELISA. Briefly, Maxisorp 96-well plates (Thermofisher Scientific) were coated overnight with 0.5 µg/mL of recombinant human HER-2 (Abcam). Plates were washed, blocked with 1% BSA-PBS, and sera were incubated for 2 hours. HRP-conjugated goat anti-mouse IgG (Thermofisher Scientific) was added for 2 hours. After washings, reaction was developed with tetramethylbenzidine as a substrate, stop with H2SO4, and the absorbance was measured at 450nm using a spectrophotometer (Molecular Devices, USA). The titer was calculated by binary logarithm regression as the reciprocal dilution of the sample, where the extinction was 2-fold the background extinction. BT474 xenografts resistant to trastuzumab were collected just after the end of treatment at D+11 in three mice treated with the combination of CoMiX-FHR4 [FHR4/VHH(T) + FHR4/VHH(P)], trastuzumab or PBS. Cryosections were performed as previously described, stained with a rat anti-mouse NKp46/NCR1 (R&D Systems, clone # 29A1.4) and revealed using a donkey AF568-conjugated anti-rat pAb (Abcam).

Statistical analysis

Statistical analysis was performed using GraphPad Prism version 10.0.0 for Windows (GraphPad Software, Massachusetts USA). For all *in vitro* experiments, multiple groups receiving the different single CoMiX or combination treatments were compared using one-way ANOVA analysis of variance and post-hoc Tukey's tests. For studies in mice, an appropriate sample size (n = 5) was calculated during the study design to obtain groups with a difference of tumor growth of 20% by taking into account a common standard deviation of 5% using a bilateral Student's T test based on a 95% confidence level. Mice with different tumor sizes were randomized between the groups. The groups were compared using one way Anova analysis of variance followed by unpaired Student's T test. A p value < 0.05 was considered as statistically significant (*$p < 0.05$, **$p < 0.01$, ***$p < 0.001$, ****$p < 0.0001$).

Data availability statement

The data generated in this study are available in the manuscript and the supplementary files or upon request from the corresponding author.

RESULTS

Molecular design of CoMiX

We used the oligomerization scaffold of the C-terminal domain of the α-chain of the C4b-binding protein (C4bp) to enable the formation of hexa- and heptamers. As described in **Fig. 1**, Fc-based complement-activating multimeric immunotherapeutic complexes (CoMiX-Fc) display a multivalent targeting function derived from trastuzumab (V_HH(T)) or pertuzumab (V_HH(P)), a monovalent tracking function (eGFP) and three dimeric C4bp alpha Fc regions (effector function) engineered with a dual hinge region between the C4bpα-scaffold and the IgG1 CH2-CH3: V_HH(T)/Fc and V_HH(P)/Fc. To evaluate the importance of the Fc dimers, Fc-based multimers without hinge (V_HH(T)/Fc Δhinge) were also generated as a control for V_HH(T)/Fc (**Fig. 1**). FHR4-based CoMiX (CoMiX-FHR4) include the FHR4 effector function instead of the Fc regions without hinge and the targeting function V_HH(T) or V_HH(P). The V_HH(T) without effector functions was also produced as a control.

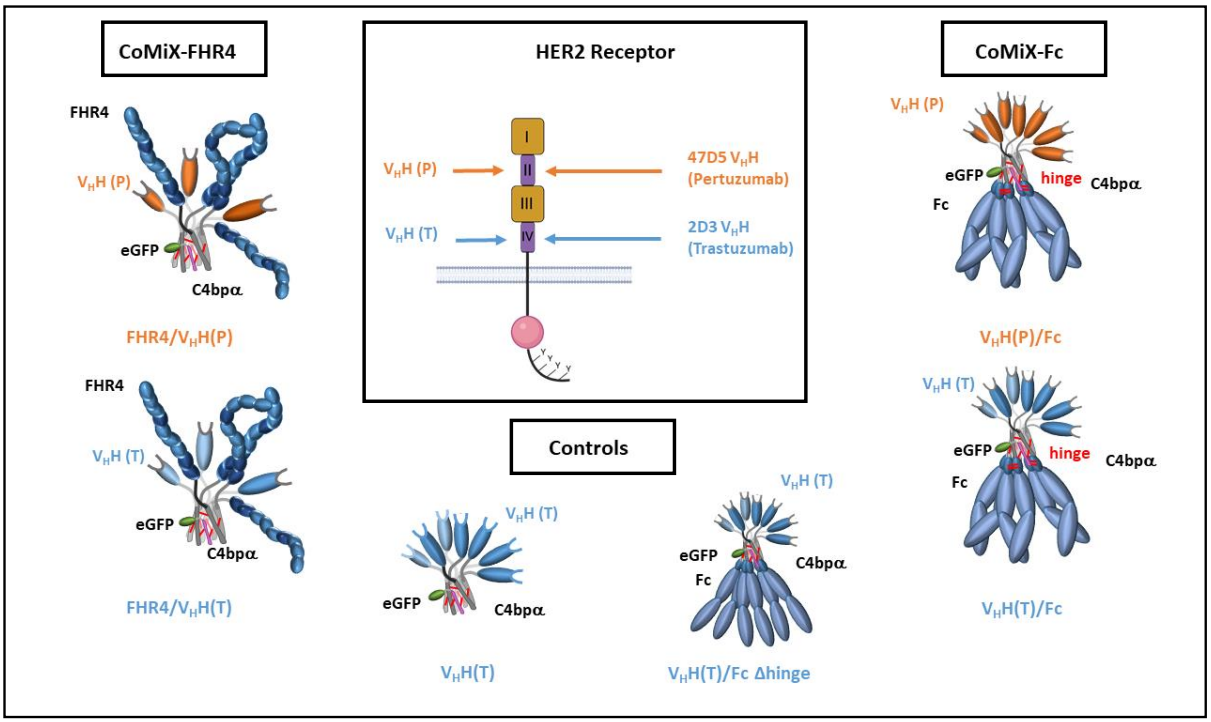

Figure 1: Design of CoMiX-FHR4, CoMiX-Fc and the controls V_HH(T) and V_HH(T)/Fc Δhinge. All constructs are co-transfected with the eGFP.C4bpβ construct, leading to the covalent association of a single eGFP tracking function with the multimeric fusion C4bp α core. We used V_HH(T) and V_HH(P), recognising trastuzumab- or pertuzumab-competing HER2 epitopes, respectively, to generate 2 types of CoMiX-FHR4 : FHR4/V_HH(T) and FHR4/V_HH(P)] or 2 types of CoMiX-Fc: V_HH(T)/Fc or V_HH(P)/Fc. C4bpα.His8x V_HH(T) is the control multimeric molecule with no effector function, and

V_HH(T)/Fc Δhinge is the control molecule of V_HH(T)/Fc without hinge that allows the formation of triple Fc dimers.

The molecular pattern of the produced multimeric immunoconjugates was analyzed under non-reducing (Supplementary Fig. S1AB) and reducing conditions (Supplementary Fig. S1C) by Western blot. Under non-reducing conditions, FHR4/V_HH(T) and FHR4/V_HH(P) display seven bands representing the number of FHR4 units in the complexes (Supplementary Fig. S1A and S1B). For CoMiX-Fc (Supplementary Fig. S1BC), all molecules have a tracking function (eGFP.C4bpβ) with a size of 50 kDa and a V_HH anti-HER2 targeting function derived from trastuzumab (V_HH(T)) or pertuzumab (V_HH(P)), with a size of 40 or 30 kDa, respectively.

Multimeric immunotherapeutic complexes promote C3b deposition, MAC formation and direct killing of BT474 tumor cells

The effect of CoMiX-Fc and CoMiX-FHR4 on complement activation was first analyzed, individually or in combination, by measuring C3b and C5b9 depositions as well as CDC on the HER2-expressing BT474 tumor cell line using flow cytometry (**Fig. 2**, Supplementary Fig. S2) in the presence of 25% of NHS, and showed a dose-response stimulation for C3b and C5b9 (Supplementary Fig. 3). The combination of CoMiX enhanced significantly C3b, C5b9 depositions and CDC as compared to the single administrations. At their highest concentration (**Fig. 2**), CoMiX-FHR4 (FHR4/V_HH(T) and FHR4/V_HH(P)) led to the highest C3b deposition and CDC, both individually and in combinations ($p< 0.0001$). CoMiX-Fc (V_HH(T)/Fc or V_HH(P)/Fc) were less efficient to facilitate C3b deposition and CDC, but surpassing the very low complement activating capacity of trastuzumab and pertuzumab (**Fig. 2A** and **2C**). C5b9 deposition-mediated by CoMiX-FHR4 and CoMiX-Fc harboring V_HH(T) was more potent than their counterpart harboring V_HH(P) (**Fig. 2B**) ($p< 0.0001$); nevertheless, all molecules exceeded the C5b9 deposition induced by trastuzumab and pertuzumab ($p< 0.05$). Combinations of CoMiX-FHR4 with CoMiX-Fc enhanced significantly C3b and C5b9 depositions and CDC as compared to CoMiX-Fc alone ($p< 0.0001$). Overall, CoMiX with the V_HH(T) targeting system activate the complement system more efficiently than their V_HH(P) counterparts. The correlation between C3b deposition and the percentage of dead cells at 15 µg/well of molecules was depicted on **Fig. 2D**. Trastuzumab and pertuzumab have little to no effect on C3b deposition and cell death when used individually. However, they show increased C3b deposition and slight increase in cell death when combined. CoMiX-FHR4 (FHR4/V_HH(T) and FHR4/V_HH(P)) demonstrated the highest complement-activating properties. CoMiX-Fc (V_HH(T)/Fc

and V_HH(P)/Fc) have a similar effect on complement activation as the combination of the two Abs. The killing activities of the different combinations with CoMiX-FHR4 and CoMiX-Fc exceeded the individual capacity of all molecules, except for FHR4/V_HH(T) being superior to the combination of the two CoMiX-Fc. Taken together, these data indicate that FHR4/V_HH(T) are the most efficient CoMiX in facilitating C3b deposition and direct killing of tumor cells.

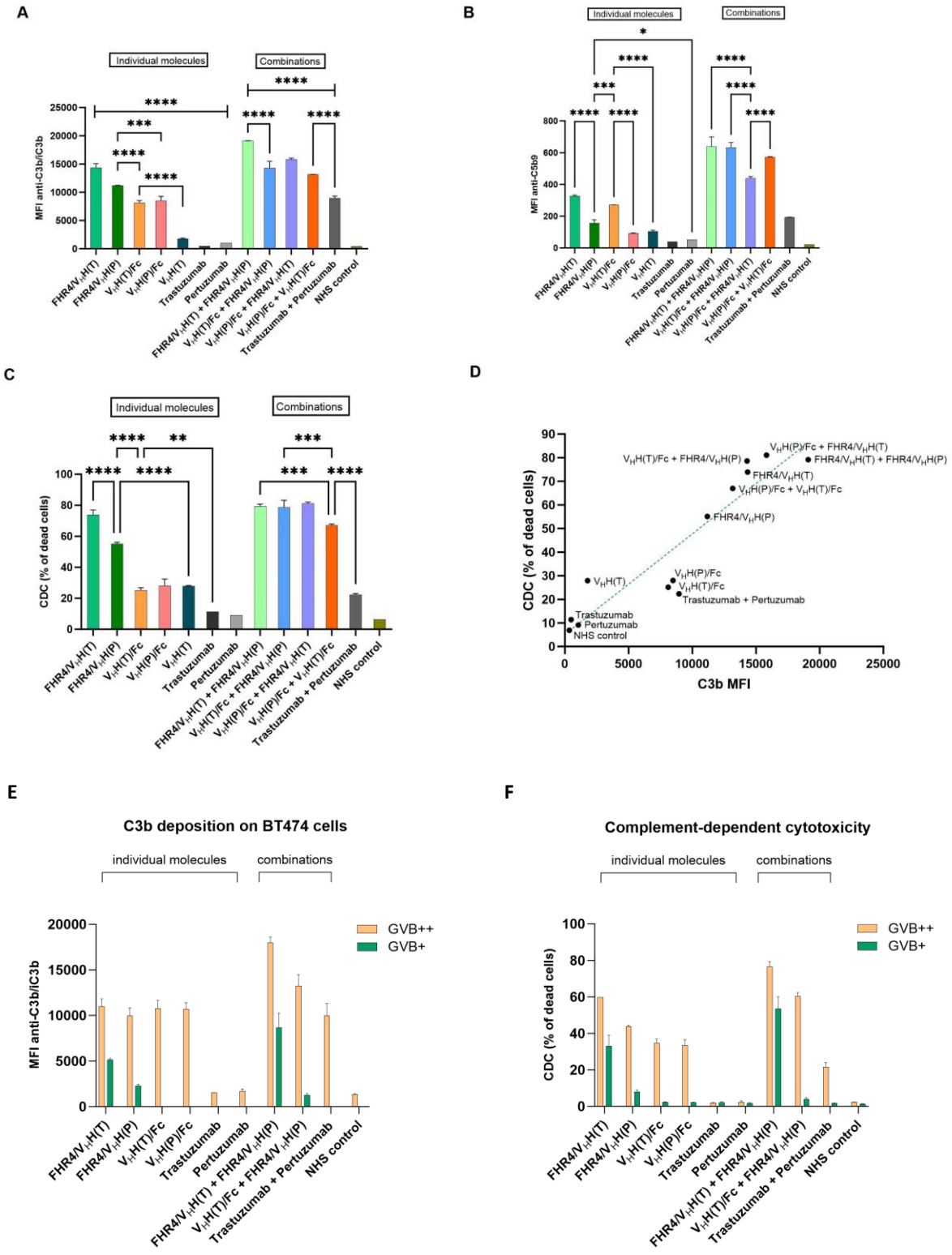

Figure 2: Flow cytometry analysis of C3b/iC3b deposition **(A),** membrane attack complex formation **(B)**, and CDC **(C)** on BT474 tumor cells incubated with 15 µg/well of multimeric immunotherapeutic complexes. **(A)** C3b/iC3b deposition was detected with mouse anti-human C3b mAb and a secondary goat anti-mouse IgG Ab conjugated with AF647. **(B)** MAC formation was analyzed using

anti-C5b9 mAb followed by PE-conjugated anti-mouse IgG pAb. MAC-formation was highest when CoMiX-Fc and CoMiX-FHR4 were combined. **(C)** The percentage of dead cells was calculated by dividing the number of live/dead-positive (dead) cells with the total number of analyzed cells. Data are presented as mean values ±SD of n = 3 independent experiments. Statistical analysis was performed using a one-way ANOVA and post-hoc Tukey test (**p < 0.005, ***p < 0.001, ****p < 0.0001). **(D)** A linear correlation between C3b deposition (MFI) and the percentage of dead cells at 15 µg/well of molecules was observed. Consistent with C3b deposition and MAC-formation, CoMiX-Fc and CoMiX-FHR4 significantly increased the percentage of dead cells compared to control multimers and Abs. **(E, F)** FHR4-CoMiX activate the alternative complement pathway, whereas Fc CoMiX facilitate classical pathway activation. C3b deposition **(E)** and CDC **(F)** of BT474 tumor cells incubated with saturating concentrations (15 µl/well) of CoMiX and control mAbs individually or in combinations. 25% NHS diluted in either GVB^{++} or GVB^{+} buffer was added for 30 minutes at 37°C. Inhibition of the classical complement pathway by using GVB^{+} buffer completely disrupts the complement activating properties of Fc-CoMiX, trastuzumab and pertuzumab. Data are presented as mean values ±SD of n = 3 independent experiments. Statistical analysis was performed using a two-way ANOVA test between GVB^{++} and GVB^{+} conditions for each molecule. All comparisons between GVB^{++} and GVB^{+} reached statistical significance (****p < 0.0001).

Mechanisms of action of CoMiX-FHR4 and CoMiX-Fc

To assess which complement pathway can be activated by the different types of CoMiX, we used 25% NHS diluted in either GVB^{++} or GVB^{+} buffer. GVB^{++} buffer contains Ca^{2+} and Mg^{2+} ions, allowing the initiation of all three pathways of the complement cascade. The absence of Ca^{2+} ions in the GVB^{+} buffer selectively inhibits the classical and lectin pathways, hence only the alternative pathway is active. As shown in **Fig. 2EF** and Supplementary Fig. S3A and S3B, C3b deposition and the percentage of dead cells were significantly reduced in GVB^{+} buffer compared to GVB^{++} in all cases (p< 0.0001) resulting in a 6.5-fold increase in C3b deposition (**Fig. 2E**) and a 20 to 30-fold increase in the percentage of dead cells (**Fig. 2F**) compared to trastuzumab and pertuzumab, respectively. Interestingly, the complement activating properties of FHR4-CoMiX were reduced only by half in GVB^{+} buffer, whereas the other Fc-based CoMiX and reference mAbs completely lose their activating effect (**Fig. 2EF**). Thus, FHR4-CoMiX facilitate alternative pathway activation, while Fc-CoMiX and Abs act as classical pathway activators.

NK cells bind IgG antibodies though their FcγRIIIa receptors (CD16) and facilitate the destruction of opsonized target cells via ADCC. We hypothesized that Fc-CoMiX could be effective NK cell activators. HER2-positive BT474 tumor cells were incubated with CoMiX and the human

CD16-expressing NK cell line (NK92^{humCD16}) for 4 hours (**Fig. 3AB** and Supplementary Fig. S5). The expression of the degranulation marker CD107a was highly upregulated on NK cells by V_HH(P)/Fc and trastuzumab and half less by V_HH(T)/Fc ($p < 0.0001$, **Fig. 3A**). Without hinge (V_HHT/Fc Δhinge) the percentage of CD107a-positive NK cells was strongly reduced when compared to CoMiX-Fc, indicating that the hinge region is mandatory for the functional assembly of multiple Fc-dimers, capable of efficiently binding to Fcγ receptors on NK cells. Pertuzumab showed a decrease capacity of degranulation as compared to CoMiX V_HH(P)/Fc ($p < 0.0001$). CoMiX-FHR4 did not induce significantly CD107a expression similarly to pertuzumab. In concordance, IFN-γ expression was significantly enhanced by V_HH(T)/Fc and V_HH(P)/Fc, as well as trastuzumab and pertuzumab ($p < 0.0001$, **Fig. 3B**) as compared to CoMiX-FHR4 and controls.

We previously showed that FHR4 induces complement-dependent macrophage-mediated phagocytosis on BT474 tumor cells [487]. We therefore compared the effects of CoMix-Fc to CoMiX-FHR4 on macrophage-mediated phagocytosis by confocal microscopy using C5-deficient serum to inhibit CDC killing (**Fig. 3CD)**. As previously described, CoMiX-FHR4 V_HH(T) enhanced phagocytosis of BT474 target cells to the extent of trastuzumab (around 20%, $p < 0.05$). CoMiX V_HH(P)/Fc increased the number of BT474 cells phagocytosed by macrophages up to 30% ($p < 0.005$) but not CoMiX V_HH(T)/Fc (**Fig. 3C)**. All combinations between CoMiX-Fc, CoMix-FHR4, trastuzumab and pertuzumab enhanced phagocytosis to a mean of around 40% ($p < 0.01$), with the exception of the trastuzumab/pertuzumab and trastuzumab/FHR4 V_HH(P) combinations. We also confirmed here that the hinge region is mandatory for functional Fc/FcγRs interactions to stimulate phagocytosis mediated by macrophages.

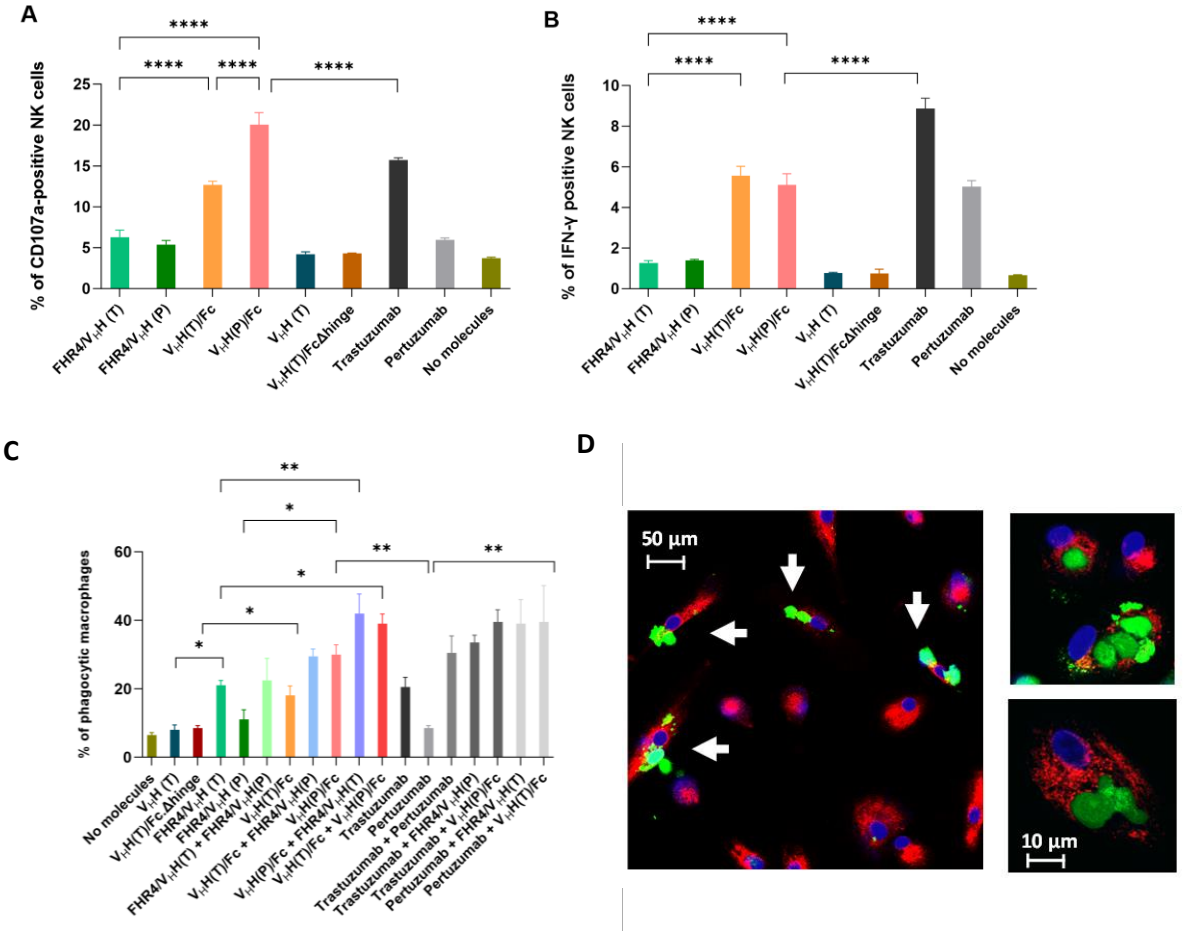
A
% of CD107a-positive NK cells
B
% of IFN-γ positive NK cells
C
% of phagocytic macrophages
D
50 µm
10 µm
E
1 hour after injection (anti-HIS or anti-IgG)
1 hour after injection (anti-C3d)
6 hours after injection (anti-HIS or anti-IgG)
6 hours after injection (anti-C3d)
CoMiX-FHR4
CoMiX-Fc
Controls
PBS
VHH(T)
Trastuzumab + pertuzumab

Figure 3: CoMiX-Fc enables NK cell activation and BT474 phagocytosis mediated by M2 macrophages. **(A)** HER2-positive BT474 tumor cells incubated with 15 µg/well of CoMiX were co-incubated with NK92^{humCD16} cells. The expression of the CD107a degranulation marker was analyzed by flow cytometry. **(B)** The intracellular accumulation of the cytokine IFN-γ was likewise analyzed by flow cytometry. Data are presented as mean values ±SD of the triplicates of one representative experiment of three independent experiments. Statistical analysis was performed using a one-way ANOVA and post-hoc Tukey test (***$p < 0.001$). **(C)** Complement-dependent macrophage-mediated phagocytosis of human BT474 cells. CFSE-stained BT474 tumor cells were incubated with controls, CoMiX, trastuzumab + pertuzumab or their combination with 25% C5-deficient human serum to prevent lysis. Percentage of phagocytic macrophages was measured. Data are presented as mean values ± SD out of n = 3 series of 10 confocal images for each condition. Statistical analysis was performed using a one-way ANOVA and post-hoc Tukey test (*$p < 0.05$, **$p < 0.01$). **(D)** Left: Confocal microscopy images of BT474 phagocytosis mediated by M2 macrophages when incubated with CoMiX V_HH(T)/Fc. The white arrows show the phagocytic macrophages (red) having engulfed BT474 cell(s) and harboring a green or yellowish color. Scale bar represents 50 µm. Right: Details of a phagocytic macrophage (red) at higher magnification (60× oil immersion). Scale bar represents 10 µm. **(E)** Immunofluorescent staining of tumor sections collected 1 or 6 hours after injection of CoMiX-FHR4 (upper panel), CoMiX-Fc (intermediate panel) or controls (lower panel with anti-C3d staining): PBS (1), V_HH(T) (2), trastuzumab + pertuzumab. CoMiX were visualized with either a rabbit anti-His mAb followed by the goat Anti-Rabbit IgG Fc AF568- or a goat anti-human IgG AF647-conjugated antibody. Complement activation was visualized using the polyclonal rabbit anti-C3d antibody followed by AF568-conjugated anti-rabbit IgG.

CoMiX-FHR4 and CoMiX-Fc reduce tumor progression *in vivo* by activating the complement

Tumor xenograft animal models are widely used in preclinical studies to evaluate the efficacy of novel anticancer therapies. We first checked the ability of CoMiX-FHR4 and CoMiX-Fc to infiltrate the tumor tissue and activate the mouse complement in a xenograft mouse model of BT474 cells (sensitive to both trastuzumab and pertuzumab) by immunohistochemistry of tumor sections (**Fig. 3E**). BT474 cells were injected into the mammary fat pads. When the tumor volumes reached ~60 mm^3, mice were injected intravenously with 100 µg of CoMiX-FHR4 (50 µg of FHR4/V_HH(T) + 50 µg of FHR4/V_HH(P)), or 100 µg of CoMiX-Fc (50 µg of V_HH(T)/Fc + 50 µg V_HH(P)/Fc), 100 µg of the V_HH (T) control, or 100 µg of Abs (50 µg trastuzumab + 50 µg pertuzumab) intravenously. One hour after injection, CoMiX were detected mainly at the tumor periphery and

co-localized with C3b-deposition (left panels). 6 hours after injection, the whole tumor was infiltrated with CoMiX-FHR4 or CoMiX-Fc (middle panels) and complement activation was not restricted to the periphery but occurred inside the whole tumor tissue (right panels). CoMiX-Fc was able to recruit C1q and activated the classical complement pathway (middle right panel) like the combination of trastuzumab or pertuzumab (lower right panel).

The effect of CoMiX was further analyzed *in vivo* on the xenograft mouse model as described in **Fig. 4A**. When the tumor volumes reached ~60 mm^3, mice were treated 9 times with 100 µg of CoMiX-FHR4, CoMiX-Fc, V_HH(T) or Abs. Three molecule combinations were also tested at half dose. No toxicity associated with the administration of CoMiX was observed by monitoring for body weight loss and other clinical symptoms. Tumor volumes were tracked for 15 days after the last drug injection and MRI was performed for several representative mice after sacrifice (**Fig. 4B**). As shown in **Fig. 4C,** both CoMiX-FHR4 reduced significantly the tumor volume compared to PBS (Mock, $p < 0.05$) as well as their combination ($p< 0.01$). V_HH(T)/Fc had no significant effect on tumor's growth whereas V_HH(P)/Fc and its combination with V_HH(T)/Fc decreased tumor growth significantly ($p<0.05$).

A

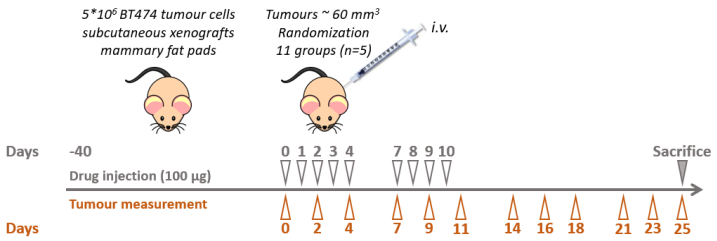
5*10⁶ BT474 tumour cells
subcutaneous xenografts
mammary fat pads
Tumours ~ 60 mm³
Randomization
11 groups (n=5)
i.v.
Days
-40
0 1 2 3 4
7 8 9 10
Sacrifice
Drug injection (100 µg)
Tumour measurement
Days
0 2 4 7 9 11 14 16 18 21 23 25

B

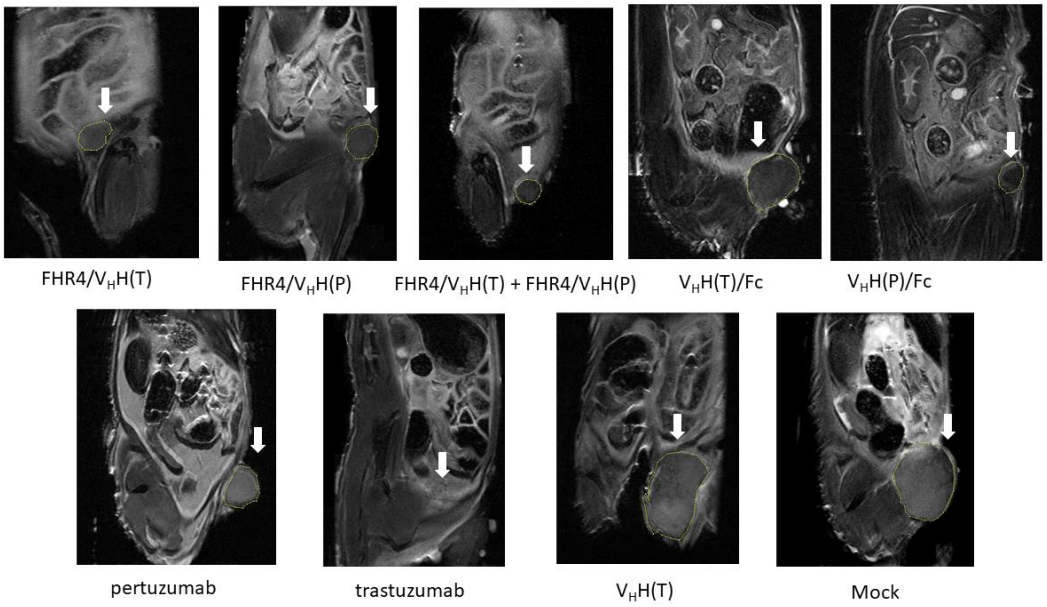
FHR4/VHH(T)
FHR4/VHH(P)
FHR4/VHH(T) + FHR4/VHH(P)
VHH(T)/Fc
VHH(P)/Fc
pertuzumab
trastuzumab
VHH(T)
Mock

C

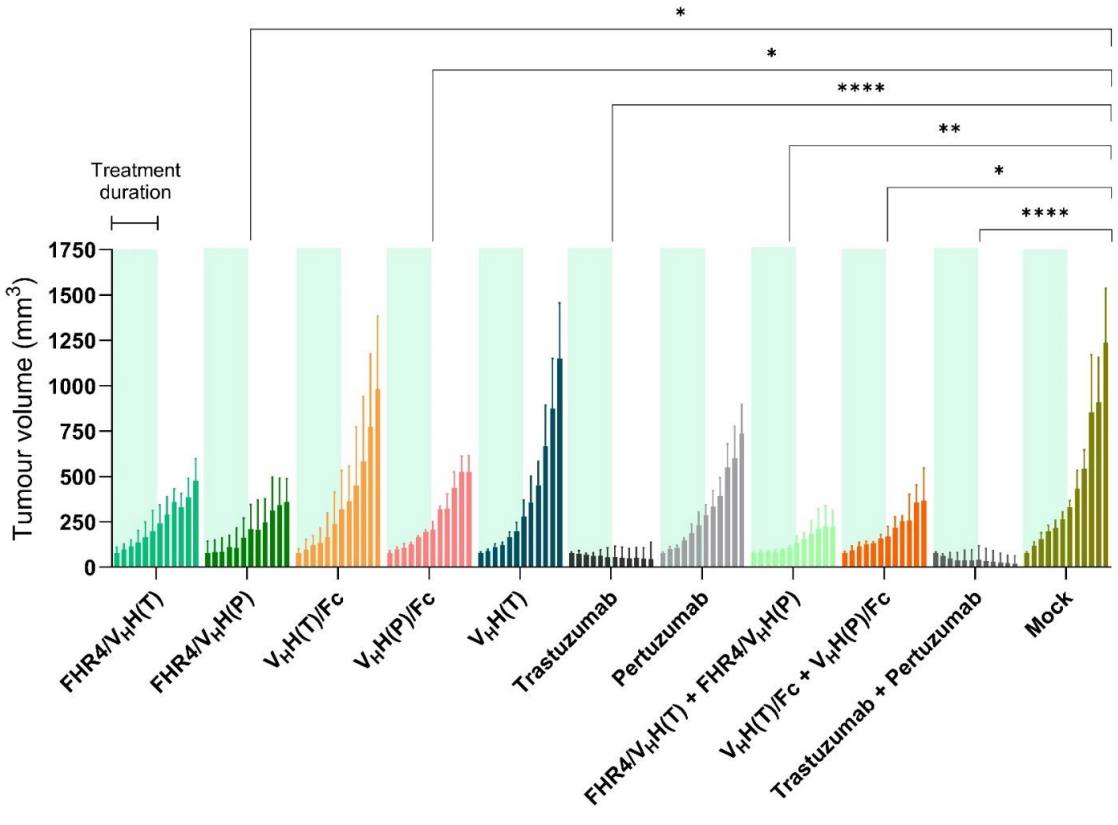
*
*
****
**
*
****
Treatment duration
Tumour volume (mm³)
1750
1500
1250
1000
750
500
250
0
FHR4/VHH(T)
FHR4/VHH(P)
VHH(T)/Fc
VHH(P)/Fc
VHH(T)
Trastuzumab
Pertuzumab
FHR4/VHH(T) + FHR4/VHH(P)
VHH(T)/Fc + VHH(P)/Fc
Trastuzumab + Pertuzumab
Mock

Figure 4: FHR4/V_HH(T), FHR4/V_HH(P) and V_HH(P)/Fc reduce tumor growth, whereas V_HH(T)/Fc has no beneficial effect. **(A)** Experimental design for the measurement of the subcutaneous xenografts mammary fat pads volume in the presence of different CoMiX and control antibodies. BT474 cells were injected into the mammary fat pads of mice. When the tumor volume reached ~60 mm^3, the mice were injected intravenously into the lateral tail vein with 100 µg of CoMiX or control antibodies, or 50 µg of each molecules for the combinations. The injection was repeated 9 times on days 1, 2, 3, 4, 7, 8, 9 and 10 after the first injection. The tumors were measured every second or third day with calipers. **(B)** MRI images of a representative tumor for each group in mice sacrificed at the end of the protocol .or when the tumor's size reached 1 000 mm^3. **(C)** The therapeutic effects of five CoMiX [FHR4/V_HH(T), FHR4/V_HH(P), V_HH(T)/Fc, V_HH(P)/Fc, V_HH(T)] and two control antibodies (trastuzumab and pertuzumab) were evaluated individually and in combination. The treatment duration is indicated for all groups in green, as mentioned for the first FHR4/V_HH(T) group in the left side of the graph. The groups were compared using unpaired Student's T test. *$p < 0.05$, **$p < 0.01$, ***$p < 0.001$, ****$p < 0.0001$).

When analyzing the tumor volume growth by single Abs or by combination (**Fig. 5A**, left panels) and at sacrifice (right panels), it is clear that V_HH(P)/Fc had a greater effect than pertuzumab but both CoMiX-FHR4 were not different than trastuzumab ($p > 0.05$). Although the combination of trastuzumab and pertuzumab was the most effective, no significant differences were observed with the two CoMiX-FHR4 and CoMiX-Fc combinations ($p > 0.05$).

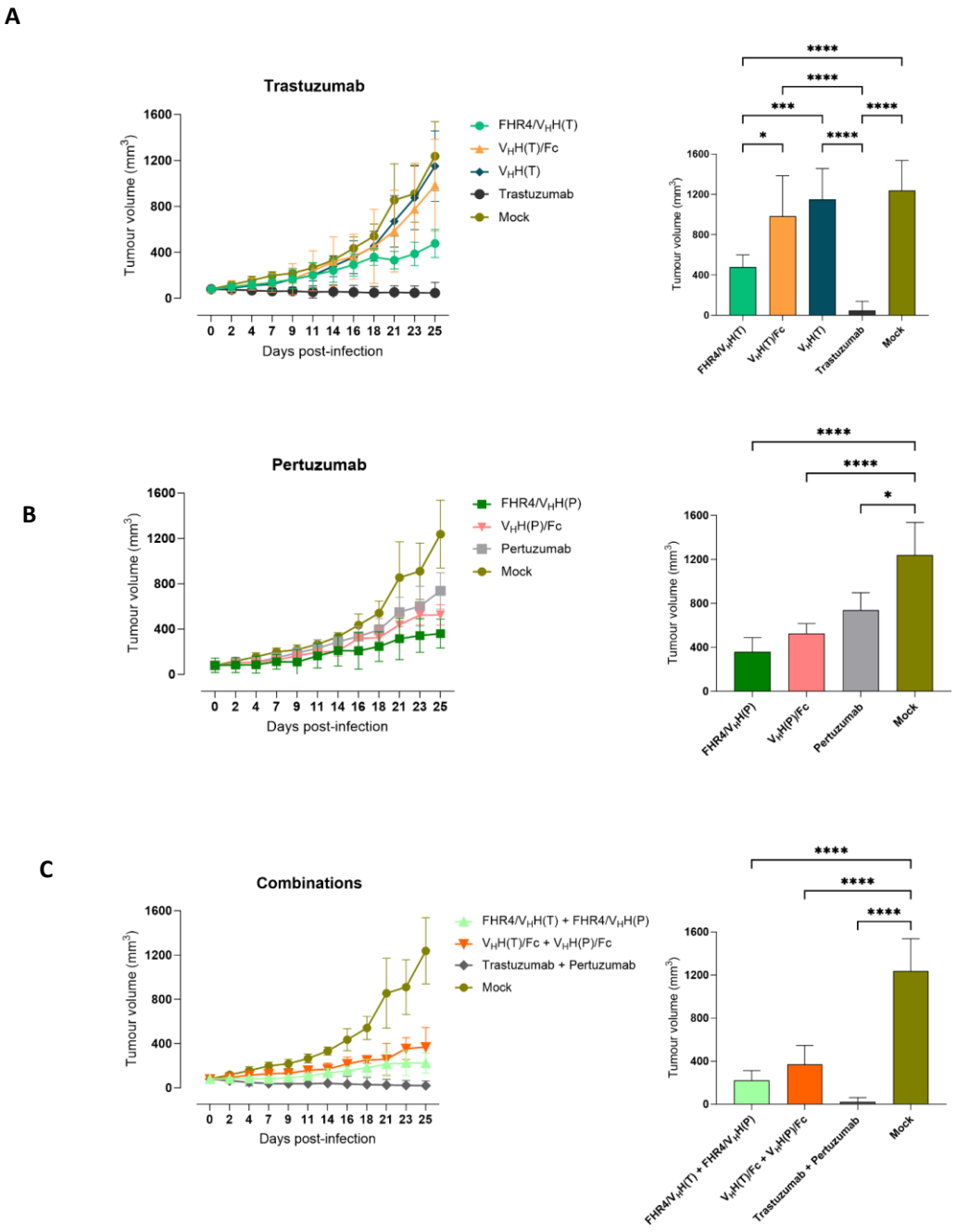

Figure 5: FHR4/V_HH(T), FHR4/V_HH(P) were not superior to trastuzumab but were as efficient as pertuzumab to reduce tumor growth. Tumor growth curve (left panels) and tumor size at sacrifice (right panels) for each treatment condition according to their HER-2 epitope. A: trastuzumab, B: pertuzumab or to their combination: C. The groups were compared using unpaired Student's T test. *p < 0.05, **p < 0.01, ***p < 0.001, ****p < 0.0001).

Immunohistochemistry was performed at day 25 or at sacrifice on when the xenograft reached 1 000 mm^3 (**Fig. 6AB)**. A large leucocyte infiltration was still found in xenografts of mice treated with trastuzumab or each combination tested, and to a lesser extend in xenografts from

the FHR4-V_HH(T), FHR4-V_HH(P) or V_HH(P)/Fc-treated mice (**Fig. 6A, left slides)**. Several spots of NK cells were detected in those infiltrations (**Fig. 6A, middle slides)** while few areas of T cells were rather concentrated at the tumor periphery or along the vessels for the mice treated with trastuzumab, V_HH(P)/Fc, FHR4-V_HH(P), and FHR4-V_HH(T) (**Fig. 6A, right slides)**. For all combinations (**Fig. 6B)**, a large leucocyte infiltration was observed including NK cells and T cells. Sera of the mice were also collected and variable anti-HER2 antibodies concentrations were measured in the mice treated with all drugs as compared to PBS (**Fig. 6C)**. Although no differences were significant, a trend towards higher anti-HER2 antibodies in trastuzumab-, V_HH(P)/Fc-, FHR4/V_HH(T)-, and trastuzumab plus pertuzumab-treated mice as compared to control mice was observed.

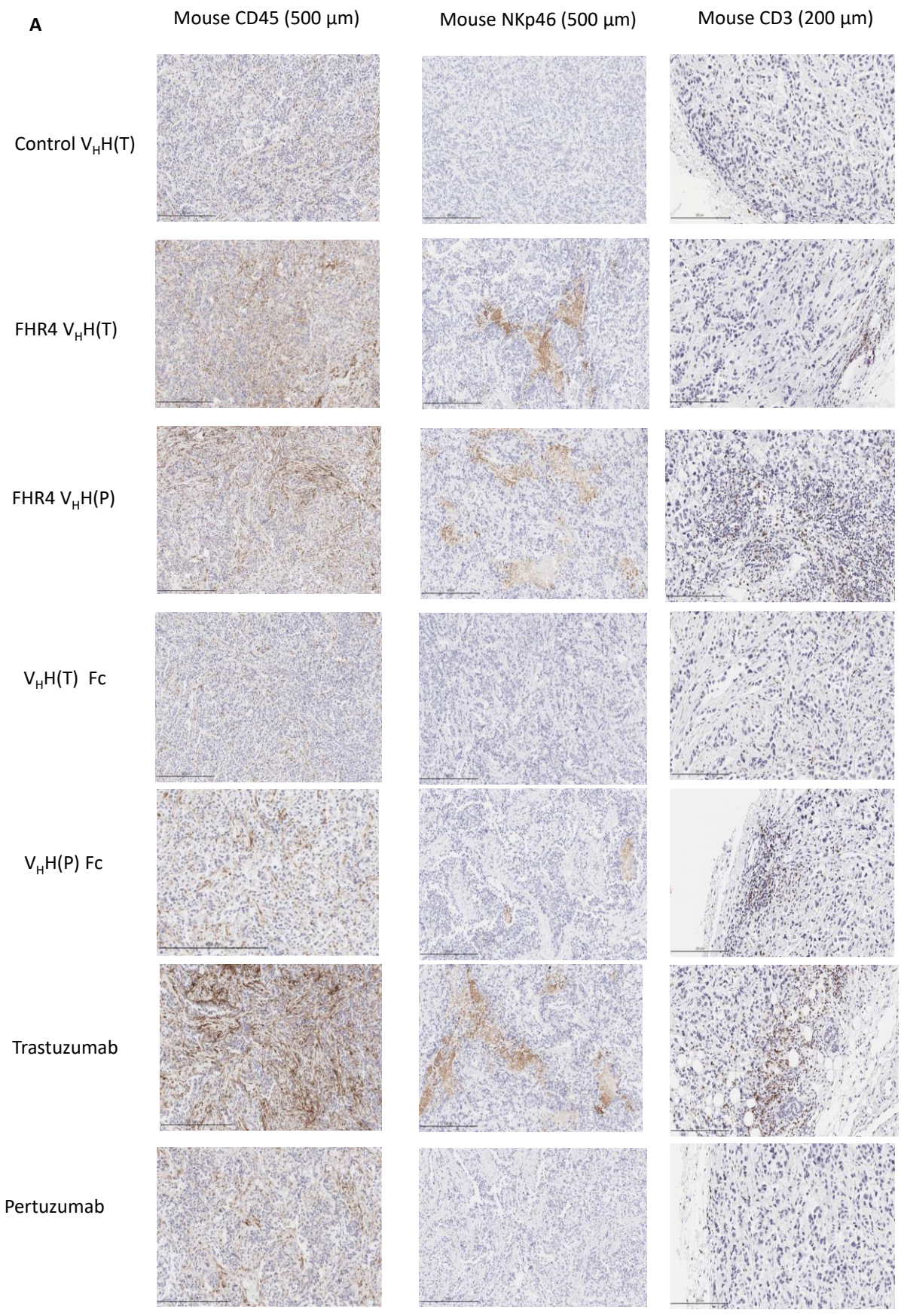
A
Mouse CD45 (500 µm)
Mouse NKp46 (500 µm)
Mouse CD3 (200 µm)
Control $V_HH(T)$
FHR4 $V_HH(T)$
FHR4 $V_HH(P)$
$V_HH(T)$ Fc
$V_HH(P)$ Fc
Trastuzumab
Pertuzumab

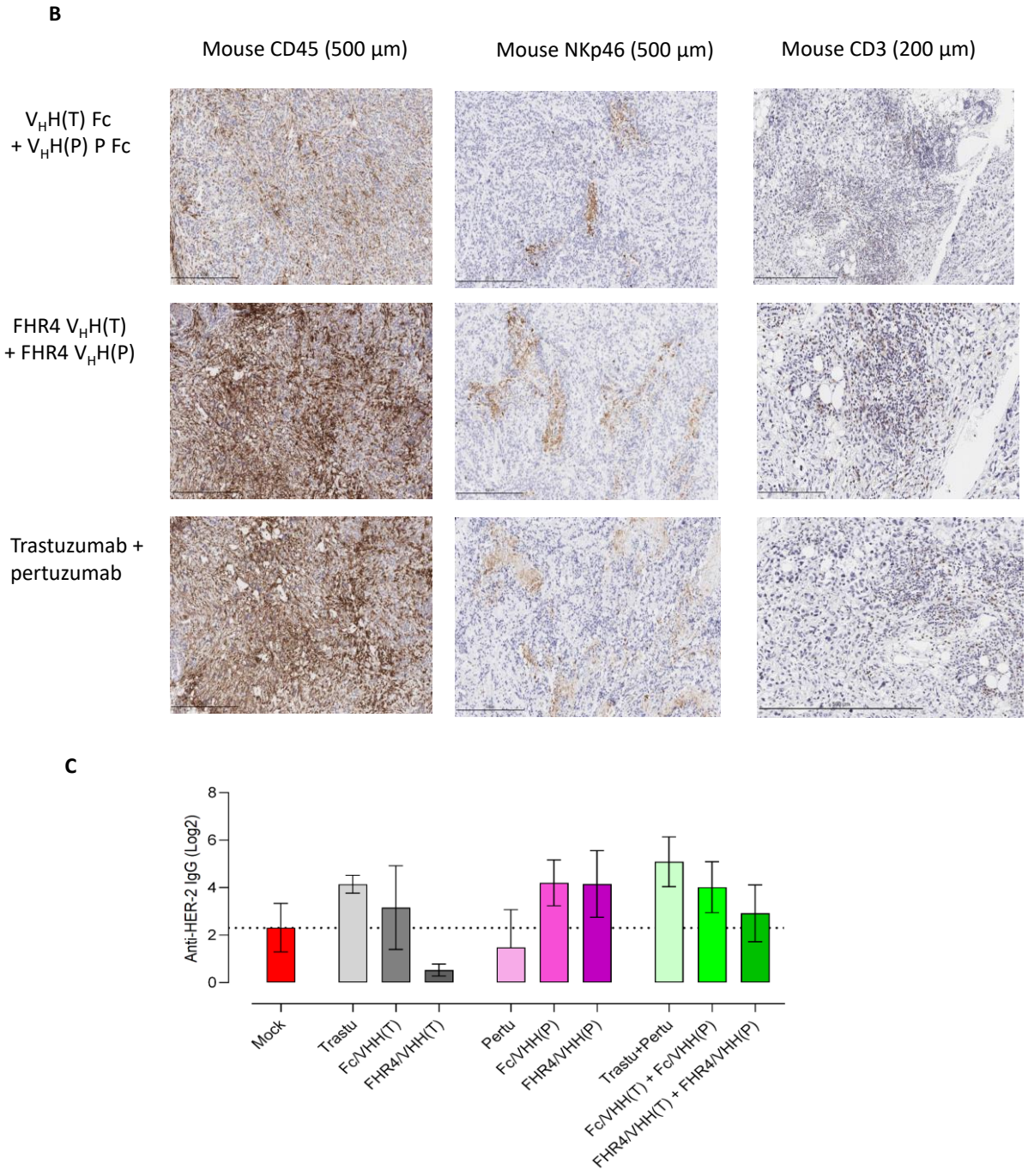

Figure 6: CoMiX stimulate leucocyte infiltration (**A**) representative pictures of immunohistochemistry staining (40X) of leucocytes (left panels) using an anti- mouse CD45 antibody, NK cells (middle panels) using an mouse NKp46/NCR1 antibody and T cells (left panels) using an anti-mouse CD3 antibody and revealed by an HRP secondary antibody. (**B**) Combination of trastuzumab with pertuzumab, CoMix FHR4/V_HH(T) with FHR4/V_HH(P), and CoMiX V_HH(T)/Fc and V_HH(P)/Fc induce large leucocyte infiltration (left panels), with a high number of NK cells (middle panels) and few areas of concentrated T cells (right panels) (**C**). Concentration of total anti-HER2 IgG in sera was determined by ELISA at days 15 after the last administration of the therapeutic

molecules. Data are represented as the mean values ± SEM. The results correspond to 4 independent experiments (n = 2-3 mice per groups).

While trastuzumab is extremely effective at the early stages of treatment, cells quickly develop various resistance mechanisms [285]. We thus explored the effects of CoMiX FHR4/V_HH(P) or in combination with CoMiX FHR4/V_HH(T) (**Fig. 7A**) on xenografts of trastuzumab-resistant BT474 cell line (ATCC-CRL-3247). Injecting trastuzumab for 10 days increased tumor growth of trastuzumab-resistant cancer cells as compared to the control PBS as previously shown [490, 491, 492]. In contrast, CoMiX-FHR4 reduced significantly their growth during treatment and up to 25 days after treatment initiation when the tumor relapsed. No difference was observed on tumor growth between CoMiX FHR4/V_HH(P) and its combination with CoMiX FHR4/V_HH(T). BT474 tumors resistant to trastuzumab treated with CoMiX-FHR4, trastuzumab or PBS where collected just after the last injection at Day 11. A massive NK cell infiltration was observed in the tumor treated with CoMiX-FHR4 (**Fig**. **7B**), whereas the infiltration was much weaker in the tumor treated with trastuzumab leading to a faster growth of the tumor. Taken together, our *in vivo* data are consistent with the data obtained *in vitro* on BT474 cells. CoMiX-FHR4 and CoMiX-Fc lead to a fast and massive complement deposition and subsequent CDC, but also to the recruitment of innate effector cells such as NK cells, that reduce tumor growth. Although the dose, treatment duration and pharmacokinetics need to be further optimized, CoMiX may offer a novel alternative for tumors that became resistant to trastuzumab, and more generally, be an alternative to optimize in combination with chemotherapy, ADC or with other immunotherapeutic approaches such as checkpoint inhibitors.

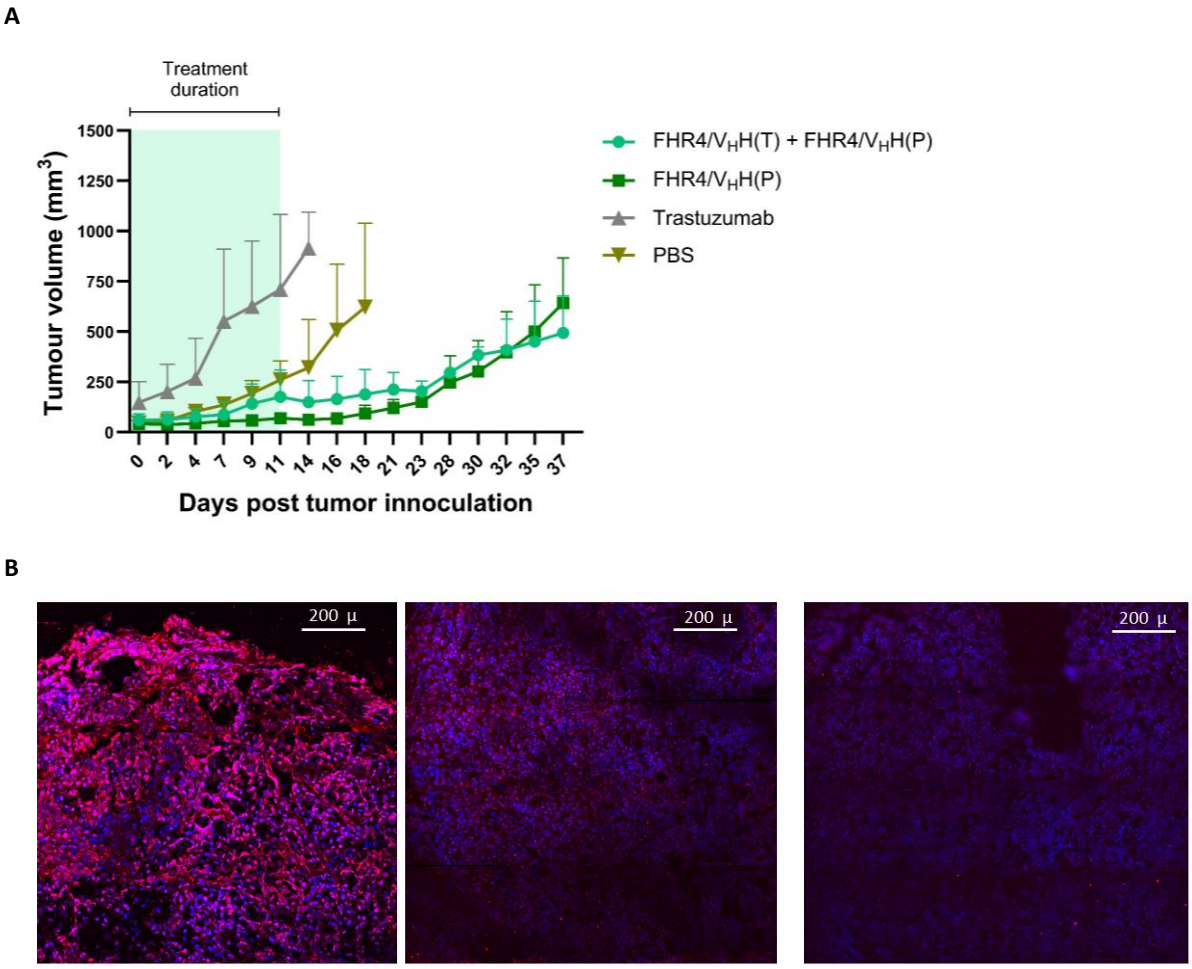

Figure 7: FHR4/V_HH(T) and FHR4/V_HH(P) CoMiX exert their anti-tumor effect on trastuzumab-resistant BT474 cells. **(A)** Trastuzumab-resistant BT474 cells were injected into the mammary fat pads of female BALB/c NUDE mice. When the tumor volume reached ~60 mm^3, the mice were injected with 100 µg of CoMiX-FHR4, trastuzumab or PBS, as described on **Fig.** 5A. The tumors were measured every second or third day until day 37 of the study or until meeting the endpoint of 10000 mm^3. **(B)** To visualize leukocyte infiltration cryosections of trastuzumab-resistant BT474 tumor xenografts collected just after the end of the treatment (at D+11). Cryosections were stained with a mouse NKp46/NCR1 antibody and revealed using a donkey anti-rat AF568-conjugated pAb. Confocal microscope was used to make pictures (lens X40), monitored by the Nikon NIS-Elements software which allowed to assemble pictures to get a large field overview of the tumors. **A)** tumor treated with combined CoMiX-FHR4 [FHR4/V_HH(T) + FHR4/V_HH(P)], **B)** tumor treated with trastuzumab, **C)** tumor treated with PBS (mock).

DISCUSSION

HER2-targeted therapies have changed the paradigm for patients and significantly improved their prognosis over the past few decades [493, 494]. For most patients with advanced HER2-positive breast cancer, trastuzumab or pertuzumab are first line treatments[495]. Breast cancer remains nevertheless a clinical challenge due to emerging resistance to HER2 therapies leading to disease progression. New HER2-targeted drugs, such as tucatinib and trastuzumab deruxtecan (T-DXd), have raised survival rates in cancers with de novo stage IV disease or that inevitably recurs [496]. However, novel effective therapies are still needed in the early and metastatic settings to prevent recurrence and advanced metastatic breast cancer.

Immunotherapy with directed complement activation is a promising approach [497]. The activation of the classical pathway of complement contributes to the therapeutic efficacy of Rituximab [498, 499, 500]. Factor H is a key complement regulator that can be hijacked by bacteria [501, 502, 503] or cancer cells[504] to evade complement-mediated cytotoxicity [500, 505]. Factor H-related protein 1 to 5 have different activation or inhibition effects [506, 507, 508]. We have previously shown that BT474 tumor cells establish a complement inhibitory threshold, overcome by high valences of FHR4 when directed to the surface of tumor cells [487]. By lacking the regulatory domains of FH, but not the surface binding region of the protein, FHR4 competes with FH for C3b, iC3b and C3d binding[487]. Fc regions, however, mediate several effector functions, including classical complement pathway activation[509], as well as activation of immune cells (phagocytes, NK cells) via various Fc receptors[510, 511].

Here, we demonstrated that both CoMiX-FHR4 and CoMiX-Fc have a complement activating capacity on HER2-positive BT474 cancer cells *in vitro* and *in vivo* that induce direct lysis of tumor cells. CoMiX-FHR4 had a superior effect *in vitro* on CDC when compared to CoMiX-Fc and Abs (**Fig. 2**). CoMiX-FHR4 serve as a platform for the assembly of the alternative pathway C3-convertase whereas CoMiX-Fc activate the classical pathway. Therefore, the combination of CoMiX-Fc with CoMiX-FHR4 resulted in enhanced complement activation. Since V_HH(T) and V_HH(P) moieties recognize different epitopes, their effect was also additive when two CoMiX-FHR4 or CoMiX-Fc constructs were combined. Alternatively, CoMiX-Fc activate NK cells and induce complement-mediated phagocytosis of BT474 cells by M2 macrophages. V_HH(P)/Fc was able to activate NK cells and complement-mediated phagocytosis with greater efficacy than pertuzumab, while V_HH(T)/Fc had a similar effect than trastuzumab.

We first tested in vivo the antitumor growth effect of CoMiX-FHR4 and CoMiX-Fc in BT474 xenografts sensitive to trastuzumab and pertuzumab. After systemic injection, the diffusion of CoMiX into the tumor was fast, and the tumor demonstrated massive complement activation 6h

after injection. FHR4/V_HH(T), FHR4/V_HH(P) and V_HH(P)/Fc reduced tumor growth but not V_HH(T)/Fc that showed less efficiency for phagocytosis by macrophages and degranulation of NK cells than V_HH(P)/Fc (**Fig.** 4) in vitro and few leucocyte infiltration in xenografts. Trastuzumab was the most potent treatment, indicating that complement activation alone is less efficient than the additive effects of cell signaling inhibition with ADCC/ADCP induced by the Abs on limiting tumor growth. Beside its cytostastic effect, the immunological engagement of trastuzumab mediates its clinical efficacy via ADCC elicited by NK cells or macrophages, resulting in cancer cell killing, but also through activation of macrophages, neutrophils, and dendritic cells, modulating the adaptive immunity. This was supported by the large leucocyte infiltration observed in xenografts of mice treated with trastuzumab but not pertuzumab. NK cells were highly represented among the leucocytes while T cells were detected to a lesser extend at the periphery of the tumor or in proximity of vessels. FHR4/V_HH(T), FHR4/V_HH(P) and V_HH(P)/Fc induced less leucocyte infiltration than trastuzumab but similar NK and T cells recruitment suggesting that the directed activation of complement on cancer cells might stimulate enough NK cell responses.

Of note, V_HH(P)/Fc was as potent as pertuzumab for reducing tumor growth *in vivo*. This might be explained by its greater efficacy to activate NK cells and complement-mediated phagocytosis, as shown in vitro, but also by the presence of NK and T cells in xenografts as compared to pertuzumab. The combined use of trastuzumab and pertuzumab enhanced their therapeutic efficacy *in vivo* as well as the combination of all FHR4/V_HH(T) and FHR4/V_HH(P) being the most potent combination of CoMiX in vivo. Ultimately, when tested on a trastuzumab-resistant BT474 cell line, FHR4/V_HH(P) and the combination of FHR4/V_HH(T) and FHR4/V_HH(P) delayed significantly tumor growth as compared to trastuzumab that showed higher growth rate than the control group with PBS as previously observed [490, 491, 492] due to the upregulation of angiogenesis factors [512, 513]. Up to 15 days after the last injection, CoMiX-FHR4 succeed to inhibit trastuzumab-resistant cell growth before the tumor relapsed suggesting that no remission was achieved at the end of the treatment. This relapse needs to be further investigated with optimized doses and timing of injection of CoMiX, when pharmacokinetics data will be known, to understand whether duration or resistance issues may have occurred. We did not observe any activation of the HER2 signaling by western-blot with our two VHH targeting HER2 (data not shown). This would imply that no resistance associated with HER2 expression or signaling may have occurred.

Our *in vivo* data corroborate with the *in vitro* data by showing a high local activation of the host complement alternative pathway in the xenograft after 6 hours of systemic injection, which leads to efficient CDC. This mechanism of action is strictly independent from the HER2 signaling pathway. Complement is currently considered as an essential effector of the tumor cytotoxic

responses of Abs but also in antitumor immunity [514]. The crosstalk of complement effectors and cellular signaling pathways is known to regulate the T and B cell responses in terms of survival, differentiation, and activation. A trend towards increased concentrations of HER2 Antibodies was therfore detected in sera of mice treated with trastuzumab, V_HH(P)/Fc, FHR4/V_HH(T), and trastuzumab plus pertuzumab. Induction of antitumor antibodies are more frequently observed in clinically responding patients [515] through endocytosis of tumor antigen–containing immune complexes or phagocytosis of antibody-opsonized tumor target cells.

Advances in HER2 breast cancer currently relies on antibody–drug conjugates (ADCs) or bi-specific antibodies using two different HER2 epitopes for higher efficacy [516]. Dual HER2 inhibition with trastuzumab plus pertuzumab improves the outcomes of patients with HER2+ metastatic breast cancer as compared to single HER2 inhibition. Dual HER2 targeting by CoMiX may overcome limited HER2 binding. A future format of CoMiX including both HER2 targeting could improve its effectiveness. Numerous attempts to stimulate the immune response against HER2+ tumor cells are under evaluation, and CoMiX may offer such perspectives under the form of an ADC or including a check-point inhibitor.

Importantly, external recruitment of the complement system is highly unlikely to lead to treatment resistance, in contrast to currently used Abs [285, 485]. The complement system has a strong potential to stimulate inflammation but is nevertheless tightly regulated. Membrane-anchored complement regulatory proteins (CD46, CD55 and CD59) are overexpressed on host cells to prevent high complement activation [257, 517]. Several other soluble complement regulatory proteins are also present in body fluids, such as FH, factor H-like protein 1 (FHL1), classical pathway inhibitors like C4b-binding protein (C4bp), C1 inhibitor as well as terminal pathway inhibitors like clusterin or vitronectin. Therefore, the tight regulation of the soluble complement cascade combined to a directed C3b activation on targeted tumor cells could represent an alternative and safe anticancer therapy [518]. Importantly, complement components are known to regulate the function of the tumor microenvironment by favoring both tumor-promoting and tumor-suppressing responses [231]; a clear understanding of the underlying mechanisms of host and tumor microenvironment will be therefore the key for the clinical development of CoMiX.

In conclusion, we made the proof of concept that directed-complement activation is able to reduce tumor growth *in vivo.* CoMiX were as effective as pertuzumab and might help to circumvent resistance to trastuzumab since their mechanism of action differs from those of trastuzumab and pertuzumab. Their combination showed enhanced effect on tumor growth that opens the way to explore combination therapies to reach a synergistic mechanism of action with Abs. As a large percentage of patients easily develop resistance to one or the two conventional

monoclonal antibodies, an optimized format of bi-specific complexes could maximize their efficacy or avoid resistance mechanisms against HER2 based therapies when used in combination.

Author's Contribution

Conceptualization, X.D., C.S.D., J.H.M.C; methodology, X.D., C.S.D., J.H.M.C, J.M.P, G.I., J.Y.S., A.P., G.K., I.B., J.Z.; validation, B.B., G.I., C.S.D., J.H.M.C, J.Z.; analysis, X.D., C.S.D., J.H.M.C, B.B., J.M.P, G.I., J.Y.S., A.P., G.K., J.Z.; data curation, J.Z, B.B, C.S.D.; writing—original draft preparation, B.B, C.S.D., J.Z., X.D. ; writing—review and editing, B.B, C.S.D., J.M.P, G.I., J.Y.S, A.P., J.Z., G.K., I.B., J.Z., J.H.M.C, X.D.; resources, C.S.D, I.B, G.I., J.M.P., J.Y.S, J.Z., X.D.; funding acquisition, C.S.D., I.B. All authors have read and agreed to the published version of the manuscript.

Acknowledgements

We would like to acknowledge Brigitte Reveil for her technical assistance and Pr Béatrice Clemenceau, University of Nantes for providing the NK92^{humCD16}cell line.

7. References

1. Turvey, S.E. & Broide, D.H. Innate immunity. *Journal of Allergy and Clinical Immunology* **125**, S24-S32 (2010).

2. Li, D. & Wu, M. Pattern recognition receptors in health and diseases. *Signal Transduction and Targeted Therapy* **6** (2021).

3. Anthoney, N., Foldi, I. & Hidalgo, A. Toll and Toll-like receptor signalling in development. *Development* **145**, dev156018 (2018).

4. Almeida-Da-Silva, C.L.C., Savio, L.E.B., Coutinho-Silva, R. & Ojcius, D.M. The role of NOD-like receptors in innate immunity. *Frontiers in Immunology* **14** (2023).

5. Rehwinkel, J. & Gack, M.U. RIG-I-like receptors: their regulation and roles in RNA sensing. *Nature Reviews Immunology* **20**, 537-551 (2020).

6. Richardson, M.B. & Williams, S.J. MCL and Mincle: C-Type Lectin Receptors That Sense Damaged Self and Pathogen-Associated Molecular Patterns. *Frontiers in Immunology* **5** (2014).

7. Mogensen, T.H. Pathogen Recognition and Inflammatory Signaling in Innate Immune Defenses. *Clinical Microbiology Reviews* **22**, 240-273 (2009).

8. Wu, S.-Y., Fu, T., Jiang, Y.-Z. & Shao, Z.-M. Natural killer cells in cancer biology and therapy. *Molecular Cancer* **19** (2020).

9. Gupta, S.C., Kunnumakkara, A.B., Aggarwal, S. & Aggarwal, B.B. Inflammation, a Double-Edge Sword for Cancer and Other Age-Related Diseases. *Frontiers in Immunology* **9** (2018).

10. Raymond, B.B.A. Pathogen evasion strategies. *Cellular Microbiology* **23** (2021).

11. Kim, S.K. & Cho, S.W. The Evasion Mechanisms of Cancer Immunity and Drug Intervention in the Tumor Microenvironment. *Frontiers in Pharmacology* **13** (2022).

12. Thakur, A., Mikkelsen, H. & Jungersen, G. Intracellular Pathogens: Host Immunity and Microbial Persistence Strategies. *Journal of Immunology Research* **2019**, 1-24 (2019).

13. Pansy, K. *et al.* Immune Regulatory Processes of the Tumor Microenvironment under Malignant Conditions. *International Journal of Molecular Sciences* **22**, 13311 (2021).

14. Merle, N.S., Church, S.E., Fremeaux-Bacchi, V. & Roumenina, L.T. Complement System Part I: Molecular Mechanisms of Activation and Regulation. *Frontiers in Immunology* **6** (2015).

15. Merle, N.S., Noe, R., Halbwachs-Mecarelli, L., Fremeaux-Bacchi, V. & Roumenina, L.T. Complement System Part II: Role in Immunity. *Frontiers in Immunology* **6** (2015).

16. Nesargikar, P., Spiller, B. & Chavez, R. The complement system: History, pathways, cascade and inhibitors. *European Journal of Microbiology and Immunology* **2**, 103-111 (2012).

17. Lu, J. & Kishore, U. C1 Complex: An Adaptable Proteolytic Module for Complement and Non-Complement Functions. *Frontiers in Immunology* **8** (2017).

18. Tan, L.A., Yang, A.C., Kishore, U. & Sim, R.B. Interactions of complement proteins C1q and factor H with lipid A and Escherichia coli: further evidence that factor H regulates the classical complement pathway. *Protein Cell* **2**, 320-332 (2011).

19. Albertí, S. *et al.* Interaction between complement subcomponent C1q and the Klebsiella pneumoniae porin OmpK36. *Infection and Immunity* **64**, 4719-4725 (1996).

20. Sjöwall, C. *et al.* Solid-phase classical complement activation by C-reactive protein (CRP) is inhibited by fluid-phase CRP–C1q interaction. *Biochemical and Biophysical Research Communications* **352**, 251-258 (2007).

21. Singh, S.K., Ngwa, D.N. & Agrawal, A. Complement Activation by C-Reactive Protein Is Critical for Protection of Mice Against Pneumococcal Infection. *Frontiers in Immunology* **11** (2020).

22. Ma, Y.J. & Garred, P. Pentraxins in Complement Activation and Regulation. *Frontiers in Immunology* **9** (2018).

23. Dobó, J. *et al.* The Lectin Pathway of the Complement System—Activation, Regulation, Disease Connections and Interplay with Other (Proteolytic) Systems. *International Journal of Molecular Sciences* **25**, 1566 (2024).

24. Dobó, J., Pál, G., Cervenak, L. & Gál, P. The emerging roles of mannose-binding lectin-associated serine proteases (MASPs) in the lectin pathway of complement and beyond. *Immunological Reviews* **274**, 98-111 (2016).

25. Pangburn, M.K. Initiation of the alternative pathway of complement and the history of "tickover". *Immunol Rev* **313**, 64-70 (2023).

26. Lachmann, P.J. Looking back on the alternative complement pathway. *Immunobiology* **223**, 519-523 (2018).

27. Serna, M., Giles, J.L., Morgan, B.P. & Bubeck, D. Structural basis of complement membrane attack complex formation. *Nature Communications* **7**, 10587 (2016).

28. Heesterbeek, D.A. *et al.* Bacterial killing by complement requires membrane attack complex formation via surface-bound C5 convertases. *The EMBO Journal* **38** (2019).

29. Tegla, C.A. *et al.* Membrane attack by complement: the assembly and biology of terminal complement complexes. *Immunol Res* **51**, 45-60 (2011).

30. Mevorach, D., Mascarenhas, J.O., Gershov, D. & Elkon, K.B. Complement-dependent clearance of apoptotic cells by human macrophages. *J Exp Med* **188**, 2313-2320 (1998).

31. Li, W. Eat-me signals: Keys to molecular phagocyte biology and "Appetite" control. *Journal of Cellular Physiology* **227**, 1291-1297 (2012).

32. Santos-López, J., De La Paz, K., Fernández, F.J. & Vega, M.C. Structural biology of complement receptors. *Frontiers in Immunology* **14** (2023).

33. Zarantonello, A., Revel, M., Grunenwald, A. & Roumenina, L.T. C3-dependent effector functions of complement. *Immunological Reviews* **313**, 120-138 (2023).

34. Hardy, M.P., Mansour, M., Rowe, T. & Wymann, S. The Molecular Mechanisms of Complement Receptor 1—It Is Complicated. *Biomolecules* **13**, 1522 (2023).

35. Erdei, A. *et al.* New aspects in the regulation of human B cell functions by complement receptors CR1, CR2, CR3 and CR4. *Immunol Lett* **237**, 42-57 (2021).

36. Vorup-Jensen, T. & Jensen, R.K. Structural Immunology of Complement Receptors 3 and 4. *Frontiers in Immunology* **9** (2018).

37. Helmy, K.Y. *et al.* CRIg: A Macrophage Complement Receptor Required for Phagocytosis of Circulating Pathogens. *Cell* **124**, 915-927 (2006).

38. Yadav, M.K. *et al.* Molecular basis of anaphylatoxin binding, activation, and signaling bias at complement receptors. *Cell* **186**, 4956-4973.e4921 (2023).

39. Barnum, S.R. C4a: An Anaphylatoxin in Name Only. *Journal of Innate Immunity* **7**, 333-339 (2015).

40. Wang, Y. *et al.* Revealing the signaling of complement receptors C3aR and C5aR1 by anaphylatoxins. *Nat Chem Biol* **19**, 1351-1360 (2023).

41. Li, X.X., Lee, J.D., Kemper, C. & Woodruff, T.M. The Complement Receptor C5aR2: A Powerful Modulator of Innate and Adaptive Immunity. *The Journal of Immunology* **202**, 3339-3348 (2019).

42. Ghosh, M. & Rana, S. The anaphylatoxin C5a: Structure, function, signaling, physiology, disease, and therapeutics. *Int Immunopharmacol* **118**, 110081 (2023).

43. Skidgel, R.A. & Erdös, E.G. Structure and function of human plasma carboxypeptidase N, the anaphylatoxin inactivator. *International Immunopharmacology* **7**, 1888-1899 (2007).

44. Klos, A. *et al.* The role of the anaphylatoxins in health and disease. *Molecular Immunology* **46**, 2753-2766 (2009).

45. Schanzenbacher, J., Köhl, J. & Karsten, C.M. Anaphylatoxins spark the flame in early autoimmunity. *Front Immunol* **13**, 958392 (2022).

46. Laumonnier, Y., Korkmaz, R.Ü., Nowacka, A.A. & Köhl, J. Complement-mediated immune mechanisms in allergy. *European Journal of Immunology* **53** (2023).

47. Evans, R. *et al.* Complement activation and increased anaphylatoxin receptor expression are associated with cortical grey matter lesions and the compartmentalised inflammatory response of multiple sclerosis. *Frontiers in Cellular Neuroscience* **17** (2023).

48. Ajona, D., Ortiz-Espinosa, S. & Pio, R. Complement anaphylatoxins C3a and C5a: Emerging roles in cancer progression and treatment. *Semin Cell Dev Biol* **85**, 153-163 (2019).

49. Li, K. *et al.* Functional modulation of human monocytes derived DCs by anaphylatoxins C3a and C5a. *Immunobiology* **217**, 65-73 (2012).

50. West, E.E., Kolev, M. & Kemper, C. Complement and the Regulation of T Cell Responses. *Annu Rev Immunol* **36**, 309-338 (2018).

51. Cho, H. Complement regulation: physiology and disease relevance. *Korean Journal of Pediatrics* **58**, 239 (2015).

52. Geller, A. & Yan, J. The Role of Membrane Bound Complement Regulatory Proteins in Tumor Development and Cancer Immunotherapy. *Frontiers in Immunology* **10** (2019).

53. Krych-Goldberg, M. *et al.* Decay Accelerating Activity of Complement Receptor Type 1 (CD35). *Journal of Biological Chemistry* **274**, 31160-31168 (1999).

54. Mácsik-Valent, B., Nagy, K., Fazekas, L. & Erdei, A. Complement Receptor Type 1 (CR1, CD35), the Inhibitor of BCR-Mediated Human B Cell Activation, Differentially Regulates TLR7, and TLR9 Induced Responses. *Frontiers in Immunology* **10** (2019).

55. Liszewski, M.K. & Atkinson, J.P. Complement regulator CD46: genetic variants and disease associations. *Human Genomics* **9** (2015).

56. Couves, E.C. *et al.* Structural basis for membrane attack complex inhibition by CD59. *Nature Communications* **14** (2023).

57. Cicardi, M., Zingale, L., Zanichelli, A., Pappalardo, E. & Cicardi, B. C1 inhibitor: molecular and clinical aspects. *Springer Semin Immunopathol* **27**, 286-298 (2005).

58. Kajdácsi, E. *et al.* Patterns of C1-Inhibitor/Plasma Serine Protease Complexes in Healthy Humans and in Hereditary Angioedema Patients. *Frontiers in Immunology* **11** (2020).

59. Ermert, D. & Blom, A.M. C4b-binding protein: The good, the bad and the deadly. Novel functions of an old friend. *Immunology Letters* **169**, 82-92 (2016).

60. Serrano, I. *et al.* The Hidden Side of Complement Regulator C4BP: Dissection and Evaluation of Its Immunomodulatory Activity. *Frontiers in Immunology* **13** (2022).

61. Mannes, M., Dopler, A., Huber-Lang, M. & Schmidt, C.Q. Tuning the Functionality by Splicing: Factor H and Its Alternative Splice Variant FHL-1 Share a Gene but Not All Functions. *Frontiers in Immunology* **11** (2020).

62. Ferreira, V.P., Pangburn, M.K. & Cortés, C. Complement control protein factor H: The good, the bad, and the inadequate. *Molecular Immunology* **47**, 2187-2197 (2010).

63. Nilsson, S.C., Sim, R.B., Lea, S.M., Fremeaux-Bacchi, V. & Blom, A.M. Complement factor I in health and disease. *Molecular Immunology* **48**, 1611-1620 (2011).

64. Watanabe-Kusunoki, K., Nakazawa, D., Ishizu, A. & Atsumi, T. Thrombomodulin as a Physiological Modulator of Intravascular Injury. *Frontiers in Immunology* **11** (2020).

65. Feng, S., Liang, X., Kroll, M.H., Chung, D.W. & Afshar-Kharghan, V. von Willebrand factor is a cofactor in complement regulation. *Blood* **125**, 1034-1037 (2015).

66. Menny, A. *et al.* Structural basis of soluble membrane attack complex packaging for clearance. *Nature Communications* **12** (2021).

67. Massri, M. *et al.* Complement C7 and clusterin form a complex in circulation. *Frontiers in Immunology* **15** (2024).

68. Sheehan, M., Morris, C.A., Pussell, B.A. & Charlesworth, J.A. Complement inhibition by human vitronectin involves non-heparin binding domains. *Clinical and Experimental Immunology* **101**, 136-141 (1995).

69. Hartmann, S. & Hofsteenge, J. Properdin, the Positive Regulator of Complement, Is Highly C-Mannosylated. *Journal of Biological Chemistry* **275**, 28569-28574 (2000).

70. Alcorlo, M., Tortajada, A., Rodríguez De Córdoba, S. & Llorca, O. Structural basis for the stabilization of the complement alternative pathway C3 convertase by properdin. *Proceedings of the National Academy of Sciences* **110**, 13504-13509 (2013).

71. Lucientes-Continente, L., Márquez-Tirado, B. & Goicoechea De Jorge, E. The Factor H protein family: The switchers of the complement alternative pathway. *Immunological Reviews* **313**, 25-45 (2023).

72. Sándor, N. *et al.* The human factor H protein family – an update. *Frontiers in Immunology* **15** (2024).

73. Kárpáti, É. *et al.* Interaction of the Factor H Family Proteins FHR-1 and FHR-5 With DNA and Dead Cells: Implications for the Regulation of Complement Activation and Opsonization. *Frontiers in Immunology* **11** (2020).

74. Papp, A. *et al.* Complement Factor H-Related Proteins FHR1 and FHR5 Interact With Extracellular Matrix Ligands, Reduce Factor H Regulatory Activity and Enhance Complement Activation. *Frontiers in Immunology* **13** (2022).

75. Renner, B. *et al.* Factor H related proteins modulate complement activation on kidney cells. *Kidney Int* **102**, 1331-1344 (2022).

76. González-Alsina, A. *et al.* Factor H-related protein 1 promotes complement-mediated opsonization of Pseudomonas aeruginosa. *Frontiers in Cellular and Infection Microbiology* **14** (2024).

77. Reiss, T. *et al.* Cutting Edge: FHR-1 Binding Impairs Factor H–Mediated Complement Evasion by the Malaria Parasite Plasmodium falciparum. *The Journal of Immunology* **201**, 3497-3502 (2018).

78. Cserhalmi, M., Papp, A., Brandus, B., Uzonyi, B. & Józsi, M. Regulation of regulators: Role of the complement factor H-related proteins. *Seminars in Immunology* **45**, 101341 (2019).

79. Van Beek, A.E. *et al.* Factor H-Related (FHR)-1 and FHR-2 Form Homo- and Heterodimers, while FHR-5 Circulates Only As Homodimer in Human Plasma. *Frontiers in Immunology* **8** (2017).

80. Medjeral-Thomas, N.R. *et al.* Circulating complement factor H–related proteins 1 and 5 correlate with disease activity in IgA nephropathy. *Kidney International* **92**, 942-952 (2017).

81. Tortajada, A. *et al.* Elevated factor H–related protein 1 and factor H pathogenic variants decrease complement regulation in IgA nephropathy. *Kidney International* **92**, 953-963 (2017).

82. Zhu, L. *et al.* Circulating complement factor H–related protein 5 levels contribute to development and progression of IgA nephropathy. *Kidney International* **94**, 150-158 (2018).

83. Cipriani, V. *et al.* Increased circulating levels of Factor H-Related Protein 4 are strongly associated with age-related macular degeneration. *Nature Communications* **11** (2020).

84. Cipriani, V. *et al.* Beyond factor H: The impact of genetic-risk variants for age-related macular degeneration on circulating factor-H-like 1 and factor-H-related protein concentrations. *The American Journal of Human Genetics* **108**, 1385-1400 (2021).

85. De Jong, S., Tang, J. & Clark, S.J. Age-related macular degeneration: A disease of extracellular complement amplification. *Immunological Reviews* **313**, 279-297 (2023).

86. Tortajada, A. *et al.* C3 glomerulopathy–associated CFHR1 mutation alters FHR oligomerization and complement regulation. *Journal of Clinical Investigation* **123**, 2434-2446 (2013).

87. Márquez-Tirado, B. *et al.* Factor H-Related Protein 1 Drives Disease Susceptibility and Prognosis in C3 Glomerulopathy. *J Am Soc Nephrol* **33**, 1137-1153 (2022).

88. Garam, N. *et al.* FHR-5 Serum Levels and CFHR5 Genetic Variations in Patients With Immune Complex-Mediated Membranoproliferative Glomerulonephritis and C3-Glomerulopathy. *Frontiers in Immunology* **12** (2021).

89. Van Beek, A.E. *et al.* Low Levels of Factor H Family Proteins During Meningococcal Disease Indicate Systemic Processes Rather Than Specific Depletion by Neisseria meningitidis. *Frontiers in Immunology* **13** (2022).

90. Xu, B. *et al.* Atypical Hemolytic Uremic Syndrome-Associated FHR1 Isoform FHR1*B Enhances Complement Activation and Inflammation. *Frontiers in Immunology* **13** (2022).

91. Bernabéu-Herrero, M.E. *et al.* Complement factor H, FHR-3 and FHR-1 variants associate in an extended haplotype conferring increased risk of atypical hemolytic uremic syndrome. *Mol Immunol* **67**, 276-286 (2015).

92. Pouw, R.B. *et al.* High Complement Factor H-Related (FHR)-3 Levels Are Associated With the Atypical Hemolytic-Uremic Syndrome-Risk Allele CFHR3*B. *Frontiers in Immunology* **9** (2018).

93. Skerka, C. *et al.* Factor H-related protein 1: a complement regulatory protein and guardian of necrotic-type surfaces. *British Journal of Pharmacology* **178**, 2823-2831 (2021).

94. Timmann, C., Leippe, M. & Horstmann, R.D. Two major serum components antigenically related to complement factor H are different glycosylation forms of a single protein with no factor H-like complement regulatory functions. *J Immunol* **146**, 1265-1270 (1991).

95. Dopler, A. *et al.* Deregulation of Factor H by Factor H-Related Protein 1 Depends on Sialylation of Host Surfaces. *Frontiers in Immunology* **12** (2021).

96. Heinen, S. *et al.* Factor H–related protein 1 (CFHR-1) inhibits complement C5 convertase activity and terminal complex formation. *Blood* **114**, 2439-2447 (2009).

97. Loeven, M.A. *et al.* Selective Binding of Heparin/Heparan Sulfate Oligosaccharides to Factor H and Factor H-Related Proteins: Therapeutic Potential for C3 Glomerulopathies. *Frontiers in Immunology* **12** (2021).

98. Csincsi, Á.I. *et al.* FHR-1 Binds to C-Reactive Protein and Enhances Rather than Inhibits Complement Activation. *The Journal of Immunology* **199**, 292-303 (2017).

99. Hannan, J.P., Laskowski, J., Thurman, J.M., Hageman, G.S. & Holers, V.M. Mapping the Complement Factor H-Related Protein 1 (CFHR1):C3b/C3d Interactions. *PLOS ONE* **11**, e0166200 (2016).

100. Zipfel, P.F., Wiech, T., Stea, E.D. & Skerka, C. CFHR Gene Variations Provide Insights in the Pathogenesis of the Kidney Diseases Atypical Hemolytic Uremic Syndrome and C3 Glomerulopathy. *J Am Soc Nephrol* **31**, 241-256 (2020).

101. Li, X., Zong, J. & Si, S. Complement Factor H related protein 1 and immune inflammatory disorders. *Mol Immunol* **145**, 43-49 (2022).

102. Józsi, M. *et al.* FHR-4A: a new factor H-related protein is encoded by the human FHR-4 gene. *European Journal of Human Genetics* **13**, 321-329 (2005).

103. Hebecker, M. & Józsi, M. Factor H-related Protein 4 Activates Complement by Serving as a Platform for the Assembly of Alternative Pathway C3 Convertase via Its Interaction with C3b Protein. *Journal of Biological Chemistry* **287**, 19528-19536 (2012).

104. Mihlan, M. *et al.* Human complement factor H-related protein 4 binds and recruits native pentameric C-reactive protein to necrotic cells. *Mol Immunol* **46**, 335-344 (2009).

105. Hebecker, M. *et al.* Molecular basis of C-reactive protein binding and modulation of complement activation by factor H-related protein 4. *Mol Immunol* **47**, 1347-1355 (2010).

106. Seguin-Devaux, C. *et al.* FHR4-based immunoconjugates direct complement-dependent cytotoxicity and phagocytosis towards HER2-positive cancer cells. *Molecular Oncology* **13**, 2531-2553 (2019).

107. Sinha, A., Singh, A.K., Kadni, T.S., Mullick, J. & Sahu, A. Virus-Encoded Complement Regulators: Current Status. *Viruses* **13**, 208 (2021).

108. Kraivong, R., Punyadee, N., Liszewski, M.K., Atkinson, J.P. & Avirutnan, P. Dengue and the Lectin Pathway of the Complement System. *Viruses* **13**, 1219 (2021).

109. Malekshahi, Z. *et al.* Interference of the Zika Virus E-Protein With the Membrane Attack Complex of the Complement System. *Frontiers in Immunology* **11** (2020).

110. Santos, N.B., Vaz Da Silva, Z.E., Gomes, C., Reis, C.A. & Amorim, M.J. Complement Decay-Accelerating Factor is a modulator of influenza A virus lung immunopathology. *PLOS Pathogens* **17**, e1009381 (2021).

111. Marschang, P., Sodroski, J., Würzner, R. & Dierich, M.P. Decay-accelerating factor (CD55) protects human immunodeficiency virus type 1 from inactivation by human complement. *Eur J Immunol* **25**, 285-290 (1995).

112. Kumar, J., Dhyani, S., Kumar, P., Sharma, N.R. & Ganguly, S. SARS-CoV-2–encoded ORF8 protein possesses complement inhibitory properties. *Journal of Biological Chemistry* **299**, 102930 (2023).

113. Kostavasili, I. *et al.* Mechanism of complement inactivation by glycoprotein C of herpes simplex virus. *J Immunol* **158**, 1763-1771 (1997).

114. Bingöl, E.N., Taştekil, I., Yay, C., Keskin, N. & Ozbek, P. How Epstein-Barr virus envelope glycoprotein gp350 tricks the CR2? A molecular dynamics study. *J Mol Graph Model* **114**, 108196 (2022).

115. Haleem, K.S. *et al.* The Pneumococcal Surface Proteins PspA and PspC Sequester Host C4-Binding Protein To Inactivate Complement C4b on the Bacterial Surface. *Infection and Immunity* **87** (2019).

116. Serruto, D., Rappuoli, R., Scarselli, M., Gros, P. & Van Strijp, J.A.G. Molecular mechanisms of complement evasion: learning from staphylococci and meningococci. *Nature Reviews Microbiology* **8**, 393-399 (2010).

117. Alitalo, A. *et al.* Lysine-Dependent Binding of OspE to the C-terminus of Factor H Mediates Complement Resistance in Borrelia burgdorferi. *Scandinavian Journal of Immunology* **59**, 624-625 (2004).

118. Yee, W.X., Barnes, G., Lavender, H. & Tang, C.M. Meningococcal factor H-binding protein: implications for disease susceptibility, virulence, and vaccines. *Trends Microbiol* **31**, 805-815 (2023).

119. Sharp, J.A. *et al.* Staphylococcus aureus Surface Protein SdrE Binds Complement Regulator Factor H as an Immune Evasion Tactic. *PLoS ONE* **7**, e38407 (2012).

120. Laabei, M. & Ermert, D. Catch Me if You Can: Streptococcus pyogenes Complement Evasion Strategies. *Journal of Innate Immunity* **11**, 3-12 (2019).

121. Moore, S.R., Menon, S.S., Cortes, C. & Ferreira, V.P. Hijacking Factor H for Complement Immune Evasion. *Frontiers in Immunology* **12** (2021).

122. Howden, B.P. *et al.* Staphylococcus aureus host interactions and adaptation. *Nature Reviews Microbiology* **21**, 380-395 (2023).

123. Honda-Ogawa, M. *et al.* Streptococcus pyogenes Endopeptidase O Contributes to Evasion from Complement-mediated Bacteriolysis via Binding to Human Complement Factor C1q. *Journal of Biological Chemistry* **292**, 4244-4254 (2017).

124. Zhang, L.F. *et al.* The Vi Capsular Polysaccharide of Salmonella Typhi Promotes Macrophage Phagocytosis by Binding the Human C-Type Lectin DC-SIGN. *mBio* **13**, e0273322 (2022).

125. Breitfelder, A.K. *et al.* Immunoglobulin M-degrading enzyme of Streptococcus suis (Ide (Ssuis)) impairs porcine B cell signaling. *Front Immunol* **14**, 1122808 (2023).

126. Seele, J. *et al.* The immunoglobulin M-degrading enzyme of Streptococcus suis, Ide Ssuis, is a highly protective antigen against serotype 2. *Vaccine* **33**, 2207-2212 (2015).

127. Zhang, A. *et al.* IgA1 protease contributes to the virulence of Streptococcus suis. *Vet Microbiol* **148**, 436-439 (2011).

128. Kuo, C.F., Lin, Y.S., Chuang, W.J., Wu, J.J. & Tsao, N. Degradation of complement 3 by streptococcal pyrogenic exotoxin B inhibits complement activation and neutrophil opsonophagocytosis. *Infect Immun* **76**, 1163-1169 (2008).

129. Woehl, J.L. *et al.* An Irreversible Inhibitor to Probe the Role of Streptococcus pyogenes Cysteine Protease SpeB in Evasion of Host Complement Defenses. *ACS Chem Biol* **15**, 2060-2069 (2020).

130. Sultan, A.R. *et al.* Production of Staphylococcal Complement Inhibitor (SCIN) and Other Immune Modulators during the Early Stages of Staphylococcus aureus Biofilm Formation in a Mammalian Cell Culture Medium. *Infect Immun* **86** (2018).

131. Amdahl, H. *et al.* Staphylococcal protein Ecb impairs complement receptor-1 mediated recognition of opsonized bacteria. *PLoS One* **12**, e0172675 (2017).

132. Jongerius, I., Garcia, B.L., Geisbrecht, B.V., van Strijp, J.A.G. & Rooijakkers, S.H.M. Convertase inhibitory properties of Staphylococcal extracellular complement-binding protein. *J Biol Chem* **285**, 14973-14979 (2010).

133. Pietrocola, G. *et al.* The Group B Streptococcus-Secreted Protein CIP Interacts with C4, Preventing C3b Deposition via the Lectin and Classical Complement Pathways. *J Immunol* **196**, 385-394 (2016).

134. Caine, J.A. *et al.* Borrelia burgdorferi outer surface protein C (OspC) binds complement component C4b and confers bloodstream survival. *Cell Microbiol* **19** (2017).

135. Laarman, A.J. *et al.* Staphylococcus aureus metalloprotease aureolysin cleaves complement C3 to mediate immune evasion. *J Immunol* **186**, 6445-6453 (2011).

136. Rooijakkers, S.H., van Wamel, W.J., Ruyken, M., van Kessel, K.P. & van Strijp, J.A. Anti-opsonic properties of staphylokinase. *Microbes Infect* **7**, 476-484 (2005).

137. Kochi, L.T. *et al.* The interaction of two novel putative proteins of Leptospira interrogans with E-cadherin, plasminogen and complement components with potential role in bacterial infection. *Virulence* **10**, 734-753 (2019).

138. Xia, X. *et al.* How Streptococcus suis serotype 2 attempts to avoid attack by host immune defenses. *J Microbiol Immunol Infect* **52**, 516-525 (2019).

139. Orth, D. *et al.* EspP, a serine protease of enterohemorrhagic Escherichia coli, impairs complement activation by cleaving complement factors C3/C3b and C5. *Infect Immun* **78**, 4294-4301 (2010).

140. Jusko, M. *et al.* A Metalloproteinase Mirolysin of Tannerella forsythia Inhibits All Pathways of the Complement System. *J Immunol* **195**, 2231-2240 (2015).

141. Laursen, N.S. *et al.* Structural basis for inhibition of complement C5 by the SSL7 protein from Staphylococcus aureus. *Proc Natl Acad Sci U S A* **107**, 3681-3686 (2010).

142. Akesson, P., Sjöholm, A.G. & Björck, L. Protein SIC, a novel extracellular protein of Streptococcus pyogenes interfering with complement function. *J Biol Chem* **271**, 1081-1088 (1996).

143. Skare, J.T. & Garcia, B.L. Complement Evasion by Lyme Disease Spirochetes. *Trends Microbiol* **28**, 889-899 (2020).

144. Hu, S. & Ottemann, K.M. Helicobacter pylori initiates successful gastric colonization by utilizing L-lactate to promote complement resistance. *Nat Commun* **14**, 1695 (2023).

145. de Haas, C.J. *et al.* Chemotaxis inhibitory protein of Staphylococcus aureus, a bacterial antiinflammatory agent. *J Exp Med* **199**, 687-695 (2004).

146. Terao, Y., Yamaguchi, M., Hamada, S. & Kawabata, S. Multifunctional glyceraldehyde-3-phosphate dehydrogenase of Streptococcus pyogenes is essential for evasion from neutrophils. *J Biol Chem* **281**, 14215-14223 (2006).

147. Postma, B. *et al.* Chemotaxis inhibitory protein of Staphylococcus aureus binds specifically to the C5a and formylated peptide receptor. *J Immunol* **172**, 6994-7001 (2004).

148. Cleary, P.P., Prahbu, U., Dale, J.B., Wexler, D.E. & Handley, J. Streptococcal C5a peptidase is a highly specific endopeptidase. *Infect Immun* **60**, 5219-5223 (1992).

149. Reynolds, D. & Kollef, M. The Epidemiology and Pathogenesis and Treatment of Pseudomonas aeruginosa Infections: An Update. *Drugs* **81**, 2117-2131 (2021).

150. Thi, M.T.T., Wibowo, D. & Rehm, B.H.A. Pseudomonas aeruginosa Biofilms. *Int J Mol Sci* **21** (2020).

151. Liao, C., Huang, X., Wang, Q., Yao, D. & Lu, W. Virulence Factors of Pseudomonas Aeruginosa and Antivirulence Strategies to Combat Its Drug Resistance. *Front Cell Infect Microbiol* **12**, 926758 (2022).

152. Colvin, K.M. *et al.* The Pel and Psl polysaccharides provide Pseudomonas aeruginosa structural redundancy within the biofilm matrix. *Environ Microbiol* **14**, 1913-1928 (2012).

153. Chung, J., Eisha, S., Park, S., Morris, A.J. & Martin, I. How Three Self-Secreted Biofilm Exopolysaccharides of Pseudomonas aeruginosa, Psl, Pel, and Alginate, Can Each Be Exploited for Antibiotic Adjuvant Effects in Cystic Fibrosis Lung Infection. *Int J Mol Sci* **24** (2023).

154. Ghssein, G. & Ezzeddine, Z. A Review of Pseudomonas aeruginosa Metallophores: Pyoverdine, Pyochelin and Pseudopaline. *Biology* **11** (2022).

155. Mateu-Borrás, M. *et al.* Molecular Analysis of the Contribution of Alkaline Protease A and Elastase B to the Virulence of Pseudomonas aeruginosa Bloodstream Infections. *Front Cell Infect Microbiol* **11**, 816356 (2021).

156. Jurado-Martín, I., Sainz-Mejías, M. & McClean, S. Pseudomonas aeruginosa: An Audacious Pathogen with an Adaptable Arsenal of Virulence Factors. *Int J Mol Sci* **22** (2021).

157. Hardy, K.S., Tessmer, M.H., Frank, D.W. & Audia, J.P. Perspectives on the Pseudomonas aeruginosa Type III Secretion System Effector ExoU and Its Subversion of the Host Innate Immune Response to Infection. *Toxin* **13** (2021).

158. Qin, S. *et al.* Pseudomonas aeruginosa: pathogenesis, virulence factors, antibiotic resistance, interaction with host, technology advances and emerging therapeutics. *Signal Transduct Target Ther* **7**, 199 (2022).

159. Huber, P. ExlA: A New Contributor to Pseudomonas aeruginosa Virulence. *Front Cell Infect Microbiol* **12**, 929150 (2022).

160. Michalska, M. & Wolf, P. Pseudomonas Exotoxin A: optimized by evolution for effective killing. *Front Microbiol* **6**, 963 (2015).

161. Homma, J.Y. *et al.* Production of leukocidin by clinical isolates of Pseudomonas aeruginosa and antileukocidin antibody from sera of patients with diffuse panbronchiolitis. *J Clin Microbiol* **20**, 855-859 (1984).

162. Tielen, P. *et al.* Interaction between extracellular lipase LipA and the polysaccharide alginate of Pseudomonas aeruginosa. *BMC Microbiol* **13**, 159 (2013).

163. Sun, Z. *et al.* Blocking phosphatidylcholine utilization in Pseudomonas aeruginosa, via mutagenesis of fatty acid, glycerol and choline degradation pathways, confirms the importance of this nutrient source in vivo. *PLoS One* **9**, e103778 (2014).

164. Morello, E. *et al.* Pseudomonas aeruginosa Lipoxygenase LoxA Contributes to Lung Infection by Altering the Host Immune Lipid Signaling. *Front Microbiol* **10**, 1826 (2019).

165. Vadakkan, K., Ngangbam, A.K., Sathishkumar, K., Rumjit, N.P. & Cheruvathur, M.K. A review of chemical signaling pathways in the quorum sensing circuit of Pseudomonas aeruginosa. *Int J Biol Macromol* **254**, 127861 (2024).

166. Pier, G.B. Pseudomonas aeruginosa lipopolysaccharide: a major virulence factor, initiator of inflammation and target for effective immunity. *Int J Med Microbiol* **297**, 277-295 (2007).

167. Maeshima, N. & Fernandez, R.C. Recognition of lipid A variants by the TLR4-MD-2 receptor complex. *Front Cell Infect Microbiol* **3**, 3 (2013).

168. Lam, J.S., Taylor, V.L., Islam, S.T., Hao, Y. & Kocíncová, D. Genetic and Functional Diversity of Pseudomonas aeruginosa Lipopolysaccharide. *Front Microbiol* **2**, 118 (2011).

169. Kintz, E. & Goldberg, J.B. Regulation of lipopolysaccharide O antigen expression in Pseudomonas aeruginosa. *Future Microbiol* **3**, 191-203 (2008).

170. Franklin, M.J., Nivens, D.E., Weadge, J.T. & Howell, P.L. Biosynthesis of the Pseudomonas aeruginosa Extracellular Polysaccharides, Alginate, Pel, and Psl. *Front Microbiol* **2**, 167 (2011).

171. Mishra, M. *et al.* Pseudomonas aeruginosa Psl polysaccharide reduces neutrophil phagocytosis and the oxidative response by limiting complement-mediated opsonization. *Cell Microbiol* **14**, 95-106 (2012).

172. Razvi, E. *et al.* Glycoside hydrolase processing of the Pel polysaccharide alters biofilm biomechanics and Pseudomonas aeruginosa virulence. *NPJ Biofilms Microbiomes* **9**, 7 (2023).

173. Wei, Q. & Ma, L.Z. Biofilm matrix and its regulation in Pseudomonas aeruginosa. *Int J Mol Sci* **14**, 20983-21005 (2013).

174. Moser, C. *et al.* Immune Responses to Pseudomonas aeruginosa Biofilm Infections. *Front Immunol* **12**, 625597 (2021).

175. Harvey, K.L., Jarocki, V.M., Charles, I.G. & Djordjevic, S.P. The Diverse Functional Roles of Elongation Factor Tu (EF-Tu) in Microbial Pathogenesis. *Front Microbiol* **10**, 2351 (2019).

176. Hallström, T. *et al.* Pseudomonas aeruginosa Uses Dihydrolipoamide Dehydrogenase (Lpd) to Bind to the Human Terminal Pathway Regulators Vitronectin and Clusterin to Inhibit Terminal Pathway Complement Attack. *PLoS One* **10**, e0137630 (2015).

177. Paulsson, M. *et al.* Identification of outer membrane Porin D as a vitronectin-binding factor in cystic fibrosis clinical isolates of Pseudomonas aeruginosa. *J Cyst Fibros* **14**, 600-607 (2015).

178. Bastaert, F. *et al.* Pseudomonas aeruginosa LasB Subverts Alveolar Macrophage Activity by Interfering With Bacterial Killing Through Downregulation of Innate Immune Defense, Reactive Oxygen Species Generation, and Complement Activation. *Frontiers in Immunology* **9** (2018).

179. Laarman, A.J. *et al.* Pseudomonas aeruginosa alkaline protease blocks complement activation via the classical and lectin pathways. *J Immunol* **188**, 386-393 (2012).

180. Mateu-Borrás, M. *et al.* Pseudomonas aeruginosa adaptation in cystic fibrosis patients increases C5a levels and promotes neutrophil recruitment. *Virulence* **13**, 215-224 (2022).

181. Engel, L.S., Hill, J.M., Caballero, A.R., Green, L.C. & O'Callaghan, R.J. Protease IV, a unique extracellular protease and virulence factor from Pseudomonas aeruginosa. *J Biol Chem* **273**, 16792-16797 (1998).

182. Tang, A., Caballero, A.R., Marquart, M.E. & O'Callaghan, R.J. Pseudomonas aeruginosa small protease (PASP), a keratitis virulence factor. *Invest Ophthalmol Vis Sci* **54**, 2821-2828 (2013).

183. Nagy, Z.A. *et al.* Ecotin, a microbial inhibitor of serine proteases, blocks multiple complement dependent and independent microbicidal activities of human serum. *PLoS Pathog* **15**, e1008232 (2019).

184. Askarian, F. *et al.* The lytic polysaccharide monooxygenase CbpD promotes Pseudomonas aeruginosa virulence in systemic infection. *Nat Commun* **12**, 1230 (2021).

185. Pelegrin, A.C. *et al.* Pseudomonas aeruginosa: a clinical and genomics update. *FEMS Microbiol Rev* **45** (2021).

186. Hassuna, N.A., Darwish, M.K., Sayed, M. & Ibrahem, R.A. Molecular Epidemiology and Mechanisms of High-Level Resistance to Meropenem and Imipenem in Pseudomonas aeruginosa. *Infect Drug Resist* **13**, 285-293 (2020).

187. McCreary, E.K., Heil, E.L. & Tamma, P.D. New Perspectives on Antimicrobial Agents: Cefiderocol. *Antimicrob Agents Chemother* **65**, e0217120 (2021).

188. McKeage, K. Finafloxacin: first global approval. *Drugs* **75**, 687-693 (2015).

189. Bush, K. & Bradford, P.A. β-Lactams and β-Lactamase Inhibitors: An Overview. *Cold Spring Harb Perspect Med* **6** (2016).

190. Yahav, D. *et al.* New β-Lactam-β-Lactamase Inhibitor Combinations. *Clin Microbiol Rev* **34** (2020).

191. Barbier, F. *et al.* Rationale and evidence for the use of new beta-lactam/beta-lactamase inhibitor combinations and cefiderocol in critically ill patients. *Ann Intensive Care* **13**, 65 (2023).

192. Shirley, M. Ceftazidime-Avibactam: A Review in the Treatment of Serious Gram-Negative Bacterial Infections. *Drugs* **78**, 675-692 (2018).

193. Cluck, D., Lewis, P., Stayer, B., Spivey, J. & Moorman, J. Ceftolozane-tazobactam: A new-generation cephalosporin. *Am J Health Syst Pharm* **72**, 2135-2146 (2015).

194. Heo, Y.-A. Imipenem/Cilastatin/Relebactam: A Review in Gram-Negative Bacterial Infections. *Drugs* **81**, 377-388 (2021).

195. Noval, M., Banoub, M., Claeys, K.C. & Heil, E. The Battle Is on: New Beta-Lactams for the Treatment of Multidrug-Resistant Gram-Negative Organisms. *Curr Infect Dis Rep* **22**, 1 (2020).

196. Lebeaux, D., Leflon-Guibout, V., Ghigo, J.M. & Beloin, C. In vitro activity of gentamicin, vancomycin or amikacin combined with EDTA or l-arginine as lock therapy against a wide spectrum of biofilm-forming clinical strains isolated from catheter-related infections. *J Antimicrob Chemother* **70**, 1704-1712 (2015).

197. Chanda, W. *et al.* Combined effect of linolenic acid and tobramycin on Pseudomonas aeruginosa biofilm formation and quorum sensing. *Exp Ther Med* **14**, 4328-4338 (2017).

198. Zhao, X.L. *et al.* Glutamine promotes antibiotic uptake to kill multidrug-resistant uropathogenic bacteria. *Sci Transl Med* **13**, eabj0716 (2021).

199. Zhan, Y. *et al.* Therapeutic strategies for drug-resistant Pseudomonas aeruginosa: Metal and metal oxide nanoparticles. *J Biomed Mater Res A* **112**, 1343-1363 (2024).

200. Dosler, S. & Karaaslan, E. Inhibition and destruction of Pseudomonas aeruginosa biofilms by antibiotics and antimicrobial peptides. *Peptides* **62**, 32-37 (2014).

201. Duplantier, M., Lohou, E. & Sonnet, P. Quorum Sensing Inhibitors to Quench P. aeruginosa Pathogenicity. *Pharmaceuticals* **14** (2021).

202. Ma, L.Z., Wang, D., Liu, Y., Zhang, Z. & Wozniak, D.J. Regulation of Biofilm Exopolysaccharide Biosynthesis and Degradation in Pseudomonas aeruginosa. *Annu Rev Microbiol* **76**, 413-433 (2022).

203. Chegini, Z. *et al.* Bacteriophage therapy against Pseudomonas aeruginosa biofilms: a review. *Ann Clin Microbiol Antimicrob* **19**, 45 (2020).

204. Reig, S., Le Gouellec, A. & Bleves, S. What Is New in the Anti-Pseudomonas aeruginosa Clinical Development Pipeline Since the 2017 WHO Alert? *Front Cell Infect Microbiol* **12**, 909731 (2022).

205. Secher, T. *et al.* The anti-Pseudomonas aeruginosa antibody Panobacumab is efficacious on acute pneumonia in neutropenic mice and has additive effects with meropenem. *PLoS One* **8**, e73396 (2013).

206. Lu, Q. *et al.* Pharmacokinetics and safety of panobacumab: specific adjunctive immunotherapy in critical patients with nosocomial Pseudomonas aeruginosa O11 pneumonia. *J Antimicrob Chemother* **66**, 1110-1116 (2011).

207. Que, Y.A. *et al.* Assessment of panobacumab as adjunctive immunotherapy for the treatment of nosocomial Pseudomonas aeruginosa pneumonia. *Eur J Clin Microbiol Infect Dis* **33**, 1861-1867 (2014).

208. Ali, S.O. *et al.* Phase 1 study of MEDI3902, an investigational anti–Pseudomonas aeruginosa PcrV and Psl bispecific human monoclonal antibody, in healthy adults. *Clinical Microbiology and Infection* **25**, 629.e621-629.e626 (2019).

209. Chastre, J. *et al.* Safety, efficacy, and pharmacokinetics of gremubamab (MEDI3902), an anti-Pseudomonas aeruginosa bispecific human monoclonal antibody, in P. aeruginosa-colonised, mechanically ventilated intensive care unit patients: a randomised controlled trial. *Critical Care* **26** (2022).

210. Horspool, A.M. *et al.* Development of an anti-Pseudomonas aeruginosa therapeutic monoclonal antibody WVDC-5244. *Frontiers in Cellular and Infection Microbiology* **13** (2023).

211. Meri, T. *et al.* The yeast Candida albicans binds complement regulators factor H and FHL-1. *Infect Immun* **70**, 5185-5192 (2002).

212. Lesiak-Markowicz, I. *et al.* Candida albicans Hgt1p, a multifunctional evasion molecule: complement inhibitor, CR3 analogue, and human immunodeficiency virus-binding molecule. *J Infect Dis* **204**, 802-809 (2011).

213. Casadevall, A. *et al.* The capsule of Cryptococcus neoformans. *Virulence* **10**, 822-831 (2019).

214. Kennedy, A.T. *et al.* Recruitment of Human C1 Esterase Inhibitor Controls Complement Activation on Blood Stage Plasmodium falciparum Merozoites. *J Immunol* **198**, 4728-4737 (2017).

215. Barrios, A.A. *et al.* Inefficient and abortive classical complement pathway activation by the calcium inositol hexakisphosphate component of the Echinococcus granulosus laminated layer. *Immunobiology* **224**, 710-719 (2019).

216. Breijo, M., Anesetti, G., Martínez, L., Sim, R.B. & Ferreira, A.M. Echinococcus granulosus: the establishment of the metacestode is associated with control of complement-mediated early inflammation. *Exp Parasitol* **118**, 188-196 (2008).

217. Kim, Y.U. & Hong, Y. Functional analysis of the first mannosyltransferase (PIG-M) involved in glycosylphosphatidylinositol synthesis in Plasmodium falciparum. *Mol Cells* **24**, 294-300 (2007).

218. Inal, J.M. Complement C2 receptor inhibitor trispanning: from man to schistosome. *Springer Semin Immunopathol* **27**, 320-331 (2005).

219. Ramírez-Toloza, G. & Ferreira, A. Trypanosoma cruzi Evades the Complement System as an Efficient Strategy to Survive in the Mammalian Host: The Specific Roles of Host/Parasite Molecules and Trypanosoma cruzi Calreticulin. *Front Microbiol* **8**, 1667 (2017).

220. Parizade, M., Arnon, R., Lachmann, P.J. & Fishelson, Z. Functional and antigenic similarities between a 94-kD protein of Schistosoma mansoni (SCIP-1) and human CD59. *J Exp Med* **179**, 1625-1636 (1994).

221. Oladiran, A. & Belosevic, M. Trypanosoma carassii calreticulin binds host complement component C1q and inhibits classical complement pathway-mediated lysis. *Dev Comp Immunol* **34**, 396-405 (2010).

222. Zhao, L. *et al.* Trichinella spiralis Calreticulin Binds Human Complement C1q As an Immune Evasion Strategy. *Front Immunol* **8**, 636 (2017).

223. Sun, R. *et al.* Trichinella spiralis Paramyosin Binds Human Complement C1q and Inhibits Classical Complement Activation. *PLoS Negl Trop Dis* **9**, e0004310 (2015).

224. Zhang, Z. *et al.* Trichinella spiralis paramyosin binds to C8 and C9 and protects the tissue-dwelling nematode from being attacked by host complement. *PLoS Negl Trop Dis* **5**, e1225 (2011).

225. Zhao, X., Hao, Y., Yang, J., Gu, Y. & Zhu, X. Mapping of the complement C9 binding domain on Trichinella spiralis paramyosin. *Parasit Vectors* **7**, 80 (2014).

226. Bergström, F.C. *et al.* Scabies mite inactivated serine protease paralogs inhibit the human complement system. *J Immunol* **182**, 7809-7817 (2009).

227. Reynolds, S.L. *et al.* Scabies mite inactive serine proteases are potent inhibitors of the human complement lectin pathway. *PLoS Negl Trop Dis* **8**, e2872 (2014).

228. Roumenina, L.T., Daugan, M.V., Petitprez, F., Sautès-Fridman, C. & Fridman, W.H. Context-dependent roles of complement in cancer. *Nat Rev Cancer* **19**, 698-715 (2019).

229. Senent, Y., Tavira, B., Pio, R. & Ajona, D. The complement system as a regulator of tumor-promoting activities mediated by myeloid-derived suppressor cells. *Cancer Lett* **549**, 215900 (2022).

230. Kourtzelis, I. & Rafail, S. The dual role of complement in cancer and its implication in anti-tumor therapy. *Ann Transl Med* **4**, 265 (2016).

231. Revel, M., Daugan, M.V., Sautés-Fridman, C., Fridman, W.H. & Roumenina, L.T. Complement System: Promoter or Suppressor of Cancer Progression? *Antibodies* **9** (2020).

232. Markiewski, M.M. & Lambris, J.D. The role of complement in inflammatory diseases from behind the scenes into the spotlight. *Am J Pathol* **171**, 715-727 (2007).

233. Markiewski, M.M. *et al.* Modulation of the antitumor immune response by complement. *Nat Immunol* **9**, 1225-1235 (2008).

234. Nabizadeh, J.A. *et al.* The Complement C3a Receptor Contributes to Melanoma Tumorigenesis by Inhibiting Neutrophil and CD4+ T Cell Responses. *J Immunol* **196**, 4783-4792 (2016).

235. Xu, Y. *et al.* Activated Hepatic Stellate Cells (HSCs) Exert Immunosuppressive Effects in Hepatocellular Carcinoma by Producing Complement C3. *Onco Targets Ther* **13**, 1497-1505 (2020).

236. Davidson, S. *et al.* Single-Cell RNA Sequencing Reveals a Dynamic Stromal Niche That Supports Tumor Growth. *Cell Rep* **31**, 107628 (2020).

237. Jackson, W.D. *et al.* C3 Drives Inflammatory Skin Carcinogenesis Independently of C5. *J Invest Dermatol* **141**, 404-414.e406 (2021).

238. Ding, P. *et al.* C5aR1 is a master regulator in Colorectal Tumorigenesis via Immune modulation. *Theranostics* **10**, 8619-8632 (2020).

239. Zha, H. *et al.* Intracellular Activation of Complement C3 Leads to PD-L1 Antibody Treatment Resistance by Modulating Tumor-Associated Macrophages. *Cancer Immunol Res* **7**, 193-207 (2019).

240. Cho, M.S. *et al.* Complement Component 3 Is Regulated by TWIST1 and Mediates Epithelial-Mesenchymal Transition. *J Immunol* **196**, 1412-1418 (2016).

241. Corrales, L. *et al.* Anaphylatoxin C5a creates a favorable microenvironment for lung cancer progression. *J Immunol* **189**, 4674-4683 (2012).

242. Vadrevu, S.K. *et al.* Complement c5a receptor facilitates cancer metastasis by altering T-cell responses in the metastatic niche. *Cancer Res* **74**, 3454-3465 (2014).

243. Bonavita, E. *et al.* PTX3 is an extrinsic oncosuppressor regulating complement-dependent inflammation in cancer. *Cell* **160**, 700-714 (2015).

244. Netti, G.S. *et al.* PTX3 modulates the immunoflogosis in tumor microenvironment and is a prognostic factor for patients with clear cell renal cell carcinoma. *Aging (Albany NY)* **12**, 7585-7602 (2020).

245. Surace, L. *et al.* Complement is a central mediator of radiotherapy-induced tumor-specific immunity and clinical response. *Immunity* **42**, 767-777 (2015).

246. Zhang, C. *et al.* C5aR1 blockade reshapes immunosuppressive tumor microenvironment and synergizes with immune checkpoint blockade therapy in high-grade serous ovarian cancer. *Oncoimmunology* **12**, 2261242 (2023).

247. Xu, D. *et al.* C5aR1 promotes the progression of colorectal cancer by EMT and activating Wnt/β-catenin pathway. *Clin Transl Oncol* **25**, 440-446 (2023).

248. Abdelbaset-Ismail, A. *et al.* Activation of the complement cascade enhances motility of leukemic cells by downregulating expression of HO-1. *Leukemia* **31**, 446-458 (2017).

249. Roumenina, L.T. *et al.* Tumor Cells Hijack Macrophage-Produced Complement C1q to Promote Tumor Growth. *Cancer Immunol Res* **7**, 1091-1105 (2019).

250. Bandini, S. *et al.* The non-inflammatory role of C1q during Her2/neu-driven mammary carcinogenesis. *Oncoimmunology* **5**, e1253653 (2016).

251. Nunez-Cruz, S. *et al.* Genetic and pharmacologic inhibition of complement impairs endothelial cell function and ablates ovarian cancer neovascularization. *Neoplasia* **14**, 994-1004 (2012).

252. Kurihara, R. *et al.* C5a promotes migration, proliferation, and vessel formation in endothelial cells. *Inflamm Res* **59**, 659-666 (2010).

253. Cho, M.S. *et al.* Autocrine effects of tumor-derived complement. *Cell Rep* **6**, 1085-1095 (2014).

254. Chen, J. *et al.* C5aR deficiency attenuates the breast cancer development via the p38/p21 axis. *Aging (Albany NY)* **12**, 14285-14299 (2020).

255. Fishelson, Z. & Kirschfink, M. Complement C5b-9 and Cancer: Mechanisms of Cell Damage, Cancer Counteractions, and Approaches for Intervention. *Front Immunol* **10**, 752 (2019).

256. O'Brien, R.M., Cannon, A., Reynolds, J.V., Lysaght, J. & Lynam-Lennon, N. Complement in Tumourigenesis and the Response to Cancer Therapy. *Cancers* **13** (2021).

257. Geller, A. & Yan, J. The Role of Membrane Bound Complement Regulatory Proteins in Tumor Development and Cancer Immunotherapy. *Front Immunol* **10**, 1074 (2019).

258. Daugan, M.V. *et al.* Intracellular Factor H Drives Tumor Progression Independently of the Complement Cascade. *Cancer Immunol Res* **9**, 909-925 (2021).

259. Kim, E.S., Kim, S.Y. & Moon, A. C-Reactive Protein Signaling Pathways in Tumor Progression. *Biomol Ther (Seoul)* **31**, 473-483 (2023).

260. West, E.E. & Kemper, C. Complosome - the intracellular complement system. *Nat Rev Nephrol* **19**, 426-439 (2023).

261. Xiao, F., Guo, J., Tomlinson, S., Yuan, G. & He, S. The role of the complosome in health and disease. *Front Immunol* **14**, 1146167 (2023).

262. Daugan, M.V. *et al.* Complement C1s and C4d as Prognostic Biomarkers in Renal Cancer: Emergence of Noncanonical Functions of C1s. *Cancer Immunol Res* **9**, 891-908 (2021).

263. Riihilä, P. *et al.* Tumour-cell-derived complement components C1r and C1s promote growth of cutaneous squamous cell carcinoma. *British Journal of Dermatology* **182**, 658-670 (2020).

264. Shimazaki, R. *et al.* Complement factor B regulates cellular senescence and is associated with poor prognosis in pancreatic cancer. *Cell Oncol (Dordr)* **44**, 937-950 (2021).

265. Harbeck, N. *et al.* Breast cancer. *Nat Rev Dis Primers* **5**, 66 (2019).

266. Tariq, M., Richard, V. & Kerin, M.J. MicroRNAs as Molecular Biomarkers for the Characterization of Basal-like Breast Tumor Subtype. *Biomedicines* **11** (2023).

267. Zografos, E. *et al.* Prognostic role of microRNAs in breast cancer: A systematic review. *Oncotarget* **10**, 7156-7178 (2019).

268. Shiovitz, S. & Korde, L.A. Genetics of breast cancer: a topic in evolution. *Ann Oncol* **26**, 1291-1299 (2015).

269. Sun, Y.S. *et al.* Risk Factors and Preventions of Breast Cancer. *Int J Biol Sci* **13**, 1387-1397 (2017).

270. Loibl, S. & Gianni, L. HER2-positive breast cancer. *Lancet* **389**, 2415-2429 (2017).

271. Lehmann-Che, J. *et al.* Immunohistochemical and molecular analyses of HER2 status in breast cancers are highly concordant and complementary approaches. *Br J Cancer* **104**, 1739-1746 (2011).

272. Hsu, J.L. & Hung, M.C. The role of HER2, EGFR, and other receptor tyrosine kinases in breast cancer. *Cancer Metastasis Rev* **35**, 575-588 (2016).

273. Bai, X. *et al.* Structure and dynamics of the EGFR/HER2 heterodimer. *Cell Discov* **9**, 18 (2023).

274. Pan, L. *et al.* HER2/PI3K/AKT pathway in HER2-positive breast cancer: A review. *Medicine* **103**, e38508 (2024).

275. Raghav, K.P.S. & Moasser, M.M. Molecular Pathways and Mechanisms of HER2 in Cancer Therapy. *Clin Cancer Res* **29**, 2351-2361 (2023).

276. Schlam, I. & Swain, S.M. HER2-positive breast cancer and tyrosine kinase inhibitors: the time is now. *NPJ Breast Cancer* **7**, 56 (2021).

277. Ruiz-Saenz, A. *et al.* HER2 Amplification in Tumors Activates PI3K/Akt Signaling Independent of HER3. *Cancer Res* **78**, 3645-3658 (2018).

278. Nahta, R. & Esteva, F.J. Trastuzumab: triumphs and tribulations. *Oncogene* **26**, 3637-3643 (2007).

279. Boekhout, A.H., Beijnen, J.H. & Schellens, J.H. Trastuzumab. *Oncologist* **16**, 800-810 (2011).

280. Sawyers, C.L. Herceptin: A First Assault on Oncogenes that Launched a Revolution. *Cell* **179**, 8-12 (2019).

281. Maadi, H., Soheilifar, M.H., Choi, W.S., Moshtaghian, A. & Wang, Z. Trastuzumab Mechanism of Action; 20 Years of Research to Unravel a Dilemma. *Cancers* **13** (2021).

282. Nami, B., Maadi, H. & Wang, Z. Mechanisms Underlying the Action and Synergism of Trastuzumab and Pertuzumab in Targeting HER2-Positive Breast Cancer. *Cancers* **10** (2018).

283. Boone, J.J., Bhosle, J., Tilby, M.J., Hartley, J.A. & Hochhauser, D. Involvement of the HER2 pathway in repair of DNA damage produced by chemotherapeutic agents. *Mol Cancer Ther* **8**, 3015-3023 (2009).

284. Vivekanandhan, S. & Knutson, K.L. Resistance to Trastuzumab. *Cancers* **14** (2022).

285. Wang, Z.H. *et al.* Trastuzumab resistance in HER2-positive breast cancer: Mechanisms, emerging biomarkers and targeting agents. *Front Oncol* **12**, 1006429 (2022).

286. Verma, S. *et al.* Trastuzumab emtansine for HER2-positive advanced breast cancer. *N Engl J Med* **367**, 1783-1791 (2012).

287. García-Alonso, S., Ocaña, A. & Pandiella, A. Trastuzumab Emtansine: Mechanisms of Action and Resistance, Clinical Progress, and Beyond. *Trends Cancer* **6**, 130-146 (2020).

288. Barok, M., Joensuu, H. & Isola, J. Trastuzumab emtansine: mechanisms of action and drug resistance. *Breast Cancer Res* **16**, 209 (2014).

289. Mosele, F. *et al.* Trastuzumab deruxtecan in metastatic breast cancer with variable HER2 expression: the phase 2 DAISY trial. *Nat Med* **29**, 2110-2120 (2023).

290. Indini, A., Rijavec, E. & Grossi, F. Trastuzumab Deruxtecan: Changing the Destiny of HER2 Expressing Solid Tumors. *Int J Mol Sci* **22** (2021).

291. Hurvitz, S.A. *et al.* Trastuzumab deruxtecan versus trastuzumab emtansine in patients with HER2-positive metastatic breast cancer: updated results from DESTINY-Breast03, a randomised, open-label, phase 3 trial. *Lancet* **401**, 105-117 (2023).

292. Lee, J. & Park, Y.H. Trastuzumab deruxtecan for HER2+ advanced breast cancer. *Future Oncol* **18**, 7-19 (2022).

293. Harbeck, N. *et al.* Trastuzumab deruxtecan in HER2-positive advanced breast cancer with or without brain metastases: a phase 3b/4 trial. *Nat Med* (2024).

294. Menderes, G. *et al.* SYD985, a Novel Duocarmycin-Based HER2-Targeting Antibody-Drug Conjugate, Shows Antitumor Activity in Uterine and Ovarian Carcinosarcoma with HER2/Neu Expression. *Clin Cancer Res* **23**, 5836-5845 (2017).

295. Capelan, M. *et al.* Pertuzumab: new hope for patients with HER2-positive breast cancer. *Ann Oncol* **24**, 273-282 (2013).

296. Barthélémy, P., Leblanc, J., Goldbarg, V., Wendling, F. & Kurtz, J.E. Pertuzumab: development beyond breast cancer. *Anticancer Res* **34**, 1483-1491 (2014).

297. Tsao, L.C. *et al.* Trastuzumab/pertuzumab combination therapy stimulates antitumor responses through complement-dependent cytotoxicity and phagocytosis. *JCI Insight* **7** (2022).

298. Yatim, K.M. & Lakkis, F.G. A brief journey through the immune system. *Clin J Am Soc Nephrol* **10**, 1274-1281 (2015).

299. Paul, S. & Lal, G. The Molecular Mechanism of Natural Killer Cells Function and Its Importance in Cancer Immunotherapy. *Front Immunol* **8**, 1124 (2017).

300. Rosales, C. & Uribe-Querol, E. Phagocytosis: A Fundamental Process in Immunity. *Biomed Res Int* **2017**, 9042851 (2017).

301. Uribe-Querol, E. & Rosales, C. Phagocytosis: Our Current Understanding of a Universal Biological Process. *Front Immunol* **11**, 1066 (2020).

302. Dahdah, A. *et al.* Neutrophil Migratory Patterns: Implications for Cardiovascular Disease. *Front Cell Dev Biol* **10**, 795784 (2022).

303. Mayadas, T.N., Cullere, X. & Lowell, C.A. The multifaceted functions of neutrophils. *Annu Rev Pathol* **9**, 181-218 (2014).

304. Winterbourn, C.C., Kettle, A.J. & Hampton, M.B. Reactive Oxygen Species and Neutrophil Function. *Annu Rev Biochem* **85**, 765-792 (2016).

305. Othman, A., Sekheri, M. & Filep, J.G. Roles of neutrophil granule proteins in orchestrating inflammation and immunity. *Febs j* **289**, 3932-3953 (2022).

306. Sørensen, O.E. & Borregaard, N. Neutrophil extracellular traps - the dark side of neutrophils. *J Clin Invest* **126**, 1612-1620 (2016).

307. Burgener, S.S. & Schroder, K. Neutrophil Extracellular Traps in Host Defense. *Cold Spring Harb Perspect Biol* **12** (2020).

308. Huang, J., Hong, W., Wan, M. & Zheng, L. Molecular mechanisms and therapeutic target of NETosis in diseases. *MedComm (2020)* **3**, e162 (2022).

309. Wu, L., Saxena, S. & Singh, R.K. Neutrophils in the Tumor Microenvironment. *Adv Exp Med Biol* **1224**, 1-20 (2020).

310. Carnevale, S. *et al.* Neutrophil diversity in inflammation and cancer. *Front Immunol* **14**, 1180810 (2023).

311. Heshmat-Ghahdarijani, K. *et al.* The neutrophil-to-lymphocyte ratio as a new prognostic factor in cancers: a narrative review. *Front Oncol* **13**, 1228076 (2023).

312. Poto, R. *et al.* Neutrophil Extracellular Traps, Angiogenesis and Cancer. *Biomedicines* **10** (2022).

313. Masucci, M.T., Minopoli, M. & Carriero, M.V. Tumor Associated Neutrophils. Their Role in Tumorigenesis, Metastasis, Prognosis and Therapy. *Front Oncol* **9**, 1146 (2019).

314. Dutta, A. *et al.* Neutrophils in Cancer and Potential Therapeutic Strategies Using Neutrophil-Derived Exosomes. *Vaccines* **11** (2023).

315. Jakubzick, C.V., Randolph, G.J. & Henson, P.M. Monocyte differentiation and antigen-presenting functions. *Nat Rev Immunol* **17**, 349-362 (2017).

316. Williams, H. *et al.* Monocyte Differentiation and Heterogeneity: Inter-Subset and Interindividual Differences. *Int J Mol Sci* **24** (2023).

317. Sreejit, G., Fleetwood, A.J., Murphy, A.J. & Nagareddy, P.R. Origins and diversity of macrophages in health and disease. *Clin Transl Immunology* **9**, e1222 (2020).

318. Mass, E., Nimmerjahn, F., Kierdorf, K. & Schlitzer, A. Tissue-specific macrophages: how they develop and choreograph tissue biology. *Nat Rev Immunol* **23**, 563-579 (2023).

319. Locati, M., Curtale, G. & Mantovani, A. Diversity, Mechanisms, and Significance of Macrophage Plasticity. *Annu Rev Pathol* **15**, 123-147 (2020).

320. Kolios, G., Valatas, V. & Kouroumalis, E. Role of Kupffer cells in the pathogenesis of liver disease. *World J Gastroenterol* **12**, 7413-7420 (2006).

321. Colonna, M. & Butovsky, O. Microglia Function in the Central Nervous System During Health and Neurodegeneration. *Annu Rev Immunol* **35**, 441-468 (2017).

322. Zheng, D., Bhuvan, T., Payne, N.L. & Heng, T.S.P. Secondary Lymphoid Organs in Mesenchymal Stromal Cell Therapy: More Than Just a Filter. *Front Immunol* **13**, 892443 (2022).

323. Yip, J.L.K., Balasuriya, G.K., Spencer, S.J. & Hill-Yardin, E.L. The Role of Intestinal Macrophages in Gastrointestinal Homeostasis: Heterogeneity and Implications in Disease. *Cell Mol Gastroenterol Hepatol* **12**, 1701-1718 (2021).

324. Joshi, N., Walter, J.M. & Misharin, A.V. Alveolar Macrophages. *Cell Immunol* **330**, 86-90 (2018).

325. Martinez, F.O. & Gordon, S. The M1 and M2 paradigm of macrophage activation: time for reassessment. *F1000Prime Rep* **6**, 13 (2014).

326. Strizova, Z. *et al.* M1/M2 macrophages and their overlaps - myth or reality? *Clin Sci* **137**, 1067-1093 (2023).

327. Viola, A., Munari, F., Sánchez-Rodríguez, R., Scolaro, T. & Castegna, A. The Metabolic Signature of Macrophage Responses. *Front Immunol* **10**, 1462 (2019).

328. Mamilos, A. *et al.* Macrophages: From Simple Phagocyte to an Integrative Regulatory Cell for Inflammation and Tissue Regeneration-A Review of the Literature. *Cells* **12** (2023).

329. Chen, S. *et al.* Macrophages in immunoregulation and therapeutics. *Signal Transduct Target Ther* **8**, 207 (2023).

330. Kerneur, C., Cano, C.E. & Olive, D. Major pathways involved in macrophage polarization in cancer. *Front Immunol* **13**, 1026954 (2022).

331. Vitale, I., Manic, G., Coussens, L.M., Kroemer, G. & Galluzzi, L. Macrophages and Metabolism in the Tumor Microenvironment. *Cell Metab* **30**, 36-50 (2019).

332. Yi, L. *et al.* Macrophage colony-stimulating factor and its role in the tumor microenvironment: novel therapeutic avenues and mechanistic insights. *Front Oncol* **14**, 1358750 (2024).

333. Pan, Y., Yu, Y., Wang, X. & Zhang, T. Tumor-Associated Macrophages in Tumor Immunity. *Front Immunol* **11**, 583084 (2020).

334. Overdijk, M.B. *et al.* Antibody-mediated phagocytosis contributes to the anti-tumor activity of the therapeutic antibody daratumumab in lymphoma and multiple myeloma. *MAbs* **7**, 311-321 (2015).

335. VanDerMeid, K.R. *et al.* Cellular Cytotoxicity of Next-Generation CD20 Monoclonal Antibodies. *Cancer Immunol Res* **6**, 1150-1160 (2018).

336. Shi, Y. *et al.* Trastuzumab triggers phagocytic killing of high HER2 cancer cells in vitro and in vivo by interaction with Fcγ receptors on macrophages. *J Immunol* **194**, 4379-4386 (2015).

337. Valone, F.H. *et al.* Clinical trials of bispecific antibody MDX-210 in women with advanced breast or ovarian cancer that overexpresses HER-2/neu. *J Hematother* **4**, 471-475 (1995).

338. Repp, R. *et al.* Phase I clinical trial of the bispecific antibody MDX-H210 (anti-FcgammaRI x anti-HER-2/neu) in combination with Filgrastim (G-CSF) for treatment of advanced breast cancer. *Br J Cancer* **89**, 2234-2243 (2003).

339. Sundarapandiyan, K. *et al.* Bispecific antibody-mediated destruction of Hodgkin's lymphoma cells. *J Immunol Methods* **248**, 113-123 (2001).

340. Borchmann, P. *et al.* Phase 1 trial of the novel bispecific molecule H22xKi-4 in patients with refractory Hodgkin lymphoma. *Blood* **100**, 3101-3107 (2002).

341. Rolin, C., Zimmer, J. & Seguin-Devaux, C. Bridging the gap with multispecific immune cell engagers in cancer and infectious diseases. *Cell Mol Immunol* **21**, 643-661 (2024).

342. Bozzano, F., Perrone, C., Moretta, L. & De Maria, A. NK Cell Precursors in Human Bone Marrow in Health and Inflammation. *Front Immunol* **10**, 2045 (2019).

343. Cooper, M.A., Fehniger, T.A. & Caligiuri, M.A. The biology of human natural killer-cell subsets. *Trends Immunol* **22**, 633-640 (2001).

344. Anfossi, N. *et al.* Human NK cell education by inhibitory receptors for MHC class I. *Immunity* **25**, 331-342 (2006).

345. Schwane, V. *et al.* Distinct Signatures in the Receptor Repertoire Discriminate CD56bright and CD56dim Natural Killer Cells. *Front Immunol* **11**, 568927 (2020).

346. Rebuffet, L. *et al.* High-dimensional single-cell analysis of human natural killer cell heterogeneity. *Nat Immunol* **25**, 1474-1488 (2024).

347. Vivier, E. *et al.* Natural killer cell therapies. *Nature* **626**, 727-736 (2024).

348. Orange, J.S. Formation and function of the lytic NK-cell immunological synapse. *Nat Rev Immunol* **8**, 713-725 (2008).

349. Capitani, N. & Baldari, C.T. The Immunological Synapse: An Emerging Target for Immune Evasion by Bacterial Pathogens. *Front Immunol* **13**, 943344 (2022).

350. Dustin, M.L. The immunological synapse. *Cancer Immunol Res* **2**, 1023-1033 (2014).

351. Krzewski, K. & Strominger, J.L. The killer's kiss: the many functions of NK cell immunological synapses. *Curr Opin Cell Biol* **20**, 597-605 (2008).

352. Dustin, M.L., Chakraborty, A.K. & Shaw, A.S. Understanding the structure and function of the immunological synapse. *Cold Spring Harb Perspect Biol* **2**, a002311 (2010).

353. Ramírez-Labrada, A. *et al.* All About (NK Cell-Mediated) Death in Two Acts and an Unexpected Encore: Initiation, Execution and Activation of Adaptive Immunity. *Front Immunol* **13**, 896228 (2022).

354. Chen, Y., Lu, D., Churov, A. & Fu, R. Research Progress on NK Cell Receptors and Their Signaling Pathways. *Mediators Inflamm* **2020**, 6437057 (2020).

355. Krzewski, K. & Coligan, J.E. Human NK cell lytic granules and regulation of their exocytosis. *Front Immunol* **3**, 335 (2012).

356. Osińska, I., Popko, K. & Demkow, U. Perforin: an important player in immune response. *Cent Eur J Immunol* **39**, 109-115 (2014).

357. Kiselevsky, D.B. Granzymes and Mitochondria. *Biochemistry (Mosc)* **85**, 131-139 (2020).

358. Kumar, S. Natural killer cell cytotoxicity and its regulation by inhibitory receptors. *Immunology* **154**, 383-393 (2018).

359. Zhang, W., Zhao, Z. & Li, F. Natural killer cell dysfunction in cancer and new strategies to utilize NK cell potential for cancer immunotherapy. *Mol Immunol* **144**, 58-70 (2022).

360. Wu, S.Y., Fu, T., Jiang, Y.Z. & Shao, Z.M. Natural killer cells in cancer biology and therapy. *Mol Cancer* **19**, 120 (2020).

361. Jones, A.B., Rocco, A., Lamb, L.S., Friedman, G.K. & Hjelmeland, A.B. Regulation of NKG2D Stress Ligands and Its Relevance in Cancer Progression. *Cancers* **14** (2022).

362. Pazina, T., Shemesh, A., Brusilovsky, M., Porgador, A. & Campbell, K.S. Regulation of the Functions of Natural Cytotoxicity Receptors by Interactions with Diverse Ligands and Alterations in Splice Variant Expression. *Front Immunol* **8**, 369 (2017).

363. Pende, D. *et al.* Killer Ig-Like Receptors (KIRs): Their Role in NK Cell Modulation and Developments Leading to Their Clinical Exploitation. *Front Immunol* **10**, 1179 (2019).

364. Shin, M.H. *et al.* NK Cell-Based Immunotherapies in Cancer. *Immune Netw* **20**, e14 (2020).

365. Myers, J.A. & Miller, J.S. Exploring the NK cell platform for cancer immunotherapy. *Nat Rev Clin Oncol* **18**, 85-100 (2021).

366. Qi, Y. *et al.* Natural killer cell-related anti-tumour adoptive cell immunotherapy. *J Cell Mol Med* **28**, e18362 (2024).

367. André, P. *et al.* Anti-NKG2A mAb Is a Checkpoint Inhibitor that Promotes Anti-tumor Immunity by Unleashing Both T and NK Cells. *Cell* **175**, 1731-1743.e1713 (2018).

368. van Hall, T. *et al.* Monalizumab: inhibiting the novel immune checkpoint NKG2A. *J Immunother Cancer* **7**, 263 (2019).

369. Sauer, N. *et al.* LAG-3 as a Potent Target for Novel Anticancer Therapies of a Wide Range of Tumors. *Int J Mol Sci* **23** (2022).

370. Lanuza, P.M. *et al.* Recalling the Biological Significance of Immune Checkpoints on NK Cells: A Chance to Overcome LAG3, PD1, and CTLA4 Inhibitory Pathways by Adoptive NK Cell Transfer? *Front Immunol* **10**, 3010 (2019).

371. Ascierto, P.A. *et al.* Nivolumab and Relatlimab in Patients With Advanced Melanoma That Had Progressed on Anti-Programmed Death-1/Programmed Death Ligand 1 Therapy: Results From the Phase I/IIa RELATIVITY-020 Trial. *J Clin Oncol* **41**, 2724-2735 (2023).

372. Rager, T. *et al.* Treatment of Metastatic Melanoma with a Combination of Immunotherapies and Molecularly Targeted Therapies. *Cancers* **14** (2022).

373. Sordo-Bahamonde, C. *et al.* LAG-3 Blockade with Relatlimab (BMS-986016) Restores Anti-Leukemic Responses in Chronic Lymphocytic Leukemia. *Cancers* **13** (2021).

374. Jiang, W. *et al.* Tim-3 Blockade Elicits Potent Anti-Multiple Myeloma Immunity of Natural Killer Cells. *Front Oncol* **12**, 739976 (2022).

375. Sanchez-Correa, B. *et al.* DNAM-1 and the TIGIT/PVRIG/TACTILE Axis: Novel Immune Checkpoints for Natural Killer Cell-Based Cancer Immunotherapy. *Cancers* **11** (2019).

376. Zhang, M., Lam, K.P. & Xu, S. Natural Killer Cell Engagers (NKCEs): a new frontier in cancer immunotherapy. *Front Immunol* **14**, 1207276 (2023).

377. Rothe, A. *et al.* A phase 1 study of the bispecific anti-CD30/CD16A antibody construct AFM13 in patients with relapsed or refractory Hodgkin lymphoma. *Blood* **125**, 4024-4031 (2015).

378. Kakiuchi-Kiyota, S. *et al.* A BCMA/CD16A bispecific innate cell engager for the treatment of multiple myeloma. *Leukemia* **36**, 1006-1014 (2022).

379. Alrubayyi, A., Ogbe, A., Moreno Cubero, E. & Peppa, D. Harnessing Natural Killer Cell Innate and Adaptive Traits in HIV Infection. *Front Cell Infect Microbiol* **10**, 395 (2020).

380. Ma, S., Caligiuri, M.A. & Yu, J. Harnessing IL-15 signaling to potentiate NK cell-mediated cancer immunotherapy. *Trends Immunol* **43**, 833-847 (2022).

381. Warlick, E.D. *et al.* GTB-3550 TriKE™ for the Treatment of High-Risk Myelodysplastic Syndromes (MDS) and Refractory/Relapsed Acute Myeloid Leukemia (AML) Safely Drives Natural Killer (NK) Cell Proliferation At Initial Dose Cohorts. *Blood* **136**, 7-8 (2020).

382. Gauthier, L. *et al.* Control of acute myeloid leukemia by a trifunctional NKp46-CD16a-NK cell engager targeting CD123. *Nat Biotechnol* **41**, 1296-1306 (2023).

383. Demaria, O. *et al.* Antitumor immunity induced by antibody-based natural killer cell engager therapeutics armed with not-alpha IL-2 variant. *Cell Rep Med* **3**, 100783 (2022).

384. Davis, Z.B., Felices, M., Verneris, M.R. & Miller, J.S. Natural Killer Cell Adoptive Transfer Therapy: Exploiting the First Line of Defense Against Cancer. *Cancer J* **21**, 486-491 (2015).

385. Kundu, S., Gurney, M. & O'Dwyer, M. Generating natural killer cells for adoptive transfer: expanding horizons. *Cytotherapy* **23**, 559-566 (2021).

386. Liang, S. *et al.* Comparison of autogeneic and allogeneic natural killer cells immunotherapy on the clinical outcome of recurrent breast cancer. *Onco Targets Ther* **10**, 4273-4281 (2017).

387. Berrien-Elliott, M.M., Jacobs, M.T. & Fehniger, T.A. Allogeneic natural killer cell therapy. *Blood* **141**, 856-868 (2023).

388. Bagus, B.I. Autologous natural killer cells as a promising immunotherapy for locally advanced colon adenocarcinoma: Three years follow-up of resectable case. *Cancer Rep* **6**, e1866 (2023).

389. Lizana-Vasquez, G.D., Torres-Lugo, M., Dixon, R.B., Powderly, J.D., 2nd & Warin, R.F. The application of autologous cancer immunotherapies in the age of memory-NK cells. *Front Immunol* **14**, 1167666 (2023).

390. Moscarelli, J., Zahavi, D., Maynard, R. & Weiner, L.M. The Next Generation of Cellular Immunotherapy: Chimeric Antigen Receptor-Natural Killer Cells. *Transplant Cell Ther* **28**, 650-656 (2022).

391. Li, J. *et al.* CAR-NK cells in combination therapy against cancer: A potential paradigm. *Heliyon* **10**, e27196 (2024).

392. Ebrahimiyan, H. *et al.* Novel insights in CAR-NK cells beyond CAR-T cell technology; promising advantages. *Int Immunopharmacol* **106**, 108587 (2022).

393. Peng, L., Sferruzza, G., Yang, L., Zhou, L. & Chen, S. CAR-T and CAR-NK as cellular cancer immunotherapy for solid tumors. *Cell Mol Immunol* (2024).

394. Kilgour, M.K. *et al.* Advancements in CAR-NK therapy: lessons to be learned from CAR-T therapy. *Front Immunol* **14**, 1166038 (2023).

395. Zhong, Y. & Liu, J. Emerging roles of CAR-NK cell therapies in tumor immunotherapy: current status and future directions. *Cell Death Discov* **10**, 318 (2024).

396. Liu, X. *et al.* Trop2-targeted therapies in solid tumors: advances and future directions. *Theranostics* **14**, 3674-3692 (2024).

397. Liu, M. *et al.* CAR NK-92 cells targeting DLL3 kill effectively small cell lung cancer cells in vitro and in vivo. *J Leukoc Biol* **112**, 901-911 (2022).

398. Su, P.L. *et al.* DLL3-guided therapies in small-cell lung cancer: from antibody-drug conjugate to precision immunotherapy and radioimmunotherapy. *Mol Cancer* **23**, 97 (2024).

399. Robbins, Y. *et al.* Tumor control via targeting PD-L1 with chimeric antigen receptor modified NK cells. *Elife* **9** (2020).

400. Guo, S. *et al.* CD70-specific CAR NK cells expressing IL-15 for the treatment of CD19-negative B-cell malignancy. *Blood Adv* **8**, 2635-2645 (2024).

401. Fitzpatrick, E.A., Wang, J. & Strome, S.E. Engineering of Fc Multimers as a Protein Therapy for Autoimmune Disease. *Front Immunol* **11**, 496 (2020).

402. Miller, A., Carr, S., Rabbitts, T. & Ali, H. Multimeric antibodies with increased valency surpassing functional affinity and potency thresholds using novel formats. *MAbs* **12**, 1752529 (2020).

403. Hofmeyer, T. *et al.* Arranged Sevenfold: Structural Insights into the C-Terminal Oligomerization Domain of Human C4b-Binding Protein. *Journal of Molecular Biology* **425**, 1302-1317 (2013).

404. Serrano, I. *et al.* The Hidden Side of Complement Regulator C4BP: Dissection and Evaluation of Its Immunomodulatory Activity. *Front Immunol* **13**, 883743 (2022).

405. Garnier, L., Hill, F. & Jullen, M. Production of multimeric fusion proteins using a c4bp scaffold. Google Patents; 2007.

406. Libyh, M.T. *et al.* A recombinant human scFv anti-Rh (D) antibody with multiple valences using a C-terminal fragment of C4-binding protein. *Blood, The Journal of the American Society of Hematology* **90**, 3978-3983 (1997).

407. Christiansen, D. *et al.* Octamerization enables soluble CD46 receptor to neutralize measles virus in vitro and in vivo. *J Virol* **74**, 4672-4678 (2000).

408. Dervillez, X., Devaux, C. & COHEN, J.H. Multifunctional heteromultimeric constructs. Google Patents; 2017.

409. Du, Y. *et al.* Incorporation of Non-Canonical Amino Acids into Antimicrobial Peptides: Advances, Challenges, and Perspectives. *Appl Environ Microbiol* **88**, e0161722 (2022).

410. Wood, S.J., Kuzel, T.M. & Shafikhani, S.H. Pseudomonas aeruginosa: Infections, Animal Modeling, and Therapeutics. *Cells* **12**, 199 (2023).

411. Miller, W.R. & Arias, C.A. ESKAPE pathogens: antimicrobial resistance, epidemiology, clinical impact and therapeutics. *Nature Reviews Microbiology* (2024).

412. Tacconelli, E. *et al.* Discovery, research, and development of new antibiotics: the WHO priority list of antibiotic-resistant bacteria and tuberculosis. *The Lancet Infectious Diseases* **18**, 318-327 (2018).

413. Seixas, A.M.M., Sousa, S.A. & Leitão, J.H. Antibody-Based Immunotherapies as a Tool for Tackling Multidrug-Resistant Bacterial Infections. *Vaccines* **10**, 1789 (2022).

414. Lu, L.L., Suscovich, T.J., Fortune, S.M. & Alter, G. Beyond binding: antibody effector functions in infectious diseases. *Nature Reviews Immunology* **18**, 46-61 (2018).

415. Mastellos, D.C., Hajishengallis, G. & Lambris, J.D. A guide to complement biology, pathology and therapeutic opportunity. *Nature Reviews Immunology* **24**, 118-141 (2024).

416. Gross, G.N., Rehm, S.R. & Pierce, A.K. The effect of complement depletion on lung clearance of bacteria. *Journal of Clinical Investigation* **62**, 373-378 (1978).

417. Cerquetti, M.C., Sordelli, D.O., Bellanti, J.A. & Hooke, A.M. Lung defenses against Pseudomonas aeruginosa in C5-deficient mice with different genetic backgrounds. *Infection and Immunity* **52**, 853-857 (1986).

418. Mueller-Ortiz, S.L., Drouin, S.M. & Wetsel, R.A. The Alternative Activation Pathway and Complement Component C3 Are Critical for a Protective Immune Response against Pseudomonas aeruginosa in a Murine Model of Pneumonia. *Infection and Immunity* **72**, 2899-2906 (2004).

419. Pont, S. *et al.* Bacterial behavior in human blood reveals complement evaders with some persister-like features. *PLOS Pathogens* **16**, e1008893 (2020).

420. Merle, N.S., Church, S.E., Fremeaux-Bacchi, V. & Roumenina, L.T. Complement System Part I: Molecular Mechanisms of Activation and Regulation. *Frontiers in Immunology* **6** (2015).

421. Bajic, G., Degn, S.E., Thiel, S. & Andersen, G.R. Complement activation, regulation, and molecular basis for complement-related diseases. *The EMBO Journal* **34**, 2735-2757 (2015).

422. González-Alsina, A., Mateu-Borrás, M., Doménech-Sánchez, A. & Albertí, S. Pseudomonas aeruginosa and the Complement System: A Review of the Evasion Strategies. *Microorganisms* **11**, 664 (2023).

423. Balducci, E., Papi, F., Capialbi, D.E. & Del Bino, L. Polysaccharides' Structures and Functions in Biofilm Architecture of Antimicrobial-Resistant (AMR) Pathogens. *International Journal of Molecular Sciences* **24**, 4030 (2023).

424. Chung, J., Eisha, S., Park, S., Morris, A.J. & Martin, I. How Three Self-Secreted Biofilm Exopolysaccharides of Pseudomonas aeruginosa, Psl, Pel, and Alginate, Can Each Be Exploited for Antibiotic Adjuvant Effects in Cystic Fibrosis Lung Infection. *International Journal of Molecular Sciences* **24**, 8709 (2023).

425. Mishra, M. *et al.* Pseudomonas aeruginosa Psl polysaccharide reduces neutrophil phagocytosis and the oxidative response by limiting complement-mediated opsonization. *Cellular Microbiology* **14**, 95-106 (2012).

426. Mateu-Borrás, M. *et al.* Molecular Analysis of the Contribution of Alkaline Protease A and Elastase B to the Virulence of Pseudomonas aeruginosa Bloodstream Infections. *Frontiers in Cellular and Infection Microbiology* **11** (2022).

427. Laarman, A.J. *et al.* Pseudomonas aeruginosa Alkaline Protease Blocks Complement Activation via the Classical and Lectin Pathways. *The Journal of Immunology* **188**, 386-393 (2012).

428. Kunert, A. *et al.* Immune Evasion of the Human Pathogen Pseudomonas aeruginosa: Elongation Factor Tuf Is a Factor H and Plasminogen Binding Protein. *The Journal of Immunology* **179**, 2979-2988 (2007).

429. Harvey, K.L., Jarocki, V.M., Charles, I.G. & Djordjevic, S.P. The Diverse Functional Roles of Elongation Factor Tu (EF-Tu) in Microbial Pathogenesis. *Frontiers in Microbiology* **10** (2019).

430. Hallström, T. *et al.* Dihydrolipoamide Dehydrogenase of Pseudomonas aeruginosa Is a Surface-Exposed Immune Evasion Protein That Binds Three Members of the Factor H Family and Plasminogen. *The Journal of Immunology* **189**, 4939-4950 (2012).

431. Seguin-Devaux, C. *et al.* Complement-Activating Multimeric Immunotherapeutic Complexes for HER2-breast cancer immunotherapy. Cold Spring Harbor Laboratory; 2024.

432. Schober, R. *et al.* Multimeric immunotherapeutic complexes activating natural killer cells towards HIV-1 cure. *Journal of Translational Medicine* **21** (2023).

433. Chauvin, D. *et al.* Targeting Aspergillus fumigatus Crf Transglycosylases With Neutralizing Antibody Is Relevant but Not Sufficient to Erase Fungal Burden in a Neutropenic Rat Model. *Front Microbiol* **10**, 600 (2019).

434. Chaudhry, W.N. *et al.* Synergy and Order Effects of Antibiotics and Phages in Killing Pseudomonas aeruginosa Biofilms. *PLoS One* **12**, e0168615 (2017).

435. Collaborators, G.B.D.A.R. Global burden of bacterial antimicrobial resistance 1990-2021: a systematic analysis with forecasts to 2050. *Lancet* **404**, 1199-1226 (2024).

436. Casadevall, A. & Paneth, N. Monoclonal Antibody Therapies for Infectious Diseases. *Curr Top Microbiol Immunol* (2024).

437. Jayne, D.R.W. *et al.* Randomized Trial of C5a Receptor Inhibitor Avacopan in ANCA-Associated Vasculitis. *J Am Soc Nephrol* **28**, 2756-2767 (2017).

438. Wilczek, E. *et al.* The possible role of factor H in colon cancer resistance to complement attack. *Int J Cancer* **122**, 2030-2037 (2008).

439. Kessel, C. *et al.* Multimerization of peptide mimotopes for blocking of factor VIII neutralizing antibodies. *ChemMedChem* **4**, 1364-1370 (2009).

440. Shinya, E. *et al.* In-vivo delivery of therapeutic proteins by genetically-modified cells: comparison of organoids and human serum albumin alginate-coated beads. *Biomed Pharmacother* **53**, 471-483 (1999).

441. Reuter, M., Caswell, C.C., Lukomski, S. & Zipfel, P.F. Binding of the Human Complement Regulators CFHR1 and Factor H by Streptococcal Collagen-like Protein 1 (Scl1) via Their Conserved C Termini Allows Control of the Complement Cascade at Multiple Levels. *Journal of Biological Chemistry* **285**, 38473-38485 (2010).

442. Motley, M.P., Banerjee, K. & Fries, B.C. Monoclonal antibody-based therapies for bacterial infections. *Curr Opin Infect Dis* **32**, 210-216 (2019).

443. Jain, R. *et al.* KB001-A, a novel anti-inflammatory, found to be safe and well-tolerated in cystic fibrosis patients infected with Pseudomonas aeruginosa. *J Cyst Fibros* **17**, 484-491 (2018).

444. Francois, B. *et al.* Safety and pharmacokinetics of an anti-PcrV PEGylated monoclonal antibody fragment in mechanically ventilated patients colonized with Pseudomonas aeruginosa: a randomized,double-blind, placebo-controlled trial. *Crit Care Med* **40**, 2320-2326 (2012).

445. Lu, Q. *et al.* Pseudomonas aeruginosa serotypes in nosocomial pneumonia: prevalence and clinical outcomes. *Critical Care* **18**, R17 (2014).

446. Jones, C.J. & Wozniak, D.J. Psl Produced by Mucoid Pseudomonas aeruginosa Contributes to the Establishment of Biofilms and Immune Evasion. *mBio* **8** (2017).

447. Digiandomenico, A. *et al.* Identification of broadly protective human antibodies to Pseudomonas aeruginosa exopolysaccharide Psl by phenotypic screening. *Journal of Experimental Medicine* **209**, 1273-1287 (2012).

448. Spiller, O.B., Hanna, S.M., Devine, D.V. & Tufaro, F. Neutralization of cytomegalovirus virions: the role of complement. *J Infect Dis* **176**, 339-347 (1997).

449. Xu, X. *et al.* Synergistic combination of two antimicrobial agents closing each other's mutant selection windows to prevent antimicrobial resistance. *Sci Rep* **8**, 7237 (2018).

450. Singh, N. & Yeh, P.J. Suppressive drug combinations and their potential to combat antibiotic resistance. *J Antibiot (Tokyo)* **70**, 1033-1042 (2017).

451. Pyzik, M., Kozicky, L.K., Gandhi, A.K. & Blumberg, R.S. The therapeutic age of the neonatal Fc receptor. *Nat Rev Immunol* **23**, 415-432 (2023).

452. McCormick, T.S. & Weinberg, A. Epithelial cell-derived antimicrobial peptides are multifunctional agents that bridge innate and adaptive immunity. *Periodontol 2000* **54**, 195-206 (2010).

453. Narazaki, M. & Kishimoto, T. The Two-Faced Cytokine IL-6 in Host Defense and Diseases. *Int J Mol Sci* **19** (2018).

454. Gierlikowska, B., Stachura, A., Gierlikowski, W. & Demkow, U. The Impact of Cytokines on Neutrophils' Phagocytosis and NET Formation during Sepsis—A Review. *International Journal of Molecular Sciences* **23**, 5076 (2022).

455. Jäger, A.V. *et al.* The inflammatory response induced by Pseudomonas aeruginosa in macrophages enhances apoptotic cell removal. *Sci Rep* **11**, 2393 (2021).

456. McElvaney, O.J., Curley, G.F., Rose-John, S. & McElvaney, N.G. Interleukin-6: obstacles to targeting a complex cytokine in critical illness. *Lancet Respir Med* **9**, 643-654 (2021).

457. Dawson, R.E., Jenkins, B.J. & Saad, M.I. IL-6 family cytokines in respiratory health and disease. *Cytokine* **143**, 155520 (2021).

458. Tsai, W.C. *et al.* CXC chemokine receptor CXCR2 is essential for protective innate host response in murine Pseudomonas aeruginosa pneumonia. *Infect Immun* **68**, 4289-4296 (2000).

459. Williams, I.R. & Parkos, C.A. Colonic neutrophils in inflammatory bowel disease: double-edged swords of the innate immune system with protective and destructive capacity. *Gastroenterology* **133**, 2049-2052 (2007).

460. Bain, W. *et al.* Increased Alternative Complement Pathway Function and Improved Survival during Critical Illness. *Am J Respir Crit Care Med* **202**, 230-240 (2020).

461. Willing, B.P., Russell, S.L. & Finlay, B.B. Shifting the balance: antibiotic effects on host-microbiota mutualism. *Nat Rev Microbiol* **9**, 233-243 (2011).

462. Wu, M. *et al.* Gut complement induced by the microbiota combats pathogens and spares commensals. *Cell* **187**, 897-913 e818 (2024).

463. Kristian, S.A. *et al.* Biofilm formation induces C3a release and protects Staphylococcus epidermidis from IgG and complement deposition and from neutrophil-dependent killing. *J Infect Dis* **197**, 1028-1035 (2008).

464. Al Ojaimi, Y. *et al.* Therapeutic antibodies - natural and pathological barriers and strategies to overcome them. *Pharmacol Ther* **233**, 108022 (2022).

465. Cavaco, M., Castanho, M. & Neves, V. The Use of Antibody-Antibiotic Conjugates to Fight Bacterial Infections. *Front Microbiol* **13**, 835677 (2022).

466. Dhole, S., Mahakalkar, C., Kshirsagar, S. & Bhargava, A. Antibiotic Prophylaxis in Surgery: Current Insights and Future Directions for Surgical Site Infection Prevention. *Cureus* **15**, e47858 (2023).

467. Kurtovic, L. & Beeson, J.G. Complement Factors in COVID-19 Therapeutics and Vaccines. *Trends Immunol* **42**, 94-103 (2021).

468. Ricklin, D., Hajishengallis, G., Yang, K. & Lambris, J.D. Complement: a key system for immune surveillance and homeostasis. *Nat Immunol* **11**, 785-797 (2010).

469. Strainic, M.G. *et al.* Locally produced complement fragments C5a and C3a provide both costimulatory and survival signals to naive CD4+ T cells. *Immunity* **28**, 425-435 (2008).

470. Serruto, D., Rappuoli, R., Scarselli, M., Gros, P. & van Strijp, J.A. Molecular mechanisms of complement evasion: learning from staphylococci and meningococci. *Nat Rev Microbiol* **8**, 393-399 (2010).

471. Sparrow, E., Friede, M., Sheikh, M. & Torvaldsen, S. Therapeutic antibodies for infectious diseases. *Bull World Health Organ* **95**, 235-237 (2017).

472. Otsubo, R. & Yasui, T. Monoclonal antibody therapeutics for infectious diseases: Beyond normal human immunoglobulin. *Pharmacol Ther* **240**, 108233 (2022).

473. Delgado, M. & Garcia-Sanz, J.A. Therapeutic Monoclonal Antibodies against Cancer: Present and Future. *Cells* **12** (2023).

474. Ain, D., Shaikh, T., Manimala, S. & Ghebrehiwet, B. The role of complement in the tumor microenvironment. *Fac Rev* **10**, 80 (2021).

475. Golay, J. & Taylor, R.P. The Role of Complement in the Mechanism of Action of Therapeutic Anti-Cancer mAbs. *Antibodies* **9** (2020).

476. Zarantonello, A., Revel, M., Grunenwald, A. & Roumenina, L.T. C3-dependent effector functions of complement. *Immunol Rev* **313**, 120-138 (2023).

477. Suzuki, H., Ohishi, T., Tanaka, T., Kaneko, M.K. & Kato, Y. Anti-HER2 Cancer-Specific mAb, H(2)Mab-250-hG(1), Possesses Higher Complement-Dependent Cytotoxicity than Trastuzumab. *Int J Mol Sci* **25** (2024).

478. Jin, S. *et al.* Emerging new therapeutic antibody derivatives for cancer treatment. *Signal Transduct Target Ther* **7**, 39 (2022).

479. Baldwin, W.M., 3rd, Valujskikh, A. & Fairchild, R.L. The neonatal Fc receptor: Key to homeostasic control of IgG and IgG-related biopharmaceuticals. *Am J Transplant* **19**, 1881-1887 (2019).

480. Maadi, H. & Wang, Z. A Novel Mechanism Underlying the Inhibitory Effects of Trastuzumab on the Growth of HER2-Positive Breast Cancer Cells. *Cells* **11** (2022).

481. Jagosky, M. & Tan, A.R. Combination of Pertuzumab and Trastuzumab in the Treatment of HER2-Positive Early Breast Cancer: A Review of the Emerging Clinical Data. *Breast Cancer (Dove Med Press)* **13**, 393-407 (2021).

482. Taylor, R.P. & Lindorfer, M.A. The role of complement in mAb-based therapies of cancer. *Methods* **65**, 18-27 (2014).

483. Diebolder, C.A. *et al.* Complement Is Activated by IgG Hexamers Assembled at the Cell Surface.

484. Singh, R., Chandley, P. & Rohatgi, S. Recent Advances in the Development of Monoclonal Antibodies and Next-Generation Antibodies. *Immunohorizons* **7**, 886-897 (2023).

485. Hunter, F.W. *et al.* Mechanisms of resistance to trastuzumab emtansine (T-DM1) in HER2-positive breast cancer. *Br J Cancer* **122**, 603-612 (2020).

486. Cserhalmi, M., Papp, A., Brandus, B., Uzonyi, B. & Józsi, M. Regulation of regulators: Role of the complement factor H-related proteins. *Semin Immunol* **45**, 101341 (2019).

487. Seguin-Devaux, C. *et al.* FHR4-based immunoconjugates direct complement-dependent cytotoxicity and phagocytosis towards HER2-positive cancer cells. *Mol Oncol* **13**, 2531-2553 (2019).

488. Hofmeyer, T. *et al.* Arranged sevenfold: structural insights into the C-terminal oligomerization domain of human C4b-binding protein. *J Mol Biol* **425**, 1302-1317 (2013).

489. Schneider, C.A., Rasband, W.S. & Eliceiri, K.W. NIH Image to ImageJ: 25 years of image analysis. *Nat Methods* **9**, 671-675 (2012).

490. Wielgos, M.E. *et al.* Trastuzumab-Resistant HER2(+) Breast Cancer Cells Retain Sensitivity to Poly (ADP-Ribose) Polymerase (PARP) Inhibition. *Mol Cancer Ther* **17**, 921-930 (2018).

491. Sanz-Álvarez, M. *et al.* Generation and Characterization of Trastuzumab/Pertuzumab-Resistant HER2-Positive Breast Cancer Cell Lines. *Int J Mol Sci* **25** (2023).

492. Lu, Y., Zi, X. & Pollak, M. Molecular mechanisms underlying IGF-I-induced attenuation of the growth-inhibitory activity of trastuzumab (Herceptin) on SKBR3 breast cancer cells. *Int J Cancer* **108**, 334-341 (2004).

493. Patel, A., Unni, N. & Peng, Y. The Changing Paradigm for the Treatment of HER2-Positive Breast Cancer. *Cancers* **12** (2020).

494. Zeng, L., Li, W. & Chen, C.S. Breast cancer animal models and applications. *Zool Res* **41**, 477-494 (2020).

495. Martínez-Sáez, O. & Prat, A. Current and Future Management of HER2-Positive Metastatic Breast Cancer. *JCO Oncol Pract* **17**, 594-604 (2021).

496. Swain, S.M., Shastry, M. & Hamilton, E. Targeting HER2-positive breast cancer: advances and future directions. *Nat Rev Drug Discov* **22**, 101-126 (2023).

497. Yuan, M., Liu, L., Wang, C., Zhang, Y. & Zhang, J. The Complement System: A Potential Therapeutic Target in Liver Cancer. *Life* **12** (2022).

498. Harjunpää, A., Junnikkala, S. & Meri, S. Rituximab (anti-CD20) therapy of B-cell lymphomas: direct complement killing is superior to cellular effector mechanisms. *Scand J Immunol* **51**, 634-641 (2000).

499. Di Gaetano, N. *et al.* Complement activation determines the therapeutic activity of rituximab in vivo. *J Immunol* **171**, 1581-1587 (2003).

500. Hörl, S. *et al.* Reduction of complement factor H binding to CLL cells improves the induction of rituximab-mediated complement-dependent cytotoxicity. *Leukemia* **27**, 2200-2208 (2013).

501. Parente, R., Clark, S.J., Inforzato, A. & Day, A.J. Complement factor H in host defense and immune evasion. *Cell Mol Life Sci* **74**, 1605-1624 (2017).

502. Moore, S.R., Menon, S.S., Cortes, C. & Ferreira, V.P. Hijacking Factor H for Complement Immune Evasion. *Front Immunol* **12**, 602277 (2021).

503. Józsi, M. Factor H Family Proteins in Complement Evasion of Microorganisms. *Front Immunol* **8**, 571 (2017).

504. Saxena, R. *et al.* Complement factor H: a novel innate immune checkpoint in cancer immunotherapy. *Front Cell Dev Biol* **12**, 1302490 (2024).

505. Hörl, S. *et al.* Complement factor H-derived short consensus repeat 18-20 enhanced complement-dependent cytotoxicity of ofatumumab on chronic lymphocytic leukemia cells. *Haematologica* **98**, 1939-1947 (2013).

506. Csincsi Á, I. *et al.* FHR-1 Binds to C-Reactive Protein and Enhances Rather than Inhibits Complement Activation. *J Immunol* **199**, 292-303 (2017).

507. Reiss, T. *et al.* Cutting Edge: FHR-1 Binding Impairs Factor H-Mediated Complement Evasion by the Malaria Parasite Plasmodium falciparum. *J Immunol* **201**, 3497-3502 (2018).

508. González-Alsina, A. *et al.* Factor H-related protein 1 promotes complement-mediated opsonization of Pseudomonas aeruginosa. *Front Cell Infect Microbiol* **14**, 1328185 (2024).

509. Lee, C.H. *et al.* IgG Fc domains that bind C1q but not effector Fcγ receptors delineate the importance of complement-mediated effector functions. *Nat Immunol* **18**, 889-898 (2017).

510. Gogesch, P., Dudek, S., van Zandbergen, G., Waibler, Z. & Anzaghe, M. The Role of Fc Receptors on the Effectiveness of Therapeutic Monoclonal Antibodies. *Int J Mol Sci* **22** (2021).

511. Lu, L.L., Suscovich, T.J., Fortune, S.M. & Alter, G. Beyond binding: antibody effector functions in infectious diseases. *Nat Rev Immunol* **18**, 46-61 (2018).

512. Hori, A. *et al.* Vasculogenic mimicry is associated with trastuzumab resistance of HER2-positive breast cancer. *Breast Cancer Res* **21**, 88 (2019).

513. Morales-Guadarrama, G. *et al.* Vasculogenic Mimicry in Breast Cancer: Clinical Relevance and Drivers. *Cells* **10** (2021).

514. Pio, R., Ajona, D., Ortiz-Espinosa, S., Mantovani, A. & Lambris, J.D. Complementing the Cancer-Immunity Cycle. *Front Immunol* **10**, 774 (2019).

515. Taylor, C. *et al.* Augmented HER-2 specific immunity during treatment with trastuzumab and chemotherapy. *Clin Cancer Res* **13**, 5133-5143 (2007).

516. Zong, H.F. *et al.* A novel bispecific antibody drug conjugate targeting HER2 and HER3 with potent therapeutic efficacy against breast cancer. *Acta Pharmacol Sin* **45**, 1727-1739 (2024).

517. Mamidi, S., Cinci, M., Hasmann, M., Fehring, V. & Kirschfink, M. Lipoplex mediated silencing of membrane regulators (CD46, CD55 and CD59) enhances complement-dependent anti-tumor activity of trastuzumab and pertuzumab. *Mol Oncol* **7**, 580-594 (2013).

518. Elvington, M. *et al.* A targeted complement-dependent strategy to improve the outcome of mAb therapy, and characterization in a murine model of metastatic cancer. *Blood* **119**, 6043-6051 (2012).